UNIVERSITY OF NOTTINGHAM

Use of steel fibres to reinforce cement bound roadbase

by

Ian Thompson BEng CEng (MICE)

May 2001

Thesis submitted to the University of Nottingham for the degree of Doctor of Philosophy

SCHOOL OF CIVIL ENGINEERING

To Jack and Adam

The highway to San Juan de la Cruz was a black-top road. In the twenties hundreds of miles of concrete highway had been laid down in California, and people had sat back and said, "There, that's permanent. That will last as long as the Roman roads and longer, because no grass can grow up through the concrete to break it." But it wasn't so. The rubber-shod trucks, the pounding automobiles, beat the concrete, and after a while the life went out of it and it began to crumble. Then a side broke off and a hole crushed through and a crack developed and a little ice in winter spread the crack, so the resisting concrete could not stand the beating of rubber and broke down.

Then the county maintenance crews poured tar in the cracks to keep the water out, and that didn't work, and finally they capped the road with an asphalt and gravel mixture. That did survive, because it offered no stern face to the pounding tires. It gave a little and came back a little. It softened in the summer and hardened in the winter. And gradually all the roads were capped with shining black that looked silver in the distance.

Chapter 9
The Wayward Bus
John Steinbeck, 1947

Abstract

An investigation of steel fibre reinforced cement bound material (FRCBM), for use as a roadbase in flexible composite pavement, is presented. It considers the laboratory-measured properties of FRCBM and the practicalities of mixing and laying the material in the field. It also presents a Design Method and Material Specification, which will enable FRCBM to be carried forward to practice.

The laboratory investigation considered the flexural, indirect tensile and flexural fatigue properties of FRCBM, and the cyclic shear behaviour across a full depth vertical crack. The behaviour of the material was compared to the properties of unreinforced cement bound material. It was shown that steel fibre reinforcement improved the post-crack properties of FRCBM, enabling the composite to carry significant static and dynamic load even after cracking had occurred. The performance of the FRCBM was found to be dependent on the steel fibre type used and the fibre volume fraction.

Field investigations showed that conventional plant and techniques could be used in FRCBM construction. Inadequacies of existing dispensing equipment for use with a continuous batcher are highlighted. Field measurements showed that the FRCBM pavement was able to retain its load carrying capacity after severe cracking had occurred, confirming the laboratory results. There is therefore a potential whole life cost saving in using FRCBM rather than the unreinforced material, which has no significant post-crack load carrying capability.

The data obtained from the laboratory and field investigations were supplemented with a theoretical analytical study into the behaviour of a concrete pavement, assuming various support and crack conditions. A Design Method was produced, which aims to avoid traffic induced cracking of the FRCBM roadbase and limit reflective cracking through the asphalt overlay.

Publications

Thom, N.H., Thompson, I, and Peaston, C.H., 2000. 'Use of Steel Fibre Reinforcement in Cement Treated Base', Proceedings of the 4th International RILEM Conference on Reflective Cracking in Pavements, Ottawa, Ontario, Canada, 26 – 30 March 2000, pp. 413 – 422.

Thompson, I, Peaston, C.H. and Thom, N.H., 1999. 'Fibre Reinforced Cement Bound Roadbase', Proceedings of the 2nd Asia-Pacific Specialty Conference on Fibre Reinforced Concrete, Singapore, 27 – 28 August 1999, pp. 213 – 220.

Acknowledgements

I am grateful to a number of people who helped me, in some large or small way, to complete this piece of work. In particular, I wish to thank my project supervisors, Dr. Chris Peaston and Dr. Nick Thom, who were of particularly assistance during the three years of study, and subsequently commented on this thesis.

The research project was carried out as part of an Engineering and Physical Sciences Research Grant, and I am grateful to them for their financial support. I am also indebted to the members of that project team for their enthusiastic support. They were David York of Sitebatch (Contracting) Ltd, Dirk Nemegeer and John Greenhalgh of N.V Bekaert S.A, John Mercer and Robert Dudgeon of the Highways Agency and Robert Armitage of Scott Wilson Pavement Engineering. I look forward to continuing the 'cause' with these people.

Also, I thank the University laboratory team, in particular Nigel Rook, who often assisted in the less pleasant task of mixing and compacting. Additionally, Barry Brodrick, Bal Loyla, Mike Bettison, Mick Langford, Andy Leyko, Ian Richardson, Geoff Mitchell, Hayley Drabble and Steve Cooper contributed in some way.

Finally, and perhaps most importantly, I thank Wendy, who has supported me on yet another of my unending adventures.

IT

Notation

A	Cross sectional area of beam
C	Subgrade friction coefficient
D	Thickness of CBM
D_a	Asphalt depth
E	Stiffness modulus
E_{ct}	Composite tensile modulus of elasticity
F	Applied load
I	Second-moment of area
$I_5, I_{10}, I_{20}, I_{50}$	ASTM toughness indices
L	Simply supported span
L'	Transverse crack spacing
L_{db}	Asphalt de-bond length
N	Number of load applications
N_f	Number of load applications to failure
P	Tyre pressure
P_{eq}	Equivalent tyre pressure
R	Tyre contact radius
$R_{e,3}$	Flexural strength ratio to a deflection of 3mm
$R_{e,2}$	Flexural strength ratio to a deflection of 2mm
R_{SP}	Equivalent indirect tensile (cylinder-splitting) strength ratio
S	Stress ratio
T_{SP}	Absolute indirect tensile (cylinder-splitting) toughness
T_{JSCE}	Absolute flexural toughness
V_f	Fibre volume fraction
$V_{f,crit}$	Critical fibre volume fraction
$V_{f,crit,fl}$	Critical fibre volume fraction in flexure
V_m	Fibre volume fraction of matrix
W	Slab width

a	Initial shear slip
b	Beam width
h	Beam depth
l	Radius of relative stiffness
l_f	Fibre length
l_{crit}	Critical fibre length
m	Deterioration gradient
r	Fibre cross sectional area to perimeter
w	Crack width
y	Net shear slip
α	Thermal coefficient of aggregate
δ_{cr}	First crack deflection
δ_{JSCE}	Measured deflection limit in JSCE toughness test (=L/150)
ε	Drying shrinkage coefficient
ε_c	Composite strain
ε_{ct}	Composite cracking strain
ε_t	Critical tensile strain
ε_{tu}	Composite ultimate tensile strain
δ_U	Deflection of loaded side of slab
δ_{UL}	Deflection of unloaded side of slab
$\Delta\delta$	Relative deflection of slab
δ_p	Permanent deflection
δ_e	Elastic deflection
δ_{SP}	Deformation of indirect tensile (cylinder-splitting) specimen
ε_t	Tensile strain in asphalt
ϕ	Fibre diameter
η_l	Bond efficiency factor

η_o	Orientation factor
σ'	Design flexural strength
σ_c	Composite stress
σ'_{cr}	Composite cracking stress
σ_{fu}	Tensile strength of fibre
σ_t	Tensile strength
σ_{cr}	First crack flexural strength
σ_{eq}	Equivalent flexural strength
σ_m	Flexural matrix strength
$\sigma_{SP,cr}$	First crack indirect tensile (cylinder-splitting) strength
$\sigma_{SP,eq}$	Equivalent indirect tensile (cylinder-splitting) strength
$\sigma_{SP,u}$	Ultimate indirect tensile (cylinder-splitting) strength
σ_u	Ultimate flexural strength
τ	Shear stress
τ_f	Interfacial bond strength
τ_u	Ultimate bond stress
θ_U	Rotation of loaded side of slab
θ_{UL}	Rotation of unloaded side of slab
θ_T	Net rotation of slab

CBM	Cement bound material
FRCBM	Steel fibre reinforced cement bound material
SFRC	Steel fibre reinforced concrete
LTE	Load transfer efficiency
LTS	Load transfer stiffness
AIF	Aggregate interlock factor
FWD	Falling weight deflectometer

Contents

Chapter 3. Fibre reinforced cementitious materials

Chapter 4. Laboratory investigation

Chapter 6. Development of a design method

Chapter 1. Introduction

1.1 Cement bound material and fibres?

Use of CBM in flexible-composite pavements

Cement bound material (CBM) is a graded aggregate or crushed rock, mixed with cement and surface compacted by rolling. As a pavement layer, the set material offers protection to the lower layers and is able to carry high traffic loads: it therefore possesses the material characteristics worthy of a roadbase. And there are a number of reasons to consider CBM as a roadbase over alternatives. CBM is able to be produced using a wide range of aggregate, enabling production on or close to the site, thereby appeasing local concerns regarding wagon movements and reducing associated haulage costs. Additionally, CBM is laid continuously, without the need to prepare steel reinforcement bars used in continuously reinforced concrete pavements. Production rates are thus not hampered by steel fixing. As CBM is significantly less expensive than bituminous materials, there are mechanical, environmental and economic reasons for selecting CBM as the roadbase over alternatives.

It is not surprising therefore that CBM has found widespread use in pavement applications throughout the world. However, terminology and design criteria of CBM vary between countries. In the United Kingdom, the term CBM covers a range of material strengths, aggregate types and gradings, allowing it to be used as a sub-base in all types of pavement, and the lower roadbase in a flexible composite pavement (the upper roadbase and surface being asphalt). CBM is therefore analogous to cement treated base used in the United States and hydraulically bound material used in other parts of Europe. In terms of material composition and construction techniques, so called roller compacted concrete (RCC) is generally the same as CBM. However, RCC tends to be higher strength than CBM and has been used outside the United Kingdom with no overlay. For the purpose of this study, CBM refers to any roller compacted cementitious material, regardless of strength.

The function of the asphalt overlay depth in flexible composite pavements is primarily to limit the migration of cracks, which originate in the CBM, to the surface. This phenomenon is commonly referred to as reflective cracking. A characteristic of CBM is transverse cracks, and effective control of these cracks is considered key to improving the mechanical behaviour of flexible composite pavements. Experience has demonstrated that a significant depth of asphalt is required to limit reflective cracking. Given that the asphalt is by far the most costly material in this type of pavement (approximately £75/m^3 compared to approximately £35/m^3 for a high strength CBM), cracking in the CBM has economic implications for the whole structure.

Steel fibre reinforcement

So why fibre reinforcement? Fibre reinforcement has been used as a mechanism to control cracking in brittle materials since ancient times. As it is well known that concrete is relatively weak in tension, so attempts to improve the 'ductility' of concrete through the addition of fibres have attempted to overcome the inherent problems associated with brittle failure. Over the past thirty years or so, fibre manufacturers have carried out considerable research to improve the shape and size of fibres to facilitate the bond with the concrete and the mixing process, enabling fibres to be effective in brittle materials. This has encouraged the use of fibre reinforced concrete in numerous civil engineering applications. In terms of pavement applications, fibre reinforcement has been widely applied to ground bearing concrete slabs.

The case for investigating fibre reinforced cement bound material (FRCBM) as a roadbase is based on a number of potential benefits for this application. As the material is roller compacted, continuous reinforcement used to control cracking in pavement quality structural concrete is not a realistic option. Research into fibre reinforced concrete has demonstrated benefits in terms of crack control - the use of fibres to control cracking in a CBM may enable a more economic flexible composite pavement to be designed. However, little research has been carried out on the reinforcement of roller compacted concretes. The

types and quantities of fibres required in such a material are not well understood, and the beneficial properties to flexible composite pavements have not been investigated.

This study provided an opportunity therefore to investigate a number of material properties pertinent to flexible composite pavements, both in the laboratory and in the field, and to demonstrate the applicability of the results to practice through the development of a design method. This could be used to compare the mechanical performance of CBM and FRCBM and to compare pavement costs.

Background to project

The impetus for this study originated from an investigation on 'Improved cement bound base design for flexible composite pavements' at the University of Nottingham in the United Kingdom by Shahid (1997). Shahid demonstrated that fibres could increase the indirect tensile (cylinder-splitting) strength, improve the post-crack ductility and increase the load transfer characteristics of a cracked CBM. The pilot study carried out by Shahid resulted in an Engineering and Physical Sciences Research Council (EPSRC) proposal to study further the potential benefits of FRCBM. The study had significant industrial support with the collaborating team comprising of: the UK Highways Agency; N.V Bekaert S.A - a steel fibre producer based in Belgium; Sitebatch (Contracting) Ltd - a producer of CBM; and Scott Wilson Pavement Engineering - a Pavement Engineering Consultancy. The Collaborators were therefore well placed to advise on many aspects of pavement construction and steel fibre reinforcement, and to exploit any of the project findings.

The vast majority of the literature available for fibre reinforced cementitious materials is based on structural grade concrete, and of relevance to this study, on concrete slabs. However, little of the experience gained on fibre reinforced structural grade concrete has found its way to highway applications. (This may in part be due to concrete slabs being designed by 'structural' engineers, and highways being designed by 'pavement' engineers). This study therefore used the opportunity to apply some of the research findings from structural concrete to the (generally) weaker CBM. The literature review retrieved only a few references to fibre reinforced roller compacted concrete. Nanni and Johari (1989) detailed a

pilot study into the practicalities of batching and laying a fibre reinforced roller compacted concrete for off-highway facilities, which involved a laying trial and some material testing. Sobhan (1997) carried out a laboratory study on a cement treated base, which led to a subsequent publication (Sobhan and Krizek 1999). Also, Ficheroulle (1998) described field trial using fibre reinforced roller compacted concrete overlaid with a thin layer of bituminous material.

Although these studies considered particular, isolated aspects of fibre reinforced roller compacted concrete, this is the first investigation into a wide range of static and dynamic material properties, measured both in the laboratory and in the field. Furthermore, the data obtained from the testing programme were incorporated into a practical design method, in part based on analytical study, and may now be carried forward to practice.

1.2 Objectives

The objectives of the study were:

1. To investigate the material properties of FRCBM in the laboratory considered important to a roadbase in a flexible composite pavement. These involved the following test modes:

    - Flexure and indirect tension (cylinder-splitting),
    - Dynamic flexure,
    - Cyclic shear.

2. To investigate the site practicalities of mixing and laying FRCBM. To achieve this, field studies were required to:

    - Assess the practicality of plant and techniques to mix and lay CBM, in particular the dispensing of fibres,
    - Monitor the accelerated deterioration of the pavement under traffic load.

3. To produce a simplified method that can be used to design flexible composite pavements using FRCBM.

1.3 Methodology and thesis layout

The methodology used to complete the research involved the five tasks described below:

1. Performing a comprehensive literature review of the design of flexible composite pavements, including literature on the load transfer characteristics at transverse cracks and the state-of-the-art for steel fibre reinforced concrete.

2. Performing laboratory tests on FRCBM to characterise the static and dynamic properties using various fibre types at various volume fractions and material strengths, and to develop a test that could be used to compare the cyclic shear behaviour of CBM and FRCBM. Material properties of FRCBM were investigated using various fibre types, fibre volume fractions and CBM strengths considered appropriate to flexible composite pavements.

3. Conducting mixing and laying trials and subsequent monitoring of the accelerated deterioration of a section of FRCBM. Field investigations included batching and laying a section of FRCBM, which was subsequently trafficked. Material tests were carried out on cored specimens, and visual observations and field measurements using the Falling Weight Deflectometer were used to investigate the *in situ* properties of the pavement.

4. Performing an analytical study of the relative influence of the components of a flexible composite pavement, including load transfer characteristics at a transverse crack, foundation support and asphalt overlay thickness. Analytical studies were carried out using the computer based multi-layer linear elastic analysis programme BISAR3 and the finite element programme ILLISLAB95 to investigate the influence of various material parameters in a pavement on the FRCBM base layer and asphalt overlay.

5. Developing a design method for flexible composite pavements with an FRCBM roadbase, which includes the contribution of the foundation, crack spacing, traffic, material characteristics, relative density of mixture and asphalt overlay thickness. Data from the

laboratory, field and analytical studies were used to develop the design method. Also, recommendations were made as to performance based criteria for the properties of FRCBM for use in a pavement, contained within the following documents for use by industry:

- Design Method (described in Chapter 6)
- Material Specification (Appendix B)
- Notes for Guidance (Appendix B)

The thesis is divided into seven chapters, following the methodology described above. An overview of the execution of the tasks, and corresponding thesis chapters, is illustrated in the flowchart in Figure 1-1.

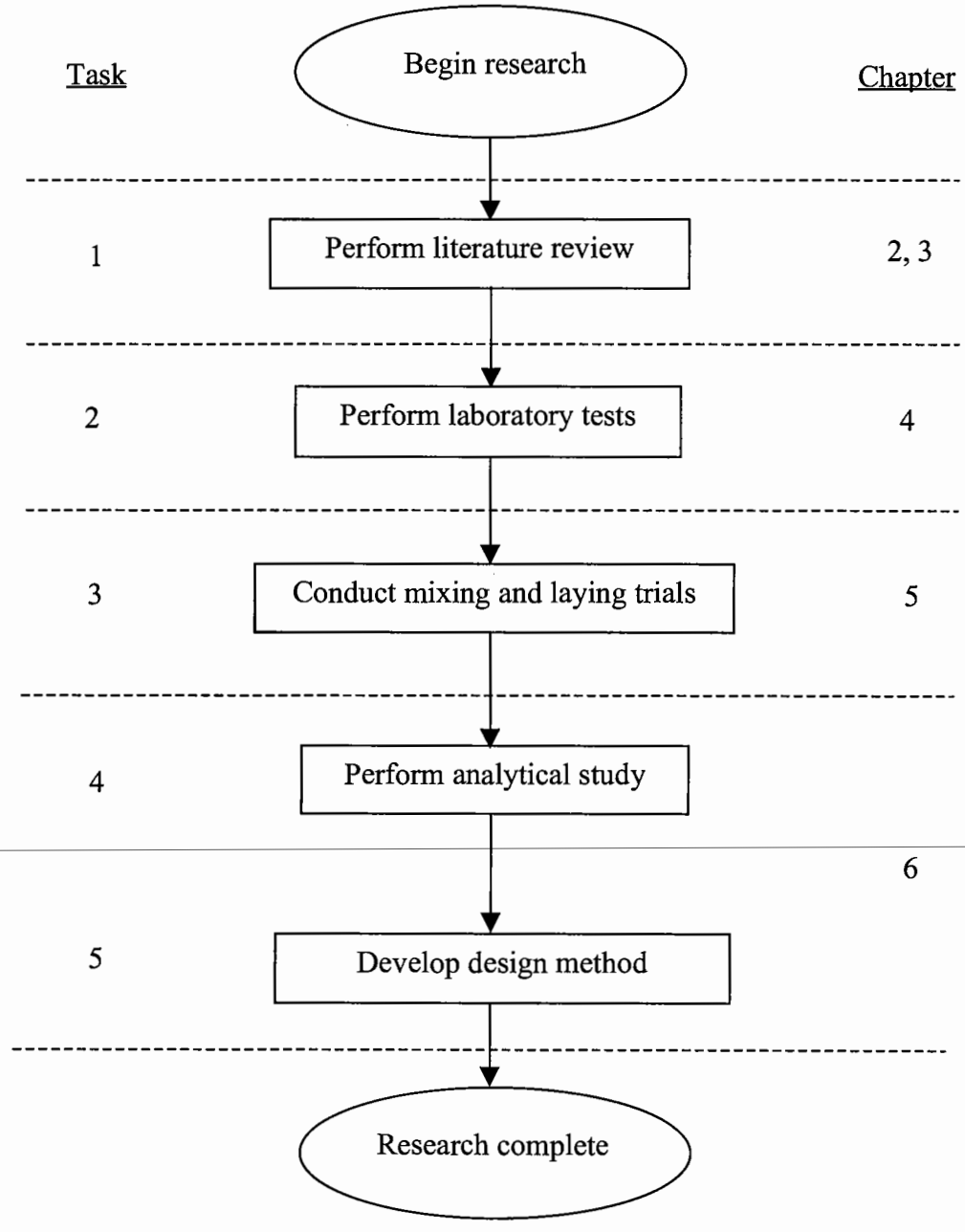

Figure 1-1 Fibre reinforced cement bound material study methodology

Chapter 2. Flexible composite pavements

2.1 Introduction

This chapter reviews literature specific to the application of CBM as part of a pavement system. In particular, it describes the design approach adopted for flexible composite pavements in the United Kingdom and overseas, and the modes and causes of deterioration.

Being a brittle material, the tendency is for CBM to crack due to excessive temperature changes and traffic load. However, cracking in the CBM itself should not be cause for concern. It is only when the consequence of such cracks to cause damage to other parts of the pavement, in particular reflection cracking through the overlay, that CBM cracking becomes problematic. Hence, the behaviour at transverse cracks is reviewed and discussed with regard to the problems associated with flexible composite pavements. Literature on load transfer at transverse cracks is drawn primarily from research carried out in the United States on pavement quality concrete. In doing so, the load transfer efficiency and concept of aggregate interlock is presented, and models of these mechanisms are also described.

Finally, the perceived benefits of steel fibre reinforcement on CBM are discussed based on the understanding of the modes of failure of flexible composite pavements and characteristics of CBM.

2.2 The design of flexible composite pavements

Flexible composite (semi-rigid) pavements are so defined when the lower roadbase is constructed using CBM and the upper roadbase and surface is asphalt (Figure 2-1). The construction is widely used throughout the world, often offering economic and environmental advantages over alternatives. However, the design approach differs somewhat between countries.

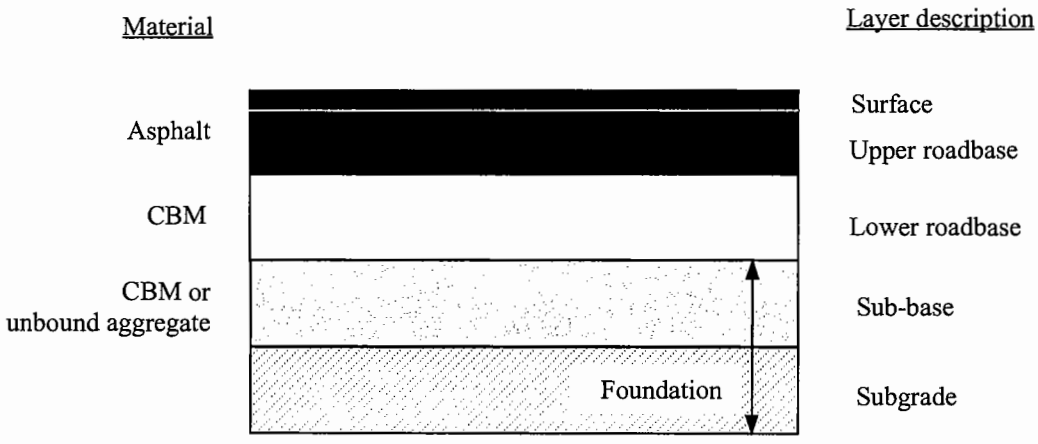

Figure 2-1 Material and layers in a flexible composite pavement

2.2.1 United Kingdom design approach

The thickness of flexible composite pavements in the United Kingdom is generally derived from a design chart presented in the Design Manual for Roads and Bridges, Volume 7 (Highways Agency 1994), reproduced in Figure 2-2. This categorises CBM on the basis of 7-day compressive cube strength, the details for which are described in the Specification for Highway Works (Highways Agency 1998) and shown in Table 2-1. The data on which the design charts are based originated from 39 sections of experimental pavement, reported in Transport Research Laboratory (TRL) report LR 1132 (Powell *et al.* 1984). The CBM used in the TRL study had 28-day compressive cube strengths between 4MPa and 20MPa. Higher strength materials were added later based in part on multi-layer linear elastic analysis.

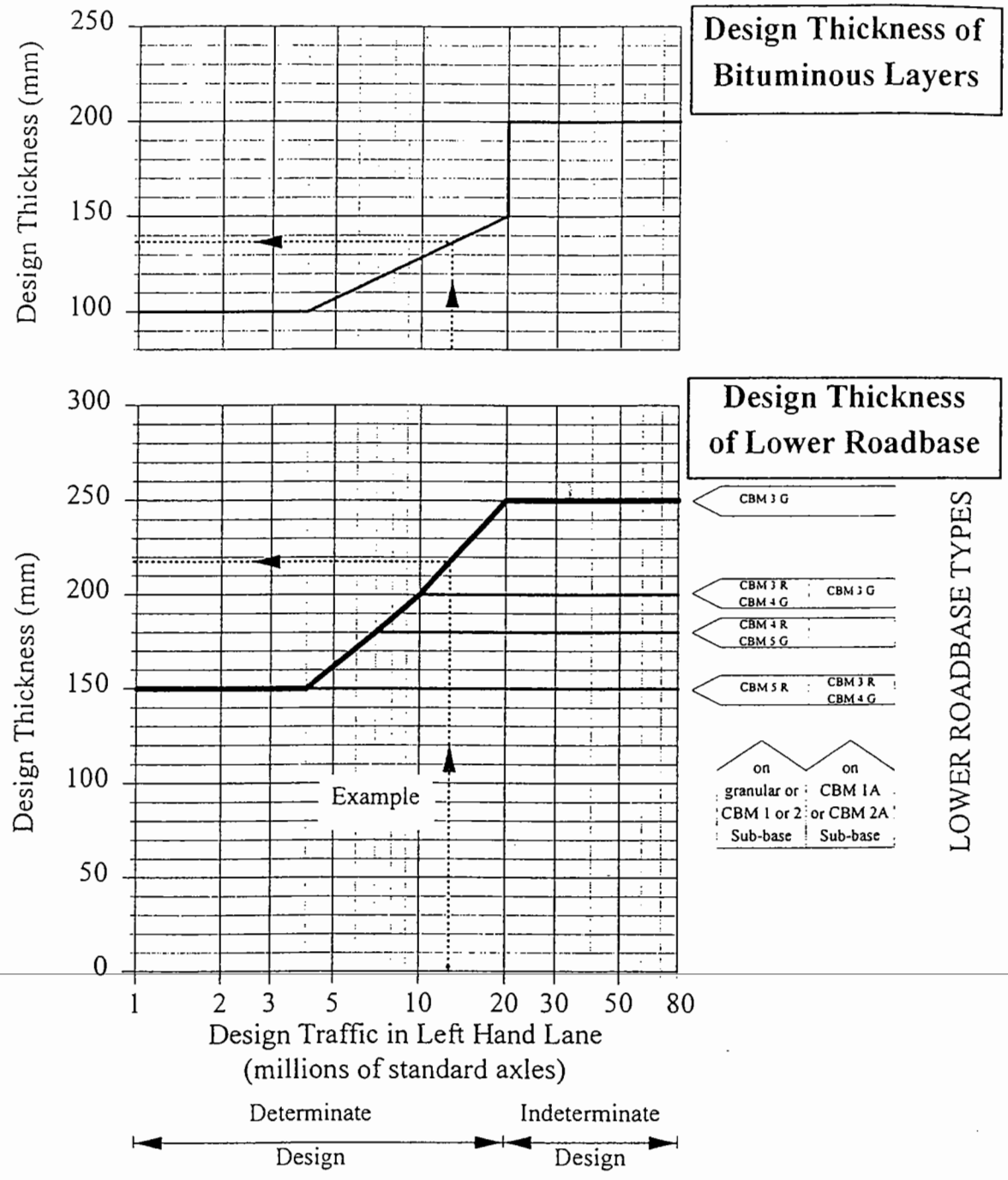

R = Roadbase having a coefficient of thermal expansion less than 10 x 10^{-6} per °C, containing crushed rock aggregate

G = Roadbase containing gravel aggregate or Roadbase that has a coefficient of thermal expansion more than 10 x 10^{-6} per °C, containing crushed rock aggregate

Figure 2-2 Design thickness chart for flexible composite pavements in the United Kingdom (*Highways Agency 1994*)

CBM category	Minimum compaction	Min. 7-day cube strength (N/mm²)	
		Average of 5 samples	Individual samples
CBM1 CBM1A	95% of cube density	4.5 10.0	2.5 6.5
CBM2 CBM2A	"	7.0 10.0	4.5 6.5
CBM3	"	10.0	6.5
CBM4	"	15.0	10.0
CBM5	"	20.0	13.0

Table 2-1 Compressive cube strength requirements for CBM in the United Kingdom (*Department of Transport 1998*)

Compressive cube strength is specified as it is a convenient method of quality control on site. However, it is well known that concrete is relatively weak in tension, so it will be no surprise that CBM invariably fails in this mode. Specifically, this can be caused by bending under the action of traffic or temperature gradients, or in direct tension due to restrained shrinkage. Flexure tests would clearly be more appropriate as they more closely reflect the in-service behaviour of the material, and would allow the contractor more freedom in the determination of aggregate selection and mix proportions. Once a relationship between flexural and compressive strength has been obtained for an individual mix, cube strength may be justifiably used as part of the site control.

The design methodology enables more economical designs (by reducing the thicknesses of the CBM and asphalt) for traffic up to 20 million standard axles (msa); such constructions are expected to deteriorate under traffic and be rectified periodically by maintenance. As cracking of these pavements is expected to occur, the design life based on Figure 2-2 is described as 'determinate' (Powell *et al.* 1984).

Intervention on higher volume roads (i.e. traffic greater than 20msa) is more costly, and the thickness of these pavement layers are designed to avoid traffic induced cracks in the CBM (Powell *et al.* 1984). At the time of the introduction of the charts, visual inspection of the experimental pavements indicated that traffic induced cracking had generally not

occurred up to 20msa when the asphalt depth was 200mm. As it was not known how much longer these pavements would perform satisfactorily, these designs were described as having an 'indeterminate' life.

Powell *et al.* (1984) observed that traffic induced cracking generally occurs when the combined stresses due to traffic and temperature in the CBM are greater than the mean 28-day flexural strength (Figure 2-3). Temperature induced stresses, which cause warping of the CBM, were derived based on a method described by Thomlinson (1940). Traffic induced stresses were determined using a multi-layer linear elastic programme.

Parry *et al.* (1999) recently carried out a retrospective study of the performance of 649km of flexible composite pavement constructed in the United Kingdom between 1959 and 1987. These pavements had carried up to 97msa by 1996. The vast majority had been strengthened using asphalt overlays and a small percentage had failed, requiring reconstruction of the CBM base. The conclusions supported the construction depths advocated by Powell *et al.* (1984) for the higher volume roads. It was also noted that of the pavements constructed using a cement bound sub-base (rather than unbound granular aggregate sub-base), comparatively very few had required reconstruction of the CBM lower roadbase.

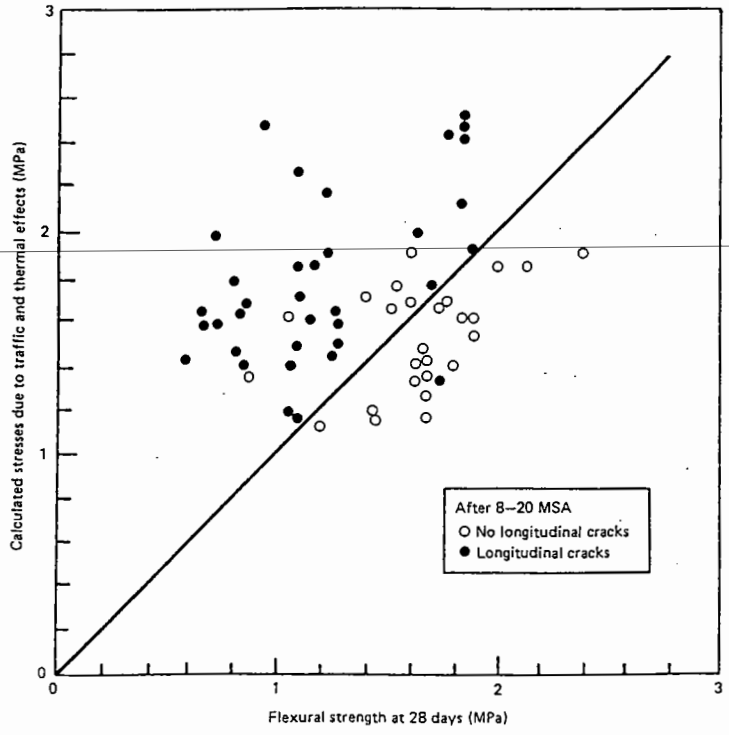

Figure 2-3 Flexural strength as an indicator of ability to resist longitudinal cracking (*Powell et al. 1984*)

The asphalt overlay thickness and properties influence the design of the lower cement bound roadbase in flexible composite structures. The asphalt serves three functions (Lister 1972):

- It insulates the CBM layer, thereby reducing temperature induced movement (expansion/contraction and warping);
- It spreads the wheel load; and
- It transfers load across transverse cracks.

The combined effect of these benefits is to reduce the stresses on the CBM and to reduce the risk of reflection cracking in the overlay. The overlay design thicknesses shown in Figure 2-2 were based on visual observations of the experimental pavements as to when surface cracking of the asphalt occurred (Figure 2-4). This type of serviceability failure was more critical than surface rutting for the asphalt used in the study.

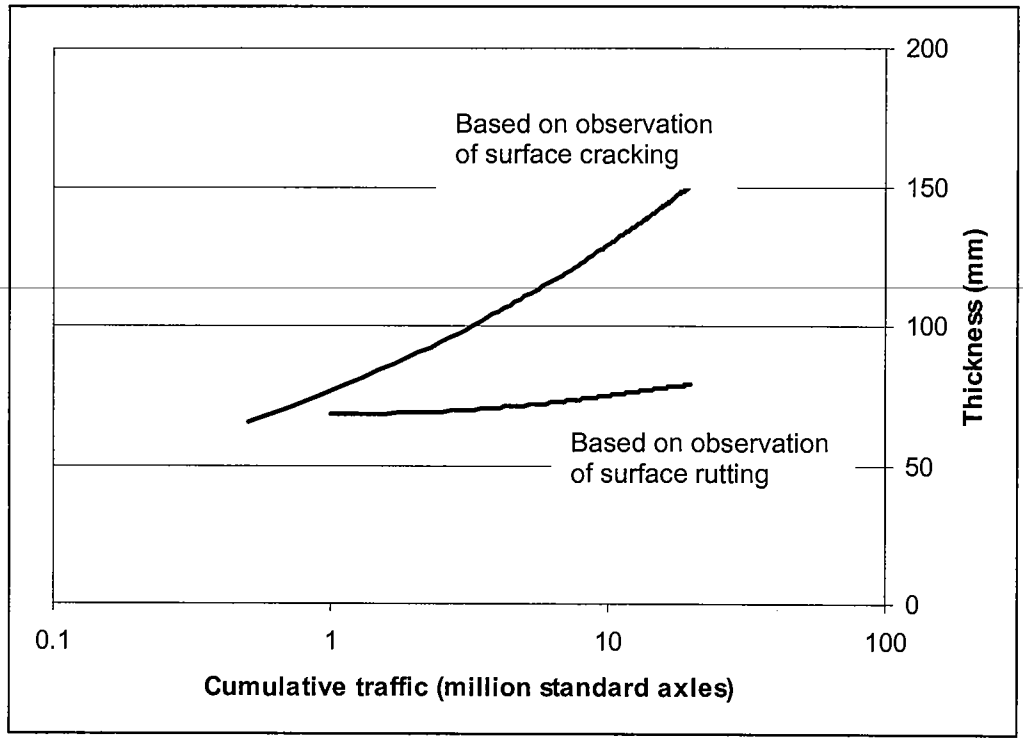

Figure 2-4 Observed cracking and rutting through the asphalt surface at various traffic for roads with a CBM lower concrete roadbase (*Powell et al. 1984*)

However, more compliant asphalts would be expected to be less susceptible to reflective cracking but more likely to fail due to excessive deformations.

Steps have recently been taken to attempt to control the width of cracks in CBM. This is carried out in practice by inducing cracks in the CBM base during construction, either by use of a physical crack inducer, or by mechanically cracking the pavement using a guillotine (Ellis *et al.* 1997). Inducing cracks at regular intervals allows controlled cracks to remain that can accommodate thermal movement and increase the load transfer efficiency over what would be expected from a natural crack. The benefits of load transfer efficiency are discussed in Section 2-4.

Outside the United Kingdom, particularly in the United States, roller compacted concrete is commonly used with no asphalt overlay. Similar structures to flexible composite pavements are used in other parts of Europe, therefore the design of these pavements is of interest to this study.

2.2.2 Overseas design approach

In the United States, roller compacted concrete is generally designed following approaches by the U.S. Army Corps of Engineers or the Portland Cement Association (Pittman 1993). The former assumes no capacity for load transfer at transverse cracks, and the critical (maximum) stress is based on a load placed at the edge of the slab. The latter is based upon flexural fatigue tests and assumes sufficient load transfer exists at cracks to make the stress resulting from a load placed at the interior of the slab control the thickness design. Neither method promotes the application of induced cracking, although the Corps' method recommends formed contraction joints where natural cracks are considered undesirable.

In Europe, France is perhaps considered the most proactive country with respect to hydraulically bound materials. The design of the French Composite Pavement, which is similar to flexible composite pavements in the United Kingdom, are described in the French Design Manual for Pavement Structures (LCPC *et al.* 1997). Composite pavements in France are designed against reflective cracking, which generally result in an asphalt surface thickness similar to the thickness of the hydraulically bound material, this being of the order

of 200mm. It is assumed in this construction, as in the United Kingdom design method, that deterioration of the cement bound layer will occur.

An alternative structure is translated from French to 'pavements with base materials with hydraulically bound materials'. The design criterion in this pavement is to avoid cracking in the cementitious layer, but accepts that some reflective cracking will occur. This results in a higher strength, thicker base design, and significantly reduced overlay thickness, when compared to the composite pavement. Indirectly, some account of transverse cracking and fatigue behaviour is included by increasing the critical stress with 'risk' factors. Although fatigue relationships and the effects of aggregate type on crack opening are well documented, no guidance is given to the potential benefit of induced cracking.

The United States' methods for RCC, and the French method for 'pavements with base materials with hydraulically bound materials', require the determination of the stress within the cementitious material under an applied load.

2.2.3 Determination of allowable stress and ultimate strength in concrete

Stresses in concrete pavements are complex and constantly varying within the material under traffic load and temperature changes. As the slab bends, the tensile stresses that are generated will cause failure if the material's tensile strength is exceeded. To take account of the complex nature of the stress distribution, variability in material properties, layer thicknesses and fatigue characteristics, safety factors are often used to ensure the strength exceeds the critical stress by a margin. The strength of the material is often determined from flexure tests, the advantage being that this test roughly represents bending under a wheel load. The main disadvantage is that it overestimates the tensile strength because of assumptions of linear elasticity, as close to failure the stress is no longer proportional to the distance from the neutral axis (Pittman 1993). However, the vast experience gained using flexural strength for pavement calculations makes flexural testing popular.

A requirement in many pavement designs is the determination of the critical stress using elastic analysis. This aims at ensuring an allowable (or working) stress, under an applied load, is less than the limit of proportionality of the material. The most widely adopted

solution using this method is by Westergaard (1926), though a number of computer based finite element programs used in the United States, such as ILLISLAB95, also use elastic analysis.

An alternative to elastic analysis is plastic analysis. This differs primarily in that the ultimate strength of the slab is determined under a given load, which will theoretically result in failure (Megson 1987). In pavement applications, standard axle loads are commonly used in analytical design, hence the strength of the structure that results in collapse based on these loads can be computed.

Plastic analysis for unreinforced concrete slabs was first proposed by Meyerhof (1962), and is a design option in the Concrete Society Technical Report TR34 (1994) for the design of fibre reinforced concrete industrial ground floors in the United Kingdom. This design method should in principle be equally valid for highway pavements.

Both Westergaard and Meyerhof computed the critical parameters (stress in the case of Westergaard and load in the case of Meyerhof) at the centre, edge and corner of the slab. In the calculations, both used the radius of relative stiffness (l), a quantity defined by Westergaard (1926) as a measure of the stiffness of the slab relative to the subgrade. Eqn...2-1 demonstrates the relative influence of the slab depth (D), and shows that if the slab stiffness (E) increases in relation to the modulus of subgrade reaction (k), l increases. Poisson's ratio is denoted by ν.

$$l = \sqrt[4]{\frac{ED^3}{12(1-\nu^2)k}} \qquad \textbf{Eqn...2-1}$$

The radius of relative stiffness is therefore required in the computation of the allowable stress or the ultimate strength in a concrete pavement, and has also been used to describe the load transfer behaviour at transverse cracks, as will be outlined in Section 2.4. Also, Meyerhof principles are currently used in the design of fibre reinforced concrete slabs in the United Kingdom, and therefore these will be discussed in more detail in Chapter 3.

Having introduced the design methods used in practice, the next section takes a more fundamental look at the deterioration and mechanical properties of CBM.

2.3 Deterioration of flexible composite pavements

Flexible composite pavements deteriorate by cracking in the CBM and reflective cracking through the asphalt layers (Highways Agency 1994). Cracking in the CBM occurs due to a combination of traffic and temperature induced stresses (which cause warping), and restrained shrinkage. Traffic induced cracks tend to appear in the longitudinal direction within the wheelpath of vehicles (Figure 2-5). Shrinkage cracks, which invariably occur, appear across the width of the CBM at regular intervals; the spacing of these cracks are dependent on the aggregate type and material strength. Transverse cracks are liable to horizontal and vertical movement, and alone or in combination with imposed traffic loads, can induce cracks in the overlying asphalt resulting in a reduction in the durability of the pavement.

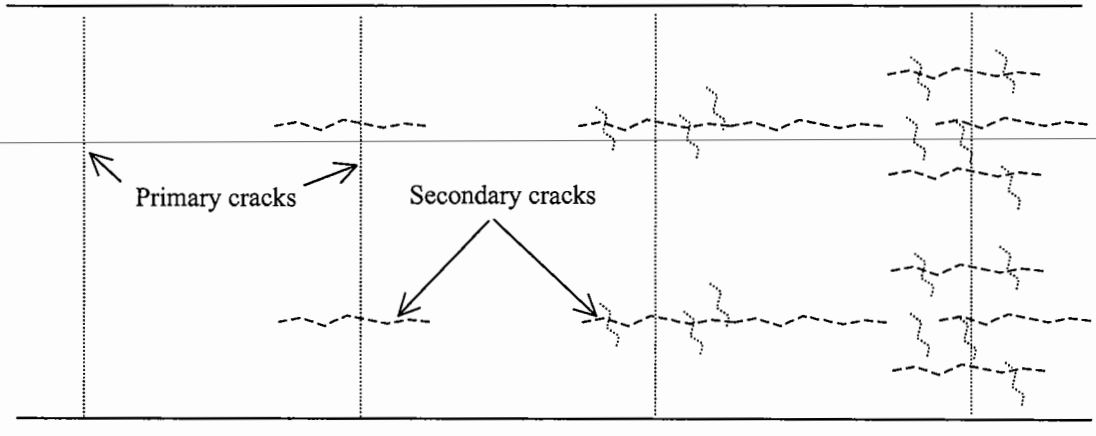

Figure 2-5 Plan of CBM layer showing longitudinal and transverse cracks

2.3.1 Traffic induced cracking

Fatigue

Traffic induced cracks are considered to be caused by load induced flexural failure (Williams 1986). Such a failure is costly as it requires the reconstruction of the failed section. Whilst cracking could occur from a single large wheel load, failure may occur after numerous smaller load applications due to material fatigue. It is customary in engineering to apply safety factors to guard against progressive failures such as those caused by fatigue. These factors are dependent on the risk associated with failure.

In the United Kingdom, some account of risk is included by differentiating between pavement life through 'determinate' and 'indeterminate' designs, although no explicit account of fatigue is included in the methodology, as is the case in the United States and France.

Lister (1972) argued that in fact damage due to fatigue is not a consideration on all but the most highly trafficked roads. This was based on a traffic study, which showed that along the section surveyed, less than ten percent of wagon wheel loads exceeded the standard wheel load of 40kN (Figure 2-6). The accumulation of damage is therefore very much lower than would be expected based on the traditional method of using cumulative standard axles.

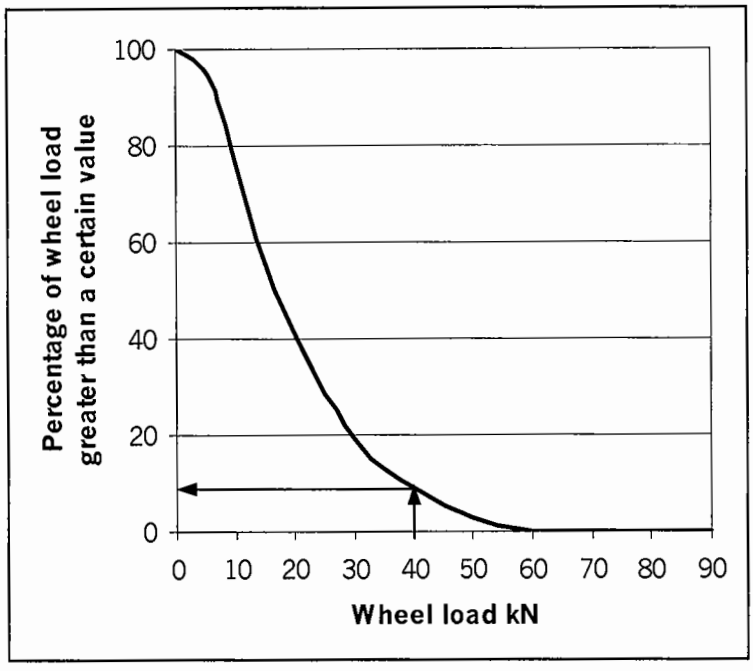

Figure 2-6 Percentage distribution of wheel loads (discounting private cars) on a UK trunk road (*Lister 1972*)

Based on laboratory fatigue relationships for CBM, in excess of 10 million load applications could be carried at an applied load of two-thirds the material strength (Shahid 1997). Considering the actual number of damaging loads as described above, dynamic behaviour may be less of a problem than, say, under-compaction. Williams (1986) reported that at a relative material density of 95% (which is the permitted minimum in the United Kingdom Specification for Highway Works), the compressive cube strength may be halved. Fatigue is often highlighted to justify the use of a safety factor, whereas under-compaction is not, although it is evident that the consequences of under-compaction on strength could be far greater than fatigue.

Under-compaction

Under compaction is clearly a cause of loss in density, though less obvious is the influence of water content on density. Too little will not provide sufficient water to lubricate all the aggregate particles necessary to facilitate compaction. Too much will result in water occupying the space of the aggregate, reducing the density of the mix. Shahid (1997) demonstrated that significant loss in cube strength occurred in CBM using both a limestone aggregate and sand and river gravel, at a water content of only 0.5% above the optimum water content. In practice, contractors often choose to lay CBM at water contents slightly above optimum to help with compaction. The potential loss in strength is generally compensated for by increasing the cement content, to make sure the minimum strength requirement is achieved.

Nanni (1989) showed from field trials on fibre reinforced and unreinforced roller compacted concrete that the lower half of the material was of significantly lower density than the upper half (Figure 2-7). This illustrates the variability of the material density with depth, and therefore the strength, increasing the susceptibility of the material to cracking.

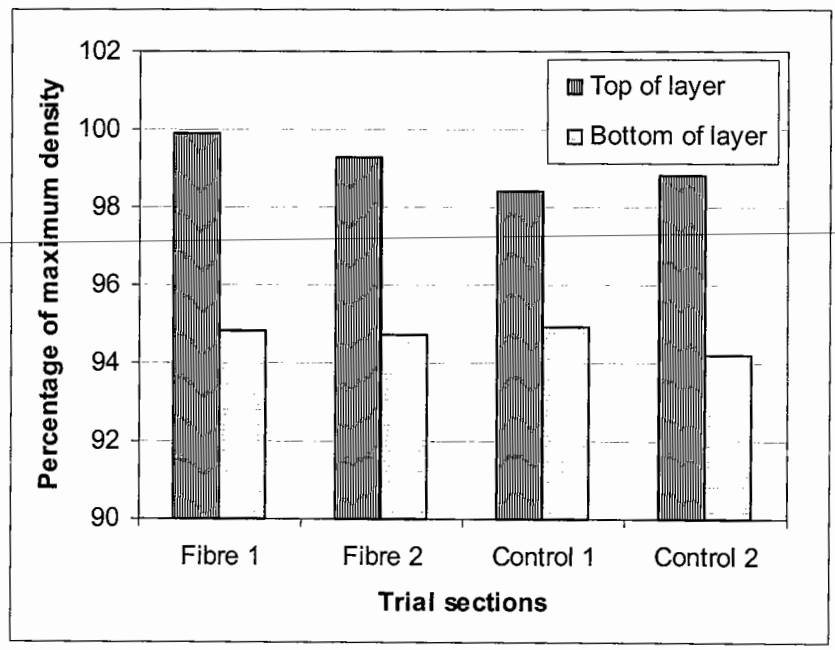

Figure 2-7 Variability in density at depths of 90mm (top) and 175mm(bottom) of a 200mm deep layer of roller compacted concrete (*based on data by Nanni 1989*).

This reduction in density and strength with depth presents a dilemma. Often the cementitious material thickness must be increased to reduce the stresses at the bottom of the layer. This in turn increases the risk of under-compaction in the bottom half of the layer, thus reducing the strength where it is most needed. Paradoxically, a reduced CBM thickness may in fact result in a pavement more able to carry load, provided a higher density can be achieved.

As failure of the CBM layer has high cost implications, the accurate determination of all material properties will reduce the risk of failure and help understanding of the inter-relationship between the various parameters. In flexible composite pavements with thin asphalt overlays, the critical stress on the CBM will be greater than pavements with deeper overlays. This loss of 'protection' where thin overlays are used make the accurate design of the base more crucial, as the stresses close to transverse cracks will be increased, and indeed its susceptibility to dynamic failure might well also increase.

2.3.2 Transverse cracks

Cracking occurs in the transverse direction shortly after laying, and occurs when restrained and warping stresses exceed the strength of the material. These stresses are developed by drying shrinkage and changes in ambient temperature (Williams 1986).

Drying shrinkage occurs as a consequence of moisture movement in the CBM resulting in a net decrease in volume. The causes of this material decrease in volume are twofold: hydration of the cement; and the loss of water through evaporation at the surface and suction from the base. Drying shrinkage cracking is increased at higher water/cement ratios and higher cement contents (Williams 1986). The cement content in CBM is traditionally low, although there has been a tendency towards higher strength mixes in recent years. The loss of water from the surface of a CBM is influenced by the wind velocity, ambient temperature and relative humidity. Drying shrinkage cracking can be eliminated by completely sealing the surface after casting and in itself is therefore generally not significant.

Thermal shrinkage occurs due to a drop in the ambient temperature, and in the main is attributable to the thermal properties of the aggregate (Shahid 1997). The ambient temperature drop (ΔT) to cause fracture is approximated in Eqn...2-2. Thermal coefficients of aggregate (α) generally range between 6 x10^{-6} and 12x10^{-6} per °C.

$$\Delta T = \frac{\sigma_t}{E}.\frac{1}{\alpha} \qquad \textbf{Eqn...2-2}$$

Assuming a CBM using a gravel aggregate (α=11.4x10^{-6} per °C) of stiffness (E) 20000MPa and tensile strength (σ_t) of 0.5MPa, then the temperature drop necessary to cause cracking through thermal shrinkage is only 2.2°C. For a carboniferous limestone (α=7.3x10^{-6} per °C) the temperature drop is 3.4°C. Such temperature changes often occur on a daily basis in most parts of Europe and North America. During the first few hours after laying, the material strength is at its lowest, and consequently CBM will invariably crack.

Given cracking is inevitable, crack width is of interest as this will be shown to influence significantly the load transfer, and therefore the stresses on the CBM close to a crack. Huang (1993) presented a relationship for the crack opening (w), developed by Darter and Barenberg (1977), which required knowledge of the subgrade friction (C), distance between cracks (L'), drying shrinkage coefficient (ε), α and ΔT (Eqn...2-3). The parameter C is an adjustment factor due to friction between the slab and sub-base. Darter and Barenberg (1977) recommended subgrade friction values (C) of 0.65 for a CBM sub-base and 0.8 for an unbound granular aggregate. ε is approximately 5x10^{-4} (Huang 1993).

$$w = L'.C.(\varepsilon + \alpha.\Delta T) \qquad \textbf{Eqn...2-3}$$

For a CBM that cracks naturally, at say 9m spacing over a temperature change of 10°C, and using the parameters described above, a gravel aggregate results in a crack opening of 1mm on a granular sub-base. For the same material, at induced crack spacing of 3m, the

crack opening is a third of this. Crack openings are lower if the slab is laid on a CBM sub-base, or if an aggregate with a lower coefficient of thermal expansion is used. Eqn...2-3 is therefore useful as it provides an indication of comparable crack widths under various temperature changes, sub-base material, crack spacing and aggregate types.

2.3.3 Cracking caused by warping

A consequence of drying shrinkage can be the propagation of cracks due to warping, caused by differential shrinkage (Neville 1995). The loss of moisture from the surface results in a moisture gradient with the depth of concrete section. The surface moves relative to the base, but is retrained by the underlying layer and the mass of the concrete. This can be of sufficient magnitude to crack the matrix whilst the material is gaining strength.

Warping poses more of a problem when the stresses are combined with traffic. Tensile stresses occur at the base of the slab, and at certain times in the day, are additive to the traffic stresses. Westergaard (1927) calculated these stresses to be of the same order as traffic stresses (up to approximately 2MPa). Thomlinson (1940) argued the stresses were in fact much lower and demonstrated this assuming a theoretical sinusoidal variation of surface temperature and research at the TRL confirmed the lower values are more in line with what is observed in practice (Lister 1972). The stresses would be further reduced by the presence of the asphalt overlay, which would insulate the layer, reducing the temperature difference as shown by Figure 2-8. The study by Lister also showed that the depth of cover was more important than the type of asphalt. However, the cracking in the CBM roadbase would not be a concern if it were not for the propagation of cracks through the overlay.

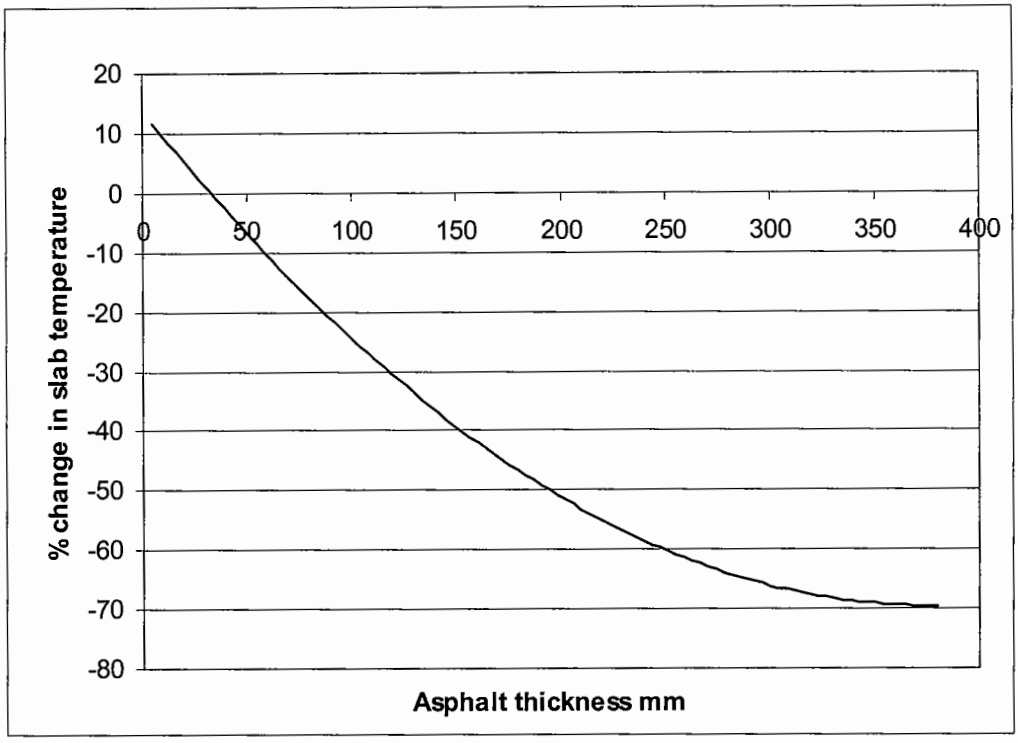

Figure 2-8 Relation between temperature difference through a concrete slab and its thickness of cover (*Lister 1972*)

2.3.4 Reflective cracking

Reflective cracking is the term given to the propagation of a crack, which has originated in the lower pavement layers, through the asphalt surfacing. In a flexible composite pavement, the source of reflective cracking is most usually from transverse shrinkage cracks in the CBM. Whilst the reflected crack is not itself a failure, the ingress of water can result in a softening of the lower layers, accelerating deterioration of the pavement. Reflection cracking is a world-wide problem, brought on by discontinuities within the pavement, though in part resulting from inadequate overlay design. Due to the relatively high cost of bitumen, various solutions have been investigated to limit the occurrences of reflective cracking without resorting to deep asphalt overlays. These include induced cracking, as previously presented, and the use of geotextiles and stress absorbing membrane interfaces (SAMI).

Nunn (1990) carried out a study of the causes of reflective cracking in flexible composite pavements. Nunn reviewed three mechanisms of reflective cracking, shown in Figure 2-9. Thermally induced cracks are caused by daily and annual temperature variations, expanding and contracting the CBM between transverse cracks. Assuming the asphalt is well bonded to the CBM, large strains would be imposed on the asphalt overlay in the vicinity of the crack, resulting in a crack in the bottom of the asphalt after a period of time. Traffic induced cracks were considered to occur when little load transfer existed across the transverse crack. Under the action of traffic, large vertical movements could be generated, causing cracking at the bottom or top of the asphalt layer. Warping induced cracks occur due to the temperature gradient through the depth of the CBM base. During the evening, when the top of the CBM is cooling at a faster rate than the bottom of the CBM, the edges of the transverse cracks would tend to lift. This would impart a tensile strain at the top of the asphalt, causing surface initiated cracking.

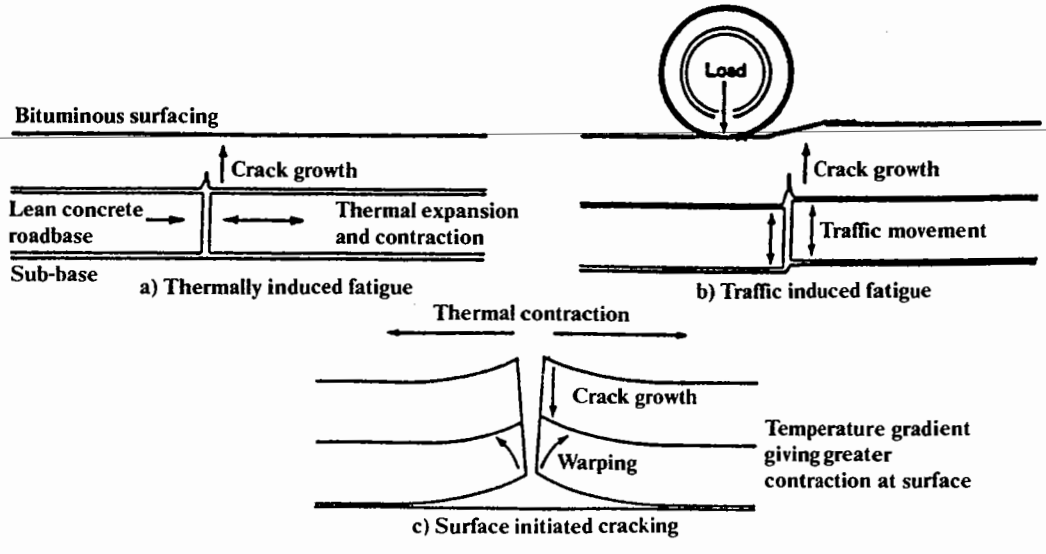

Figure 2-9 Mechanisms of reflective cracking in flexible composite pavements (*Nunn 1990*)

Nunn (1990) described theoretical modelling by Foulkes (1986 and 1988), who claimed that warping stress, in combination with increased strain due to contraction of the CBM, was the most likely cause of reflective cracking. This would result in surface initiated cracks; such cracks have been shown to occur in trial sections of pavement investigated by Nunn. Even in areas where trafficking had not occurred, surface cracks were proven to occur in cores taken from the site. The consequences of warping strains were shown to be most onerous in asphalts of low yield strain and penetration, due to the material being brittle. This being the case, an increase in the ductility of the asphalt might limit reflection cracking, but is likely to contribute to increased rutting, particularly in deeper asphalt sections.

Nunn's work provides useful evidence as to the causes of reflective cracking in flexible composite pavements. It is apparent that the severity of the three modes of reflection cracking considered is all related in some way to the crack width in the CBM roadbase. It follows that an improvement in the characteristics of the crack will limit the effects of reflection cracking. Such crack characteristics have generally been measured in terms of load transfer.

2.4 Load transfer at transverse cracks

Few studies have been conducted on the load transfer of CBM, though extensive research has been carried out on transverse shrinkage cracks in jointed reinforced and unreinforced concrete pavements in the United States. A notable exception to this is an extensive study by Pittman (1993) into the load transfer of roller compacted concretes at various formed joints. The loss of aggregate interlock across cracks is reported to have resulted in increased slab deflections, infiltration of water, pumping and spalling. Continued pumping can eventually lead to loss of support beneath the slab and can result in fatigue cracking (Raja and Snyder 1991). An additional effect requiring consideration in flexible composite pavements is the consequence of increased slab deflections on the asphalt surfacing, a cause of reflective cracking. The load transfer characteristics of a CBM are therefore of great importance to understanding the stresses in the CBM, and the imposed strains in the asphalt.

2.4.1 Load transfer efficiency

Load transfer is commonly quantified in terms of load transfer efficiency (*LTE*). This is often derived from deflection measurements on laboratory test slabs, or *in situ* using, for example, a Falling Weight Deflectometer (FWD). *LTE* is most commonly determined from deflection measurements on account of the relative ease of measuring deflection rather than stress. Different researchers have defined deflection *LTE* in different ways. In carrying out FWD measurements in the field, Ellis *et al.* (1997) used the ratio between the deflections on the unloaded side of the crack (δ_{UL}) and the loaded side of the crack (δ_L), expressed as a percentage (Eqn...2-4):

$$LTE = \frac{\delta_{UL}}{\delta_L}.100 \qquad \textbf{Eqn...2-4}$$

In laboratory studies, Colley and Humphrey (1967) used the expression shown in Eqn...2-5:

$$LTE = \frac{2.\delta_{UL}}{\delta_L + \delta_{UL}}.100 \qquad \textbf{Eqn...2-5}$$

Less commonly, *LTE* is computed on the basis of stress. Pittman (1993) demonstrated that the relationship between *LTE* based on deflections (using Eqn...2.4) and *LTE* based on stress is not linear, and is dependent on the loaded contact area (a) and the radius of relative stiffness (l), which was previously defined in Eqn...2-1 (Figure 2-10).

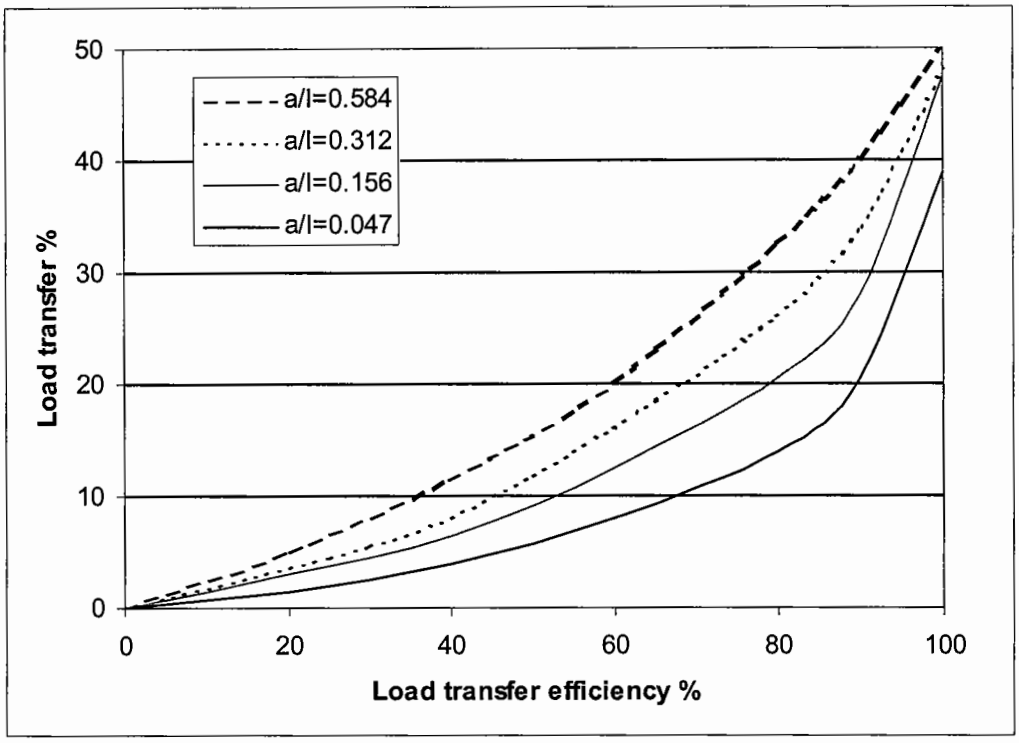

Figure 2-10 Relationships between load transfer efficiency obtained using stress and deflection measurements (*Pittman 1993*)

LTE is of practical use in that it is a measure of the behaviour of the pavement under an applied load, which can be used to indirectly compare stresses in the CBM and strains in the asphalt. Figure 2-11 illustrates theoretical longitudinal profiles of a pavement base with no cracks, and with cracks with a high *LTE* and low *LTE*, produced assuming a load close to a transverse crack using the finite element programme ILLISLAB95 (referred to in Chapter 6). It is apparent that as soon as a crack forms, the bending profile of the pavement results in a sharp tip. When the *LTE* is high, the loaded and unloaded sides of the crack deflect by the same amount, demonstrating all the imposed load is transferred across the crack. Even at a high *LTE*, the bending profile is causing additional stress to be imparted onto the base, and would add strain to the overlying asphalt at the tip. When the *LTE* is low, little load is transferred across the crack, causing an increase in the deflection of the loaded side of the crack. The base is then put under additional stress, and the strain in the asphalt will be greatly increased at the 'step'. As little load is transferred across the crack, the underlying layer must carry the load that is not transferred. It can therefore be concluded that any cracking is undesirable, but given cracks do occur, an improvement in the load transfer across the crack will have benefits to the sub-base, base and the surface.

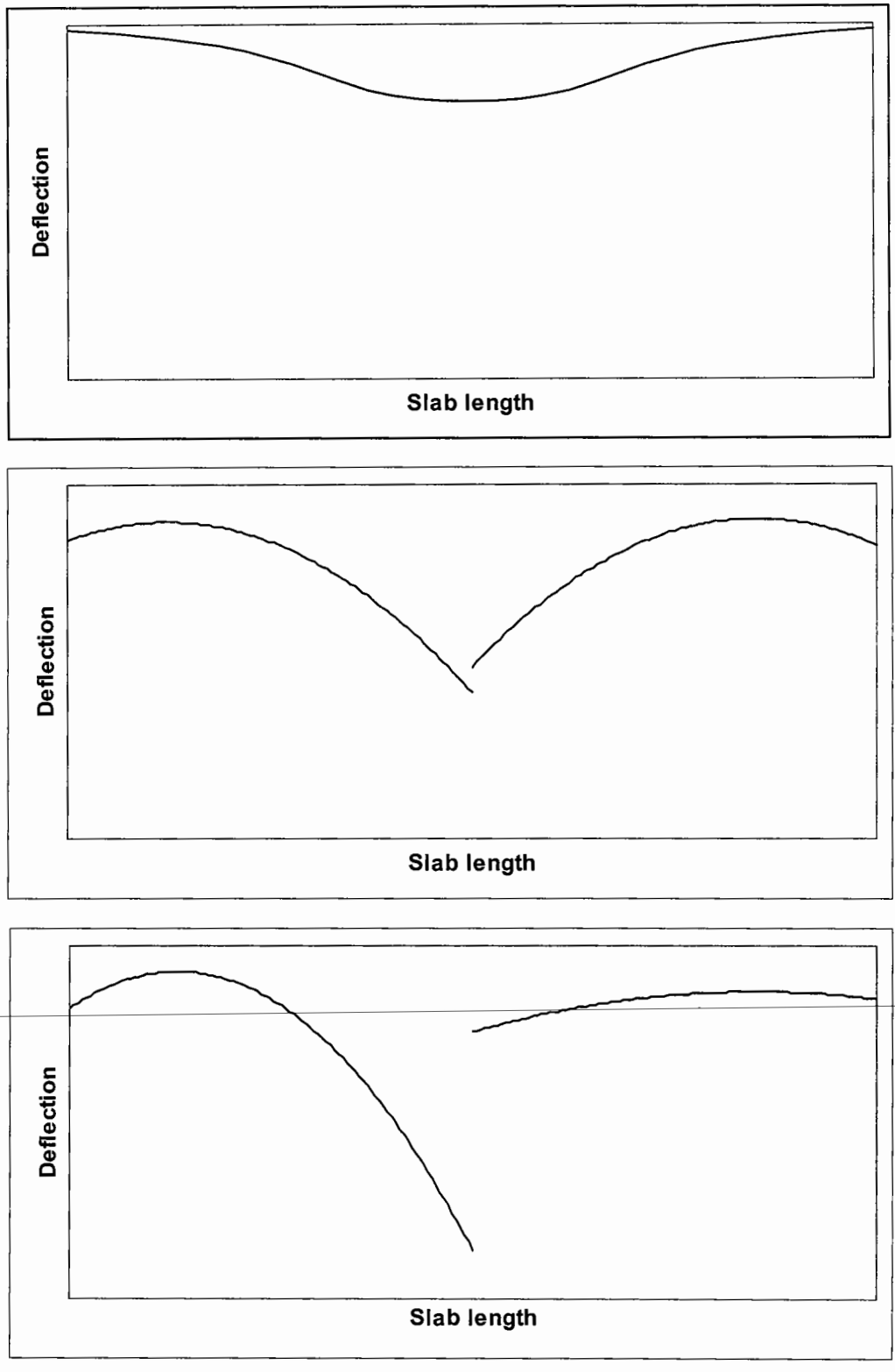

Figure 2-11 Longitudinal deflection profile in an uncracked pavement, and a cracked pavement with a high *LTE* and low *LTE*

2.4.2 Aggregate interlock

Load transfer across a cracked CBM must occur by aggregate interlock only, and therefore to increase *LTE*, it follows that this property should be understood.

The load transfer through aggregate interlock is dependent on crack width, aggregate type, aggregate size, paste-aggregate bond strength, compressive strength, aggregate hardness (resistance to abrasion), magnitude of applied load, number of load repetitions and foundation support (Buch 1994). The transfer of load is brought about by the protruding aggregate from one face of the crack coming in contact with the other face.

Two aggregate interlock models have been widely discussed (Raja and Snyder 1991, Buch 1994, Millard and Johnson 1984). The local and global roughness model postulates that local roughness (micro-texture) causes interlocking of the fine aggregate particles, which is principally a bearing or crushing action. Global roughness (macro-texture) causes interlocking of coarser aggregate particles, principally a sliding and overriding action (Figure 2-12).

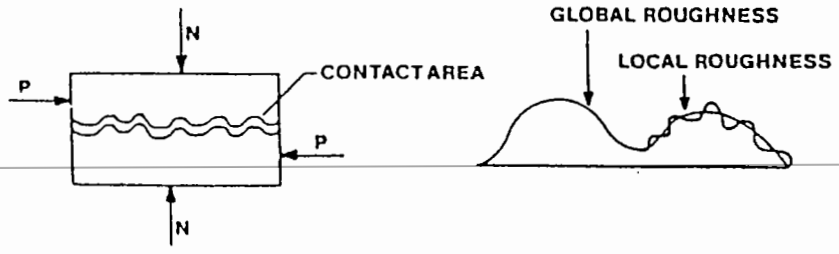

Figure 2-12 Local and global roughness model (*Buch 1994*)

Local roughness is believed to be responsible for most aggregate interlock effects when crack widths are less than 0.25mm. It is considered that the local roughness also provides the interlock mechanism during the early load cycles, and the global roughness provides the interlock later when the local roughness has been eroded.

An alternative model suggests that concrete is a two-phase material of aggregate and cement, that can be modelled as a distribution of rigid spheres within a deformable rigid-plastic matrix (Figure 2-13). Shear forces are resisted by a combination of crushing and sliding of the rigid spheres into and over the softer cement matrix. Millard and Johnson (1984) devised a test to investigate aggregate interlock, and concluded the two-phase model was the most realistic.

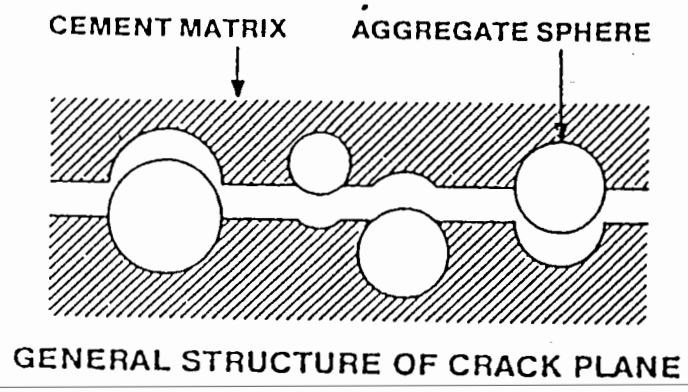

Figure 2-13 Two phase model (*Buch 1994*)

Buch (1994) reported that the load-slip relationship during the later cycles was non-linear. This was explained by an increase in aggregate contact increasing resistance, resulting in an upward curving load-slip relationship. This was demonstrated by results obtained in cyclic shear carried out by Abdel-maksoud *et al.* (1997), a load-deflection output from which is shown in Figure 2-14.

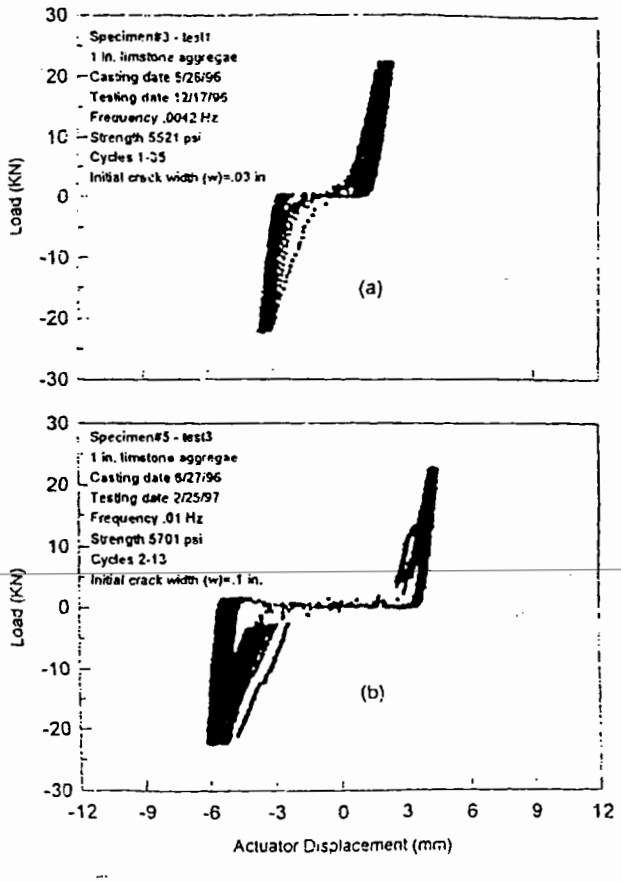

Figure 2-14 Load-deflection output obtained from dynamic shear tests carried out by *Abdel-maksoud et al. (1997).*

2.4.3 Shear stress

Under an applied load, shear resistance created through particle contact determines the portion of the load being transferred. Substantial shear forces are transmitted through this mechanism if the cracks remain tight (Raja and Snyder 1991). Buch (1994) presented theoretical relationships between non-dimensional shear stress (Eqn...2-4) and the ratio of the aggregate interlock factor (*AIF*) – a parameter used to describe crack effectiveness (Tabatabaie and Barenberg 1978) - to *kl*. This ratio had previously been adopted by Ioannides and Korovesis (1990) to relate load transfer efficiency to aggregate interlock, and is presented in Section 2.4.5. These showed that as the *AIF* increased, for given pavement thickness (*D*), material properties and load (*F*), the shear stress increased (τ) (Figure 2-15). With all other parameters constant, an increase in the modulus of subgrade reaction (*k*) decreases the shear stress.

$$\textit{Non-dimensional shear stress} = \frac{\tau D^2}{F} \qquad \textbf{Eqn...2-6}$$

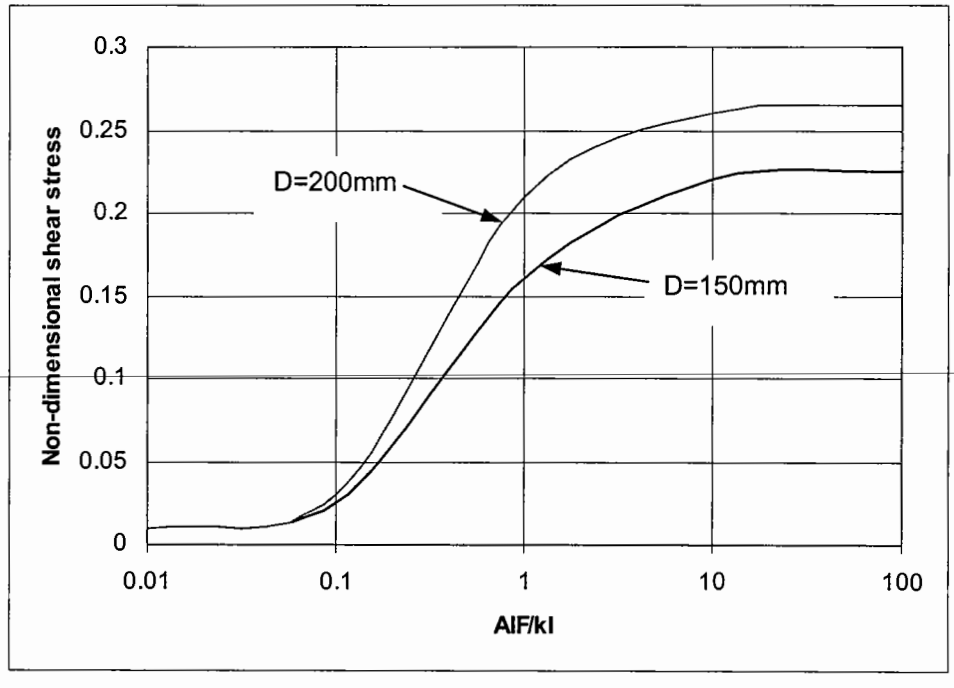

Figure 2-15 Relationship between non-dimensional shear stress and *AIF/kl for k=0.16N/mm³*

Based on a standard wheel load of *F*=40kN, and when *D*=150mm and *k*=0.16N/mm³, the shear stress can be calculated as ranging between approximately 20kPa and 220kPa.

2.4.4 Durability of cracks

Being a ratio, *LTE* only tells us the relative vertical movement of the loaded and unloaded sides of a crack. It says nothing of the total vertical deflection. This too is an important consideration in the development of stresses and strains at critical positions within the pavement layers. Even at an *LTE* of 100%, a base with a low stiffness will allow the pavement to deflect a large amount. Larger deflections can increase the rate of deterioration of the crack. Colley and Humphrey (1967) studied the effects of load magnitude, crack width, pavement depth and sub-base type on the deterioration of cracks on large scale slabs in the laboratory. They demonstrated the importance of joint opening in achieving effective aggregate interlock and a high *LTE* (Figure 2-16).

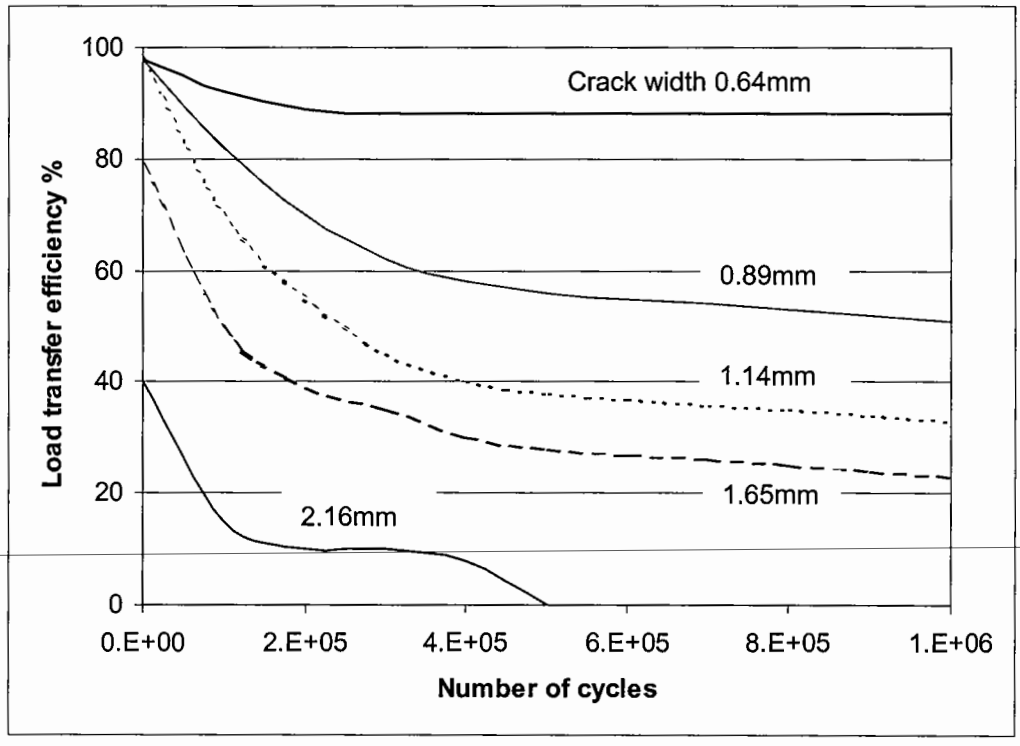

Figure 2-16 Influence of joint opening on load transfer efficiency, 225mm concrete slab, 150mm gravel sub-base (*Colley and Humphrey 1967*)

To take account of the crack width, sub-base restraint and magnitude of load, Colley and Humphrey introduced the endurance index as a descriptor of the long term performance of cracks. This was defined as the ratio of the area under the curve of *LTE* (using Eqn...2-5)

verses the number of repetitions (N) to the corresponding area under the curve by setting the *LTE* at 100% for 1 million cycles. It was found that the sub-base modulus had a significant affect on the endurance index (Figure 2-17). Even at identical *LTE*, a strengthened sub-base results in a more durable crack as the total vertical movement is reduced, decreasing the rate of deterioration. Similarly, an increase in load causes more movement at the crack, and increases the rate of crack deterioration.

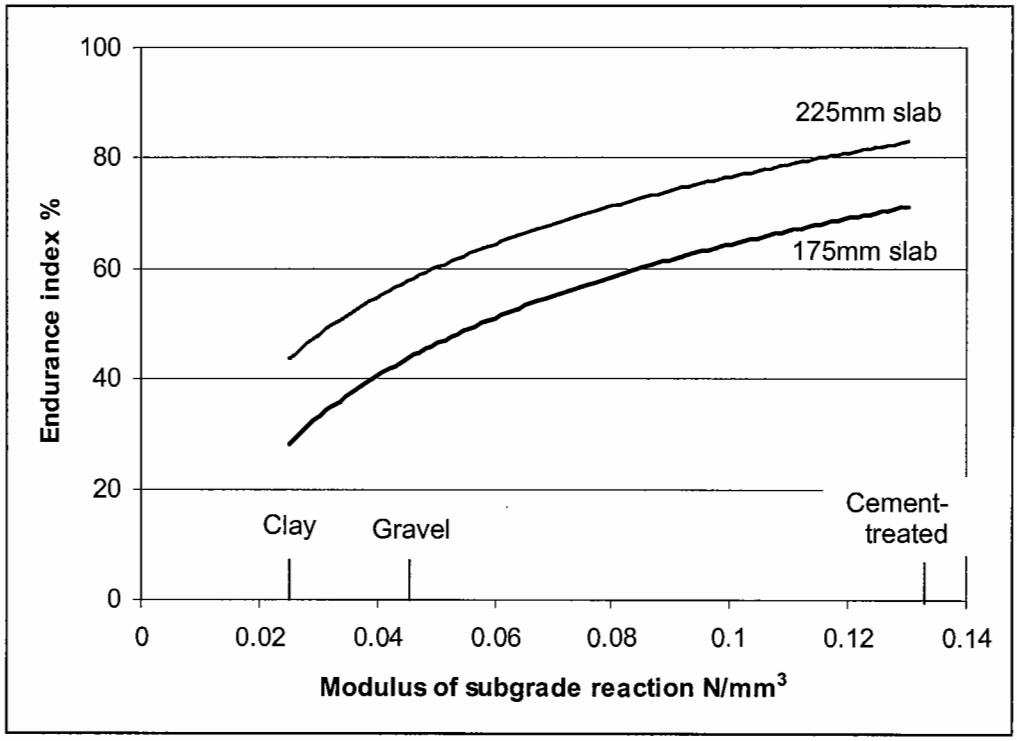

Figure 2-17 Effect of foundation strength on endurance index (*Colley and Humphrey 1967*)

Based on these data, Colley and Humphrey (1967) showed that an increase in depth and sub-base restraint, and decrease in the crack width, increases the endurance of a crack.

Abdel-maksoud (2000) carried out a comprehensive literature review into the effect of aggregate size and strength and material strength for the load transfer of concrete joints. From the conclusions, it was shown that:

- Aggregate size has a significant affect on load transfer, with larger aggregate particles performing better than smaller ones
- Material strength had little affect on load transfer

2.4.5 Theoretical analysis of load transfer

Ioannides and Korovesis (1990) demonstrated a relationship between *LTE* and the spring constant used in ILLISLAB95 to transfer load in shear (Figure 2-18). In doing so, they defined a non-dimensional joint stiffness, by dividing the aggregate interlock factor (*AIF*) by the subgrade modulus (k) and radius of relative stiffness (l). Ioannides and Korovesis conceded that the choice of parameters in the dimensionless parameter for joint stiffness were a combination of engineering judgement, imagination and experience. Nonetheless, a range of independent laboratory and field results and dimensional analysis has confirmed the validity of the relationship.

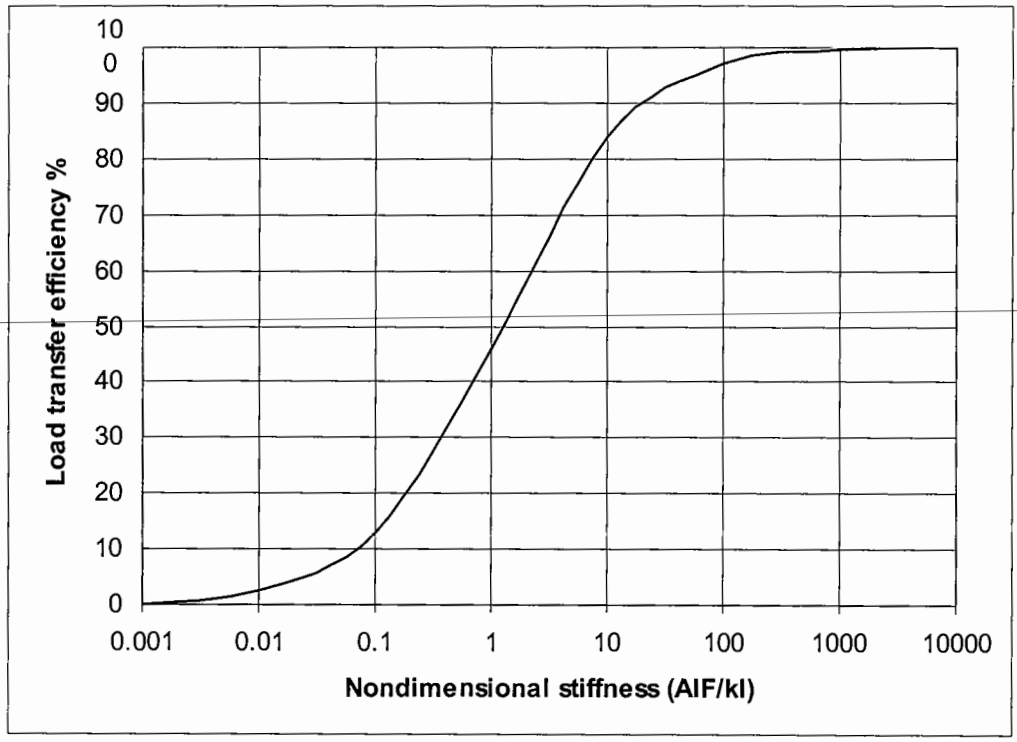

Figure 2-18 Load transfer efficiency as a function of dimensionless joint stiffness (*Ioannides and Korovesis 1990*)

The relationship demonstrates that *LTE* is a function of the subgrade properties, and a higher subgrade modulus would result in a lower *LTE* for a given joint stiffness. This is of interest as *LTE* can be readily obtained on site using an FWD. It is clear that interpretation of *LTE* should not be carried out without knowledge of the sub-base properties. Perhaps more importantly, the relationship allows FWD results to be back-analysed to determine a field measure of the spring stiffness. Such an analysis was carried out using *LTE* data reported by Ellis *et al.* 1997 (Table 2-2). These data are of interest as the study by Ellis compared naturally cracked CBM and induced cracking. The results demonstrated a visual difference between natural and induced cracking.

	[1]Test section	[1]CBM depth (D) mm	[2]Modulus subgrade reaction (k) N/mm³	Radius of relative stiffness (l) mm	*LTE* %	$\frac{AIF}{kl}$	AIF MPa	AIF MPa [3](95%)	[1,4]Observed crack width
Natural crack	1	205	0.08	612	80.5	6	294		-
	6	145	0.08	472	62.6	3	113	217	wide
	8	183	0.08	562	77.8	6.5	292	(89)	wide
	11	158	0.16	423	60.3	2.5	169		wide
Induced cracks at 3m	2	210	0.08	623	88.6	16	798		n. v
	3	186	0.08	569	89.3	18	819		v. fine
	4	205	0.08	612	93.4	50	2448		-
	5	165	0.08	520	84.0	11	458	982	med.-wide
	7	201	0.08	603	91.0	25	1206	(447)	v. fine
	9	141	0.16	389	82.1	10	622		med.
	10	163	0.16	433	78.8	7	485		fine-wide
	12	161	0.08	511	91.2	25	1021		fine-wide

Notes: [1]after Ellis *et al.* (1997), [2]estimated, [3]95% confidence, [4]n.v – not visible, v. – very, med. –medium.

Table 2-2 Back-analysed values of *AIF* from FWD tests

In situ AIF were found to be in the range of 217 ± 89MPa at 95% confidence for a natural crack. Induced cracks on CBM were in the range of 982 ± 447MPa. There was therefore statistically a significant difference between induced and naturally cracked pavements. Also, the crack stiffness values appear to correlate with the observed crack widths; cracks with a low *AIF* were generally found to be wide, whereas cracks with a high *AIF* were generally found to be narrow.

Back-analysed FWD data may therefore be used to determine the *AIF*, independent of the subgrade properties that effect the *LTE*.

2.5 Fibre reinforced cement bound material

So in what way might steel fibre reinforcement benefit a CBM? This may be considered in terms of the main modes of deterioration of a CBM, which are traffic and temperature induced cracking of the CBM layer, and reflective cracking through the asphalt overlay, caused by inadequate load transfer at transverse shrinkage cracks and/or insufficient thickness of asphalt overlay.

Steel fibres may improve the fatigue characteristics of the material, and in the event of cracking, provide a mechanism to maintain narrow cracks. The 'tying' together of the CBM in this way will ensure the pavement has a high residual effective stiffness, thus maintaining protection to the lower layers. Indeed, the current Highways Agency design for a flexible composite design of 'determinate' life accepts the CBM will deteriorate, with a view to strengthening the pavement once serviceability limits have been reached. FRCBM, in such an instance, might require significantly less strengthening than CBM, reducing the whole life cost of the material. The load carrying capacity of the pavement post-crack will be a consideration in the determination of such properties.

In order to understand the potential of fibre type, fibre volume fraction and matrix strength on CBM, it is necessary to review research carried out on steel fibre reinforced concrete (SFRC).

Chapter 3. Fibre reinforced cementitious materials

3.1 Introduction

Fibres have been added to cementitious materials for many years, with the intention of improving the ductility of an otherwise brittle material. Concrete is known to be relatively weak in tension when compared to compression, and the resulting failure may occur with little warning. The primary reason for reinforcing concrete with fibres is to redistribute the stresses as the material cracks, providing a mechanism for a more controlled failure.

Attempts have more recently been made to determine the improvement in the fatigue characteristics of steel fibre reinforced concrete (SFRC), which is of particular benefit to pavement applications.

Almost without exception research into SFRC has been carried out on structural grade concrete, as opposed to weaker cementitious mixes as traditionally used as the base layer in flexible composite pavements. However, a small number of practical studies have been carried out which aimed to determine whether fibres could be successfully mixed with plant produced cement treated materials.

This chapter describes the influence of fibre characteristics on the properties of SFRC; these being fibre type, aspect ratio, volume fraction, bond and orientation. Specific properties of SFRC relevant to pavements are discussed, along with some theoretical models that aim to predict material strength and toughness and direct measurement methods. In particular, the determination of toughness parameters is described as this property most distinguishes SFRC from the unreinforced material, and allows the influence of fibre reinforcement on the CBM properties to be evaluated. Finally, the design methodology of ground bearing slabs is described as a method to determine the ultimate bearing capacity of an FRCBM pavement.

3.2 Influence of fibre characteristics on properties of SFRC

3.2.1 Fibre types

Fibre type distinguishes between various fibres on the basis of the material they are manufactured from, and in the case of steel fibres the shape, length and diameter. Fibres are manufactured from steel, glass, synthetic materials such as nylon and polypropylene, and organic materials such as sisal. The fibre material, shape, dimensions and content effects the properties of the composite material (Bentur and Mindess 1990). High modulus, high strength fibres (steel, asbestos and carbon) produce strong composites. Low modulus, high elongation fibres (nylon, polypropylene and polyethylene) do not lead to significant strength improvements, but are capable of large energy absorption under impact (Swamy *et al.* 1974). The range of fibre properties is illustrated by Table 3-1.

Fibre	Diameter (μm)	Modulus of elasticity (GPa)	Tensile strength (MPa)	Elongation at break (%)
Steel	5-500	200	500-2000	0.5-3.5
Glass	9-15	70-80	2000-4000	2-3.5
Polypropylene	20-200	5-77	500-750	8.0
Carbon	9	230	2600	1.0
Nylon	-	4.0	900	13.0-15.0
Polyethylene	-	0.3	0.7	10
Sisal	10-50	-	800	3.0
(Cement matrix)	-	10-45	1-7	0.02

Table 3-1 Typical fibre properties (*Bentur and Mindess 1990*)

The static and dynamic tensile strength, energy absorbing characteristics, toughness and fatigue endurance of concrete reinforced with steel fibres is particularly beneficial to pavement applications (ACI Committee 544 1996). Steel fibres are further categorised for specifications, either by manufacturing process following American Standard ASTM A 820 (1995), or by fibre shape following Japanese Standard JSCE (1984). Various manufacturing methods are used, which result in a range of geometries, and allow steel fibres to be supplied collated or loose (ACI Committee 544 1996).

The fibre properties and geometries ultimately contribute to the fibre-matrix bond, affecting the mechanical properties of the cementitious composite.

3.2.2 Fibre-matrix bond

The fibre-matrix bond describes the interaction between the fibre and the cementitious matrix. This is dependent on the matrix strength, fibre type (in terms of length, diameter and shape), and fibre volume fraction.

The ratio of the length of the fibre to the diameter of the fibre is defined as the aspect ratio. For fibres with a shaped end, an effective length is measured between the extremities of the fibre rather than along the length of the fibre. Aspect ratios are generally between 40 and 80. Higher aspect ratio fibres improve the first crack strength, ultimate strength and toughness of a composite more than lower aspect ratio fibres (Swamy *et al.* 1974). However, upper limits on the aspect ratio are determined by construction practicalities. The aspect ratio influences the workability of the wet mix and the tendency of the fibres to become entangled during mixing, known as 'balling'. Workability is affected at high fibre volumes, though such problems have been largely overcome through the use of superplasticisers. Balling generally occurs on high aspect ratio fibres (ACI Committee 544 1990), and to avoid this some fibre manufacturers supply the fibres collated with a soluble glue. Therefore, for a given mix design, the aspect ratio could be optimised in terms of performance, whilst avoiding practical difficulties during the mixing process.

The effectiveness of the fibre-matrix bond is quantified by the interfacial bond strength (τ_f). Values for the interfacial bond strength are given by Bentur and Mindess (1990) to be in the range of 0.8 to 13MPa. The interfacial bond strength is a measure of the ability of the matrix to restrain the fibre, and is a function of the matrix strength. Prior to cracking, the influence of the fibres is measured in the relation of their modulus of elasticity with that of concrete. Due to the relatively minor proportion of fibres in relation to the total volume in pavement applications, this influence is minimal (Maidl 1995). The main influences of the fibres on the composite follow cracking of the matrix. The fibres provide a mechanism to transfer stresses into the uncracked part of the matrix as the applied load is increased. The effectiveness of the bond between the fibre and the matrix determines the increase in load sustainable before fibre slip takes place. In addition, as the load increases, the fibres and the matrix-fibre bond is required to withstand increasing tensile stresses.

3.2.3 Fibre shape

The pull-out behaviour of individual fibres can be measured indirectly in the laboratory using a direct tensile test. The interfacial bond strength is calculated by dividing the ultimate direct tensile load post-crack by the total fibre area bridging the cracked specimen. The test can also provide a relationship between the bond shear stress and fibre slip (Weiler and Grosse 1996). This type of test was used to demonstrate the effectiveness of fibre shape by comparing the relative influence between the hooks and straight section of shaped fibres. This was achieved by measuring the bond shear stress due to the hook (by lubricating the straight section of fibre) and then the bond shear stress of the straight section of fibre (by removing the hook). The results are shown in Figure 3-1, and indicate that hooked-ends are a significant contributor to the bond shear stress of the fibre. Furthermore, the summation of the bond due to the hooks and the straight sections approximates to the total contribution of the fibre.

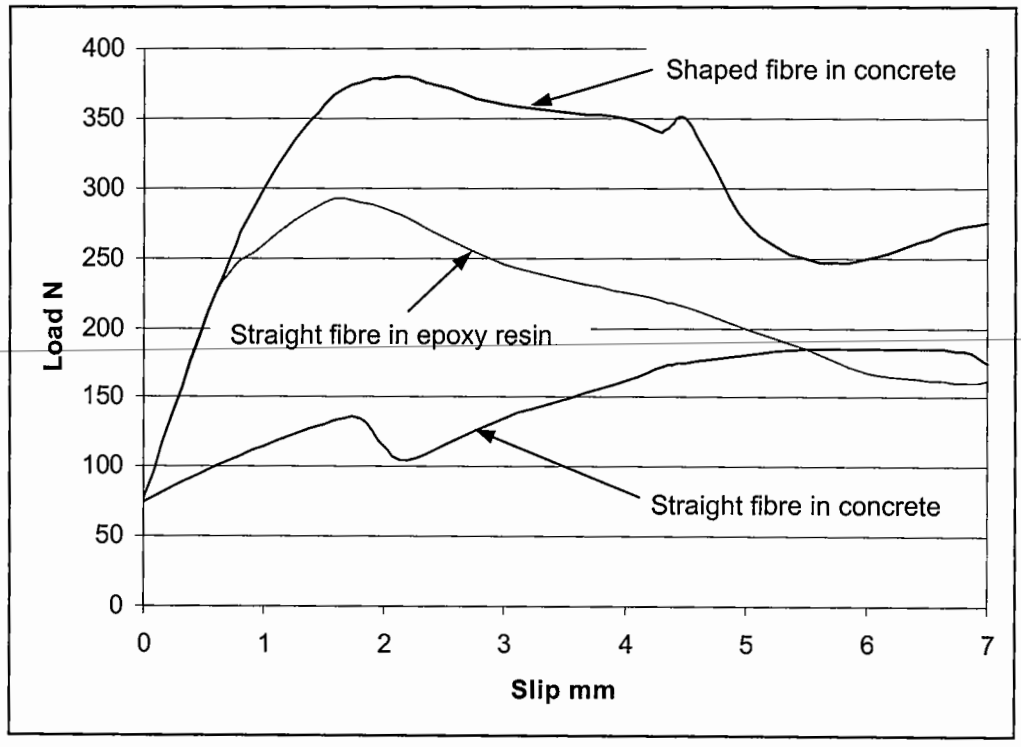

Figure 3-1 Load-slip curves of a shaped and straight fibre in concrete and a waxed shaped fibre in epoxy resin (*Weiler and Grosse 1996*)

3.2.4 Fibre length

The critical fibre length is the minimum fibre length required for a fibre to achieve its full tensile capacity. Beyond this, the fibre will fracture. Fibres less than critical will not be stressed to their full capacity, and they will pull-out of the matrix. A relationship in terms of a critical fibre length (l_{crit}) was described by Maidl (1995), by assuming the shear resistance along the fibre to be constant. As illustrated in Eqn...3-1, the critical fibre length and interfacial bond strength (τ_f) are inversely proportional, where ϕ is the fibre diameter and σ_{fu} is the tensile strength of the fibre.

$$l_{crit} = \frac{\phi \sigma_{fu}}{2\tau_f} \qquad \textbf{Eqn...3-1}$$

By using a fibre of length greater than the critical fibre length, the greatest composite strength will be achieved, though fibre fracture will result in a less ductile failure. Therefore, to maximise both ductility and strength, a fibre length just less than the critical fibre length would be most beneficial. Other aspects may limit the length of the fibre though, such as balling during distribution. Maidl (1995) illustrated the use of Eqn...3-1 with an example for a straight, round fibre, where τ_f =1.47MPa, ϕ =0.4mm and σ_{fu}=1000MPa, showing l_{crit}=136mm. This is known to be an impractical length of fibre as it would be prone to balling (ACI Committee 544 1996). To improve the fibre-matrix bond, it is therefore necessary to increase the interfacial bond strength by improving the shape of the fibre, or increasing the matrix strength. Different shaped fibres have therefore been manufactured to increase the interfacial bond strength (Figure 3-2).

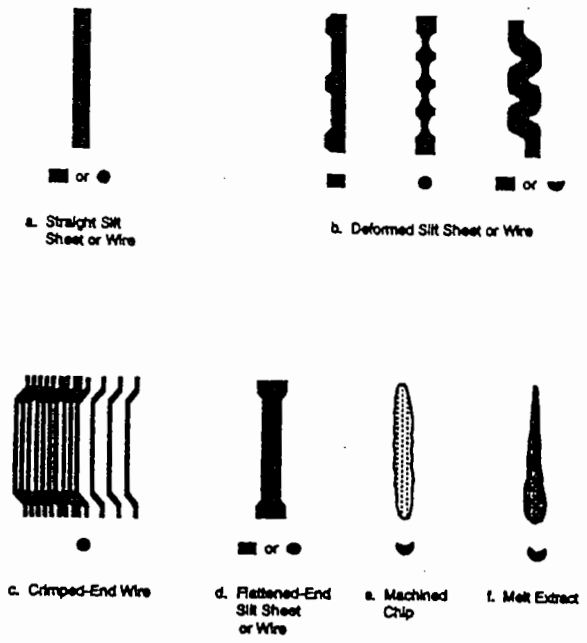

Figure 3-2 End shapes available with steel fibres (*ACI Committee 544 1996*)

3.2.5 Fibre orientation

Fibres mixed with a cementitious material would be expected to be randomly orientated, though their orientation in the set matrix may well be influenced by the method of compaction. The orientation is significant in that the fibres that are favourably aligned most effectively redistribute the tensile stresses that they are there to resist. The application of the SFRC will dictate what an ideal orientation is, whether it is a general alignment in one direction, or a random orientation.

In modelling SFRC, researchers have defined an orientation factor, η_θ, which modifies the relative influence of the fibre on the composite (Paine 1998). The orientation factor, η_θ, ranges from 1.0, for fibres aligned in the direction of stress, to less than 0.2 for a worst case. For the random, 3-dimension case where the fibre has an equal probability of orientation in any direction, an orientation factor of 0.41 has been derived, and has been used

by a number of authors (Paine 1998). In a pavement material, where it is expected that the fibres will be randomly distributed in 2-dimensions, a factor between 0.33 and 0.67 is suggested (Lanu 1996). It is expected that an alignment in two dimensions (in the plane of the layer) will provide the most effective reinforcement in a pavement. This resists stresses created in direct tension by early age shrinkage, and in bending due to warping and flexural fatigue.

Despite the expectation that fibres aligned in the direction of stress will perform most effectively, paradoxically, fibres askew to the direction of tensile stress may more effectively increase the post-cracking strength of the composite (Bentur and Mindess 1990). The explanation for this relates to the additional energy required to overcome local frictional forces at the interface of the deformed fibre as the matrix resists fibre pull-out, in what is termed 'snubbing'. Unlike the orientation factor, snubbing improves the ductility of the composite, and has a factor greater than unity. Li *et al.* (1993) applied the snubbing effect in models, assigning a value of 1.9 for stiff steel fibres.

3.2.6 Fibre volume fraction

Fibre volume fraction (V_f) is the quantity of fibres used in a mix, and is usually expressed in terms of a percentage by volume. A mix quantity of 80kg/m³ equates to a fibre volume fraction of approximately 1.0%. As the fibre volume fraction is increased, the post-cracking ductility of SFRC is improved (ACI Committee 544 1996). The post-crack behaviour is also dependent on the fibre type and matrix strength, therefore the fibre volume fraction should not be considered in isolation. If the fibre volume fraction is sufficient for a given matrix strength and fibre type, an increase in load following first crack would be expected. The fibre volume fraction at which this first occurs is known as the critical fibre volume ($V_{f,crit}$). Additionally, $V_{f,crit}$ also indicates the onset of multiple cracking (Mangat and Gurusamy 1987). This would result in a tensile specimen (without a neck) failing at a number of points along its length. The maximum load is reached once the fibres start pulling-out of the matrix or yield. At significantly lower fibre volume fractions than $V_{f,crit}$, the composite is unable to carry load following first crack.

At fibre volume fractions between the limits described above, the load-bearing capacity of the composite reduces after matrix cracking, but the fibres sustain a certain

proportion of the transferred stress. No increase in composite strength is observed over the first crack strength, but the failure is ductile due to the fibres pulling-out of the matrix.

However, in flexure an increase in ultimate strength over first crack strength may occur at fibre volume fractions less than $V_{f,crit}$. The fibre volume fraction when this first occurs is defined as the critical fibre volume fraction in flexure ($V_{f,crit,fl}$). In concrete, these are related by (Lanu 1995):

$$V_{f,crit,fl} = 0.41 V_{f,crit} \qquad \textbf{Eqn...3-2}$$

The behaviour of SFRC in terms of the above mechanism is dependent on many attributes, not least the modulus of elasticity and strength of the fibres and matrix, fibre volume fraction, fibre-matrix bond and fibre orientation. The fibre-matrix bond is in turn dependent on the matrix strength, fibre type and fibre dimensions. Therefore, in understanding the behaviour of SFRC, the interaction of the concrete mix, fibre type and fibre volume fraction should be considered.

3.3 Properties of SFRC

3.3.1 Static tension

The distinguishing properties of SFRC over unreinforced concrete can readily be demonstrated using a load-deflection plot from a tensile test. The ascending portion of the graph is identical to unreinforced concrete, such that there exists a section of proportionality, generally assumed to be elastic. In an unreinforced concrete, failure would be expected to occur at or shortly after the limit of proportionality, generally defined as the first crack. An SFRC would continue to deflect, indicating an increase in pseudo-ductility of the composite. Whilst the pre-cracking strength is almost wholly dependent on the matrix properties, the post-cracking behaviour is governed by the fibre type, fibre volume fraction and matrix strength.

The tensile properties of SFRC are measured directly using the direct tensile test, or indirectly using the indirect tensile (cylinder-splitting) test and the flexural test. Toughness, which is the parameter that most distinguishes SFRC from unreinforced concrete (ACI Committee 544 1996), is a measure of the energy required to fracture a specimen. It is calculated from the area beneath a load-deformation curve from any of the tensile tests.

3.3.2 Fatigue

Fatigue is an important design parameter in concrete pavements as it is a cause of traffic induced cracks. It is characterised by the initiation of a crack within the material, which propagates until failure occurs. There is evidence to suggest that the propagation of a crack in SFRC is arrested by fibres, resulting in an improved endurance (ACI Committee 544 1996).

Experimental studies show that fibre reinforcement increases the endurance of concrete in flexure, as illustrated by typical S-N curves, comparing data from various sources using unreinforced and fibre reinforced cementitious material (Figure 3-3). The increase is dependent on the fibre type and the fibre volume fraction (ACI Committee 544 1996).

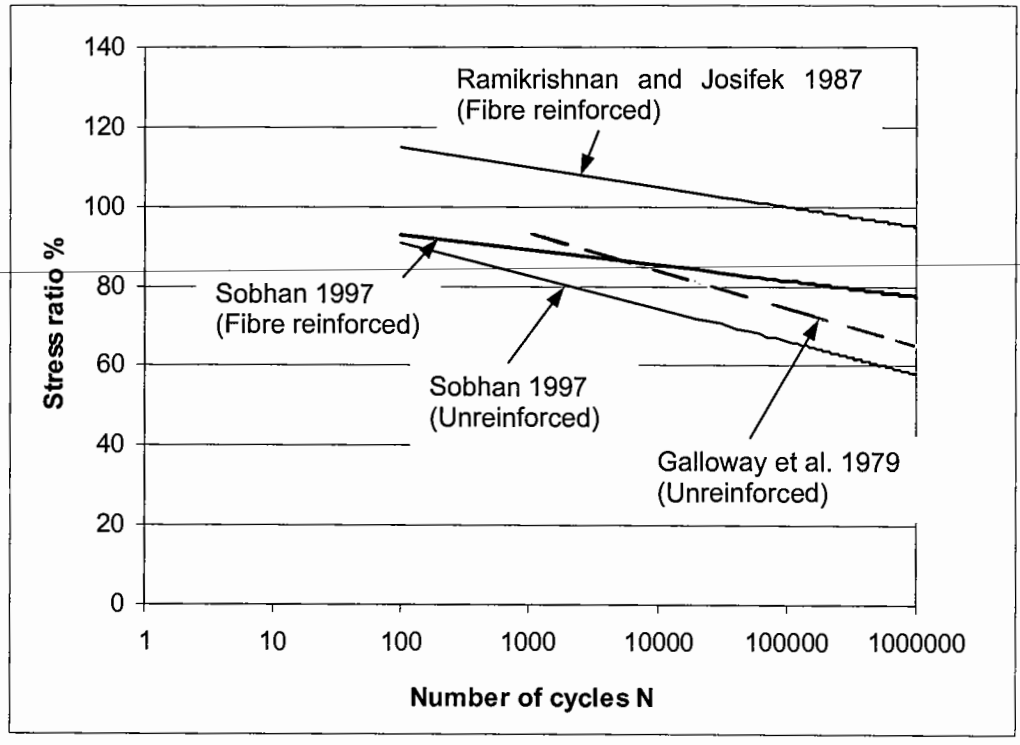

Figure 3-3 S-N curves for unreinforced and fibre reinforced cementitious material

Jun and Stang (1998) did not observe any difference in endurance between straight and hooked steel fibres. They also noted that an 'optimum' fibre volume fraction exists between 0 and 2%, over which the endurance decreases to a value comparable to plain concrete. Grzybowski and Meyer (1992) made similar observations from fatigue compression tests, and found the greatest improvement at fibre volume fractions of less than 0.5%.

Sobhan and Krizek (1999) demonstrated differences between the endurance of unreinforced and steel fibre reinforced cement stabilised material. The respective endurance relationships were used to determine relative stresses. These were equated by varying the base depth using multi-layer linear elastic analysis, and presented as a design chart so that base depths could be compared at various cumulative traffic loads (Figure 3-4).

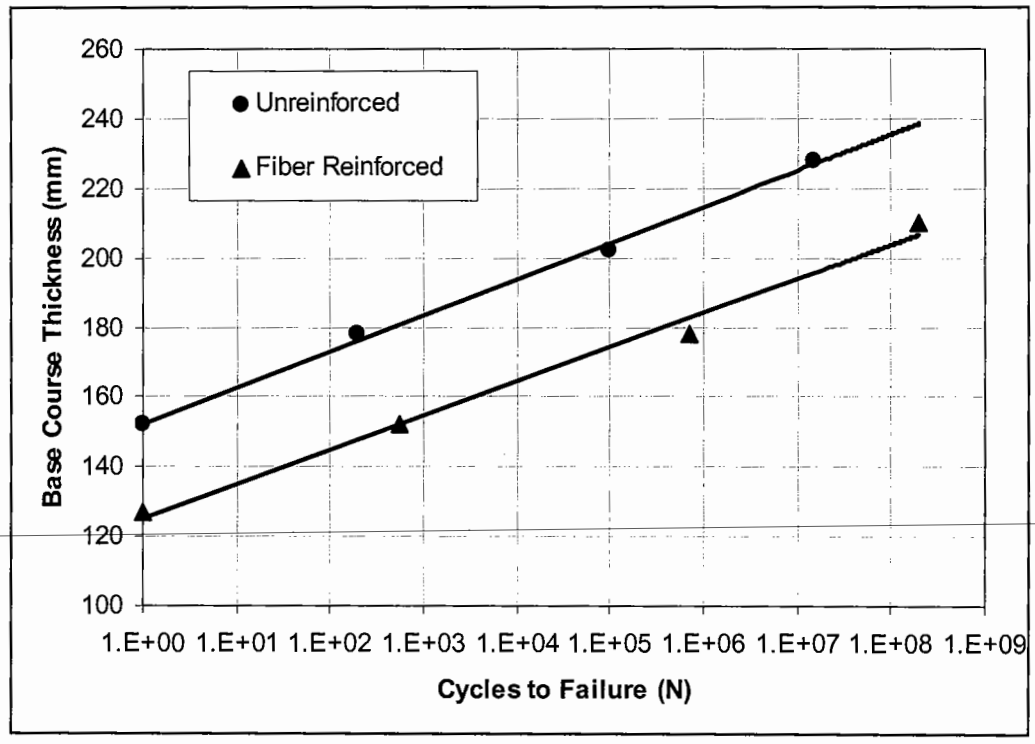

Figure 3-4 Relationship between base thickness and traffic load for an unreinforced and waste plastic fibre reinforced cement stabilised material (*Sobhan and Krizek 1999*).

Sobhan (1997) carried out fatigue tests on cement stabilised materials using steel and waste plastic fibres. He showed that during the tests the elastic deflections of the beam specimens went through three phases, expressed in terms of elastic stiffness. The initial phase saw a significant decrease in elastic stiffness; this accounted for approximately 10% of the life of the beam. Over the following 80% of the life, the stiffness remained reasonably constant, prior to rapid stiffness loss taking place during the last 10% of the life.

Sobhan (1997) demonstrated that as the dynamic tests progressed, a gradual increase in elastic deflection occurred over the life of the specimen. This may be contrasted with the behaviour of strain measurements on unreinforced concrete made by Saito and Imai (1983), who showed that the elastic strain was reasonably constant throughout the tests (Figure 3-5).

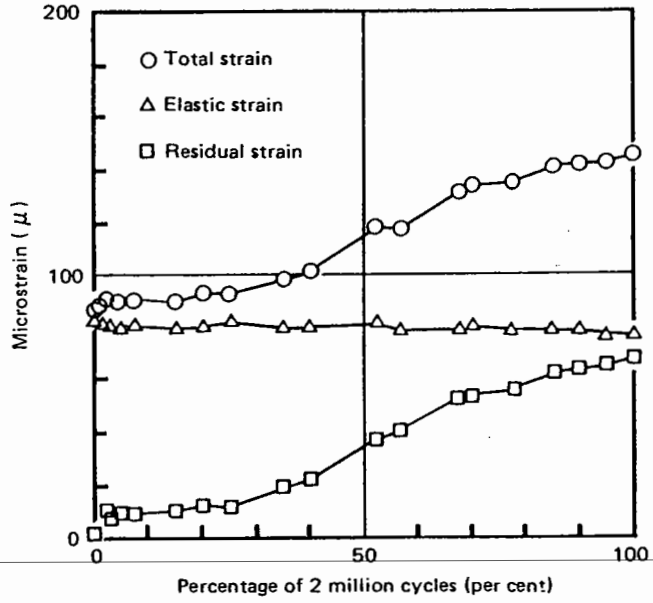

Figure 3-5 Elastic strain accumulation during fatigue tests (*Saito and Imai 1983*)

3.3.3 Shrinkage cracking

Tests show that steel fibres have little effect on free shrinkage of SFRC (Hannant 1978). However, when shrinkage is restrained, as is the case in pavement applications due to friction of with the sub-base, cracking occurs. Steel fibres provide a mechanism to transfer tensile stresses across shrinkage cracks, allowing the cracked material to maintain some residual tensile strength. The extent of shrinkage is dependent on a number of factors, including the properties of the materials, temperature and relative humidity of the environment, the age when the concrete is subject to the drying environment and the size of the concrete mass (ACI Committee 544 1996). The amount of cracking is further influenced by the degree of the restraint, fibre parameters and bond characteristics of the fibre-matrix interface (Grzybowski and Shah 1989).

Several studies were highlighted by Grzybowski and Shah (1990) as demonstrating that fibres had beneficial effects on concrete by increasing the frequency of cracking, and therefore reducing the average crack width (Figure 3-6).

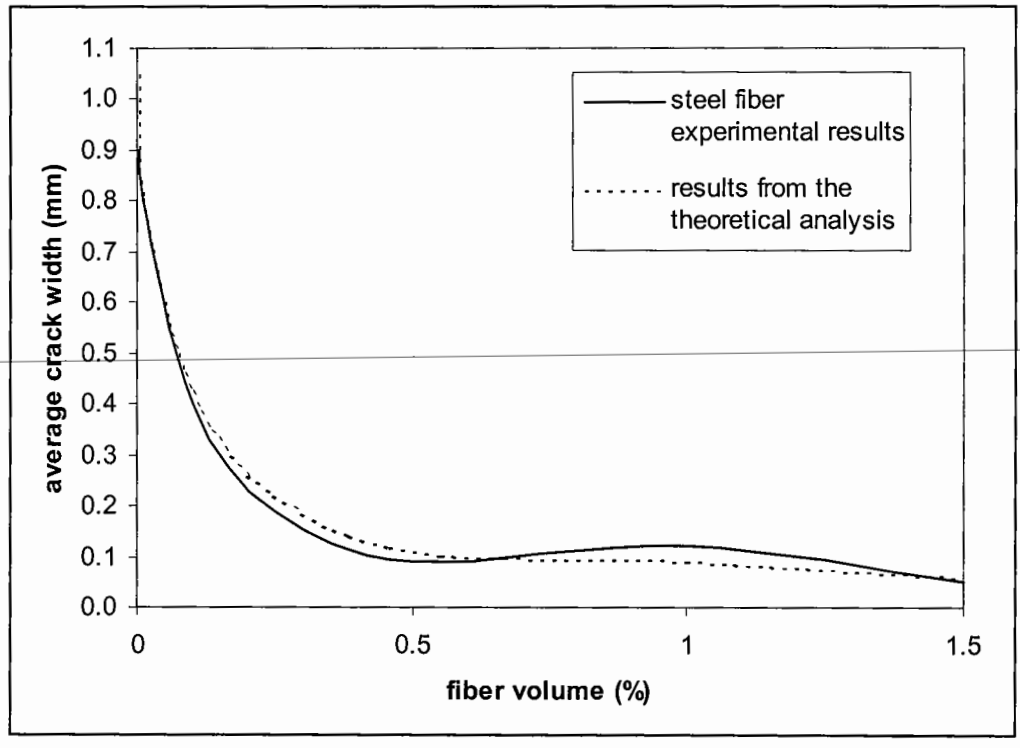

Figure 3-6 Relationship between average crack width and fibre volume fraction for a straight steel fibre under restrained shrinkage *(Grzybowski and Shah 1990)*

The researchers went on to determine a theoretical model, which took account of the time-dependent constitutive properties of concrete. The numerical analysis was compared to experimental results using a ring specimen, and demonstrated that at even low fibre volume fractions, the average crack width in an SFRC is less than a comparable unreinforced material. They also showed that the number of observed cracks were less than those indicated by strain measurements, suggesting the presence of micro-cracks.

These tests show that multiple cracking could occur in pavements even if the fibre volume fraction is significantly less than the critical fibre volume fraction. (It was described in Section 3.2.6 that for multiple cracking to occur in a laboratory test, the fibre volume fraction would have to exceed the critical fibre volume fraction). The multiple cracking in pavements is possibly due to the relationship between the fibre-matrix bond and the material bond at an early age. Multiple cracking in FRCBM could be advantageous, as it is the presence of sizeable transverse cracks that result in reflection cracking. Frequent cracks will result in more narrow crack widths, increasing load transfer and reducing the damaging strains on the asphalt overlay. Currently crack widths are controlled in practice by inducing cracks at shorter spacing than would occur naturally, and the 'assistance' of fibre reinforcement in this role would take away the need for this operation. However, this aspect was not investigated as part of this study, and considering the relatively low cost of induced cracking compared to the cost of the total construction, controlled cracking by mechanical means is recommended.

3.3.4 Durability of steel

The durability of steel fibres is a concern in pavements as it is after a period of time, when some material cracking has occurred, that the fibres will be most beneficial in increasing the bearing capacity of the cracked structure.

The durability of steel fibres is largely dependent on the corrosion protection offered by the composite. Corrosion of the fibres is generally not a problem in uncracked concrete or in cracked composites when the crack width is less than 0.1mm, or the crack depth is small (ACI Committee 544 1996). The small surface area of steel fibres means that the subsequent increase in volume, brought about by the chemical corrosive process, is insufficient to cause spalling. Furthermore, as the fibres are discontinuous, there is no conductive path to carry current to other parts of the material, therefore corrosion elsewhere is unlikely. However, corrosion occurs within the carbonation zone and surface staining can be expected.

The durability of steel fibres was not investigated as part of this project. However, given the importance of durability within a long-life structure and the relatively pervious nature of a CBM when compared to structural concrete, this aspect warrants a comprehensive study.

3.4 Theoretical determination of tensile properties

Theoretical models are required to predict the behaviour of a material without having to resort to extensive laboratory studies. For SFRC, this is necessary to allow a wide range of matrix variations in terms of composite materials, and fibre types, to enable variations to be made to the product to produce the most economically advantageous composite.

3.4.1 Direct tension

A theoretical model was proposed by Lim *et al.* (1987) to predict the behaviour of a fibre reinforced material in direct tension (Figure 3-7). In this figure, σ'_{cr} is the ultimate strength in direct tension and ε_{cr} is the corresponding strain, E_{ct} is the modulus of elasticity and ε_{tu} is the composite ultimate tensile strain.

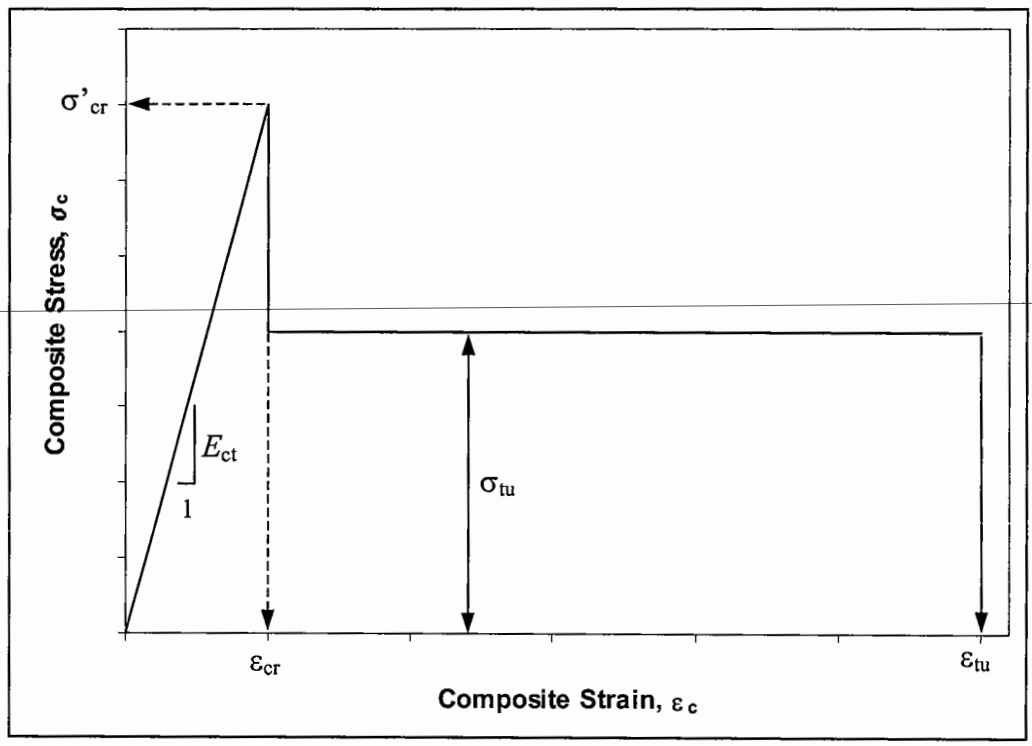

Figure 3-7 Idealised tensile stress-strain curve (Lim *et al.* 1987)

The model allows the direct tensile behaviour to be predicted without resorting to direct measurement using a test that can be difficult to perform. The composite post-cracking strength (σ_{tu}) was given as (Lim *et al.* 1987):

$$\sigma_{tu} = \eta_l \eta_0 V_f \ell_f \frac{\tau_u}{2r} \qquad \textbf{Eqn...3-3}$$

Where η_l is the snubbing factor, η_0 is the orientation factor, V_f is the fibre volume fraction, l_f is the fibre length, τ_u is the interfacial bond strength and r is the ratio of the fibre cross-sectional area to its perimeter.

3.4.2 Flexure

In flexure, fracture mechanics models and interface mechanics models are considered the most suitable for predicting the inelastic processes in fibre composites (ACI Committee 544 1996). Linear elastic fracture mechanics is used to study the effects of crack initiation, growth, arrest and stability in the presence of fibres through appropriate changes in the stress intensity factor. Such models typically assume perfect bond between the fibre and the matrix. Fictitious crack models aim to implicitly account for the inelastic interface response during crack growth, through a non-linear stress-displacement relationship for the fibre-bridging zone. This requires a singular assumption for the behaviour at the crack tip. Jenq and Shah (1986) used fracture mechanics to predict the crack propagation resistance of SFRC by considering four regimes: pre-cracking; crack growth to the beginning of fibre bridging; steady state crack growth; and resistance to cracking provided solely by the fibres. All of these models rely on the stress-crack width relationship being obtained experimentally.

Studies have also been carried out of the mechanics of the fibre-matrix interface, and these have been used to predict macroscopic stress-crack width relationships. These are based on models described as shear-lag theory, fracture mechanics interface models and numerical models (ACI Committee 544 1996). These models are useful in understanding the basic mechanics of stress transfer at the interface and showing that the interface softening and de-bonding play an important role in the fracture of such composites.

The theoretical evaluation of flexural strength of SFRC beams was first approached by Romualdi and Batson (1963), who used fracture mechanics to determine the first crack and ultimate flexural strength of the composite using the so-called 'spacing theory'. Swamy *et al.* (1974) demonstrated the inaccuracy of the expression using empirical data, and went on to produce their own expression using the 'law of mixtures'. This considers the material as consisting of two distinct components, concrete and steel, and assumes the strains in the matrix, fibres and the composite are equal. Each component bears a part of the applied load, according to their proportion of the total volume and stiffness ratio. The length and orientation of the fibres, and fibre-matrix bond, have an important role to play in this model. Mangat and Gurusamy (1987) demonstrated that although Swamy's expression was valid, it was a special case. They derived a similar expression using stress blocks, but noted differences in the interfacial bond strength. (Swamy *et al.* had argued that the interfacial bond strength was approximately constant irrespective of the matrix strength). However, the special case derived by Swamy *et al.* (1974) is quoted in Design Considerations for Fiber Reinforced Concrete (ACI Committee 544 1998), probably because it discounts the interfacial bond strength (which is difficult to measure) and uses only fibre geometry.

The expression derived by Swamy *et al.* (1974) for the first crack flexural strength and ultimate flexural strength of an SFRC was based on the unreinforced flexural strength, fibre aspect ratio and the fibre volume fraction. The interfacial bond stress was considered and found to be reasonably constant for all fibre types up to the ultimate load. However, it should be noted that at the time of the tests the range of fibre types available was relatively limited compared to the wide range of fibre types and shapes marketed today.

The average bond stress when slip occurred at first crack was found to be 3.57 MPa. The average ultimate bond strength was found to be 4.15 MPa. The first crack flexural strength (σ_r) was given by (Eqn...3-4 *after* Swamy *et al.* 1974), where; σ_m and V_m is the flexural strength and volume fraction of the matrix; V_f is the fibre volume fraction; and l_f and ϕ is the fibre length and diameter respectively.

$$\sigma_r = 0.843\sigma_m V_m + 2.93V_f\left(l_f/\phi\right) \qquad \textbf{Eqn...3-4}$$

The ultimate strength (σ_u) was given by (Swamy *et al.* 1974):

$$\sigma_u = 0.97\sigma_m V_m + 3.41V_f\left(l_f/\phi\right) \qquad \textbf{Eqn...3-5}$$

The modified expression by Mangat and Gurusamy (1987) was given by:

$$\sigma_u = A\sigma_m(1 - BV_m) + BV_f\left(l_f/\phi\right) \qquad \textbf{Eqn...3-6}$$

Constants A and B accounted for the shift in the neutral axis at ultimate stress, fibre-matrix interfacial bond strength and orientation of fibres, and are derived empirically for any fibre type. Whilst more fundamental, Eqn...3-6 requires a measure of the interfacial bond strength. Eqn...3-4 and Eqn...3-5 assume the interfacial bond strengths quoted, and have been found to be valid for a wide range of SFRC. These expressions are therefore convenient as a knowledge of the fibre geometry, fibre volume fraction and material strength only are required.

Eqn...3-4 and Eqn...3-5 imply that the fibre shape does not influence the first crack flexural strength or the ultimate flexural strength. Hence a straight fibre would be expected to increase the flexural strength by the same amount as a hook-ended fibre. This observation was confirmed in laboratory flexure tests carried out by Jun and Stang (1998). Differences

between straight fibres and hooked fibres are therefore more noticeable in the descending part of the load-deflection curve.

These expressions, whilst useful in the understanding of the contribution of fibres to first crack and ultimate strength, may not be widely adopted in design. At fibre volume fractions likely to be economically acceptable in pavement applications, the first crack and ultimate strength of SFRC, and modulus of rupture of an unreinforced material, will be comparable. The main benefit of fibres in such instances will be in the post-crack ductility, as measured by the toughness of the composite. Some theoretical approaches to predict the behaviour in the inelastic region of a fibre reinforced composite were discussed at the beginning of this section, though practically the only method currently available to determine toughness characteristics with some reliability is through direct measurement.

3.5 Measurement of tensile properties of SFRC

Despite the attractiveness of theoretical modelling, direct measurement remains the most common method of determining the tensile properties of SFRC.

3.5.1 Direct tensile strength

RILEM have recently proposed a standard test method for determining the direct tensile strength of SFRC (Nemegeer 2001). Direct tensile test specimens are necked or notched and are difficult to produce, particularly for a CBM which is compacted in layers. Care needs to be taken during testing to ensure failure occurs at the centre of the specimen and the load is not applied eccentrically. Further difficulties can be encountered following matrix cracking due to machine instability, especially if the fibre volume fraction is less than critical (Paine 1998). This is due to the sudden reduction in stress across the section. The specimens should be cast in such a manner so that fibre alignment is consistent with the end use. For FRCBM, this poses further problems, as the compaction will tend to align the fibres perpendicular to the orientation expected in the field.

In spite of the difficulties, the direct tension test provides the 'purest' measure of tensile strength, and by counting the fibres following failure, the actual fibre contribution can

most realistically be determined. At the French research laboratory, Laboratoire Central des Ponts et Chaussées, direct tensile hydraulically bound material specimens are compacted using a vibrating rig. This overcomes many of the preparation problems highlighted and may result in a random distribution of fibres across the necked area. Such a test rig is not available in the United Kingdom, though its introduction would allow this type of test to be performed on FRCBM.

3.5.2 Indirect tensile strength

The indirect tension (cylinder-splitting) test can be used on unreinforced concrete in lieu of the direct tension method. The specimens for the indirect method are simpler to prepare and test, and allow direct comparison with the *in situ* material by taking cores.

A case for using the indirect tension test in lieu of the flexural test for SFRC was made by Nanni (1988). Nanni compared results from flexural tests with those from indirect tension tests. However, the test is considered unsuitable for testing SFRC by many researchers (ACI Committee 544 1996) due to the unknown stress distribution following cracking. Nanni justified its use using finite element analysis by showing that the stress distribution up to ultimate did not differ substantially from that up to first crack. The implication from both Nanni's work and other research (ACI Committee 544 1996, Maidl 1995) suggest the test cannot be used beyond the ultimate load.

3.5.3 Flexural strength

Flexural strength is often of direct relevance to the design of concrete pavements. Increases in flexural strength of SFRC are substantially greater than in direct tension or compression (ACI Committee 544 1996). This is due to a redistribution of stresses and strains over the depth of the beam in the tensile zone. The strain distribution in direct tension is generally constant, whereas in flexure it is assumed to be linear. The bending created by loading a simply supported specimen creates a tensile stress, which is always accompanied by a compressive stress.

Once the tensile strength of the specimen is exceeded, a crack occurs and the stress is carried in part by the fibres. If the tensile strength of the composite is reduced due to the cracking, the neutral axis can wander in the direction of the compressive stress. As a result, the depth of the tensile zone increases and the compressive zone decreases. As the formation of the crack does not immediately decrease the tensile strength to zero, and the compressive strength is considerably greater than the tensile strength, it is possible for a new equilibrium to be established (Figure 3-8). The SFRC specimen is therefore able to continue carrying loads even when cracked, unlike unreinforced concrete, and at lower fibre volume fractions than in direct tension (Maidl 1995).

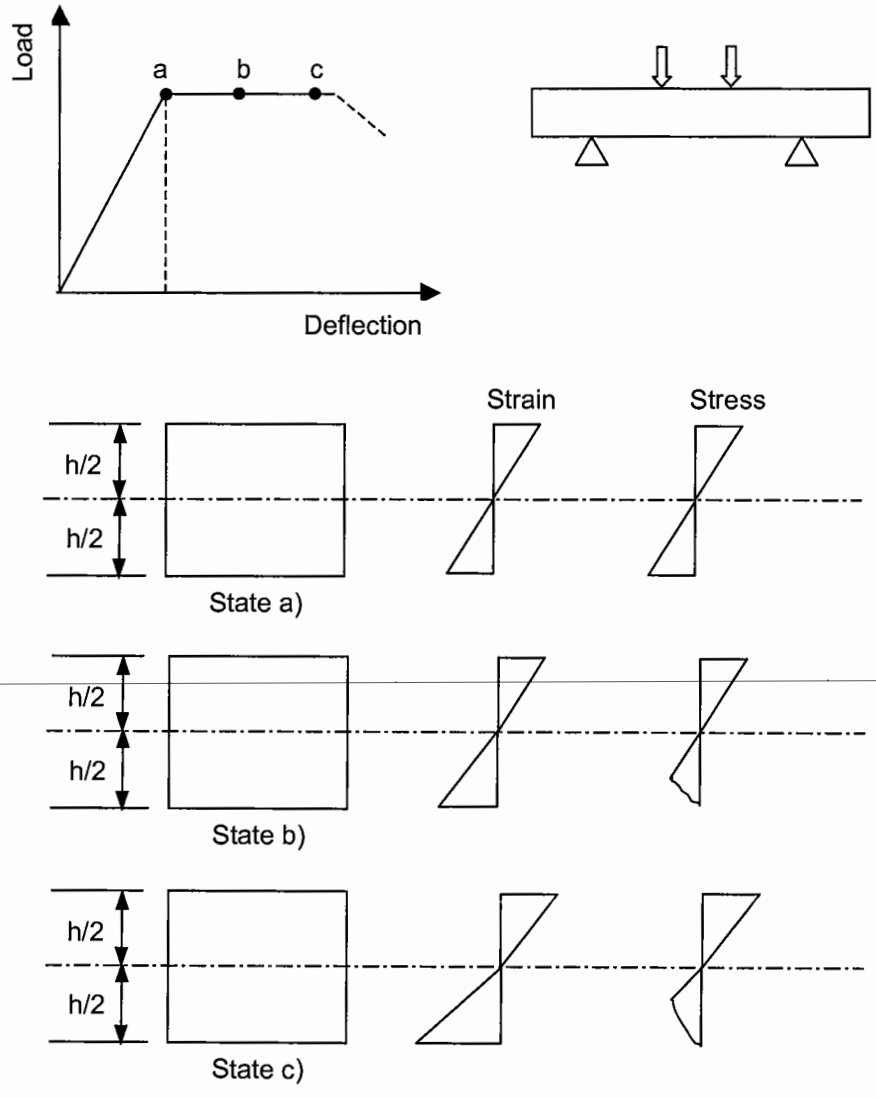

Figure 3-8 Redistribution of stress in SFRC under flexural load (*Maidl 1995*)

Flexural strength is measured in four point bending following the procedure described in BS 1881: Part 118 (1983). By instrumenting the beams, central deflections can be measured and used to control the rate of loading in accordance with the American Standard ASTM C1018, which is necessary in the determination of toughness. Three-point bending can also be carried out, though the former arrangement subjects a greater proportion of the beam to maximum bending moment. There is therefore a greater chance that the weakest part of the specimen is subjected to the maximum stress. For this reason, flexural strengths determined from four point bending are lower than the strengths derived from three point bending. It is common in unreinforced concrete to equate the ultimate flexural strength (σ_u) to the modulus of rupture. In four point bending, this is determined using elastic theory based on the specimen width (b) and depth (h), load (F) and span (L) as shown in Eqn...3-7.

$$\sigma_u = \frac{FL}{bh^2} \qquad \textbf{Eqn...3-7}$$

In SFRC, for a given fibre type, a significant increase in the modulus of rupture over the first crack strength can occur if the critical fibre volume fraction is exceeded.

3.5.4 Flexural toughness

The preferred method for determining toughness is in flexure, as this reflects the stress condition in the majority of applications, including pavements, and is simpler to perform than the direct tensile test. Toughness is measured from the area beneath the load-deflection curve, and indicates the energy expended in failing the specimen. The two most common methods are the American Standard ASTM C 1018 (1994) and the Japanese Standard JSCE SF-4 (1983). The former is based on energy based dimensionless indices, which provide a relative measure of toughness to the composite's first crack toughness; the latter is based on an absolute toughness up to a specified deflection.

The toughness indices calculated using the American Standard (I_5, I_{10}, I_{20}) correspond to the ratio of the toughness values as multiples of the first crack deflection (δ_{cr}) for a perfectly elastic-plastic material (Figure 3-9).

The deflection values defined in Figure 3-9 are $3\delta_{cr}$, $5.5\delta_{cr}$, $10.5\delta_{cr}$ and $25.5\delta_{cr}$, and correspond to toughness values of 1 for elastic-brittle behaviour, and 5, 10, 20 and 50 respectively for perfectly elastic-plastic behaviour. The suffixes therefore reflect the index for perfectly elastic-plastic behaviour. Index I_5 is the ratio of area OACD to OAB, index I_{10} is the ratio of area OAEF to OAB, index I_{20} is the ratio of area OAGH to OAB and index I_{50} is the ratio of area OAIJ to OAB. A wider range of indices may be defined for specific applications following these principles, as was the case for index I_{50} used in this study.

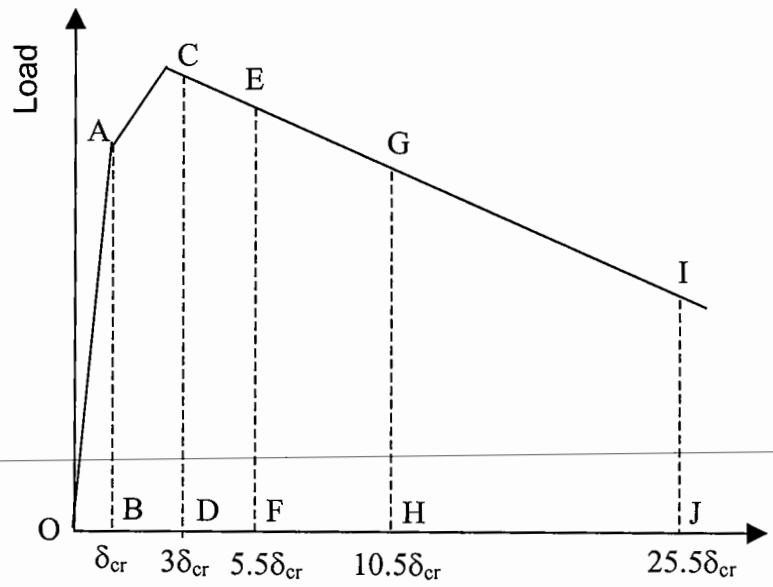

Figure 3-9 Definition of ASTM toughness indices (*ACI Committee 544 1996*)

Research into energy based dimensionless toughness indices was carried out by Johnston (1982), who tested relatively ductile beams. As a consequence, the first crack deflections he recorded were higher than those generally noted for most concretes. Stiffer

mixes can lead to error, as the first crack deflection can be more difficult to identify. Despite this, an advantage of the ASTM method is that the indices reflect the ductility brought about by fibre-matrix bond, and discount apparent increases in toughness due to strength increases. This is necessary if the influence of the matrix composition on the fibre types and fibre volume fractions are to be compared.

Nemegeer and Tatnall (1995) proposed using strength-based dimensionless indices to avoid errors in identifying the first crack deflection. This method makes use of a strength index ($R_{\delta 2-\delta 1}$), which is defined as the average strength over a deflection range to the first crack strength. The first crack strength is determined objectively to avoid similar errors to finding the first crack deflection. Despite being dimensionless, a fixed beam geometry is recommended when using this method until further research identifies the effects of varying dimensions.

Unlike the American Standard, the Japanese Standard JSCE SF-4 specifies a toughness parameter (T_{JSCE}) to a prescribed deflection of 1/150 of the flexural span (L) (Figure 3-10), and therefore does not rely on qualitative interpretation of the first crack. Furthermore, for most concretes, the Japanese Standard measures the toughness over a greater deflection unless large ASTM indices are used. In doing so, it indicates a more marked difference between fibre types and fibre volume fractions.

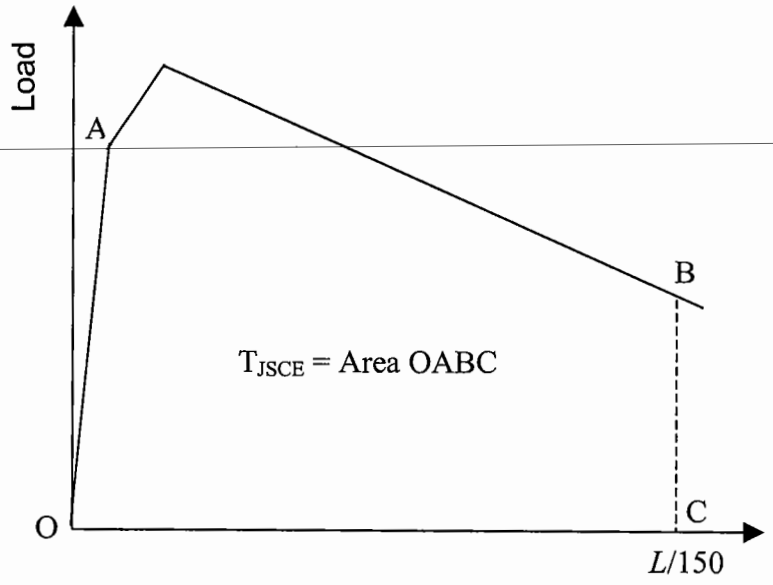

Figure 3-10 Definition of JSCE SF-4 toughness (*ACI Committee 544 1996*)

The method also has its limitations though. As the toughness is a direct measure to a stated deflection, the value is dependent on the strength of the material. Also, JSCE toughness values can be shown to be similar for very different composite behaviour, depending on the material strength and post-crack performance (Figure 3-11). Therefore knowledge of the material strength, fibre type and fibre volume fraction is required when using these values.

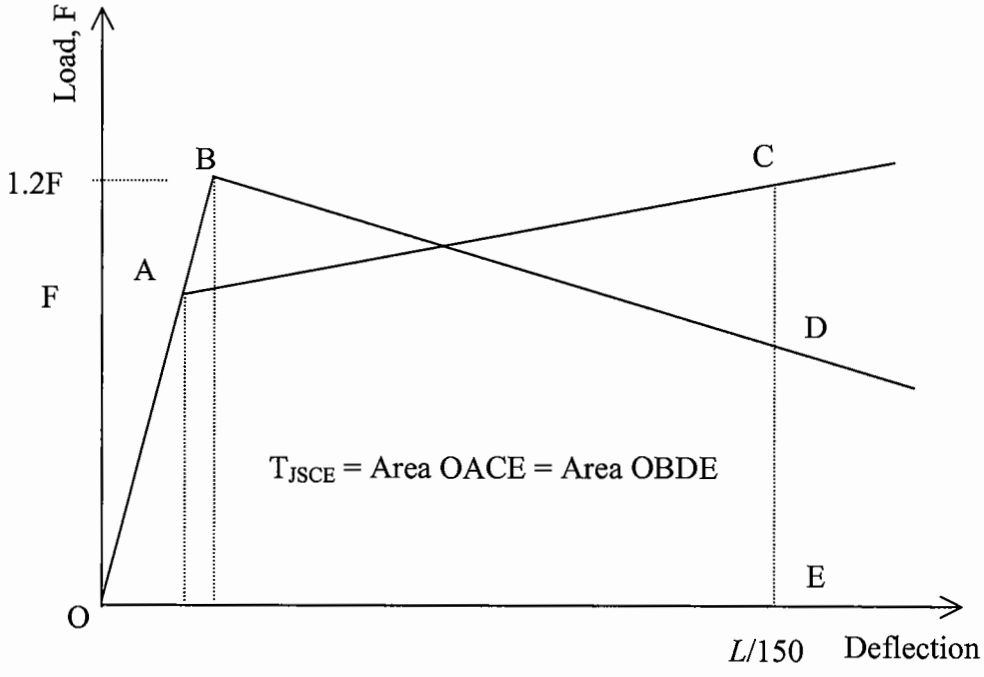

Figure 3-11 Schematic load-deflection curves showing the same absolute toughness for different first crack strengths (*Johnston 1985*)

3.5.5 Equivalent flexural strength and flexural strength ratio

The limitations of the JSCE SF-4 toughness parameter (T_{JSCE}) may be overcome by defining an index based on the equivalent and ultimate flexural strengths. The equivalent flexural strength is calculated by dividing the toughness by the prescribed deflection, so that:

$$\sigma_{eq} = \frac{T_{JSCE} L}{\delta_{JSCE} b h^2} \qquad \textbf{Eqn...3-8}$$

where the Japanese standard JSCE SF-4 defines δ_{JSCE} as $L/150$.

For a span of 300mm, δ_{JSCE} is 2mm. The index, referred to as the flexural strength ratio ($R_{e,2}$ for δ_{JSCE} = 2mm) is shown in Eqn...3-9. For a span of 450mm, the index is $R_{e,3}$. The index $R_{e,3}$ is used as a design parameter in the Concrete Society Technical Report TR 34 (1994), possibly as it is more objective than the American indices. It has some practical use in that it is used in the design of ground bearing floor slabs to modify the ultimate bearing capacity, though ASTM indices could also be applied using similar principles.

$$R_{e,\delta_{JSCE}} = \frac{\sigma_{eq}}{\sigma_u} \qquad \textbf{Eqn...3-9}$$

In addition to the energy based dimensionless indices, ASTM C 1018 (1994) requires the computation of dimensionless residual strength factors. These factors, termed $R_{5,10}$ and $R_{10,20}$ are computed as $20.(I_{10}-I_5)$ and $10.(I_{20}-I_{10})$ respectively, and represent the average strength between the two cut off deflections as a percentage of the first crack strength. These may be used to compare residual strengths of composites at given deflections.

3.5.6 Fatigue

There is no common approach to fatigue testing. Fatigue loading can be applied in compression, tension, or shear (Balaguru and Shah 1992), though most investigations are carried out in flexural fatigue on account of the end use. The basic fatigue characteristics of a material are usually illustrated on an S-N curve, a graph of the stress ratio - applied load/ultimate load (S) - against the logarithm of the number of cycles (N). However, for fibre reinforced composites, where the objective is to demonstrate the comparative performance against an unreinforced material, the first crack load, rather than the ultimate strength, may be preferable. The use of the ultimate load may imply less favourable performance if the ultimate load exceeds the first crack load significantly, as is the case at higher volume fractions. The definition of the stress ratio should therefore be clearly indicated in the reporting of fatigue tests on SFRC.

Testing was stopped by a number of researchers (Ramikrishnan *et al.* 1987, Jun and Stang 1998, Batson *et al.* 1972) at two million cycles. Specimens that had not failed after two million load repetitions were tested statically to determine a residual flexural strength. In some cases, this residual static flexural strength has been 10 to 30 percent greater than for similar beams with no fatigue history (ACI Committee 544 1996). One explanation of this increase is that the cyclic loading reduces initial residual tensile stresses caused by shrinkage of the matrix. Similar behaviour has been reported for unreinforced concrete (Mallet 1991).

Results from fatigue tests are notorious for scatter, and repetition of tests at the lower stress ratios is necessary to achieve a statistically meaningful curve. This scatter has been attributed to differences in specimen strengths (Galloway *et al.* 1979a, Cornelissen and Reinhardt 1984). By using the stress ratio, differences in flexural strength, cement content and mix proportion have been shown to be 'normalised' (Mallet 1991). SFRC fatigue results, presented by Ramikrishnan and Josifek (1987), have been shown to have superior performance to unreinforced concrete, reported by Galloway *et al.* (1979a), as previously shown in Figure 3-3, possibly due to the arrest mechanism created by a fibre, slowing the rate of progression of the crack. These data were supported by comparative fatigue tests on unreinforced and fibre reinforced cement stabilised base material, reported by Sobhan (1997).

Loading rates of between 1 and 15 Hz, and short rest periods are thought to have little effect on the fatigue life, though the minimum applied stress can have a considerable effect (Balaguru and Shah 1992). However, Galloway and Raithby (1973) showed from uni-axial tensile fatigue tests that the load rate does have a significant affect on the static strength of the material, therefore influencing the magnitude of the stress ratio. This will affect the remaining data as shown in Figure 3-12.

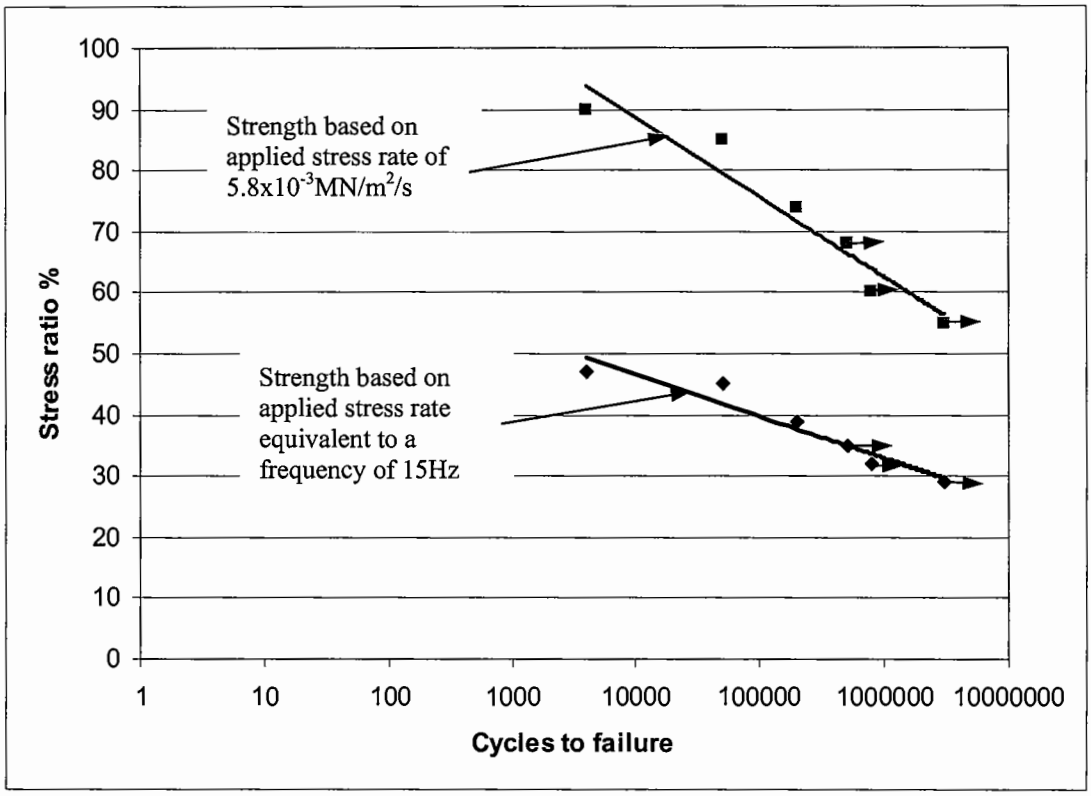

Figure 3-12 Effect of rate of loading on static strength and resulting dynamic data based on uni-axial tensile fatigue tests (*Galloway and Raithby 1973*)

Therefore, by way of summary, it is evident that *S-N* curves may be used to compare the performance of unreinforced and fibre reinforced cementitious material. However, the rate of loading of the static test to determine the first crack or ultimate load, from which the stress ratio is based, should be clearly defined, and whether the first crack or ultimate load has been used in the determination of stress ratio. In this regard, a standard approach to fatigue testing and reporting of fibre reinforced cementitious composites would be beneficial.

3.6 Application of material properties in design

Bischoff *et al.* (1998) had outlined two options available in rigid slab design, shown in Figure 3-13. Option 1 was to determine all working stresses (loading, shrinkage, curling and differential settlement) and design the slab with sufficient safety factors using elastic methods so that the strength of the material exceeds the stresses, and cracking does not occur. In such an instance, reinforcement is not required. Option 2 was to accept that some cracking will occur and design the slab based on serviceability (crack control) criteria. Nominal reinforcement in this case may be required.

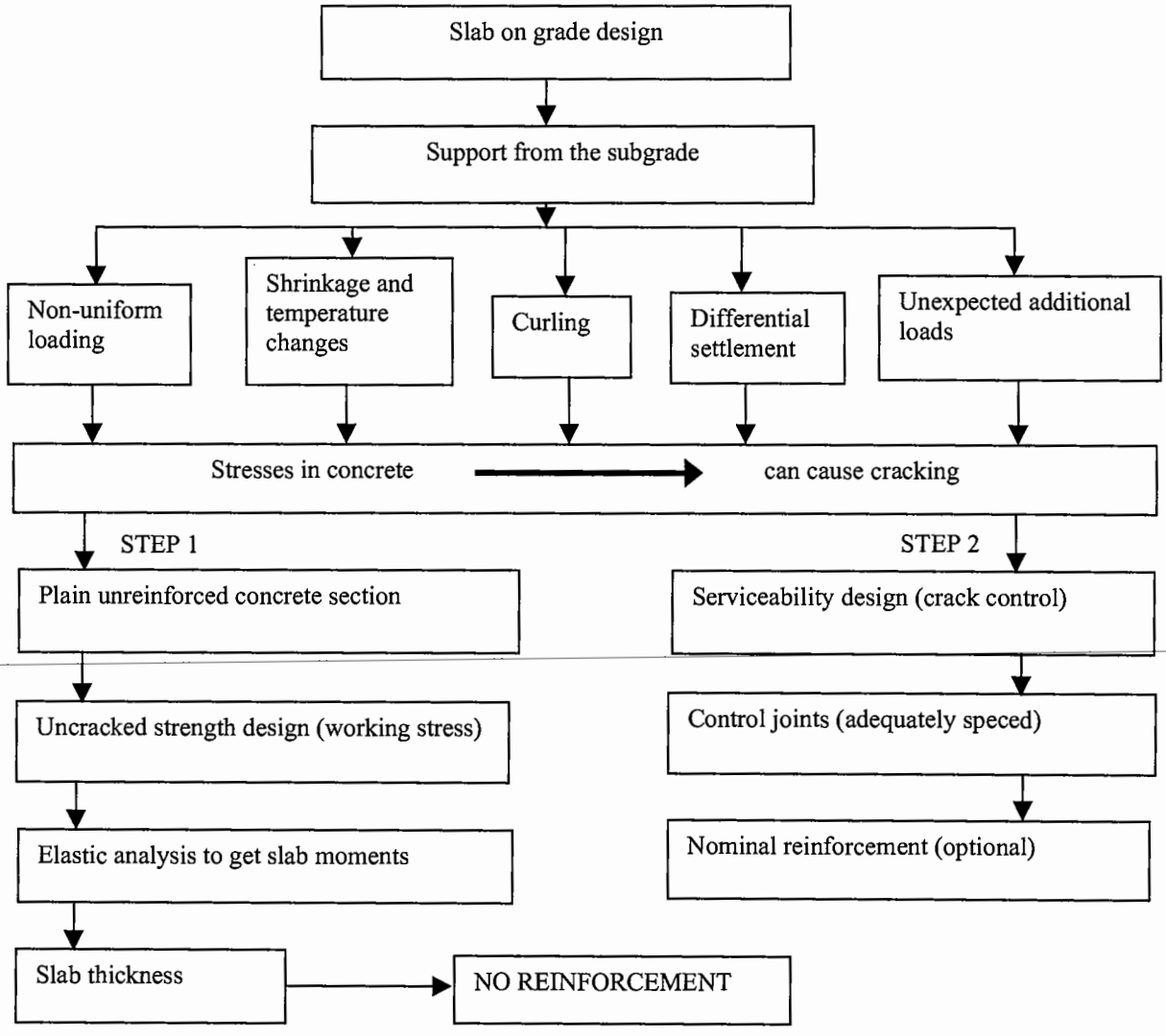

Figure 3-13 Concrete slab design options (Bischoff *et al.* 1998)

As the failure criterion was based on surface cracks, the fibres provided a mechanism to increase the load bearing capacity of the slab. Additionally, as cracking occurs, the sub-base also contributes by the degree of support offered. It was felt that the method was suitable for FRCBM as the contributions of the fibres and sub-base restraint could be readily incorporated. A similar method has widespread acceptance by industry in the design of ground bearing floor slabs (Concrete Society 1994).

Beckett and Humphreys (1989) showed from numerous full-scale slab tests that the increase in post-crack ductility could be used practically using a method proposed by Meyerhof (1962), which applied plastic analysis. Comparisons of SFRC slabs with control slabs had demonstrated a substantial increase in both first crack and ultimate strength. The method assumed that cracks occur in the underside of the layer from a centre or edge load (Figure 3-14). Results reported by Beckett and Humphreys demonstrating the increase in load is shown in Table 3-2.

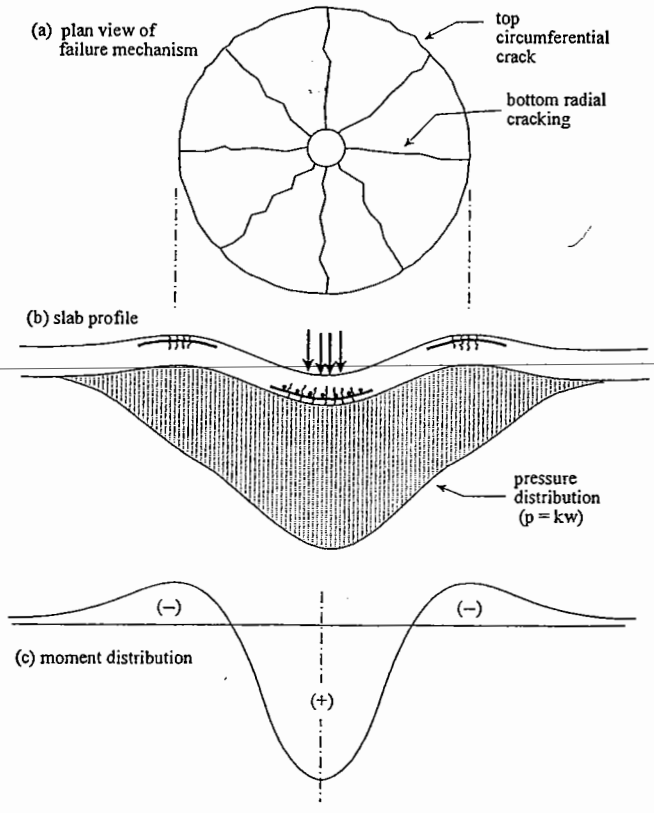

Figure 3-14 Model of crack mechanism in concrete slab

Test no	Slab depth mm	Fibre type[1]	Load kN		Comments
			At first observed crack	At failure	
1	150	No reinforcement	180	200	Cracks through full depth of slab and punching.
2	150	No reinforcement	200	200	Cracks through full depth of slab and punching.
3	150	Hook ended (60/100) @ 30kg/m^3	290	>345	Maximum load attained, no cracks on top surface.
4	150	Hook ended (60/100) @ 30kg/m^3	240	340	(Repeat of Test 2). Cracks through full depth of slab and punching.
5	150	Hook ended (60/100) @ 20kg/m^3	220	350	Cracks through full depth of slab and punching.
6	150	Hook ended (60/100) @ 20kg/m^3	200	300	(Repeat of Test 4). Cracks through full depth of slab and punching.
7	150	Hook ended (60/100) @ 20kg/m^3	290	350	(Repeat of Test 4). Punching.
8	130	Hook ended (60/100) @ 20kg/m^3	240	320	Cracks through full depth of slab and punching.
9	150	Hook ended (60/80) @ 20kg/m^3	260	390	Cracks through full depth of slab and punching.
10	150	Hook ended (60/80) @ 30kg/m^3	320	360	Punching, no cracks on top surface.
11	150	Undulating @ 30kg/m^3	260	370	Cracks through full depth of slab.
12	150	Undulating @ 30kg/m^3	260	380	Cracks through full depth of slab and punching.
13	150	Undulating @ 20kg/m^3	220	260	Cracks through full depth of slab and punching.
13	150	Straight fibres (19mm) @ 22.5kg/m^3	220	240	Cracks through full depth of slab and punching.

Note: [1]Notation 60/100 etc refers to fibre aspect ratio/length in mm.

Table 3-2 Comparative first crack and ultimate loads due to an applied centre load, measured on 3m x 3m concrete slabs on grade, using various steel fibres and volume fractions (*Beckett and Humphreys 1989*)

Toughness parameters obtained from tensile tests are largely used to determine the comparative performance of fibre type, fibre volume fraction and matrix strength, and to this extent, are largely used as in research. However, in the design of concrete industrial floors, the flexural strength ratio $R_{e,3}$, obtained from flexural tests as described in Section 3.5.5, enable a comparison of the ultimate bearing capacity of steel fibre reinforced slabs and unreinforced slabs. The design method, which applies theoretical plastic analysis based on work by Meyerhof (1962), is described in Appendix F of the Concrete Society Technical Report TR 34 (1994). It provides an alternative to the expressions derived by Westergaard

(1926) based on elastic analysis, though follows a similar approach in that loads are considered in the centre, edge and corner of the slab.

The analysis shows that although the simply supported flexural strength is often not increased, due to the moment redistribution that takes place in a slab, which is increased significantly by fibre reinforcement, the ultimate bearing capacity of the slab is increased. This was illustrated by Bischoff (1999) in full-scale tests (Figure 3-15).

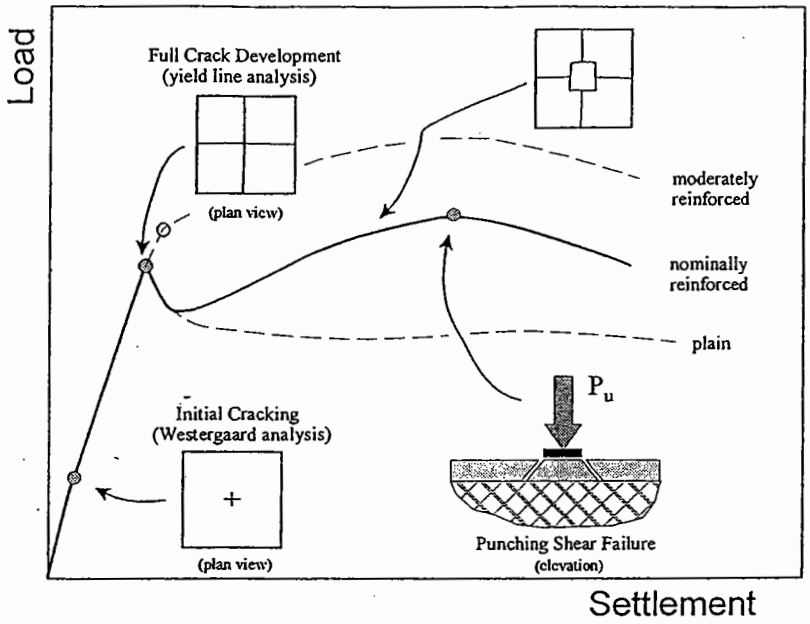

Figure 3-15 Comparative ultimate load carrying capacity of unreinforced and fibre reinforced concrete slabs (Bischoff 1999).

The analysis shows that for a fibre reinforced composite with an $R_{e,3}$ value of 50%, the collapse load in the centre or edge of the fibre reinforced slab will be 50% greater than that of an unreinforced concrete. At the edge, the first crack will appear at the surface, therefore the ultimate bearing capacity of both the fibre reinforced and unreinforced slabs would be expected to be the same.

The $R_{e,3}$ (and similarly $R_{e,2}$) can therefore be used in design. As flexural testing is recommended in this study for determining the material strength, the determination of the flexural strength ratio may therefore be carried out on the same specimens, to achieve performance based criteria. In practice, an increase in ultimate bearing capacity may be used to reduce the slab thickness, with no overall increase in pavement life.

Chapter 4. Laboratory investigation

4.1 Introduction

A laboratory study was carried out to investigate the properties of steel fibre reinforced cement bound material (FRCBM) considered applicable to the behaviour of a cementitious roadbase. The literature review showed that cracking of the CBM was a major contributory factor in the failure of a flexible composite pavement. Specifically of interest are the static and dynamic flexural strengths and post-crack behaviour, and the transverse crack characteristics. For these reasons, the following testing was carried out:

- Static flexure and indirect tensile (cylinder-splitting)
- Dynamic flexure
- Cyclic shear

This Chapter describes the test materials used, specimen preparation and the individual tests. The objectives, test arrangements, results and discussion of each test are described within the individual section for that test. Descriptions are given in Section 4-3 and results for the static tests are in Section 4-4, dynamic tests are in Section 4-5 and 4-6 and cyclic shear tests are in Section 4-7 and 4-8.

Tests were carried out using gravel CBM and limestone CBM at a range of strengths. The strengths were chosen to cover the range of CBM strengths currently used in the United Kingdom. Higher strengths were also studied on account of overseas experience with CBM with thinner overlays than are used in the United Kingdom, or with no overlay. Three commercially available steel fibre types with hooked ends were compared in the study, at fibre volume fractions up to 1%. Additionally, a fourth fibre type, with a conical end, was investigated by Munt (1999), using nominally the same gravel CBM mix described in this study.

4.2 Laboratory test materials, mixing and specimen preparation

4.2.1 Laboratory test materials

Two aggregate types were used in the study; these were gravel and limestone, both with a nominal maximum aggregate size of 20mm. The aggregates were selected to provide some variation in aggregate strength and angularity as these properties are known to affect the tensile strength of CBM (Williams 1986). Also, any differences in the post-crack behaviour of the reinforced specimens due to aggregate type were also of interest. The river gravel originated from the Trent Valley and was a rounded aggregate. The crushed rock siliceous limestone was from Ballidon Quarry in Derbyshire. All aggregate was dried and stored prior to use. The particle size distribution for these aggregates, determined following BS 1377: Part 2 (BSI 1990a), is shown in Figure 4-1. The gradings lay within the envelope defined by the Specification for Highway Works for CBM3 and above (see Table 2-1 for strengths and categories), when used as the lower roadbase in a flexible composite pavement (Highways Agency 1998).

Cement contents, determined by mass of dry aggregate, were 4.5%, 6.0%, and 8.5% for the gravel CBM and 3.5%, 4.5% and 5.5% for the limestone CBM. The water content of each mix (shown in Table 4-1) was the optimum water content, determined following BS1924 (BSI 1990) for the unreinforced mix. Water was added to all mixes by mass of dry aggregate, cement and fibres.

Three commercially available steel fibres were used in the study, supplied by N.V Bekaert S.A under the trade name Dramix. These were referenced 65/60, 65/35 and 45/50 (Plate 4-1). The fibres were cold-drawn steel wires with a minimum tensile strength of 1000MPa. Fibre types were referenced by aspect ratio and length, the aspect ratio being the ratio of the effective fibre length to its diameter. Hence, fibre type 65/60 had an aspect ratio of 65, length of 60 mm and diameter of 0.9mm. Fibre types 65/60 and 65/35 were supplied collated (i.e. in bundles held together by a soluble glue), and fibre type 45/50 was supplied loose. Reinforcement was at fibre volume fractions (V_f) up to 1.0%.

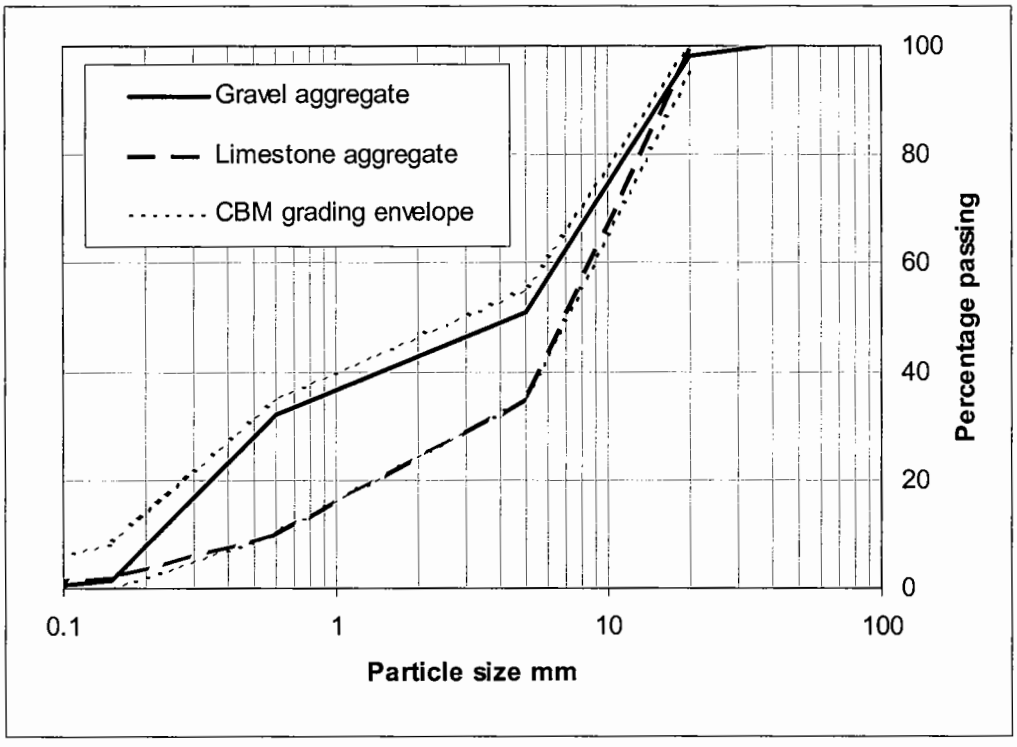

Figure 4-1 Particle size distribution for laboratory mixes showing grading envelope for CBM used as a lower roadbase in flexible composite pavements

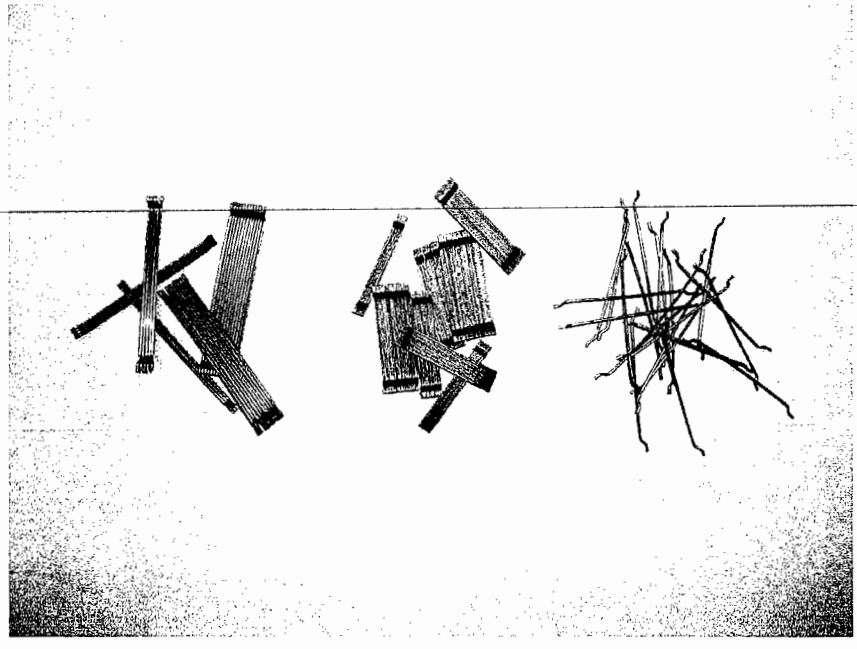

Plate 4-1 Hook ended Bekaert steel fibre types 65/60, 65/35 and 45/50 used in laboratory study

Tests carried out for each mix are summarised in Table 4-1. Details of fibre types and volume fractions used in each test are presented with the description of that test in subsequent sections.

Mix ref.	Aggregate type	[1]CC %	[2]WC %	[3]Cube strength MPa	Static flexure	Static indirect tension	Dynamic flexure	Cyclic shear
G1	Gravel	4.5	5.0	10	x		x	x
G2	Gravel	6.0	5.2	17	x	x		x
G3	Gravel	8.5	5.2	26	x		x	x
L1	Limestone	3.5	4.5	18	x			
L2	Limestone	4.5	4.5	26	x			
L3	Limestone	5.5	4.5	32	x	x		

Notes: [1]CC (cement content) by mass of dry aggregate, [2] WC (water content) by mass of dry aggregate, cement and fibres, [3]7-day compressive cube strength average of unreinforced mixes shown in Appendix A.

Table 4-1 Summary of mix designs and tests carried out

4.2.2 Mixing and specimen preparation

All mixing took place in a 0.1m³ capacity pan type mixer. The unreinforced material was mixed for a total of three minutes, broken down as follows: dry aggregate and cement mixed for one minute prior to water being added, then mixed for a further two minutes. The fibre reinforced mixes were mixed for a total of four minutes, broken down as follows: dry aggregate and cement mixed for one minute prior to water being added. This was then mixed for a further minute before adding the fibres. The material was then mixed for a further two minutes.

The test specimens comprised of cubes, beams and cylinders. The cubes were used in the compression tests, the beams in the static and dynamic flexure tests and the cyclic shear tests and the cylinders in the static indirect tension (cylinder-splitting) tests. Specimens were produced in steel moulds of the following dimensions: cubes, 100mm; beams, 100mm x 100mm x 500mm; and cylinders, 150mm diameter x 300mm. Cylinders were cut in half to produce two test specimens of dimensions 150mm diameter x 150mm.

Each specimen was compacted in three layers of material using a 75 watt Kango 365 vibrating hammer, fitted with a flat plate to suit the mould's shape and dimensions. Each

layer was compacted to refusal. Beam and cube moulds were fitted with a specially fabricated extension. This was so that the final layer of material could be surcharged and compacted more effectively. Any material protruding above the specimen after the extension was removed was cut away, and the surface was levelled by placing a wooden plank on the mould and re-compacting. Compaction of all the material from any mix was completed within 45 minutes.

Completed specimens were stored in their moulds for two days under wet hessian and a polythene sheet. They were then stripped and cured in a water tank held at 20°C until they were tested. The cylinders were cut to length (150mm) the day before testing. Immediately prior to any test being carried out, the weight of the specimen in and out of water was measured to calculate the saturated density.

4.3 Static tests

The objectives of the static tests were to determine the effect of aggregate type, cement content, fibre type and fibre volume fraction on the strength and post-crack ductility of the composite. An additional aim was to recommend a test parameter that could be used in design to distinguish between CBM and FRCBM based on the post-crack ductility. The static tests were carried out in:

- Compression
- Flexure
- Indirect tension (cylinder-splitting)

Cubes were prepared and tested in compression from the same mix as that used in the preparation of the beams and cylinders. The investigation into differences between fibre types and volume fractions were on the whole carried out in flexure. This is valid as the vast majority of research on SFRC is also in flexure, and this stress state is most representative of the bending behaviour of a pavement. However, investigations in indirect tension were also carried out to assess the practicality of using cored specimens, which would facilitate measurements from material in the field.

The three fibre types were used in the flexural and indirect tensile tests, at the fibre volume fractions shown in Table 4-2 and Table 4-3. A minimum of three specimens was tested at 7-days for each test.

Mix ref.	Control	Fibre type						
		65/60			65/35		45/50	
		Fibre volume fraction						
		0.25	0.5	1.0	0.5	1.0	0.5	1.0
G1	x		x	x				
G2	x		x	x	x	x	x	x
G3	x		x	x				
L1			x					
L2			x					
L3	x	x	x	x				

Note: Aggregate, cement content and water content for each mix given in Table 4-1. Aggregate gradings shown in Figure 4-1.

Table 4-2 Details of tests carried out in flexure showing fibre types and fibre volume fractions

Mix ref.	Control	Fibre type													
		65/60						65/35					45/50		
		Fibre volume fraction													
		0.1	0.2	0.25	0.5	0.75	1.0	0.1	0.25	0.5	0.75	1.0	0.25	0.5	1.0
G2	x	x	x	x	x	x	x	x	x	x	x	x	x	x	x

Note: Aggregate, cement content and water content for each mix given in Table 4-1. Aggregate gradings shown in Figure 4-1.

Table 4-3 Details of tests carried out in indirect tension showing fibre types and fibre volume fractions

Comparisons of the results from this study are made with published research into CBM, and the results from an undergraduate project study carried out at the University of Nottingham using FRCBM (Munt 1999).

4.3.1 Static test arrangements and data acquisition

Compressive cube tests

A 2500kN capacity compression testing machine was used to test the cubes in accordance with BS 1881 (BSI 1983) at an applied load rate of 160kN/min.

Flexural tests

Flexural and indirect tensile tests were carried out using a 200kN capacity Zwick universal testing machine. The test arrangement is shown in Figure 4-2.

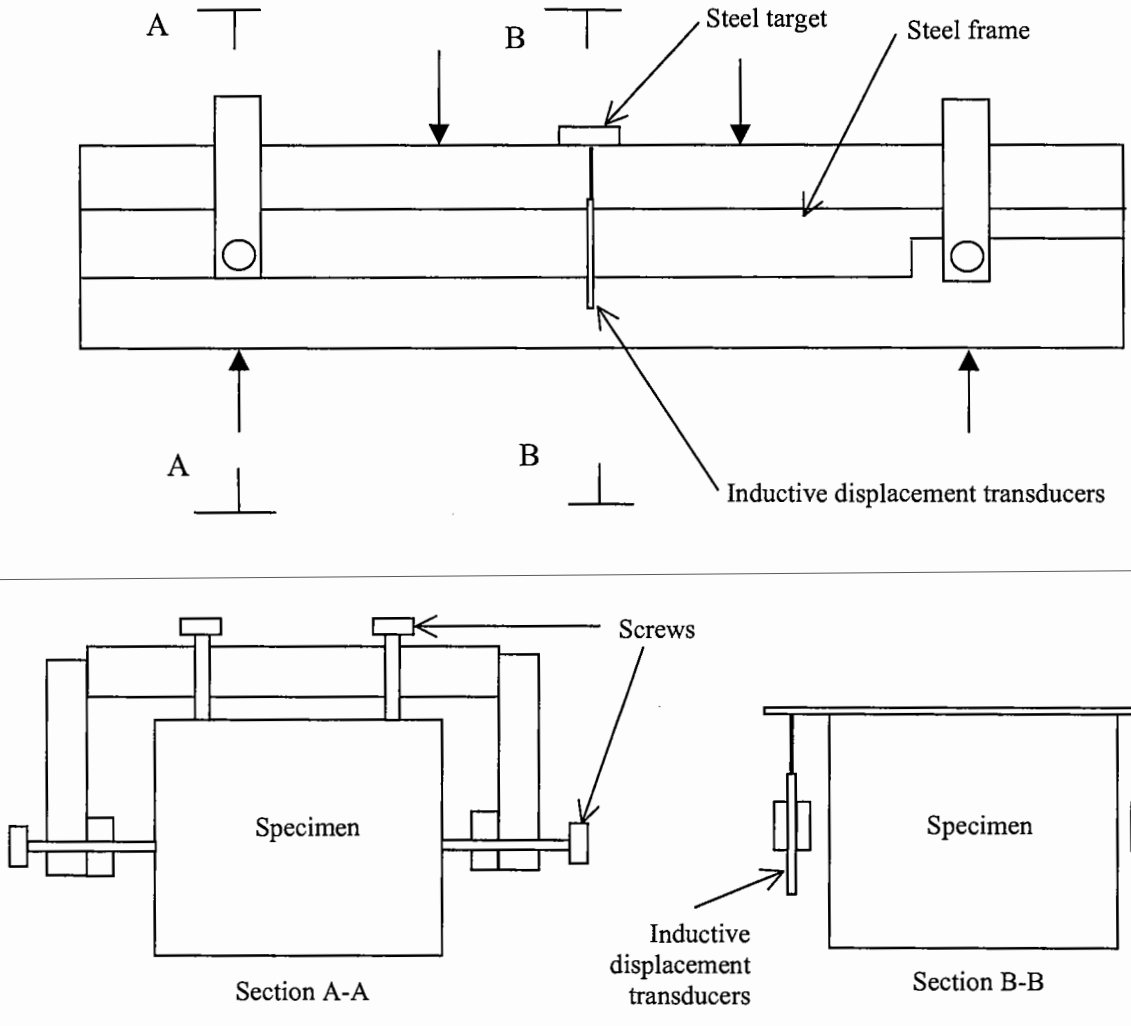

Figure 4-2 Testing arrangement for static flexure tests

The beams were tested in four point bending over a span of 300mm, in accordance with the American Society for Testing and Materials (ASTM) standard C1018 (1994) and the Japanese Society of Civil Engineers (JSCE) standard SF4 (1983). Inductive displacement transducers were mounted using a 'yoke' arrangement to measure the net mid-span deflection between the mid-height and the top surface of each beam. The yoke ensured accurate measurement, independent of extraneous deformations resulting from crushing of the specimen at the supports.

Tests were carried out under closed-loop deflection control at a rate of specimen deflection of 0.1mm/min, and stopped at a total deflection of 2mm. Zwick software was used to control the test and automatically log data at deflection intervals of 0.001mm to a deflection of 0.1mm, and at intervals of 0.01mm thereafter. Data were then transferred to a Microsoft Excel spreadsheet for analysis.

Indirect tensile tests

Indirect tensile (cylinder-splitting) tests involved measuring the horizontal deformation, using linear potentiometers, at the diametrical centre of the cylinder under an applied load, as shown in Figure 4-3.

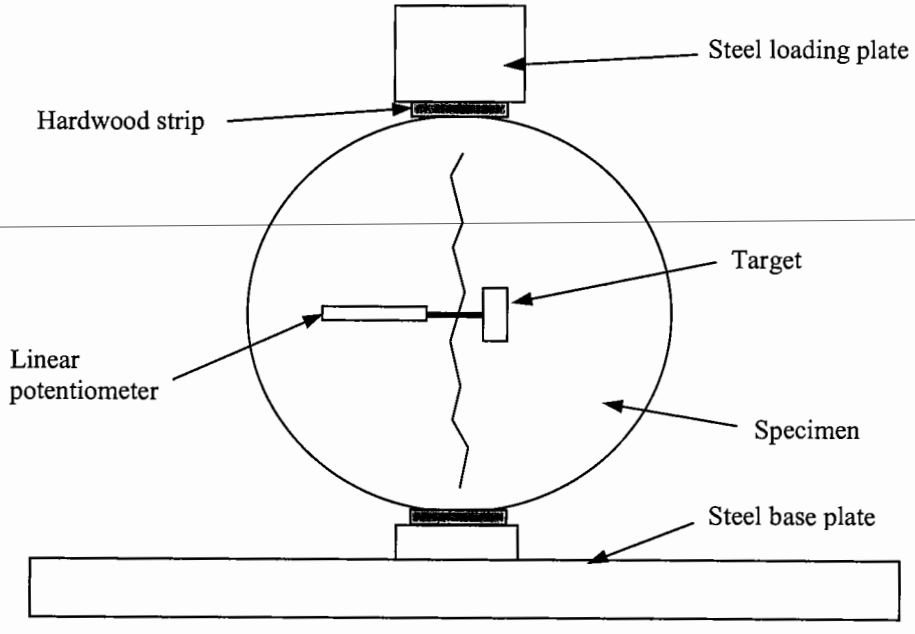

Figure 4-3 Indirect tension test arrangement

The linear potentiometers and targets were stuck to each face of the specimen using a rapid set glue. The load was applied at a constant cross head stroke rate of 0.2mm/min through two hardwood strips 15mm wide and 4mm thick, controlled through the interface of the Zwick testing machine. Load-cell and sensor total voltage outputs were automatically recorded at 10 second intervals and stored digitally using an external logger. Testing was stopped at a total horizontal deformation of 1.5mm. Data were then transferred to a Microsoft Excel spreadsheet for analysis.

4.3.2 Definition of flexure and indirect tension test parameters

Flexural tests

The static material properties of FRCBM reported are indirect tensile and flexural strengths, ASTM toughness indices, JSCE toughness values, JSCE equivalent flexural strengths and flexural strength ratio. As there is no universally accepted test method for characterising the flexural toughness of fibre reinforced concrete, ASTM C1018 (1992) and JSCE-SF4 (1983) were adopted since they are the most widely used and reported methods for characterising fibre reinforced concrete behaviour.

The parameters calculated from the flexural tests to evaluate strength and ductility of FRCBM were: first crack strength (σ_{cr}) and ultimate flexural strength (σ_u); four energy-based dimensionless indices (I_5, I_{10}, I_{20}, I_{50}) as defined by ASTM C1018; and from JSCE-SF4 an absolute toughness value (T_{JSCE}), which measures the energy-absorption capacity of the material. The derivation of the flexural toughness indices used in this study was shown in Figures 3-9 and 3-10 (Section 3.5.4). The equivalent flexural strength (σ_{eq}) was determined using Eqn...3-8 and the flexural strength ratio expressed as a percentage ($R_{e,2}$) was determined to a total deflection of 2mm using Eqn...3-10 (Section 3.5.5).

Indirect tensile tests

The parameters calculated from the indirect tensile tests to evaluate strength and ductility of FRCBM were: first crack strength ($\sigma_{SP,cr}$) and ultimate indirect tensile strength ($\sigma_{SP,u}$); and an absolute toughness value following a similar approach to JSCE-SF4 (T_{SP}).

This was defined as the total area under a load-deflection plot to a deformation (δ_{SP}) of 1.5mm. Additionally, an equivalent indirect tensile strength ($\sigma_{SP,eq}$) and equivalent indirect tension strength ratio expressed as a percentage (R_{SP}) was defined using similar principles to those defined for the flexure tests.

Hence: $$\sigma_{SP,eq} = \frac{T_{SP}}{\delta_{SP}}$$ **Eqn...4-1**

And: $$R_{SP} = \frac{\sigma_{SP,eq}}{\sigma_{SP,u}}.100$$ **Eqn...4-2**

4.4 Static test results

The results from the compressive, flexural and indirect tensile (cylinder-splitting) tests are presented in this section. A full table of results from the static tests is shown in Appendix A. The results include average values, standard deviations, coefficients of variation and 95% confidence limits. The Figures presented below use the average of three specimens; where appropriate, 95% confidence limits are also included. Regression lines were used in some instances to demonstrate perceived relationships.

Compressive cube results are shown to demonstrate the effect of fibres on compressive strength, based on the fact that this parameter is used to distinguish between CBM in the current Highways Agency Specification in the United Kingdom. These data were compared to those presented by Shahid (1997) for a nominally identical material.

The effect of fibre volume fraction on flexural strength is investigated as this is of direct relevance to the design of CBM; any increase in strength would lend itself to a lower cement content or reduced material thickness for the same traffic. As increases in ultimate strength over first crack strength have been reported for SFRC, these parameters are investigated for the gravel and limestone CBM, at three CBM cement contents, and at three steel fibre types and various fibre volume fractions.

Flexural toughness is presented in terms of the ASTM index I_{50} and the flexural strength ratio $R_{e,2}$, derived from parameters determined following the method described in JSCE-SF4. These parameters were chosen as they are a measure of the post-crack ductility of the composite, and in SFRC this behaviour more than any other was shown to increase when compared to the unreinforced material. Other ASTM indices (I_5, I_{10}, I_{20} etc.) could have been used as described in Section 3.5.4, though an index over a greater deflection was chosen as this was considered more representative of potential deflections in a cracked pavement. Toughness values were compared to those for an FRCBM using an alternative fibre type as reported by Munt (1999), and to concrete mixes of various strengths as reported by Middleton (1998).

Relationships between indirect tensile (cylinder-splitting) strength and toughness were compared to the flexural parameters. The use of cylinder specimens would allow cores to be taken and *in situ* measurements to be made.

The conclusions and discussion within this section draw together the main findings from the compressive, flexural and indirect tensile tests, and discuss the applicability of the findings to practice.

4.4.1 Compressive cube results

The results from the average 7-day compressive cube tests are summarised in Table 4-4 and presented below; the full set of results, including the compressive cube results, is shown in Appendix A.

Mix ref.	Cement content %	Saturated density (at V_f=0.5%) kg/m³	Compressive cube strength MPa		
			Control	V_f=0.5%	V_f=1.0%
G1	4.5	2408 (3)	9.2 (0.6)	12.9 (1.0)	9.2 (0.8)
G2	6.0	2393 (6)	16.9 (1.4)	17.7 (0.9)	17.9 (0.5)
G3	8.5	2419 (3)	32.9 (1.7)	25.9 (1.5)	25.8 (1.2)
L1	3.5	2482 (0)	-	18.0 (0.6)	-
L2	4.5	2483 (0)	-	25.5 (3.8)	-
L3	5.5	2504 (3)	38.9 (0.5)	34.2 (1.3)	30.9 (3.4)

Table 4-4 Summary of average 7-day compressive cube strengths and 95% confidence values (± in brackets) using fibre type 65/60

Effect of cement content on compressive cube strength

Compressive cube strength increased linearly with cement content for the gravel CBM (Figure 4-4) and the limestone CBM (Figure 4-5), both reinforced using fibre type 65/60. The increase in cube strength was matched by an increase in the saturated densities of the materials (Table 4-4). The increases in compressive strength for both the gravel CBM and limestone CBM was approximately 100% between the cement contents studied.

The relationship between compressive cube strength, flexural strength and density is known to be dependent on the aggregate type, water content and degree of compaction of the mix (Croney and Croney 1991, Shahid 1997). The relationship between cement content and compressive cube strength is known to be linear (Kennedy 1983), therefore these data agree with such findings.

Although an increase in strength and density may be predicted with increasing cement content, the prediction of these parameters is not straightforward. Strength is dependent on aggregate shape, strength, angularity, gradation, water content of the mixture and compaction applied to the material. The density is also dependent on these items and additionally on the specific gravity of the aggregate (Croney and Croney 1991). Therefore, whilst a unique relationship between cement content and compressive cube strength would be desirable for CBM, no such relationship exists due to the inter-relationship between the various constituent materials already indicated. Cube strength for a given aggregate type, gradation and water content at various cement contents can only therefore be determined by direct measurement.

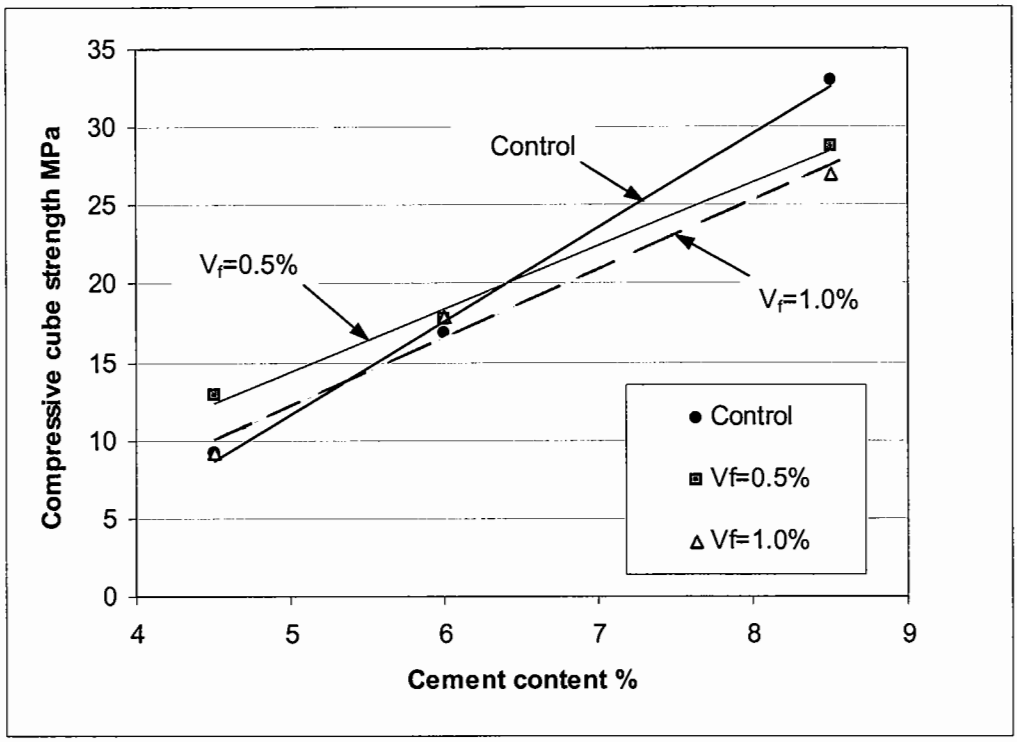

Figure 4-4 Relationship between 7-day compressive cube strength and cement content for gravel CBM and FRCBM reinforced with fibre type 65/60

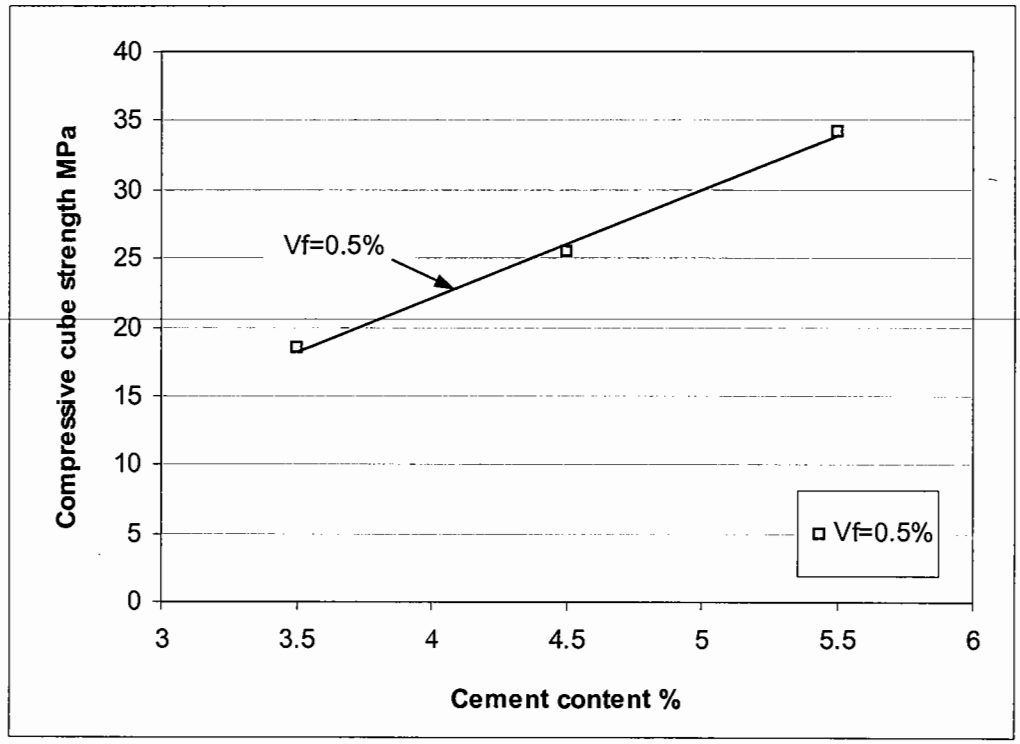

Figure 4-5 Relationship between 7-day compressive cube strength and cement content for limestone FRCBM reinforced with fibre type 65/60 at a fibre volume fraction of 0.5%

The CBM mix using the gravel aggregate used in the study was nominally identical to that reported by Shahid (1997). However, comparison with Shahid's data shows the increase in 7-day compressive strength with cement content was similar in this study, although the actual strength at a given cement content was lower (Figure 4-6). The difference may be explained by small variations in aggregate grading, in particular the source of the sand, which differed between studies. Variations in the strength of limestone mixes could be explained by differing aggregate sources, grading, water content and the fact that the data in Figure 4-5 are taken from a fibre reinforced material. The results serve to demonstrate the variability in compressive cube strength for very similar materials.

It was observed whilst compacting the specimens that the gravel CBM tended to 'flow' under the action of the vibrating plate, probably due to the rounded aggregate. The limestone CBM, however, was much more stable, and the aggregate appeared to interlock and even crush to form a more solid mass. In the field, this variability in density may be expected to increase as it is dependent on not only the aggregate properties, but also the compaction applied, the pavement depths and the degree of support offered by the lower layers.

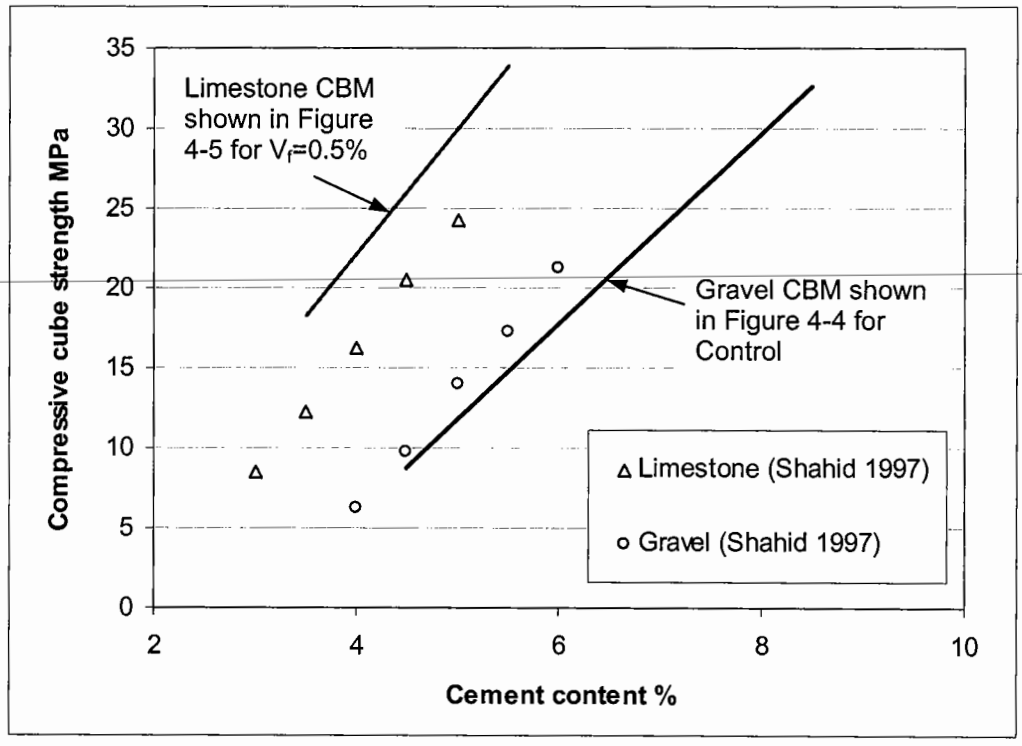

Figure 4-6 Comparison of relationship of 7-day cube strengths with cement content with data reported by *Shahid (1997)*

The mix design of CBM is an important element in ensuring the design strength is achieved. The reduction in material strength in an under-compacted CBM was explored during the field trials, and is discussed in Chapter 5. The data here serve to confirm the variability of CBM as a function of the aggregate type and gradation. Additionally, it should be borne in mind that water content (as reported by Shahid 1997) and method of compaction will further influence the achievable density and material strength. To ensure strength requirements are achieved in the field, all these elements must be carefully controlled. In practice, to allow for the variability in strength, additional cement tends to be added to compensate for the potential reduction.

Effect of fibre volume fraction on compressive cube strength

There was no tendency for the 7-day compressive cube strength of the gravel CBM to increase with fibre volume fraction (Figure 4-7), which is consistent with experience gained using structural grade concrete (ACI committee 544 1996). An increase in cement content is the most effective method to increase this property.

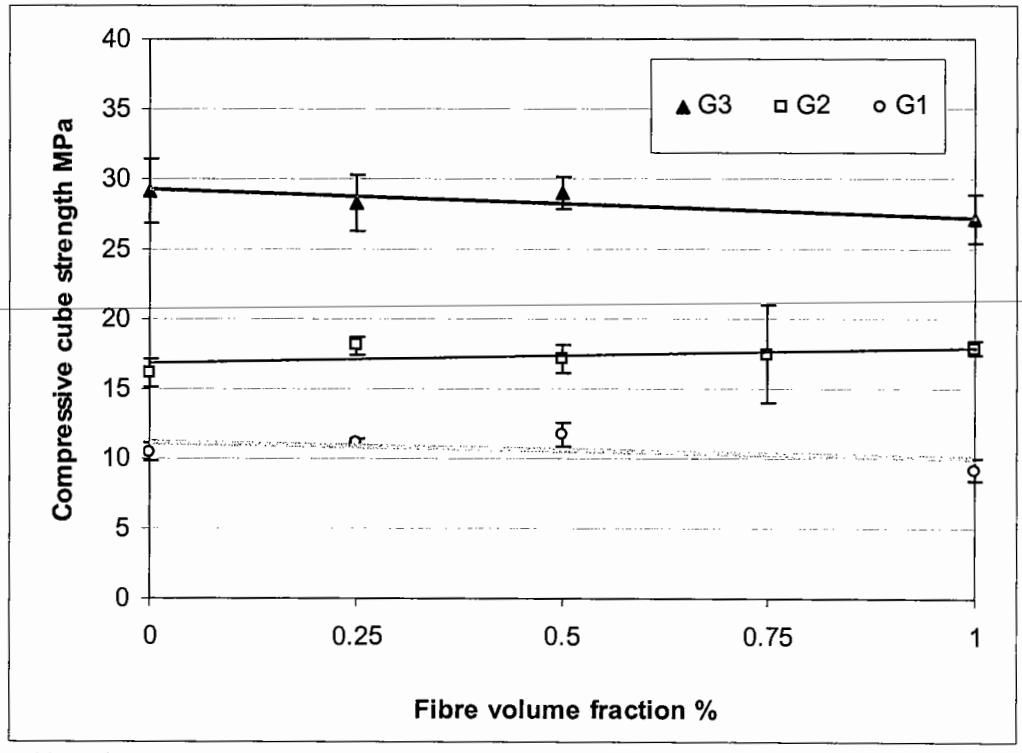

95% confidence limits shown.

Figure 4-7 Relationship between 7-day compressive cube strength and fibre volume fraction for gravel CBM.

In fact, the addition of steel fibres may reduce the compressive cube strength. The cause of this apparent loss in strength with fibre addition could be explained by the failure plane in a compressive cube test being influenced by the orientation of the fibres. During compaction, fibres tend to lay flat under the action of the vibrating plate. When tested, so that the compressed surfaces are flat and parallel, the cube is turned through 90°. The fibres are therefore orientated in a vertical plane in the test, in the same direction as the load is applied. Thus, the orientation of fibres in this test might encourage failure at a lower strength than without fibres. This seems to be supported by data presented by Shahid (1997) in a pilot study of FRCBM, who observed that whilst compressive cube strength did not increase with fibre addition, compressive cylinder strength increased by 12%. In a compressive cylinder test, the fibres would be orientated in a plane perpendicular to the direction of load application, and therefore may not contribute to failure in the same way.

4.4.2 Flexural strength results

The flexural strength results for fibre type 65/60 from the 7-day flexural tests are shown in Table 4-5, and the results for fibre types 65/60, 65/35 and 45/50 from mix G2 is shown in Table 4-6. These data were taken from the full set of flexural results shown in Appendix A.

Mix ref.	C.C %	Fibre volume fraction %							
		Control		0.25		0.5		1.0	
		First crack strength MPa	Ultimate strength MPa	First crack strength MPa	Ultimate strength MPa	First crack strength MPa	Ultimate strength MPa	First crack strength MPa	Ultimate strength MPa
G1	4.5	1.3 (0.2)	1.4 (0.2)	-	-	1.4 (0.1)	1.5 (0.1)	1.4 (0.1)	1.8 (0.3)
G2	6.0	2.2 (0.1)	2.2 (0.1)	-	-	1.9 (0.1)	2.0 (0.1)	2.7 (0.4)	2.9 (0.1)
G3	8.5	2.8 (0.3)	2.8 (0.3)	-	-	3.3 (0.2)	3.7 (0.6)	-	-
L1	3.5	-	-	-	-	2.2 (0.1)	2.4 (0.1)	-	-
L2	4.5	-	-	-	-	3.6 (0.1)	3.7 (0.2)	-	-
L3	5.5	4.4 (0.1)	4.4 (0.1)	4.5 (0.1)	4.5 (0.1)	4.7 (0.2)	5.9 (0.3)	4.7 (0.9)	5.9 (1.1)

Table 4-5 Summary of average 7-day flexural strengths and 95% confidence values (± in brackets) for gravel CBM and limestone CBM using fibre type 65/60

Fibre volume fraction %	Control		Fibre type			
			65/60		65/35	45/50
	First crack strength MPa	Ultimate strength MPa	First crack strength MPa	Ultimate strength MPa	Ultimate strength MPa	Ultimate strength MPa
0	2.2 (0.1)	2.2 (0.1)	-	-	-	-
0.5	-	-	1.9 (0.1)	2.0 (0.1)	2.1 (0.1)	2.2 (0.1)
1.0	-	-	2.7 (0.4)	2.9 (0.1)	2.6 (0.5)	2.4 (0.3)

Table 4-6 Summary of average 7-day ultimate flexural strengths and 95% confidence values (± in brackets) for gravel CBM mix G2 for three fibre types

The results are used to investigate the effects of cement content, fibre volume fraction and fibre type on flexural strength and toughness. Also, the ability of the toughness parameters to distinguish between the fibre types and volume fractions is discussed.

Effect of cement content on strength

The flexural strength of a CBM increases linearly with cement content (Figure 4-8). For a given cement content, the 7-day flexural strength of the CBM using the limestone aggregate was significantly greater than that of the CBM using the gravel aggregate. At a cement content of 5.5%, the ultimate flexural strength of gravel was 1.7MPa, whereas for limestone it was 4.8MPa, an increase of 180%. To achieve a flexural strength of 3MPa, the limestone mix would require approximately 4% cement (by mass of dry aggregate) as opposed to over 7% for the gravel CBM. Generally, local aggregate is used in the CBM to reduce haulage costs, although it is apparent that if alternative aggregates are available, an investigation of the sort carried out above may enable significant cost savings to be made by reducing the cement content of the mix for higher performing aggregate.

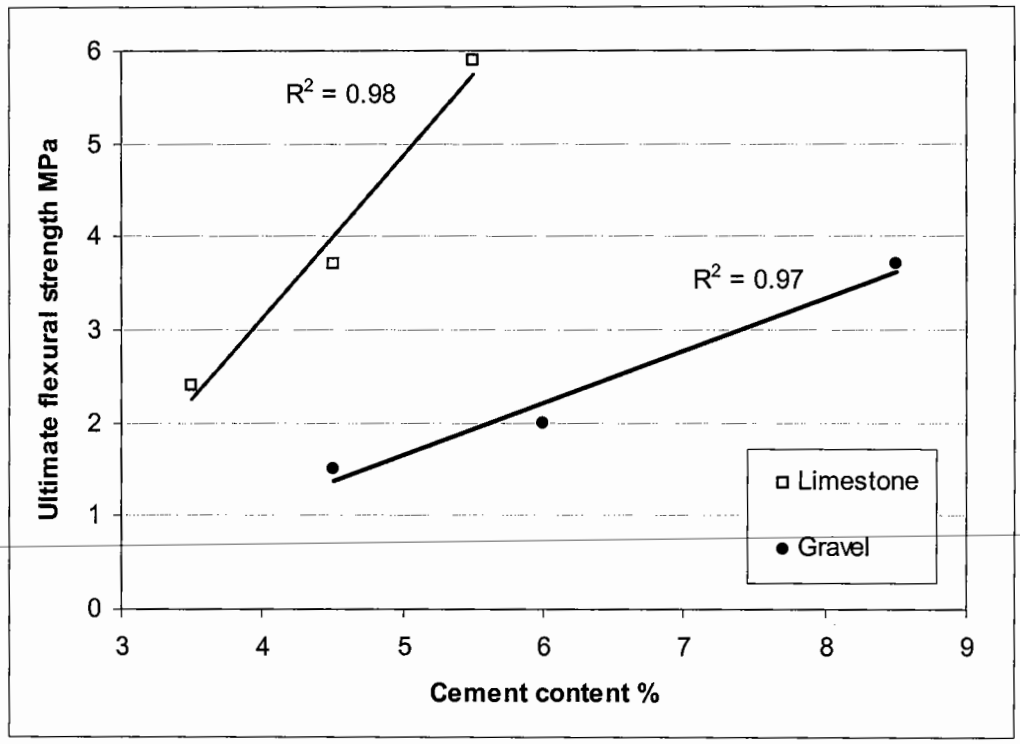

Figure 4-8 Relationship between cement content and ultimate flexural strength using fibre type 65/60 at a fibre volume fraction of 0.5%

Crushed aggregate is known to result in higher compressive and flexural strengths on account of the aggregate shape (Neville 1995). In addition, calcium carbonate contained in limestone may contribute to the cementitious process, further improving the bond between the aggregate and cement paste (William 1986).

Effect of fibre volume fraction on flexural strength

There is a trend for the ultimate flexural strength to increase with fibre volume fraction (Figure 4-9). For mix L3, the increase at a fibre volume fraction of 1% over the unreinforced material is approximately 34%; the increase is therefore significantly less than that produced by a modest increase in cement content, as presented above.

It may therefore be concluded that flexural strength is more readily increased by increasing the cement content rather than steel fibre reinforcement. However, whilst strength increase may not be the primary function of fibres, any increase is beneficial. More importantly, the apparent loss in compressive cube strength with fibre addition (as shown in Figure 4-7) is not replicated in flexure.

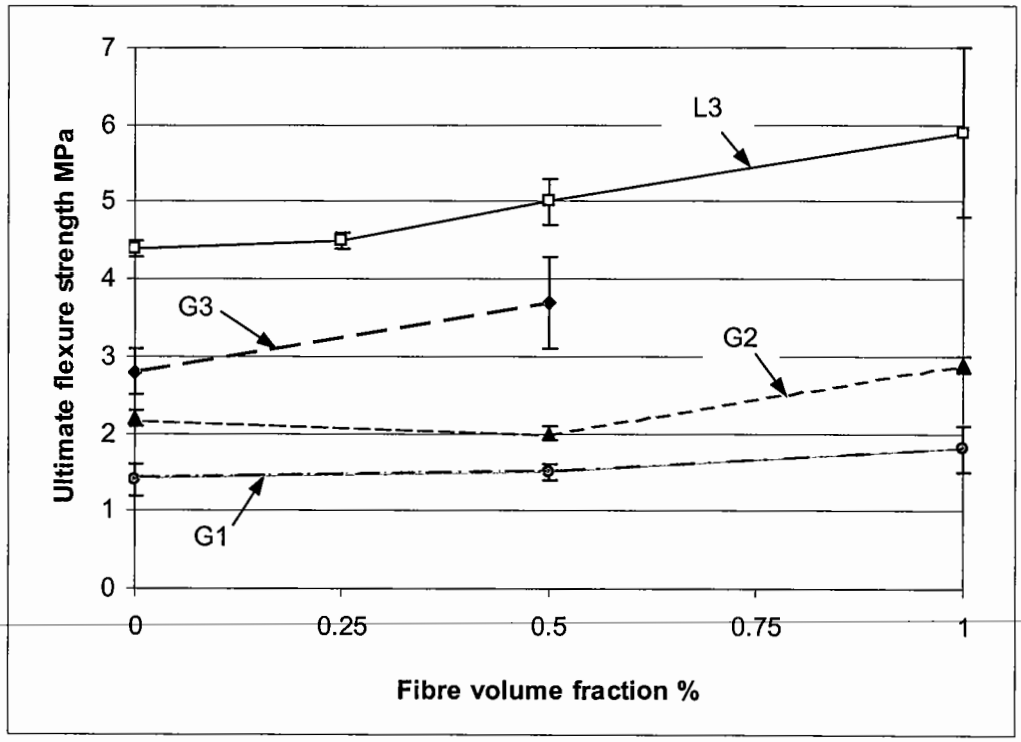

95% confidence limits shown.

Figure 4-9 Relationship between 7-day ultimate flexural strength and fibre volume fraction for fibre type 65/60

The increase in strength shown in Figure 4-9 appears to be bi-linear, with increases in the fibre reinforced specimen strengths occurring at a fibre volume fraction greater the 0.25% (in mix L3) or 0.5% (in mixes G2 and G1). Increases in strength occurred in SFRC when the critical fibre volume fraction in flexure was exceeded, and there is no reason to suspect the behaviour is dissimilar for FRCBM based on these results.

Differences in ultimate flexural strength over first crack flexural strength with fibre volume fraction were most apparent at a fibre volume fraction of 1%. This can be illustrated by comparing the first crack and ultimate strengths of the highest strength mix, L3, and the lowest strength mix, G1 (Figure 4-10). The increase in ultimate flexural strength over first crack flexural strength at a fibre volume fraction of 1% is 25% in mix L3 and 30% in mix G1. However, the 95% confidence limits were also significantly greater at a fibre volume fraction of 1% than at lower fibre volume fractions. This may be explained by the number of fibres bridging the cracked zone. It can also be seen that the first crack strength does not increase appreciably with fibre volume fraction. This is at odds with a theoretical model proposed by Swamy *et al.* (1974), which predicted increases in first crack strength at greater fibre volume fractions and fibre aspect ratios.

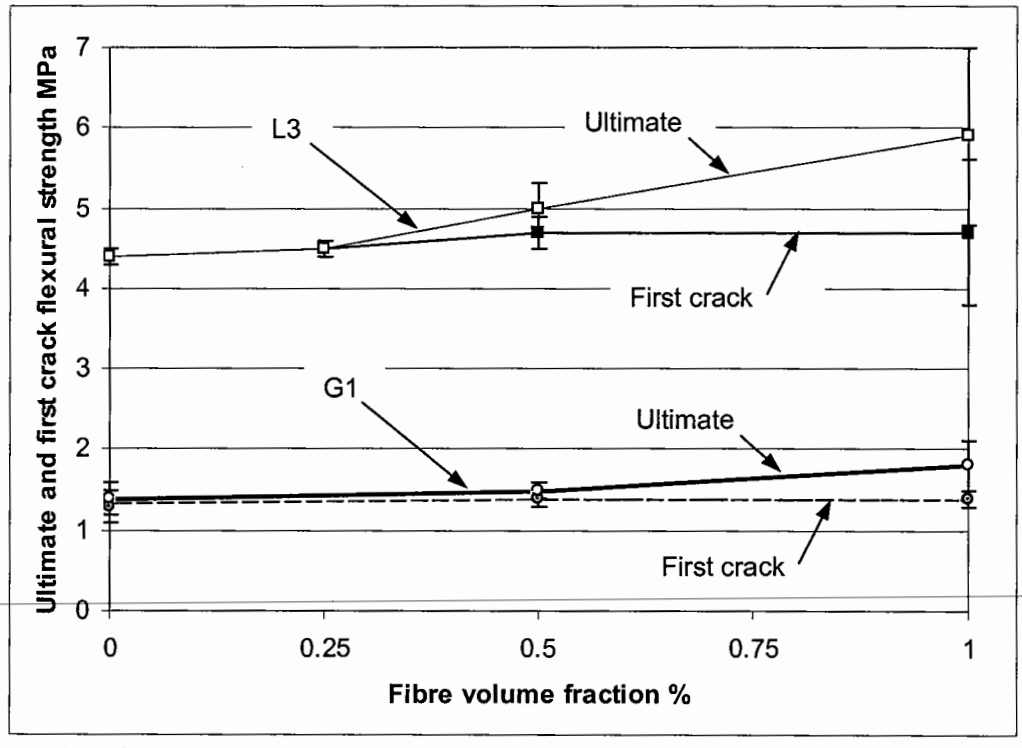

95% confidence limits shown.

Figure 4-10 Relationship between first crack and ultimate flexural strengths for limestone mix L3 and gravel mix G1

As the variability for the first crack and ultimate strength is similar at a given fibre volume fraction (Figure 4-10), it may also be concluded that the fibres are influencing the material behaviour prior to an appreciable crack occurring.

At current costs, it is unlikely that FRCBM will be economic at fibre volume fractions greater than 0.5%. It has been shown that any increase in ultimate flexural strength over first crack flexural strength at this reinforcement level would be low and for all practical purposes, the first crack and ultimate strengths may be assumed to be equal to those of the unreinforced material.

Effect of fibre type on ultimate flexural strength

Fibres with higher aspect ratios were expected to increase the flexural strength of a mix more than fibres with lower aspect ratios, as described in Section 3.2.2. Therefore, fibre types 65/60 and 65/35 are expected to result in a higher ultimate flexural strength than fibre type 45/50. This may be supported to a degree by data at a fibre volume fraction of 1.0% for the gravel CBM mix G2 (Figure 4-11). However, considering the variability in strength of FRCBM already demonstrated, such differences at a fibre volume fraction of 0.5% do not appear to be practically observable.

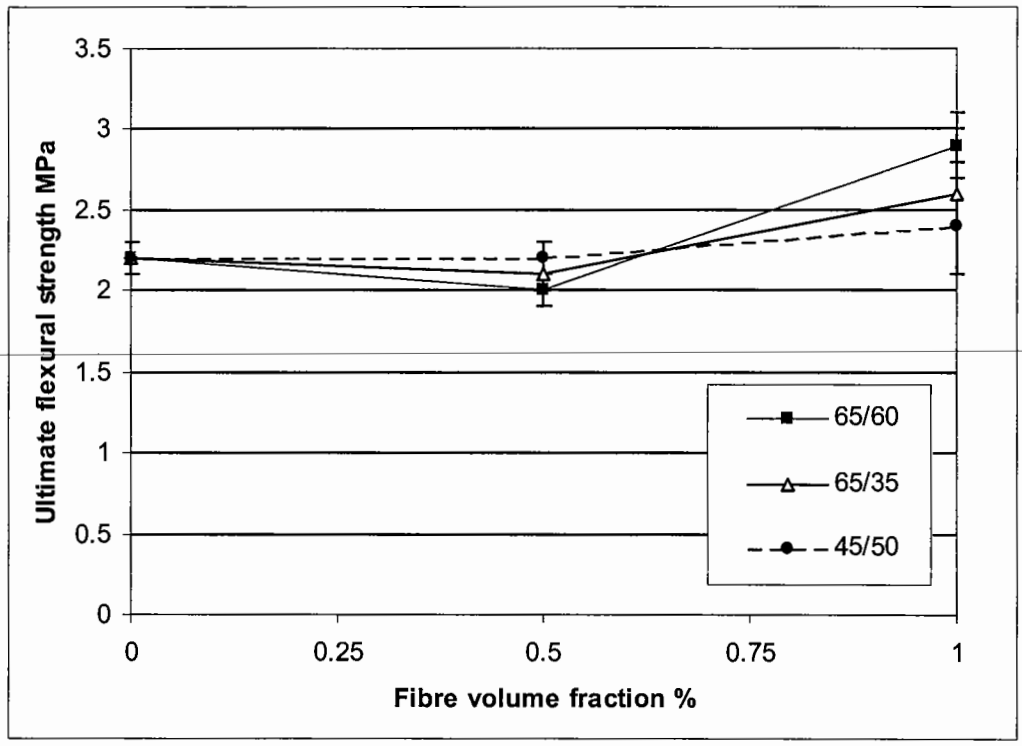

Figure 4-11 Comparison of 7-day ultimate flexural strengths from gravel CBM mix G2 for fibre types 65/60, 65/35 and 45/50

The foregoing results and discussion demonstrates that whilst steel fibres may increase the flexural strength of FRCBM, this will only occur at relatively high fibre volume fractions. At fibre volume fractions considered economical, the first crack and ultimate strengths of FRCBM, and unreinforced strength of CBM, can for all practical purposes be assumed to be equal. Any desired flexural strength increase can be realised more effectively by increasing the cement content and optimising the mix properties (aggregate type, gradation and water content).

4.4.3 Flexural toughness results

The flexural toughness results from the 7-day flexural tests are shown below. The data are presented in Table 4-7 in terms of ASTM toughness indices I_{10} and I_{50} and the flexural strength ratio $R_{e,2}$. The full set of flexural toughness results is shown in Appendix A.

Mix ref.	C.C %	Fibre type	Fibre volume fraction %	Toughness parameter			
				ASTM I_{10}	ASTM I_{50}	σ_{eq} MPa	$R_{e,2}$ %
G1	4.5	65/60	0.5	8.1 (3.8)	43.1 (9.4)	1.2 (0.1)	82 (3)
G2	6.0	65/60	0.5	6.5 (0.1)	27.5 (1.8)	1.6 (0.4)	82 (17)
G3	8.5	65/60	0.5	7.7 (1.4)	33.0 (8.6)	2.2 (0.4)	60 (6)
G2	6.0	65/35	0.5	8.4 (1.7)	38.5 (10.9)	1.7 (0.4)	81 (16)
G2	6.0	45/50	0.5	6.9 (1.6)	27.1 (7.8)	1.2 (0.1)	53 (3)
G2	6.0	65/60	1.0	8.3 (1.3)	40.6 (7.6)	2.7 (0.1)	90 (6)
G2	6.0	65/35	1.0	8.9 (2.8)	43.7 (18.4)	1.9 (0.9)	75 (21)
G2	6.0	45/50	1.0	6.7 (1.4)	30.9 (11.2)	1.7 (0.1)	68 (4)
L1	3.5	65/60	0.5	7.5 (1.6)	31.3 (11.4)	1.6 (0.4)	68 (16)
L2	4.5	65/60	0.5	7.9 (1.8)	34.4 (11.8)	2.6 (0.7)	71 (15)
L3	5.5	65/60	0.25	5.3 (0.2)	18.0 (5.9)	1.7 (0.7)	39 (16)
L3	5.5	65/60	0.5	10.9 (0.6)	52.4 (2.8)	4.4 (0.3)	89 (7)
L3	5.5	65/60	1.0	10.9 (3.1)	55.2 (14.5)	5.0 (0.9)	86 (8)

Table 4-7 Summary of average 7-day flexural toughness and 95% confidence values (± in brackets) for gravel and limestone CBM using three fibre types

Load-deflection plots from unreinforced mixes G1 and G3 and FRCBM mixes G1 and G3 with a fibre volume fraction of 0.5% are compared in Figure 4-12 to illustrate the different behaviour exhibited post-crack by fibre reinforced specimens.

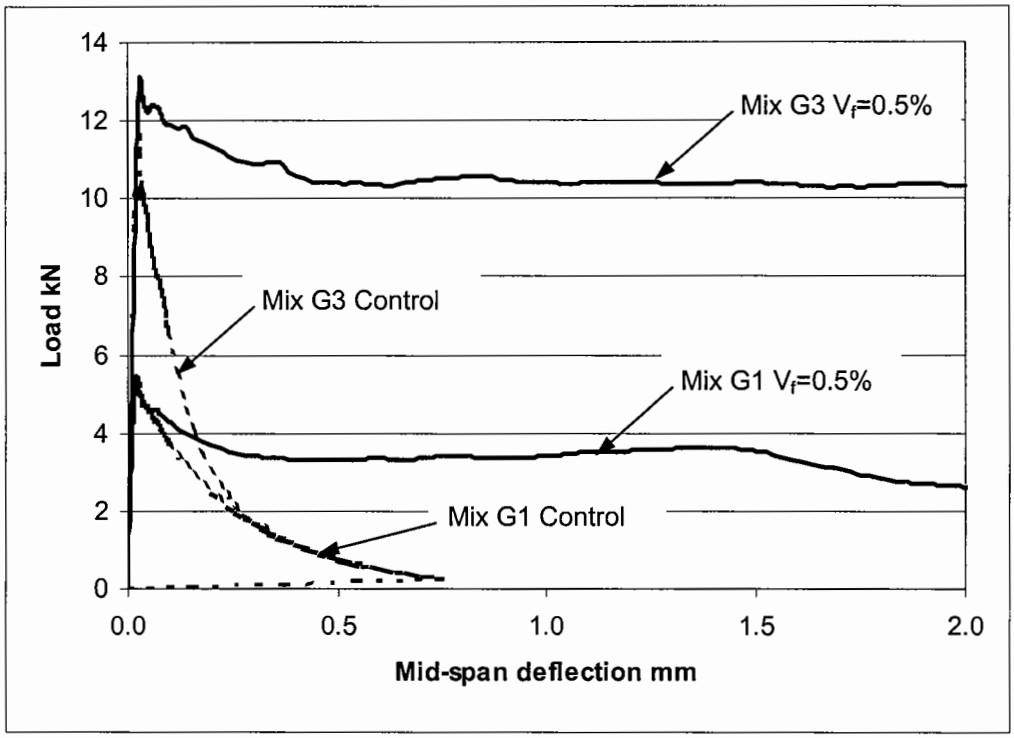

Figure 4-12 Load-deflection plots for CBM and FRCBM reinforced at 0.5% using fibre type 65/60

Once the first crack strength of the unreinforced specimens had been reached, the CBM was unable to carry any significant load post-crack, resulting in a brittle failure. However, the FRCBM was able to carry significant load to a deflection of 2mm, where the test was stopped, even in the lower strength FRCBM mix.

The post-crack behaviour of the FRCBM was compared using various toughness values, described in Sections 3.5.4 and 3.5.5. The objectives of the comparisons were to assess any effect of fibre type and fibre volume fraction on the toughness characteristics, and to comment on the suitability of the toughness values for use in design.

Effect of flexural strength on ASTM toughness

The effect of strength on toughness was investigated using ASTM toughness indices I_{10} and I_{50}, the equivalent flexural strength (σ_{eq}) and the flexural strength ratio ($R_{e,2}$). The objectives were to comment on the influence of the matrix strength on the various toughness parameters, and to determine whether one toughness parameter was preferable to the others.

Overall, there was a general tendency for the ASTM toughness to increase by a small amount (discounting the result from the lowest strength gravel CBM) (Figure 4-13). The ASTM toughness indices have been shown to be a measure of post-crack ductility, independent of matrix strength effects (Section 3.5.4). The increases in toughness with strength, demonstrated by Figure 4-13, are therefore considered to be due to an improvement in the fibre matrix bond. However, over the CBM strength range studied (7-day compressive cube strengths from 10MPa to 35MPa), there is a significant increase in toughness, although the variability is also high by comparison to the increase (shown by 95% confidence limits).

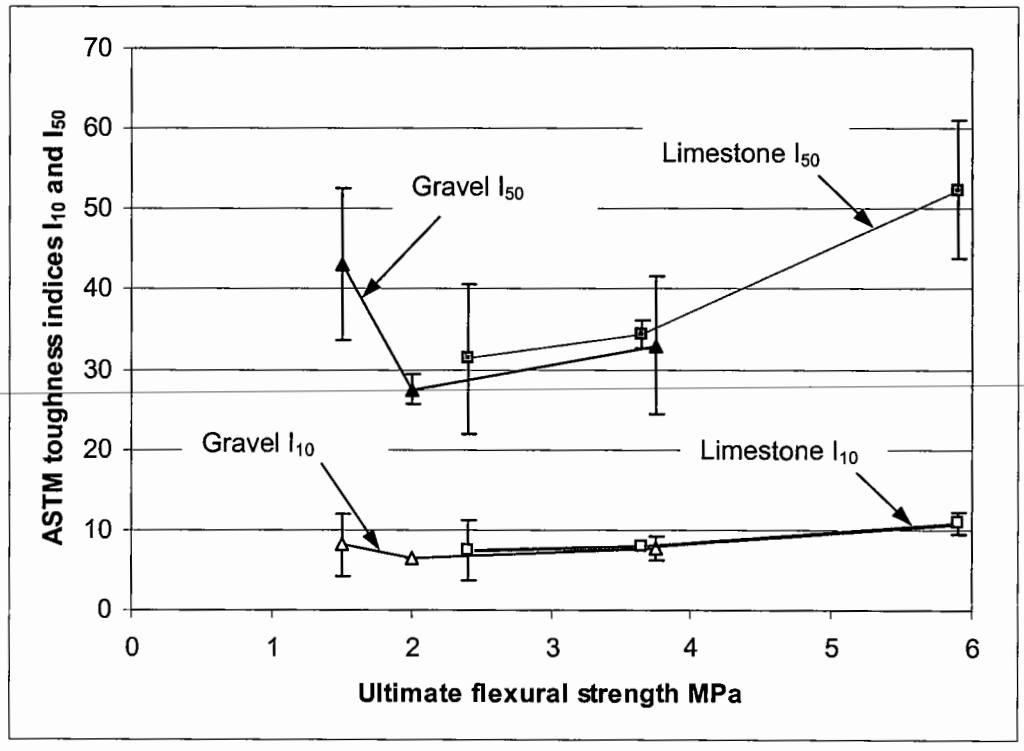

Figure 4-13 ASTM toughness indices I_{10} and I_{50} for gravel and limestone CBM using fibre type 65/60 at a fibre volume fraction of 0.5%

ASTM C 1018 (1997) gives guidance on the acceptable variability of the toughness indices I_5, I_{10} and I_{20}, measured in terms of the coefficient of variability. The upper limits given by ASTM are compared to those obtained in this study and shown in Appendix A (Table 4-8).

Mix ref.	[1]CC %	Fibre type	Fibre volume fraction %	Coefficient of variability %			
				ASTM I_5	ASTM I_{10}	ASTM I_{20}	ASTM I_{50}
ASTM limit				**12**	**14**	**16**	**None given**
G1	4.5	65/60	0.5	33.9	33.6	27.7	19.2
G2	6.0	65/60	0.5	4.1	0.9	2.2	5.7
G3	8.5	65/60	0.5	9.5	17.8	27.2	22.9
G2	6.0	65/35	0.5	13.9	17.8	21.5	25.0
G2	6.0	45/50	0.5	18.7	20.7	25.2	25.5
G2	6.0	65/60	1.0	15.7	14.0	18.1	16.6
G2	6.0	65/35	1.0	18.2	27.4	35.3	37.2
G2	6.0	45/50	1.0	14.8	18.9	26.1	32.1
L1	3.5	65/60	0.5	10.0	18.6	25.6	32.2
L2	4.5	65/60	0.5	12.9	19.7	26.1	30.3
L3	5.5	65/60	0.25	4.4	2.9	11.4	29.2
L3	5.5	65/60	0.5	9.2	5.1	8.5	4.8
L3	5.5	65/60	1.0	12.7	24.9	17.6	23.1

Note: [1]CC = Cement content

Table 4-8 Summary of coefficients of variation for ASTM toughness indices

Table 4-8 shows that, generally, as the ASTM index increases, the variability increases, although it can be seen that there are very large differences within the coefficient of variability measured. Comparisons with the limits proposed by ASTM show that generally the variability of the FRCBM was greater than that allowable under ASTM C 1018 (1997), often by a large amount. The greater variability in CBM when compared to concrete may, in part, be due to the method of specimen preparation (compaction using a Kango hammer as described in Section 4.2.2). Clearly, the fact that the average was based on three tests only would increase the variability.

Effect of flexural strength on equivalent flexural strength

The equivalent flexural strength increases with ultimate flexural strength, as shown in Figure 4-14. Regression lines (through zero) at a fibre volume fraction of 0.5% suggest the relationship between ultimate flexural strength and equivalent flexural strength is not dependent on aggregate type.

It is also evident there was a measurable increase in equivalent flexural strength between fibre volume fractions of 0.5% and 1%, and a decrease between 0.5% and 0.25%, as shown for fibre type 65/60. Equivalent flexural strength measured for fibre type 65/35 suggests the performance is similar to the 65/60 fibre, and the 45/50 fibre was shown to perform slightly less well at the volume fractions of 0.5% and 1.0%. The comparative performance of the fibre types is in agreement with the ASTM toughness index I_{50} reported above.

A discussion regarding the relative advantages between these toughness measurements for research and design, with respect to distinguishing between fibre types, volume fractions and material strengths, is included at the end of this section.

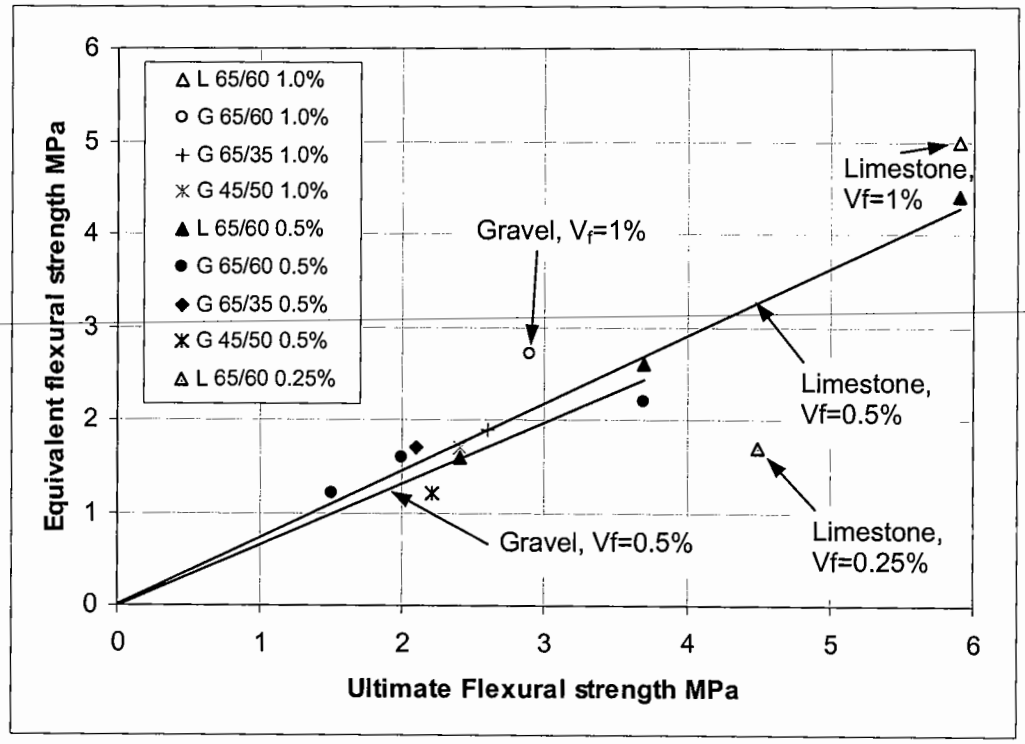

Figure 4-14 Relationship between equivalent flexural strength and ultimate flexural strength for gravel CBM and limestone CBM using 65/60 fibre

Effect of flexural strength on flexural strength ratio

There did not appear to be any correlation between the flexural strength ratio and the ultimate flexural strength (Figure 4-15). In fact, the pattern of the results was less varied than those reported for the ASTM toughness indices in Figure 4-13. It may therefore be stated at this stage that if ASTM indices are representative of fibre performance, largely independent of strength (and the above discussion suggests they are), then the flexural strength ratio has the same advantages.

An advantage of the flexural strength ratio over the ASTM indices is that the first crack deflection and strength do not need to be interpreted; only the ultimate strength is required, which is more easily determined.

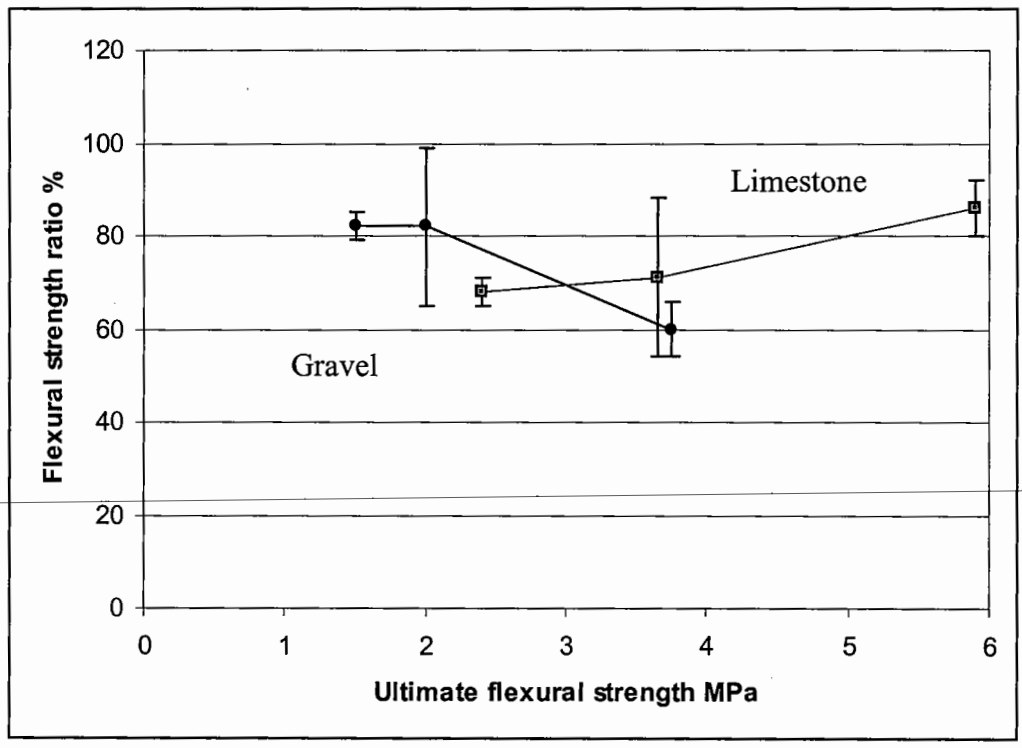

Figure 4-15 Relationship between ultimate flexural strength and flexural strength ratio for gravel CBM and limestone CBM using fibre type 65/60

Effect of fibre type on toughness

The comparative post-crack ductility of the composite using fibre types 65/60, 65/35 and 45/50 was demonstrated using ASTM index I_{50}, equivalent flexural strengths and the flexural strength ratio.

ASTM I_{50} indices were compared for fibre types 65/60, 65/35 and 45/50 (Figure 4-16). It should be noted that the indices I_{50} were less than 50 - the value that theoretically denotes perfectly elastic-plastic behaviour (see Section 3.5.4). The I_{50} index for an unreinforced material (not shown in Figures) is by definition unity. It should also be noted at this stage that these fibres were all of similar shape, having hooked ends. These data were also compared to data presented by Munt (1999), who carried out tests on a nominally identical gravel FRCBM mix to that used in this study, but using a fibre type with a conical end, referenced 54/cone (aspect ratio 54, length 54mm, diameter 1.0mm).

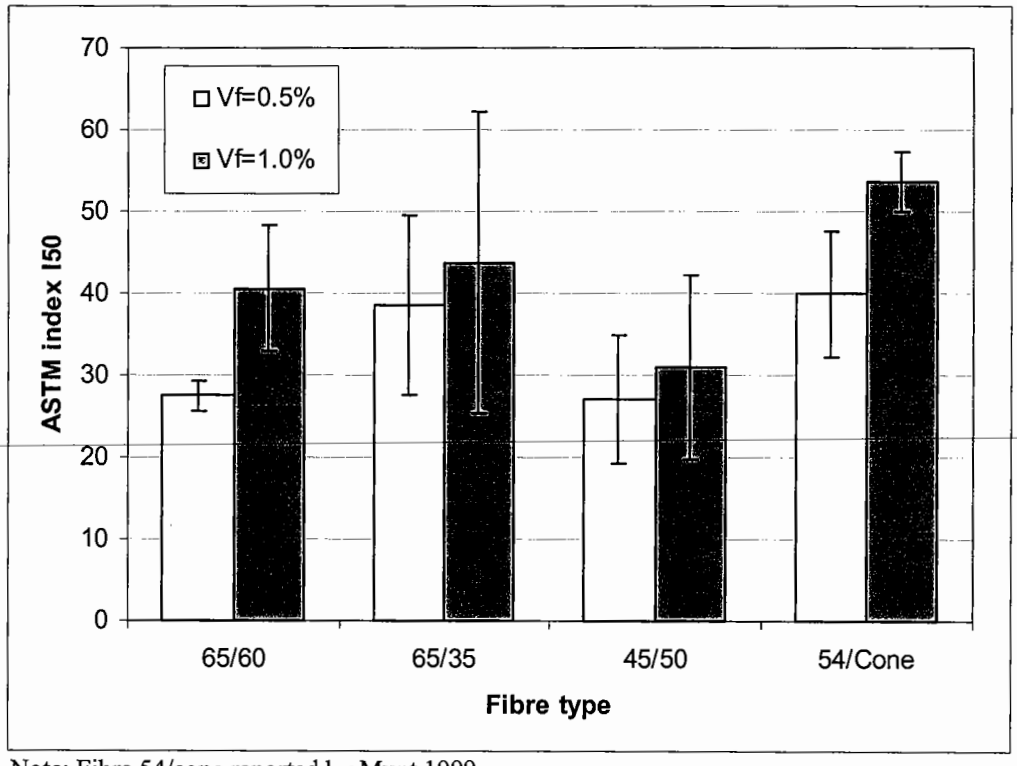

Note: Fibre 54/cone reported by Munt 1999.

Figure 4-16 Comparison of ASTM toughness index I_{50} for gravel CBM mix G2 reinforced with various fibre types

The expectation was for the higher aspect ratios to exhibit greater toughness characteristics than lower aspect ratio fibres, based on the review (Section 3.2.2). This was supported to a degree by the hook ended fibres at a fibre volume fraction of 1%, where fibre type 45/50 (aspect ratio 45) exhibited lower ASTM toughness than the 65/60 and 65/35 fibres (aspect ratio 65). However, Munt's tests showed that FRCBM using conical ended fibres has similar or higher I_{50} index values than those reported for the hook-ended fibres, despite the lower aspect ratio.

It is evident that the magnitude of the differences is significant. At a fibre volume fraction of 0.5%, the increase is 50% between the minimum value for the 45/50 fibre (27.1) and maximum value for the 54/conical fibre (39.9). At 1%, the difference is 70% between the minimum (30.9) and maximum (53.6) values. This difference is more significant than an increase in toughness for a given fibre between volume fractions 0.5% and 1% (e.g. value of 39.9 and 53.6 for 54/cone fibre, or 35%).

It is apparent that the fibre shape is at least partly responsible for post-crack ductility, though, for similar shapes, the aspect ratio may be used to distinguish between fibre types. Considering the fibre type therefore, it follows that the post-crack ductility may be improved by improving the anchorage by modifying the shape and increasing the aspect ratio. New shapes of fibre continue to be researched and marketed by fibre manufactures, though there is no simple technique to predict the effectiveness of the anchorage other than by experience and testing of the type described here. Aspect ratio may readily be increased by increasing the fibre length and reducing the diameter, though there are practical limits to the aspect ratio if balling of the fibres during mixing is to be avoided. Hence practical limitations exist on the magnitude of this parameter, and indeed Munt (1999) reported mixing problems with the conical ended fibre.

In mix G2, the average equivalent flexural strengths for fibres 65/60 and 65/35 were found to be similar at a fibre volume fraction of 0.5%, although at 1% the 65/60 fibre performed significantly better (Figure 4-17). However, the variability of the mix using fibre type 65/35 was found to be much higher than the variability with the 65/60 fibre, in particular at a volume fraction of 1%. The average equivalent flexural strength with the 45/50 fibre was found to marginally less than with the other fibres.

These results are consistent with the ASTM toughness indices, shown above. Therefore in mixes of nominally identical strength, it is evident that the equivalent flexural strength may be used to compare fibre types and fibre volume fractions.

Table 4-5 showed that the ultimate flexural strengths of mix G2 at fibre volume fractions of 0.5% and 1.0% were 2.0MPa and 2.9MPa respectively (for the 65/60 fibre). It can be seen from Figure 4-17 that, within the 95% confidence limits, the equivalent flexural strengths of the 65/60 and 65/35 fibres at volume fractions 0.5% and 1.0% approach or exceed that value. (Note that the ultimate flexural strength is the highest strength achieved immediately after the beam cracks, and does not include strength increases above the 'ultimate' brought about by the fibres). However, the equivalent flexural strength using the 45/50 fibre is significantly less than the ultimate strength of the 45/50 fibre, since at 0.5% the ultimate flexural strength is 2.2MPa and at 1% the value is 2.4MPa (Table 4-6). This is presenting the data shown in Figure 4-13 to further illustrate the lower toughness achieved using fibre type 45/50, demonstrating at a given material strength, the equivalent flexural strength is able to distinguish between fibre types.

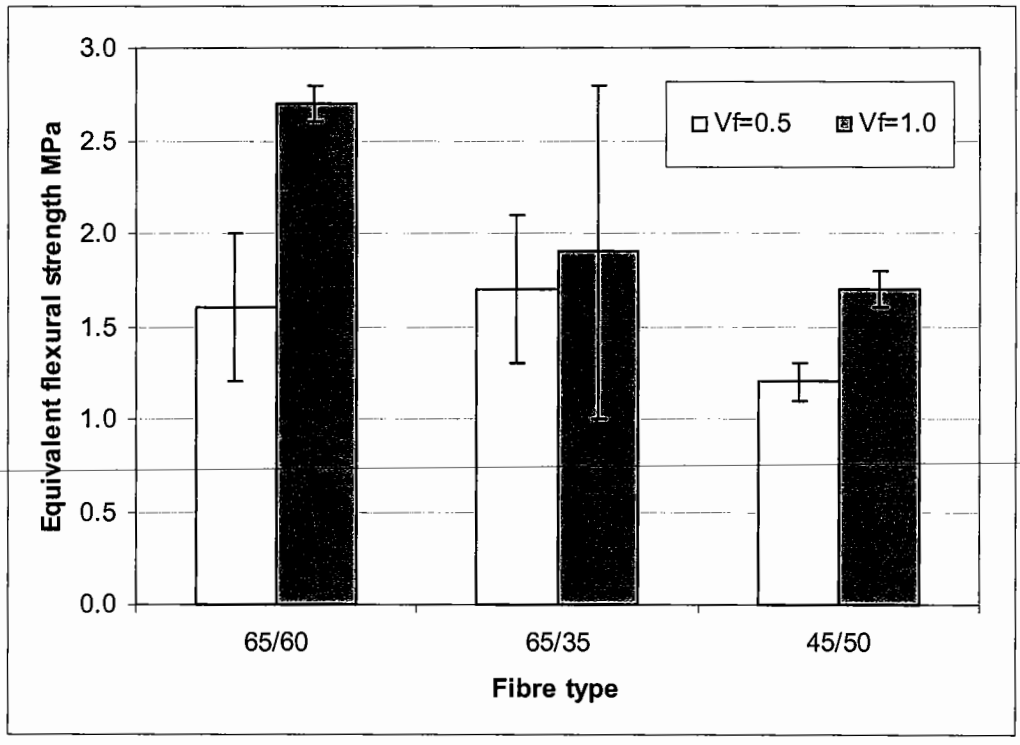

Figure 4-17 Comparison of equivalent flexural strength for fibre types 65/60, 65/36 and 45/50 for mix G2

The relationship between fibre volume fraction and the flexural strength ratio is shown in Figure 4-18. This demonstrates that the flexural strength ratio is similar at 0.5% and 1.0% fibres. The difference between a fibre volume fraction of 0.5% and 1.0% is less marked than is shown by the ASTM toughness index I_{50} and equivalent flexural strength, shown above. This is because the flexural strength ratio is based on the ratio of the equivalent and ultimate flexural strengths. At a volume fraction of 1.0%, it was shown that the ultimate flexural strength exceeds the first crack flexural strength by up to 30% (see Section 4.4.2). A relative increase in equivalent flexural strength also occurs at this fibre volume fraction, hence the flexural strength ratio at this fibre volume fraction is similar to that when the fibre volume fraction is 0.5%. Therefore, when the ultimate flexural strength is significantly greater than the first crack flexural strength, it may be concluded that the flexural strength ratio does not readily demonstrate the comparative improvement in toughness.

If an increase in the ultimate strength over the first crack flexural strength is likely to occur, the flexural strength ratio will not readily distinguish between fibre types over a range of fibre volume fractions.

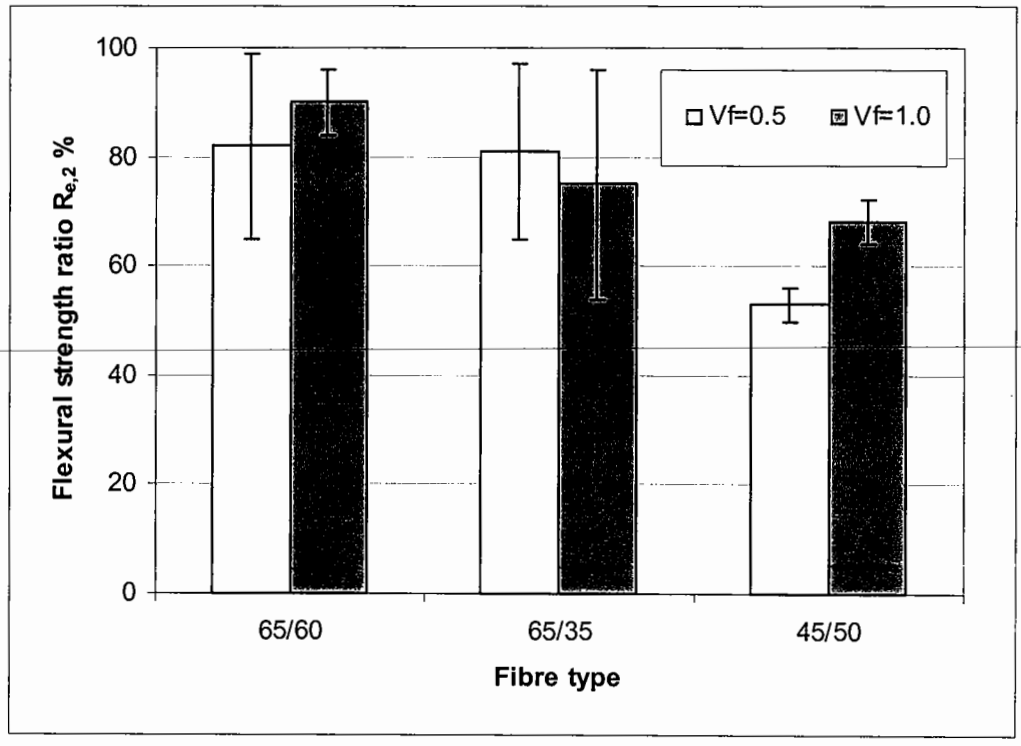

Figure 4-18 Relationship between flexural strength ratio and fibre volume fraction for mix G2 using fibre types 65/60, 65/35 and 45/50

Discussion of flexural toughness measurements

The foregoing discussion presents three parameters that are used to determine the toughness characteristics of a fibre reinforced cementitious material. It has been demonstrated that the ASTM index is able to distinguish between fibre types and fibre volume fractions, and has the advantage over the other methods of being independent of material strength. However, the determination of the ASTM toughness indices requires interpretation of the first crack deflections and strength. This means that the calculated values, which are themselves somewhat tedious to determine, may vary between investigators. As this method calculates the toughness, independent of matrix strength, it is perhaps the preferable parameter to use in research to distinguish between fibre types and volume fractions. Additionally, by using different toughness indices (I_5, I_{10}, I_{20} etc) some account of the envisaged in-service deflections can be taken.

The equivalent flexural strength is a measure of toughness to a defined deflection, and is therefore dependent on the flexural strength of the material. However, this parameter may be used to compare fibre types and volume fractions in materials of nominally the same strength. It has the advantage over the ASTM toughness values of not requiring interpretation of the first crack deflection or strength, and of having a value that pavement engineers familiar with flexural strength values are able to relate to.

The flexural strength ratio does not require interpretation of the first crack, but does not readily distinguish between fibre types over a range of fibre volume fractions.

It is therefore suggested that, whilst the ASTM toughness indices are most necessary for research, the equivalent flexural strength may be used in practice. It is proposed that, for design, an ultimate flexural strength and equivalent flexural strength is specified. The ultimate flexural strength will enable the designer to determine the cement content for a given aggregate type, grading and water content, and the equivalent flexural strength can be used to determine the fibre volume fraction for a given fibre type.

4.4.4 Indirect tensile strength results

Indirect tensile tests have the potential advantage over flexure tests of readily enabling comparisons between laboratory prepared specimens and the *in situ* material by testing cores. Laboratory specimens are relatively simple to prepare, and compaction is better controlled than in the preparation of the flexure beams. However, such a test has not met with universal approval. Williams (1986) concluded after 20 years of using the test that "it involved unrealistic assumptions, did not simulate the behaviour of a layer under load and that the maximum load sustained was dependent more on wedges that occur in the vicinity of the packing strips rather than the load to induce splitting." The latter criticism should be noted as specimens tested in indirect tension as part of this study universally exhibited 'wedging' following cracking (Plate 4-2). The subsequent post-crack behaviour must therefore be dependent in some way on this, though the precise contribution to the toughness characteristics is not easily quantifiable. Nonetheless, researchers have advocated this approach using a roller compacted concrete (Nanni 1989), and CBM reinforced with steel fibres (Shahid 1997). If an empirical relationship can be demonstrated with the flexure tests, this test may still have some practical potential.

Plate 4-2 Cylinder specimen showing 'wedging'

The average indirect tensile strength and toughness results at 7-days are shown in Table 4-9. Toughness is expressed in terms of the indirect tensile strength ratio (R_{SP}), defined in Section 4.3.2. The full set of results is shown in Appendix A.

Fibre volume fraction %	Fibre type 65/60			Fibre type 65/35	Fibre type 45/50
	First crack strength MPa	Ultimate strength MPa	Indirect tensile strength ratio %	Indirect tensile strength ratio %	Indirect tensile strength ratio %
0	1.0	1.0	0.1 (0)	0.1 (0)	0.1 (0)
0.1	1.0	1.0	35.9 (5.7)	30.2 (3.8)	-
0.2	1.0	1.1	35.4 (5.0)	-	-
0.25	1.1	1.2	50.0 (5.2)	35.5 (4.4)	36.4
0.5	1.1	1.3	59.2 (6.2)	61.0 (8.7)	44.7
0.75	1.1	1.3	62.3 (4.3)	65.2 (7.8)	63.9
1.0	1.1	1.4	64.8 (2.9)	59.1 (4.5)	54.8

Table 4-9 Summary of average 7-day flexural strengths and indirect tensile strength ratio with 95% confidence values (± in brackets) for gravel CBM G2

Effect of fibre volume fraction on indirect tensile strength

Figure 4-19 shows the effect of fibre volume fraction on the indirect tensile strength for gravel CBM mix G2 using the 65/60 fibre. The ultimate and first crack strengths are indicated. It is apparent in indirect tension that an increase in the ultimate strength over the first crack strength occurs at a fibre volume fraction as low as 0.2%, which is at a significantly lower fibre volume fraction than occurred in flexure. The increase in ultimate strength over the unreinforced material is approximately 30% at a fibre volume fraction of 0.5%, and 40% at a volume fraction of 1.0%. Shahid (1997) reported an increase of 38% in ultimate over first crack indirect tensile strength using a hook-ended steel fibre of aspect ratio 60 and length 30mm at a fibre volume fraction (V_f) of 1%.

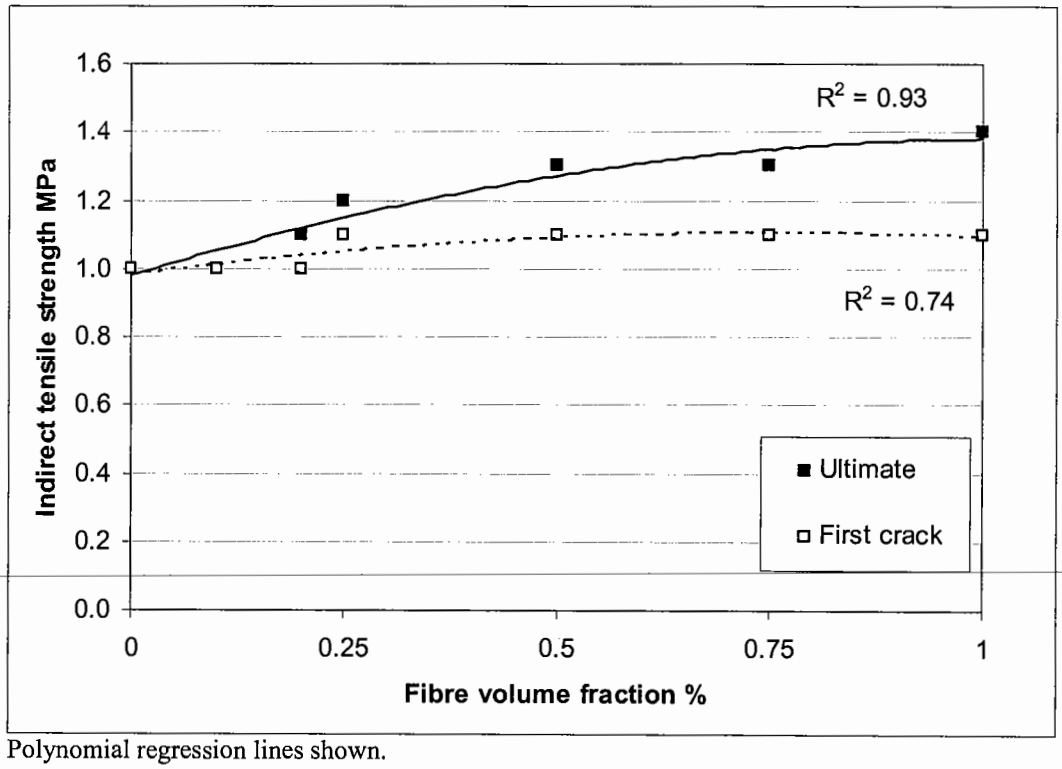

Polynomial regression lines shown.

Figure 4-19 Relationship between indirect tensile strength and fibre volume fraction for gravel aggregate CBM G2 using fibre type 65/60

It is worth noting that an increase in the ultimate over the first crack strength occurs at a V_f as low as 0.2%. This may be contrasted with the increase in ultimate over first crack strength in flexure, which occurred when $V_f > 0.5\%$ (see Figure 4-10). This may be influenced (perhaps significantly) by the wedging. Shear stresses generated at the wedge

would be expected to be affected by the interface at the wedge, and if fibres bridge this zone, the strength and post-crack behaviour may be enhanced. Such an enhancement is peculiar to this test, which may explain why an increase in ultimate indirect tensile strength occurred at a fibre volume fraction as low as 0.2%.

4.4.5 Indirect tensile toughness results

At a fibre volume fraction of 0.5% (Figure 4-20), an increase in load following first crack load occurs in indirect tension. No sudden decrease in load occurs. This may be contrasted with the flexural test behaviour, shown in Figure 4-12, where generally no increase in strength after first crack occurs, and there is a decrease in strength as the mid-span deflection increases.

In a theoretical model for the direct tensile test, as presented in Section 3.4.1, a substantial decrease in load is predicted to occur following first crack. However, once a 'steady state' has been established, in theory the composite material is able to carry load to significant deformations.

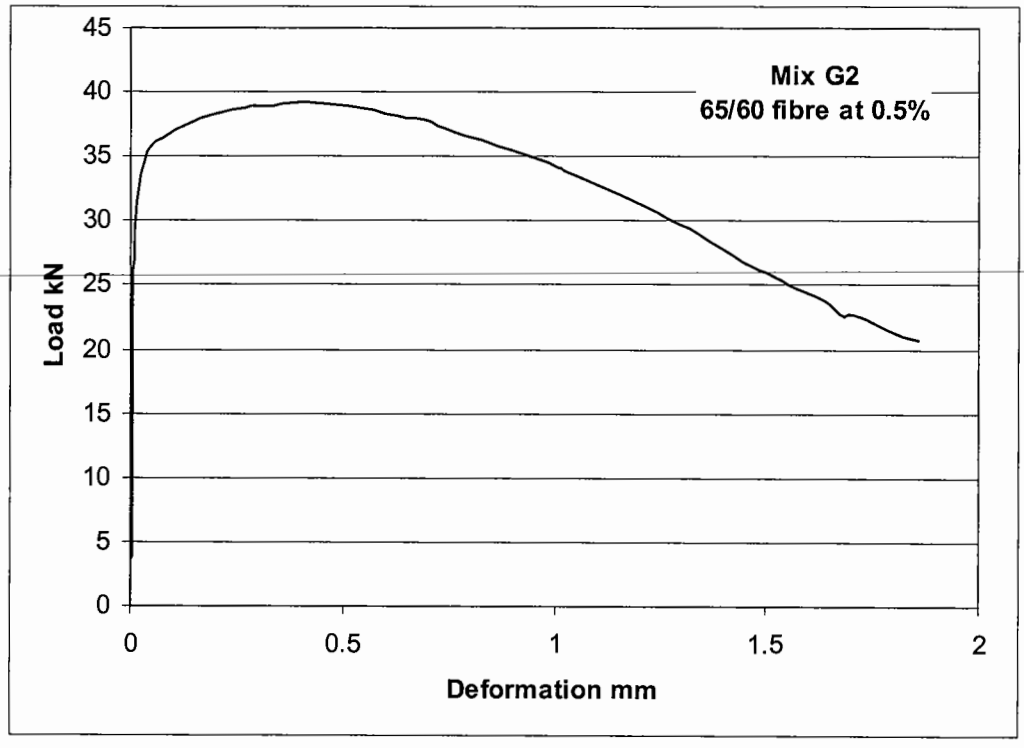

Figure 4-20 Typical load-deflection plots in indirect tension and flexure for mix G2 and model in direct tension.

Effect of fibre volume fraction and fibre type on indirect tensile toughness

Toughness for the three steel fibre types and fibre volume fractions was compared using the indirect tensile strength ratio (R_{SP}). Figure 4-21 shows the effect of fibre volume fraction on R_{SP} to a deformation of 1.5mm, for fibre types 65/60, 65/35 and 45/50. Even at very low fibre volume fractions, a significant toughness was recorded. The regression line demonstrates that the 65/60 and 65/35 fibres performed similarly, and the 45/50 fibre performed less well. This is consistent with the results from the flexure tests. There is no guidance on the variability, though the coefficient of variability shown for the specimens in Appendix A is generally less than that from the flexural tests.

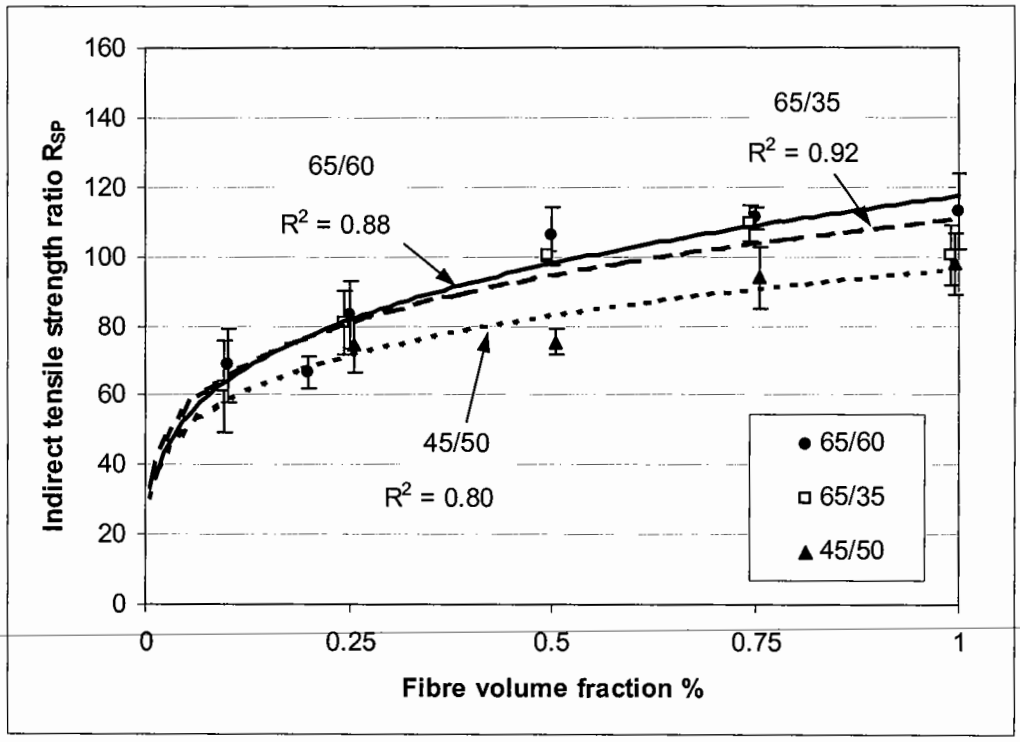

Figure 4-21 Increase in indirect tensile strength ratio with fibre volume fraction for gravel aggregate CBM (G2)

It would appear that the indirect tensile test is able to distinguish between fibre types and fibre volume fractions, and the results do not contradict the flexural strength results. However, it is not clear what effect wedging had on the determination of strength and toughness parameters of a fibre reinforced composite. These concerns should be addressed if this test is to be adopted as a site and laboratory means of determining FRCBM properties.

4.4.6 Inter-relationships between compressive, flexural and indirect tensile parameters

Relationships between compressive strength and flexural strength

The relationship between compressive cube strength and flexural strength is of interest as cube strength is commonly used as a site control, whereas pavement analysis requires knowledge of flexural stresses. There is no unique relationship between cube and flexural strength for a CBM (Croney and Croney 1991). The relationship is dependent on aggregate properties and grading. Figure 4-22 compares data from this study based on first crack flexural strengths with a relationship assumed for CBM using gravel aggregate and crushed rock aggregate by Parry *et al.* (1999). The gravel CBM and limestone CBM used in this study lie between the relationships used by Parry, demonstrating that such generalised expressions cannot be relied upon to determine flexural strength from compressive cube strength.

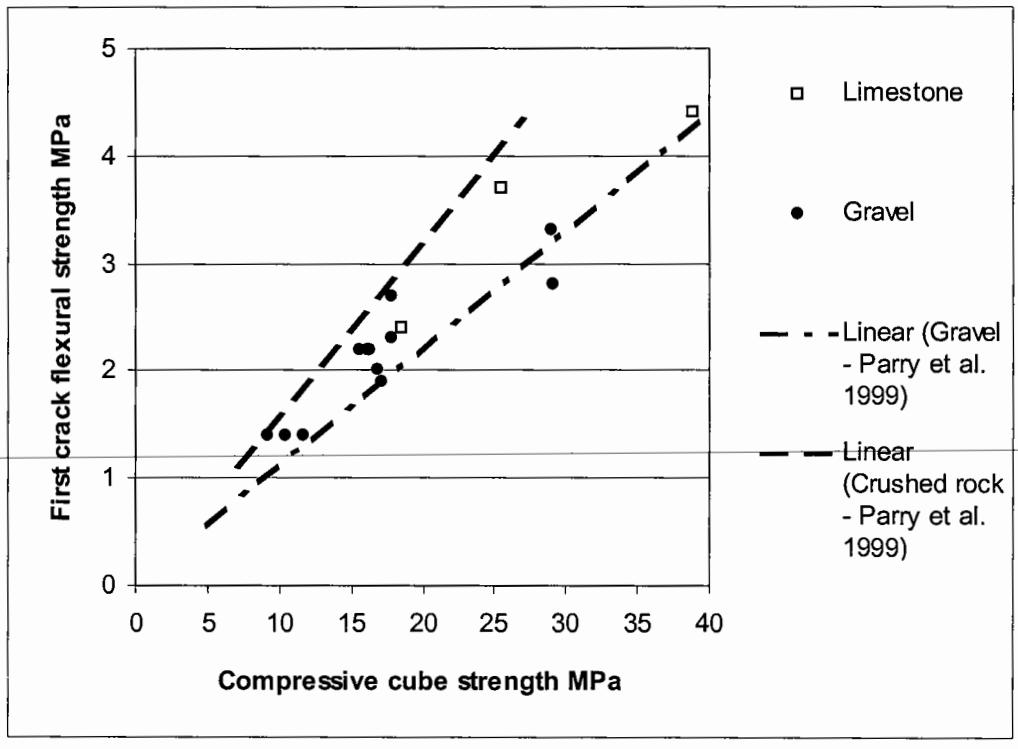

Figure 4-22 Compressive strength and first crack flexural strength relationship at 7-days compared to data reported by *Parry et al. 1999*

The relationship further demonstrates that the strength properties of CBM and FRCBM must be determined on an individual mix basis. In particular, the prediction of flexural strength based on cube strength could result in significant error.

Relationship between flexural toughness and indirect tensile toughness

Flexural toughness and indirect tensile toughness were correlated using the flexural strength ratio ($R_{e,2}$) and the indirect tensile strength ratio (R_{SP}) for the three fibre types using gravel CBM mix G2 (Figure 4-23). These data were shown in Tables 4-7 and 4-9. There appeared to be a relationship between the strength ratios in spite of the concerns regarding wedging in indirect tension. However, in order to use such a relationship with confidence, more tests would be required at a range of material strengths and fibre types and volume fractions, to investigate the effects of wedging.

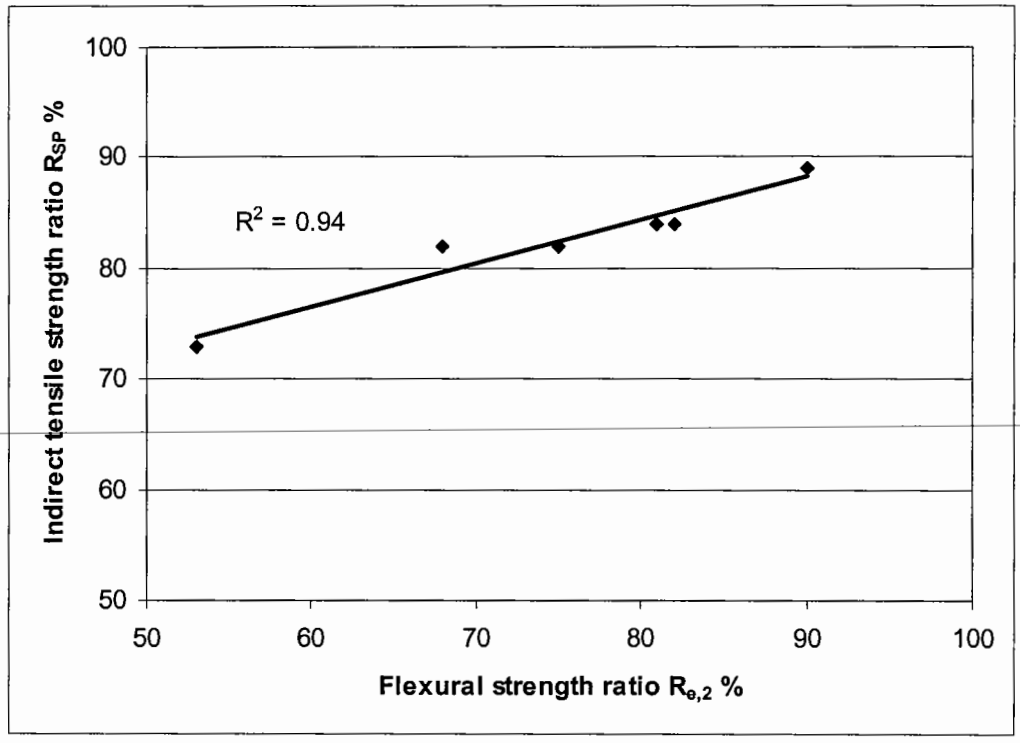

Figure 4-23 Correlation between flexural strength ratio and indirect tensile strength ratio for gravel CBM G2

4.4.7 Variability in material properties

The variability in material properties is investigated using coefficients of variability for fibre type 65/60, shown in Appendix A and summarised below in Table 4-10.

	Parameter	G2			L3		
		Control	0.5	1.0	Control	0.5	1.0
Compressive cube tests	Strength σ_{cu}	7.2	4.6	2.6	1.0	4.0	10.0
Flexural test	First crack strength σ_{cr}	4.5	5.3	13.9	3.0	4.6	16.2
	Ultimate strength σ_U	4.5	5.9	2.0	3.0	5.0	16.3
	ASTM toughness I_{10}	24.8	0.9	14.0	1.6	5.1	24.9
	ASTM toughness I_{50}	4.5	5.7	16.6	4.6	4.8	23.1
	Equivalent flexural strength	60.1	22.1	4.1	1.6	6.3	15.2
	Flexural strength ratio $R_{e,2}$	60.7	18.1	5.4	4.7	6.7	7.8
Indirect tensile test	First crack strength $\sigma_{SP,cr}$	6.4	4.2	9.4	-	-	-
	Ultimate strength $\sigma_{SP,U}$	6.3	5.1	3.3	-	-	-
	Absolute toughness T_{SP}	-	9.2	3.9	-	-	-

Table 4-10 Summary of coefficients of variability (expressed as a %) from static tests

Strength

There appears to be no apparent relationship between the coefficient of variability and the compressive cube, flexural or indirect tensile strengths. The coefficients vary between 1.0% (L3 Control) and 16.3% (L3 1.0%). ASTM C 1018 (1997) specifies an upper limit of 5% based on flexural first crack and ultimate strength. It is evident many tests failed this criterion, some by a considerable margin. However, the average values quoted are based on only three test specimens; an investigation into whether the differences are due to the material characteristics or due to the small number of samples warrants further study.

By comparing the coefficient of variability at increasing fibre volume fraction for all the tests, it can be seen that generally the variability increases with increasing fibre volume fraction. It is apparent that steel fibre reinforcement has an affect on the predictability of the

first crack and ultimate strengths, in spite of the tendency for strength to increase in flexure and indirect tension.

Toughness

The variability in toughness was compared using the ASTM indices I_{10} and I_{50}, the equivalent flexural strength and the flexural strength ratio. It was discussed in Section 4.4.3 the relatively higher variability in ASTM toughness indices of FRCBM when compared to those specified by ASTM C 1018 (1997). It can be seen from Table 4-10 that the variability based on the equivalent flexural strength and the flexural strength ratios were comparable to the ASTM variability for the limestone, although there appeared to be no correlation between the parameters for the gravel mix.

There appears to be a tendency for the variability in all toughness parameters to increase with fibre volume fraction, in particular at a fibre volume fraction of 1.0%. No explanation can be offered as to why the variability at a fibre volume fraction of 1.0% is so much more than at 0.5%. This result is contrary to expectations; with fewer fibres, it would seem that there is less likelihood of fibres bridging the cracked zone and being effective.

Summary

The results here serve to demonstrate, albeit briefly, the variability in strength and toughness characteristics of FRCBM. The variability of FRCBM was found to be higher than what is expected in SFRC, and this is likely to be due in part to the inherent variability of CBM properties, as has already been discussed in Chapter 2. This being so, knowledge of the material's variability is important to enable parameters to be specified and achieved in practice, and to allow designers the opportunity to include appropriate safety factors.

The data in this study may be used as a basis for assessing the strength and toughness variability of the tests described. However, given the relatively large variability highlighted with fibre volume fraction, a more extensive study into the effect of steel fibres on the strength and toughness properties is recommended.

4.4.8 Conclusions and discussion based on static test results

Influence of fibre reinforcement on compressive, flexural and indirect tensile strength

1. Fibres appear to have little or even a detrimental effect on the compressive cube strength of FRCBM, most likely due to the orientation of fibres with respect to the direction of the applied load.

2. The first crack flexural and indirect tensile strengths were generally unaffected by fibre reinforcement. At low fibre volume fractions (i.e. those less than the critical fibre volume fraction in flexure), no increase in flexural strength over first crack strength was observed. However, where the critical fibre volume fraction in flexure was exceeded, the ultimate strength was greater than the first crack strength, and by a significant amount (up to 30%) at a fibre volume fraction of 1%. The ultimate indirect tensile strength was increased at fibre volume fractions as low as 0.2%, although this was thought to be a function of 'wedging' in combination with fibre reinforcement, and the effects of the two were not distinguishable.

3. Strength increase is more readily brought about by increasing the cement content. Therefore, at a given cement content, it is proposed for design that the flexural strength of FRCBM and CBM should be assumed to be equal.

Influence of fibres on post-crack flexural ductility

4. Fibre reinforcement was shown to increase the load carrying capability post crack of FRCBM, and the effect of this was significantly greater than the effect of fibre reinforcement on flexural strength.

5. ASTM toughness indices and the flexural strength ratio showed that significant post-crack ductility occurred in even the lowest strength mix (7-day compressive cube strength of approximately 10MPa). The toughness is thought to be influenced more by the end shape of the fibre than the adhesion between concrete and steel. Toughness was found to vary with fibre type and fibre volume fraction.

6. ASTM toughness indices appeared to be a measure of fibre performance, largely independent of matrix strength. However, ASTM toughness indices require interpretation of the first crack deflection, and calculation of the indices is somewhat tedious.

7. The equivalent flexural strength was shown to be a measure of both fibre performance and material strength, and could not be used to measure fibre performance in FRCBM of variable strength. This difficulty could be overcome however by comparing fibre types in materials of nominally equal strength. In practice, the equivalent flexural strength may be preferred as a design parameter as the magnitude of the equivalent flexural strength is a value engineers will be able to relate to.

8. The flexural strength ratio was shown to be a measure of fibre performance, but was also influenced by any increase in ultimate flexural strength over first crack flexural strength. An advantage of this parameter over the ASTM toughness indices was that interpretation of the first crack deflection was not required. At fibre volume fractions where increases in strength are not expected, the flexural strength ratio is therefore a convenient parameter to compare fibre types.

9. The indirect tensile test revealed similar benefits to the flexural test based on fibre type and volume fraction, and has the added benefit of being a simpler test, conveniently enabling the comparison of field and laboratory data. The results have shown that indirect tensile strength ratio, along the lines of the flexural strength ratio, would serve this test well. The effects of wedges that occur in this test have not been fully researched, in particular post-crack. This issue should be addressed before this test is widely adopted.

Design considerations

10. The tests demonstrated that there is significant variability in the toughness properties of FRCBM compared to cast concrete, probably caused by variability in the fibre distribution, orientation and method of producing specimens (surface compaction). To accommodate this variability, the design should be based on characteristic, rather than average, values.

11. All fibres tested in this study were known, and marketed as, high quality performance steel fibres. There were measurable differences between the fibre types, and 'poorer' fibres can in practice be compensated for by increasing the fibre volume fraction. The fact that none of the fibres significantly outperformed the others should not be surprising. For such fibres at a given fibre volume fraction, dispersion in the mix is probably more important than fibre type. However, other fibre types may not perform in the same way, and static tests should be performed to demonstrate the post-crack ductility in accordance with the Material Specification in Appendix B.

12. A criticism of the HA's Specification for Highway Works (Highways Agency 1998) may be that the variability of flexural strength is not accurately reflected by compressive cube test results. Given the variability between mixes, the most economic pavement structure may only be determined by testing an individual CBM in flexure. The flexure test is not a difficult test to perform and the production and testing of site specimens surely cannot be over ambitious. In order to produce a design, assumptions must be made regarding the CBM strength at a time when knowledge regarding the likely aggregate to be used is limited. This is needed to cost the project. The use of flexural strength rather than cube strength would allow the design to be costed and enable the contractor to benefit from material properties using a more realistic strength parameter. In producing a mix design, a relationship between the cube and flexural strength can be obtained for that individual mix, and cube strength used thereafter for quality control purposes during construction. Any economic savings through improved mechanical performance may then be taken advantage of, and should the aggregate be found to perform more poorly than is currently assumed, steps may be taken to ensure acceptable *in situ* strengths are achieved.

4.5 Dynamic flexure tests

Cementitious materials, like steel, are known to fail over a period of time at a lower applied stress than their ultimate strength, and this is therefore considered to be a consequence of fatigue (Mallet 1991). The understanding of the fatigue behaviour of materials therefore has implications when designing pavements.

Dynamic flexure tests were carried out on beams and tested in four-point bending. Tests were carried out on CBM and FRCBM beams, primarily to investigate the fatigue behaviour up to first crack. However, the post-crack behaviour was considered relevant as CBM is prone to cracking, and static tests showed that it was here where fibres had most influence. Therefore, a limited number of additional tests were carried out on the FRCBM post-crack at various load magnitudes. The objective of these tests was to go some way to presenting a possible post-crack dynamic test arrangement. The overall objectives of the fatigue tests were therefore:

- To compare the fatigue endurance of CBM and FRCBM at various fibre volume fractions for two strengths of gravel CBM,

- To present a dynamic post-crack test arrangement and comment on the effect of fibre volume fraction on the post-crack dynamic behaviour.

An investigation into the dynamic flexure properties of FRCBM up to first crack was carried out by the author as part of an MSc study (Thompson 2000). Some of the endurance characteristics reported in that study are included here for completeness; data previously presented are attributed as such.

Dynamic flexure tests were carried out on the low and high strength gravel CBM referenced G1 and G3 respectively, reinforced using fibre type 65/60 at the fibre volume fractions shown in Table 4-11.

Mix ref.	Endurance tests				Post-crack tests		
	Control	Fibre volume fraction			Fibre volume fraction		
		0.25	0.5	1.0	0.25	0.5	1.0
G1	x		x				
G3	x	x	x	x	x	x	x

Note: Aggregate, cement content and water content for each mix given in Table 4-1. Aggregate gradings shown in Figure 4-1.

Table 4-11 Details of tests carried out in dynamic flexure

4.5.1 Dynamic flexure testing arrangement

Pre-crack (endurance) study

Dynamic flexure tests were carried out in four-point bending over a span of 300mm. The same 'yoke' arrangement was used as for the static tests, described in Section 4.3.1, though mid-span deflection measurements were made on one face only. Dynamic tests were carried out on a 100kN capacity Mand hydraulic testing machine in load control using a sinusoidal waveform at a frequency of 6Hz. The machine control and data acquisition were automated using Rubicon software. As endurance is traditionally presented on a logarithmic scale, a schedule of data collection points were produced so that a greater number of cycles could be recorded early in the test, and fewer cycles recorded as the number of load applications increased. This kept the data stored to a manageable size. For each cycle, approximately fifty data points were recorded so that a load – deflection plot could be produced.

In the endurance tests, a series of six beams was used in the higher strength mix (G3), and a series of three beams was used in the lower strength mix (G1). The first beam in each series was tested monotonically in the same way as described for the static flexure tests. The remaining beams were then tested dynamically, between an applied maximum and minimum load. Each series of beam tests was completed within four days of the first static test. The applied maximum load was chosen based on the first crack flexural load, determined in the

static test for the first beam. Subsequent beams were tested at progressively lower applied loads. The stress ratio (S) for each beam was defined as the ratio between the maximum applied load for that beam and the first crack flexural load recorded for the first beam. The minimum applied load was 10% of the maximum applied load for each beam. For each series of beams, three compressive cube strengths were obtained at 7-days and reported in Appendix A.

Post-crack study

Post-crack dynamic tests were carried out on 'failed' beams tested for endurance using mix G3 at fibre volume fractions 0.25%, 0.5% and 1% as shown in Table 4-11. Loads were applied at ratios between 25% and 64% of the static first crack flexural load, and the permanent and elastic deflections measured over 2000 cycles. Permanent and elastic deflections were compared to investigate the behaviour at each fibre volume fraction post-crack, and to enable comment to be passed on the applicability of the test set-up.

4.5.2 Definition of dynamic test parameters

Endurance study

Endurance was defined as the number of load applications to cause failure (N_f) at a given applied load (F). Many of the fibre reinforced specimens were found to be able to carry load once a crack had formed. 'Failure' of these specimens was therefore defined as the occurrence of the first crack, which was detected as a step increase recorded by the inductive displacement transducer that measured mid-span deflection.

The endurance study related the number of cycles to failure to stress ratio, referred to as an S-N plot (Mallet 1991). Based on the static flexure test results, it was concluded that the first crack strength of the FRCBM specimens were approximately equal to the flexural strength of CBM (see Section 4.4.2). The first crack flexural strength was therefore used in the determination of stress ratio.

The load-deflection relationship was continually recorded during the endurance tests (Figure 4-24). From the load-deflection plot, the permanent and elastic deflections were

determined by measuring the deflections corresponding to the maximum and minimum applied load. Permanent deflection (δ_p) and elastic deflection (δ_e) measured mid-span for a given number of load cycles are defined Figure 4-24. If a specimen had not failed at 1 million cycles, the test was stopped. The cycle data were 'normalised' by using the ratio of the number of applied cycles (N) to the number of cycles at failure (N_f), so that comparisons could be made over the life of the specimens. This 'normalising' of the cycle data allowed common trends to be investigated irrespective of the number of cycles to failure. Permanent and elastic deflections were determined from the data at the start of the test and at failure, and at cycle ratios of 0.1, 0.5 and 0.9.

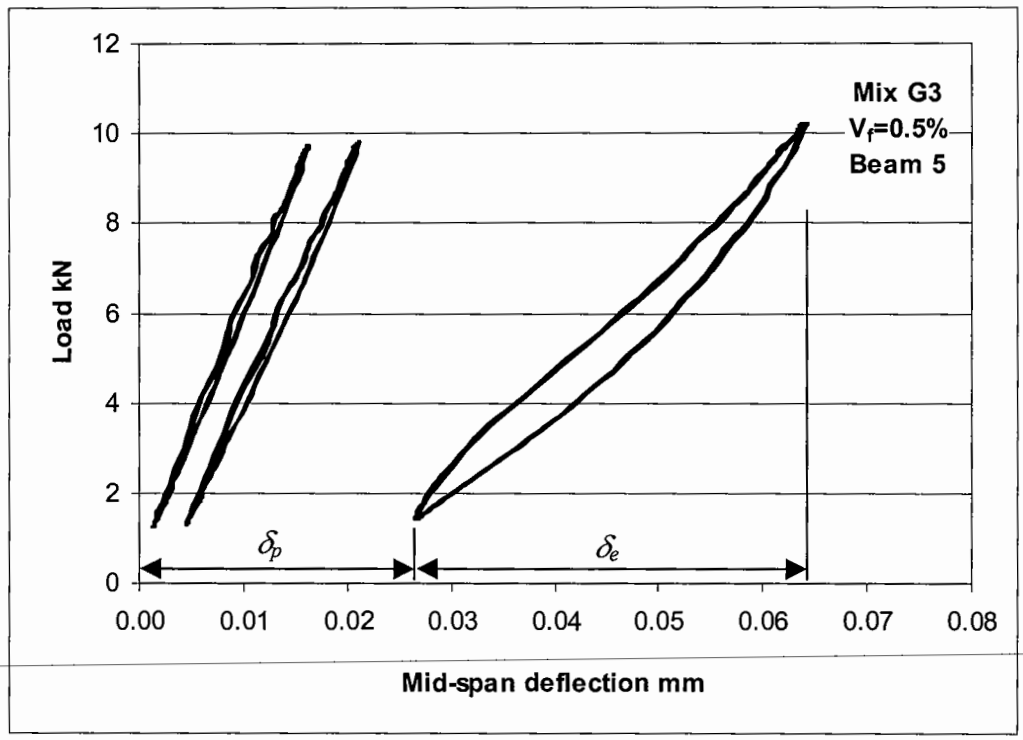

Figure 4-24 Load deflection plots at start, middle and towards end of endurance test on mix G3, V_f=0.5%, with definition of permanent deflection (δ_p) and elastic deflection (δ_e)

The design of pavements requires a knowledge of the material stiffness to determine the stresses imposed on the lower layers. A change in the elastic deflection means a change in the elastic stiffness. Elastic stiffness moduli (E) were computed as the tests progressed using Eqn...4-5, which may be derived using elastic bending theory with knowledge of the applied load (F), span (L), second moment of area (I) and elastic deflection (δ_e):

$$E = \frac{23FL^3}{1296I\delta_e} \qquad \textbf{Eqn...4-5}$$

It should be noted that Johnston (1985) showed that the contribution of shear in bending can be significant, and for the dimensions of the beams used in this study, predicted that the true stiffness would be 25% higher than reported here.

Post-crack study

No published data were found for dynamic tests once cracking has occurred. In this study, permanent and elastic mid-span deflections were generally determined post-crack up to 2000 cycles (although a small number of tests were carried out up to 450000 cycles) to investigate the effect of fibre volume fraction on specimen deterioration.

Relationships between the permanent and elastic deflections and number of load applications were investigated at various applied loads. It was found that permanent deflection tended to increase throughout the tests, whereas the elastic deflections were reasonably constant. For this reason, to compare the effects of permanent deflection, the number of loads to deflect the specimen 'permanently' through 0.2mm was reported. The value of 0.2mm was chosen as this gave a spread of values based on the output data, which could be used to make comparisons, and did not seem to be an unreasonable deflection 'limit'.

Initial investigations indicated that specimens with a fibre volume fraction of 0.5% or less were unable to carry load at over approximately 70% of the specimen's first crack load. The applied loads reported are therefore significantly lower than the first crack load.

4.6 Dynamic test results and discussion

4.6.1 Endurance

The results from the endurance tests are summarised in Table 4-12. This shows the age of each beam at testing, the static first crack and ultimate strengths obtained from the first beams, the maximum applied dynamic stress, the calculated stress ratio (S) and the number of cycles to failure (N_f).

Mix reference	Fibre volume fraction	Beam no.	Age of beam at test Days	Static flexure		Dynamic flexure		
				Ultimate strength MPa	First crack strength MPa	Maximum applied stress MPa	Stress ratio (S) %	Number of cycles to failure (N_f)
G3	0	1	51	3.54	3.34			
		2	51			2.91	87	2400
		3	51			2.81	84	2900
		4	51			2.64	79	10900
		5	52			2.51	75	164900
		6						no data
G3	0.25	1	70	4.20	4.20			
		2	70			3.72	89	7750
		3	71			3.57	85	143910
		4	72			3.18	76	318800
		5	73			2.70	64	1000000+
		6	76			2.34	56	1000000+
G3	0.50	1	72	3.93	3.84			
		2	72			3.48	91	1300
		3	72			3.18	83	1600
		4	72			3.06	80	33800
		5	73			2.82	73	40800
		6						no data
G3	1.00	1	28	5.01	3.75			
		2	28			4.02	107	410
		3	28			3.51	94	1080
		4	28			3.21	86	15000
		5	29			3.00	80	382
		6	29			2.82	75	1000000+
G1	0	1	47	1.62	1.62			
		2	47			1.32	81	940
		3	47			1.26	78	135500
G1	0.50	1	41	1.65	1.47			
		2	41			1.47	100	1800
		3	41			1.23	84	42800

Note: Aggregate, cement content and water content for each mix given in Table 4-1.
Aggregate gradings shown in Figure 4-1.

Table 4-12 Summary of results from dynamic flexure tests (*Thompson 2000*)

The number of cycles to failure (N_f) with stress ratio (S) is presented graphically in Figure 4-25. It is worth noting that an underestimation of first crack strength would result in apparent enhanced *S-N* behaviour. This highlights an important point regarding the *S-N* relationship. The strength on which the stress ratio is based must be accurately determined. The use of one test only to derive this parameter, as in this study, may therefore lead to inaccuracies in the position of the endurance line.

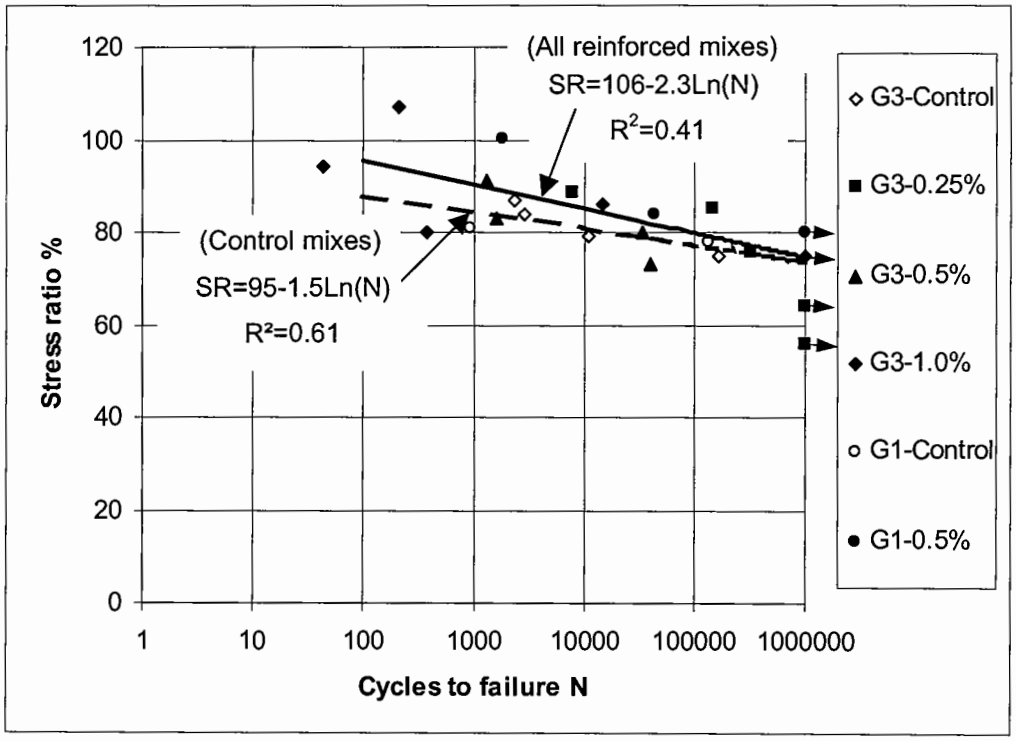

Figure 4-25 *S-N* relationship for high strength (G3) and low strength (G1) gravel CBM at various fibre volume fractions

The S-N relationship for CBM and FRCBM obtained in this study compares well with published research by Galloway *et al.* (1979) on unreinforced concrete and Sobhan (1997) on a weakly bound fibre reinforced stabilised base material (Figure 4-26). There are, though, some points of difference worthy of discussion.

Ramikrishnan and Josifek (1987) carried out simply supported flexural fatigue tests reinforced using a hook ended fibre at a fibre volume fraction (V_f) of 0.5%. This was a similar fibre type to the 65/60 fibre used in this study. The major difference was that the tests were carried out using a structural concrete. It is evident that such a material leads to a greatly enhanced fatigue life, most likely because (in this instance) the static ultimate strength was significantly greater than the first crack strength - hence the stress ratios exceeding 100%. For an FRCBM, it was demonstrated in the static flexure tests that the first crack and ultimate strengths at V_f=0.5% are similar. However, even for FRCBM reinforced at V_f=1%, where the ultimate strength exceeds the first crack strength, the fatigue behaviour was not demonstrably improved. This may be due to the failure criterion being the first crack, as detected by a step change in mid-span deflection as measured by the inductive displacement transducers. In fact, the specimens at a fibre volume fraction of 1% were able to carry significant load post-crack, as will be demonstrated later, and therefore the endurance results shown may not do justice to this mix. However, this does illustrate the need to carefully define 'failure' when comparing dynamic results, and the need for users of fatigue data to understand any assumptions made.

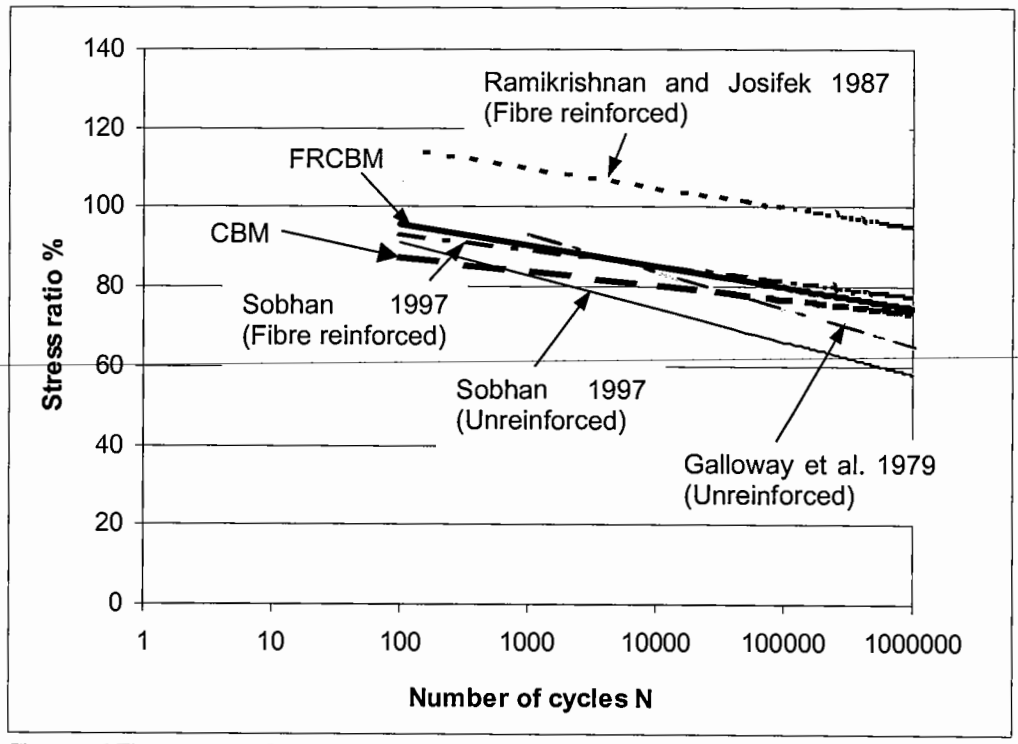

CBM and FRCBM line from Figure 4-25.

Figure 4-26 Comparison of endurance relationships for FRCBM with various published data

The results suggest that the material behaviour is reasonably similar to extensive data reported by Galloway *et al.* (1979) and Sobhan (1997) which cover a wide range of matrix strengths. The tests also suggest that there is little difference between the endurance of CBM and FRCBM in fatigue. The relationship for FRCBM was found to be very similar to the relationship obtained by Sobhan (1997) for the fibre reinforced material. It is worth noting though that Sobhan detected a very different relationship for the unreinforced specimens, which is at odds with what was found for CBM.

4.6.2 Permanent and elastic deflections to first crack

Throughout the tests, the permanent and elastic deflections were found to increase, although the magnitude of the increases was dependent on the fibre volume fraction. It was observed that the permanent deflections increased progressively throughout the tests for both the control (unreinforced) and reinforced specimens. There appeared to be a tendency for the permanent deflections to increase at a greater rate with increasing fibre volume fractions (Figure 4-27). The permanent deflections recorded for the low strength material were lower than those for the high strength material (Figure 4-28). By observation of Figure 4-27 and Figure 4-28, the rate of accumulation of permanent deflection for the unreinforced mixes was reasonably linear. Some of the reinforced specimens exhibited increased rates of deflection during the latter half of the material's life.

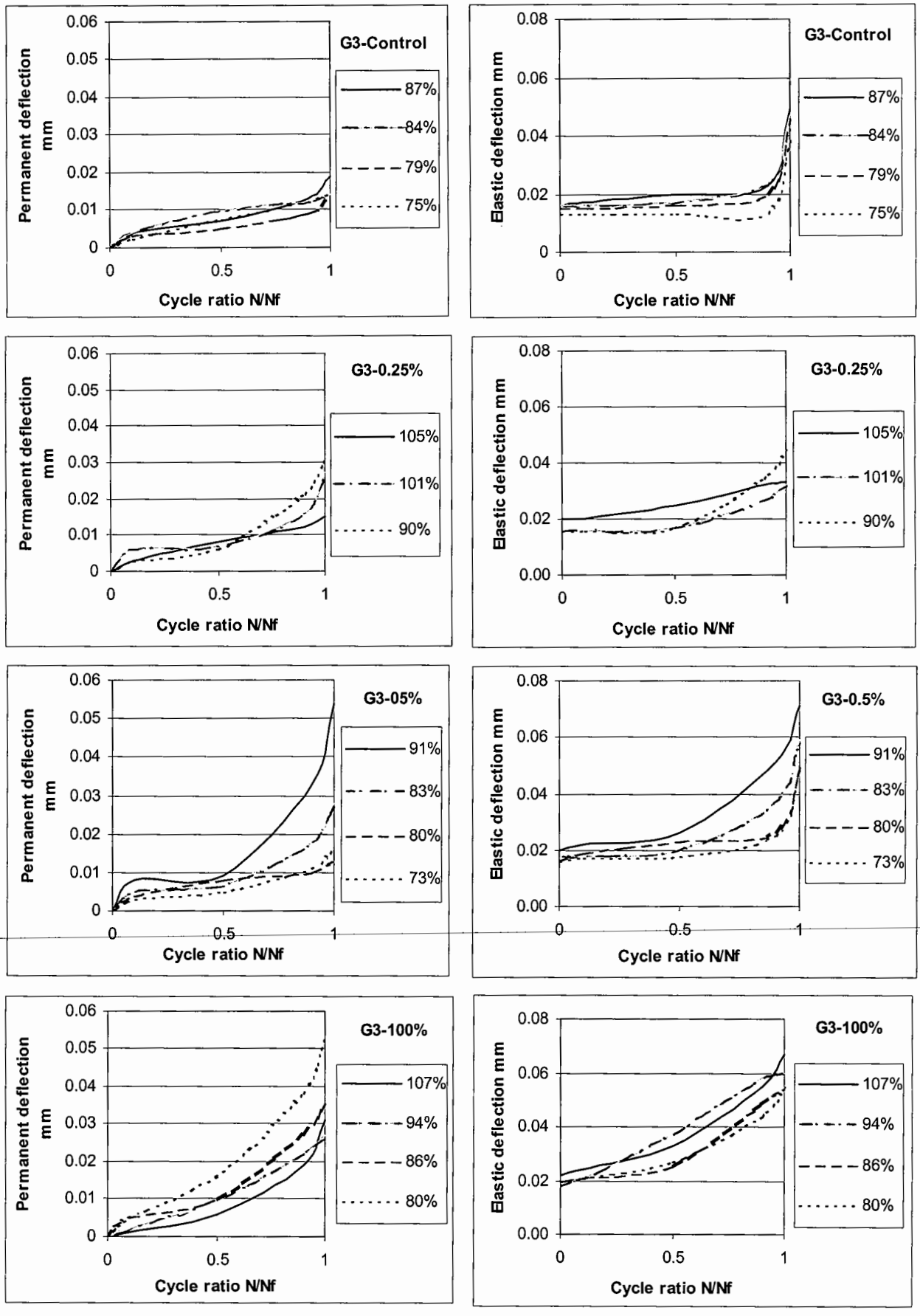

Figure 4-27 Permanent and elastic deflections in gravel CBM mix G3 at various stress ratios

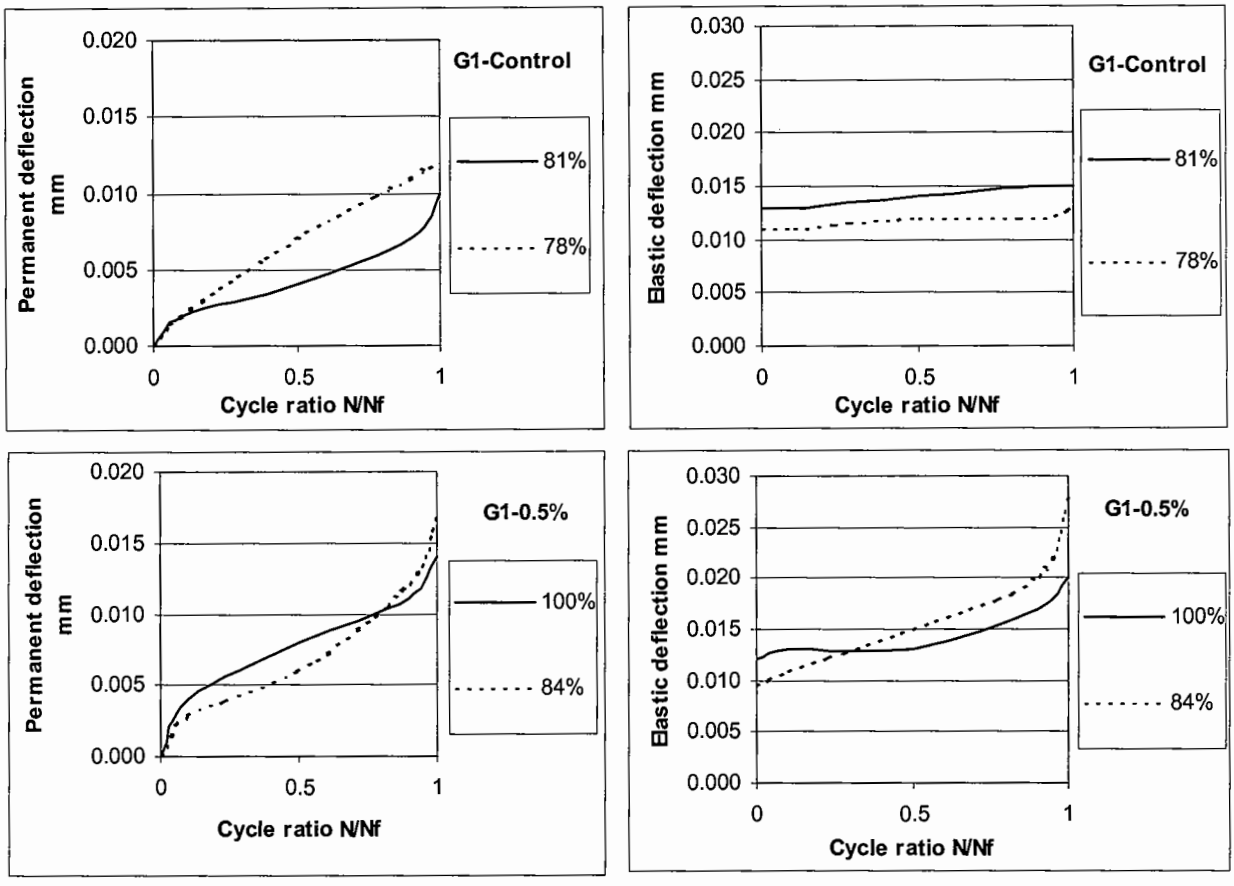

Figure 4-28 Permanent and elastic deflections in gravel CBM mix G1 at various stress ratios

The elastic mid-span deflections were shown to remain reasonably constant with the number of cycles for the unreinforced mixes, at least over 90% of the specimen life. This may be contrasted with fibre reinforced specimens, which experienced progressively increasing elastic deflections. The behaviour of the unreinforced material was similar to that reported by Saito and Imai (1983) who showed plastic strains increased linearly whilst elastic strain remained reasonably constant, as discussed in Section 3.3.2.

Average total mid-span deflections were calculated for all beams tested at each fibre volume fraction, at 90% of the specimen's life (Table 4-13). Whilst the use of an average may not be appropriate to dynamic testing at various stress levels (in particular as elastic deflection is stress dependent), the results provide an indication of the contribution of fibre volume fraction to the dynamic response of the material. Figure 4-29 indicates that as the fibre volume fraction increases, the total (permanent and elastic) deflection increases. A possible explanation for this is that micro-cracking is encouraged by the addition of fibres,

and the combined effect of these cracks and the resistance to failure offered by the reinforcement results in a more ductile mix. It should be noted that this ductility is occurring prior to a crack forming. The increase in ductility for FRCBM over CBM is marked, and unlike for the static tests - where the fibres were primarily effective post-crack - in dynamic flexure the fibres also appear to be influential pre-crack.

Mix reference	fibre volume fraction %	Average mid-span deflections				Total deflection mm
		Permanent mm	95% confidence	Elastic mm	95% confidence	
G3	Control	0.012	0.002	0.020	0.005	0.032
G3	0.25	0.016	0.005	0.031	0.004	0.047
G3	0.50	0.018	0.010	0.035	0.012	0.053
G3	1.00	0.027	0.008	0.051	0.006	0.078
G1	Control	0.009	0.004	0.014	0.003	0.023
G1	0.50	0.012	0.001	0.019	0.002	0.031

Table 4-13 Average mid-span permanent and elastic deflections at 90% of the specimen's life for all mixes (*Thompson 2000*)

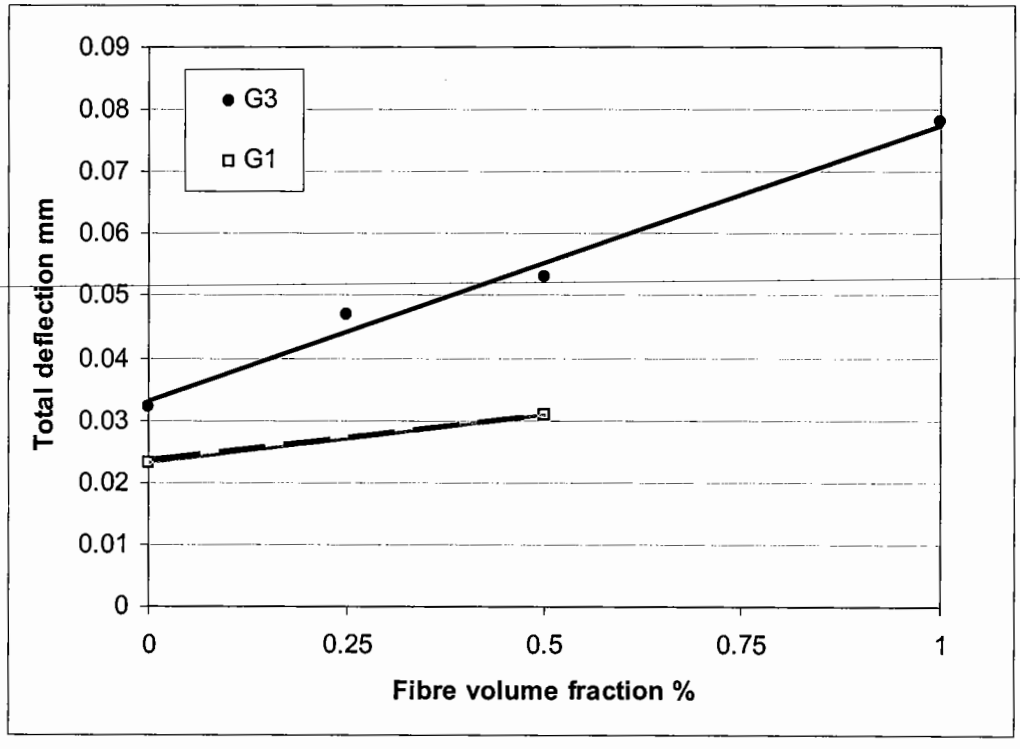

Figure 4-29 Comparison of total mid-span deflections for gravel aggregate CBM at 90% of the pre-crack life (*Thompson 2000*)

It appears as though fibre reinforcement has an affect on the fatigue behaviour of a CBM before the point of first crack. The fibres appear to increase the flexibility of the material before failure occurs. This may be explained by the fibres being a source of micro-cracking in the material. This is evidenced by the progressive increase in elastic deflection throughout the life of the material, behaviour which was not exhibited to the same degree in unreinforced specimens. The expectation was for failure to occur over a small number of cycles once progressive increases in elastic deflection occurred. This was the case for unreinforced specimens, but not for FRCBM, which continued to carry dynamic load at significant increases in deflection. As the fatigue life of FRCBM was comparable to CBM (see Figure 4-26), it is considered that the propagation of micro-cracks into macro-cracks, that would cause failure, is inhibited by the fibres. It is concluded that fibres are a cause of micro-cracking in a FRCBM, but provide a mechanism that delays the onset of macro-cracking and therefore increases the number of cycles that result in material failure.

4.6.3 Dynamic stiffness determined from elastic deflections

Pre-crack behaviour

Engineers use the stiffness of a pavement material to analyse the protection provided to the layer below it and the support to that above, and to determine the stress within the material itself. For the design of cementitious materials, the stress is often computed at the base of the cementitious layer, and this is used as a basis for the determination of the required material strength. The dynamic stiffness is therefore presented to demonstrate how the elastic deflection data may be used in the analysis of an FRCBM pavement.

Dynamic stiffness during fatigue tests was computed from elastic deflection measurements using Eqn...4-5. It was found that the dynamic stiffness reduced during the tests, and the manner of the reduction appeared to be a function of the fibre volume fraction. Control specimens showed little loss in stiffness before fracture occurred (Figure 4-30). However, the dynamic stiffness of fibre reinforced specimens reduced progressively during the tests, often quite considerably.

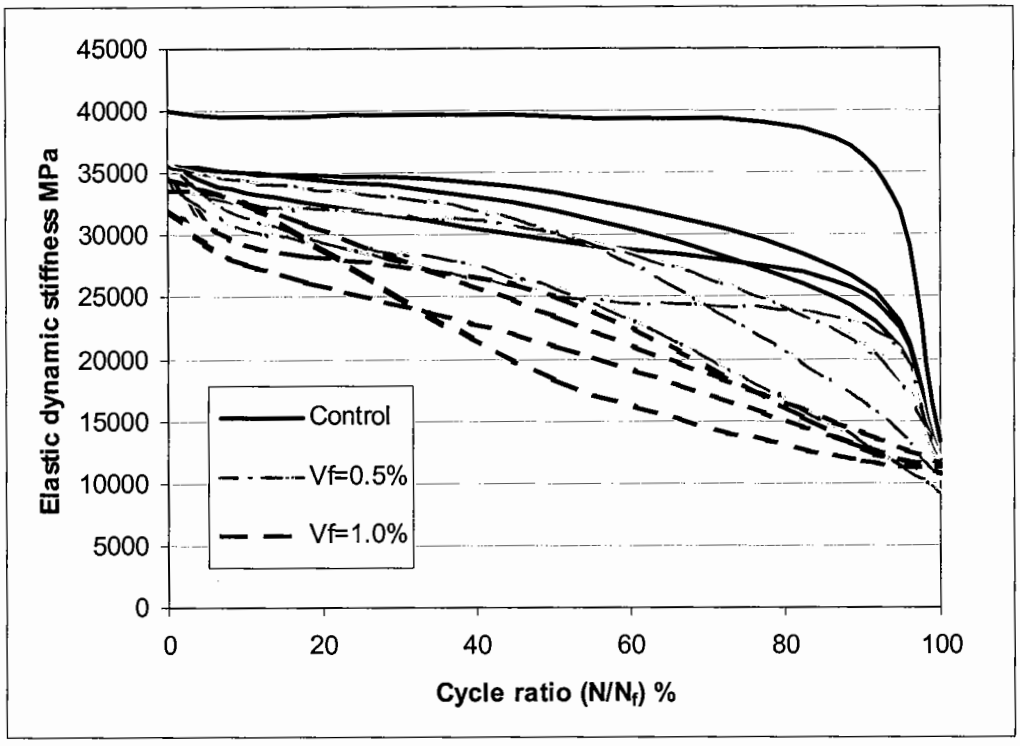

Figure 4-30 Relationship between elastic dynamic stiffness and cycles ratio for gravel aggregate CBM G3 at various fibre volume fractions

The fibres appear to prevent a unique crack from developing early in the life of the specimen, resulting in an accumulation of damage over the most highly stressed section. The resulting failure is therefore much more ductile than the control. Furthermore, the gradual reduction in dynamic stiffness would reduce the stress at the critical point in the CBM in a pavement. Such a reduction in stress would be expected to result in an increased fatigue life. However, the reduced stiffness will result in greater stresses and strains being imparted to the lower layers. Therefore whilst a stiffness reduction might benefit the cementitious material, the lower layers must be designed to withstand the additional vertical stresses imposed on them. The smaller loss in stiffness of the control material may be credited to micro-cracking around the aggregate, although this is less apparent than micro-cracking caused by the fibres.

Post-crack behaviour

At a fibre volume fraction of 1.0%, specimens were able to carry load for a considerable time after the beam had cracked (Figure 4-31). It is apparent that when the fibre volume fraction is sufficiently high so as to allow a significant increase in ultimate strength over first crack strength in a static test. The composite is also able to carry dynamic load after first crack in a simply supported test. This aspect of the material's behaviour will be explored further in the next section.

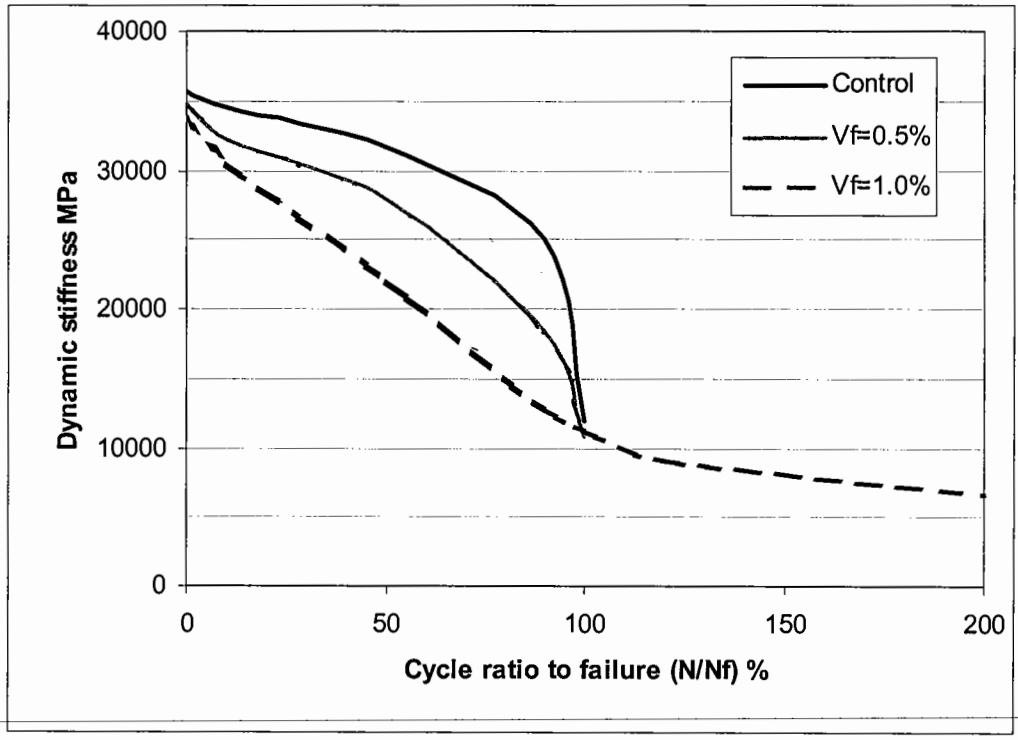

Figure 4-31 Graph showing ability of gravel aggregate CBM mix G3 reinforced at 1.0% to carry load following first crack

4.6.4 Post-crack dynamic test results

Following first crack, static flexure tests showed that CBM is unable to carry load, resulting in a brittle failure and collapse. By contrast, FRCBM was able to carry significant load to a mid-span deflection of 2mm, as described in Section 4.4.3. Dynamic tests post-crack showed that FRCBM was able to carry load following first crack. The number of load applications it was able to sustain was dependent on the maximum applied load and fibre volume fraction.

A summary of the dynamic test results post-crack is shown in Table 4-14. This shows the load ratio, defined as the ratio of the applied load to the first crack load from Table 4-11, expressed as a percentage. Elastic post-crack deflections are shown at 500 cycles. The number of cycles to permanently deflect the specimens through 0.2mm is also shown. This value is used to compare the effect of fibres on permanent deflection under a dynamic load.

Fibre volume fraction	First crack load kN	Applied load kN	Load ratio %	Elastic post-crack deflection (Δ_e) mm at N=500	Number of cycles to reach a permanent deflection (Δ_p) of 0.2mm
0.25%	11.8	3.0	25	0.131	1473
		4.0	34	0.153	2100
		5.0	42	0.169	120
		6.0	51	0.179	95
0.5%	12.8	4.0	31	0.130	10940
1.0%	12.5	4.0	32	0.116	450000
		6.0	48	0.158	450000
		8.0	64	0.176	2000

Note: *Elastic deflection not constant denoting rapid failure

Table 4-14 Summary of results from post-crack dynamic tests for mix G2 using fibre type 65/60

Effect of load on permanent deflections

As the number of cycles increased, the permanent deflections increased to an asymptote up to a certain 'critical load'. The critical load was defined as the load at which an asymptote would not be reached (and failure occurred), shown to be 6kN in Figure 4-32. This 'slowing down' of permanent deflection per cycle suggests that if the maximum applied load is sufficiently lower than the first crack load, the material will deflect to a steady state. This may occur as some initial fibre slip within the matrix takes place prior to the fibre anchorage becoming effective. The expectation might be for this anchorage to break down if sufficient cycles are applied, though in the test development study described below this aspect of 'endurance' was not studied. The initial fibre slip and increase in interfacial bond strength between the fibre and matrix is not unlike 'snubbing', which, in Section 3.2.5, was used to explain how the toughness in static flexure might be enhanced by re-orientating fibres. Therefore, it is suggested a similar mechanism might also be responsible for the asymptotic permanent deflection behaviour shown in Figure 4-32.

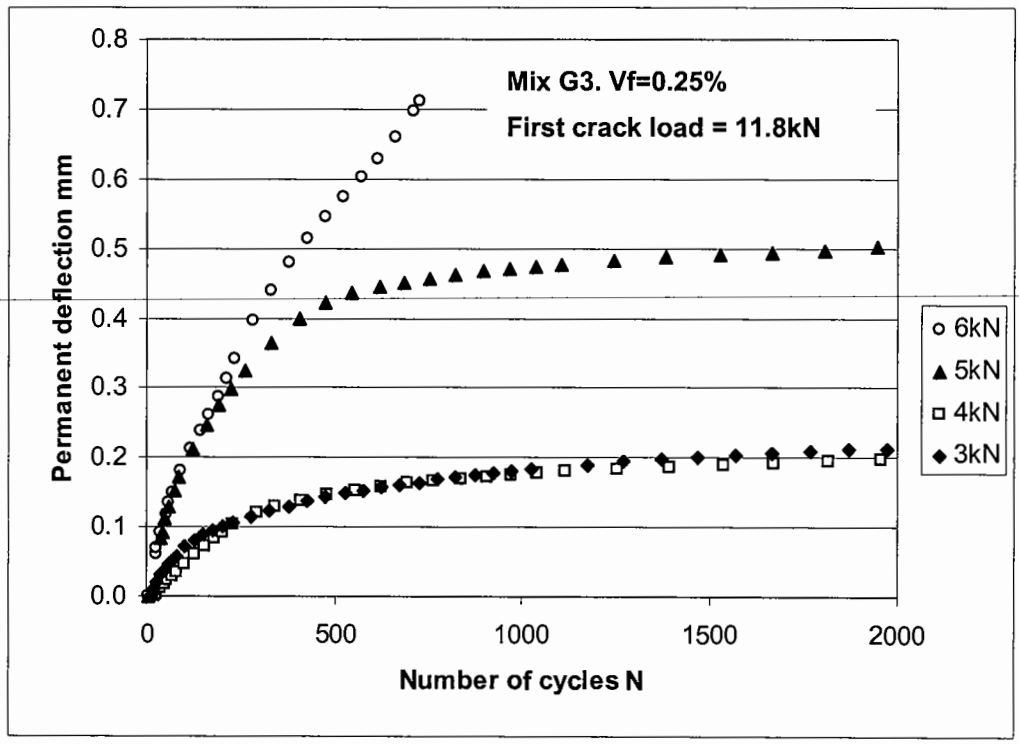

Figure 4-32 Accumulation of permanent deflections post-crack for gravel CBM mix G3 at a fibre volume fraction of 0.25%

Effect of load on elastic deflections

The elastic deflections appear to remain constant or even reduce throughout the tests at various loads and various fibre volume fractions, provided the critical load is not exceeded (Figure 4-33). As a visible crack had formed in all these tests, the majority of the tensile load would have been expected to be carried by the fibres. The fact that the elastic deflections were not increasing demonstrates that the increase in permanent deflection was not adversely affecting the fibre-matrix bond. This may be explained by the relative influence of the end anchorage of the fibres studied compared to the bond along the length of the fibre. Weiler and Grosse (1996) showed the effectiveness of the end anchorage post-crack, as described in Section 3.2.3. This behaviour supports the belief that fibre reinforcement 'holds together' formed cracks, ensuring a cracked fibre reinforced composite has significant post-crack stiffness and load carrying capability.

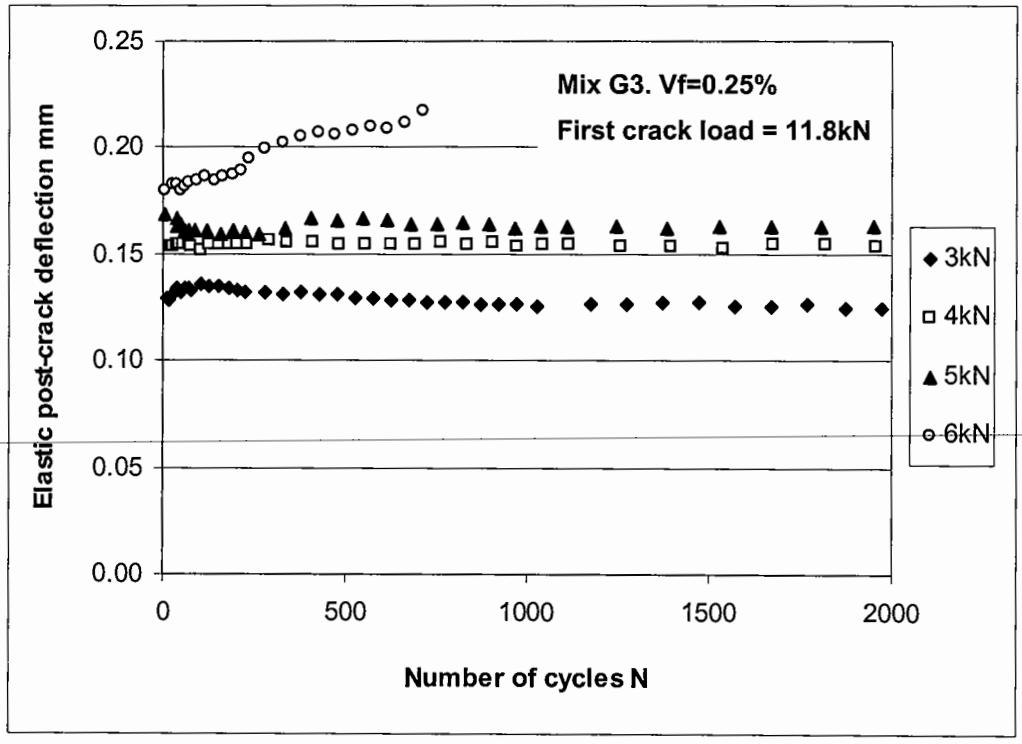

Figure 4-33 Accumulation of elastic deflections post-crack for gravel CBM mix G3 at a fibre volume fraction of 0.25%

Effect of number of cycles on permanent deflections

Although it was shown in Figure 4-32 that the permanent deformations reached an asymptote after a number of cycles, the expectation was that eventually the fibre anchorage in the FRCBM would break, after a number of cycles, resulting in failure. This was supported by the test data shown in Figure 4-34, which demonstrates that at a V_f=0.25%, the FRCBM was unable to carry significant load at the load level applied. However, the material with V_f=0.5% did carry approximately 150000 cycles, at which point the anchorage broke down and failure occurred. this can be contrasted to the specimen with V_f=1.0%, which was able to carry load to 450000 cycles, where the test was stopped.

Although these comments are based on one set of results only, the expectation is for the 'post-crack endurance' to be dependent on the magnitude of the load, the number of load applications and the fibre volume fraction.

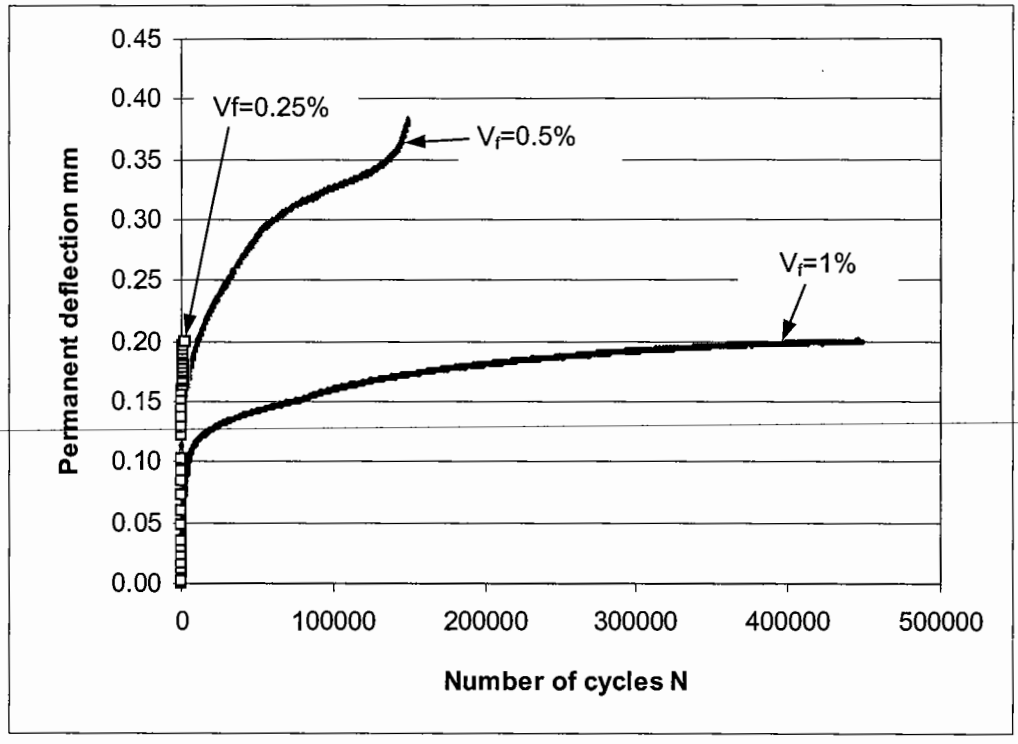

Figure 4-34 Permanent deflection output with load cycles at fibre volume fractions of 0.25%, 0.5% and 1% and a maximum load of 4kN

Effect of load on dynamic elastic deflections

The relationship between applied load and elastic deflection after 500 cycles is shown in Figure 4-35. This shows that, as the applied load increases, the elastic deflection increases as would be expected, and the relationship between the two is approximately linear. Although the elastic deflections are shown at 500 cycles, Figure 4-33 showed that the elastic deflections were reasonably constant throughout the tests. It may therefore be concluded that the post-crack elastic deflections are independent of number of cycles, provided the critical load has not been exceeded, and an 'endurance' failure has not occurred.

It can also be seen from Figure 4-35 that an increase in the fibre volume fraction reduces the post-crack elastic deflections.

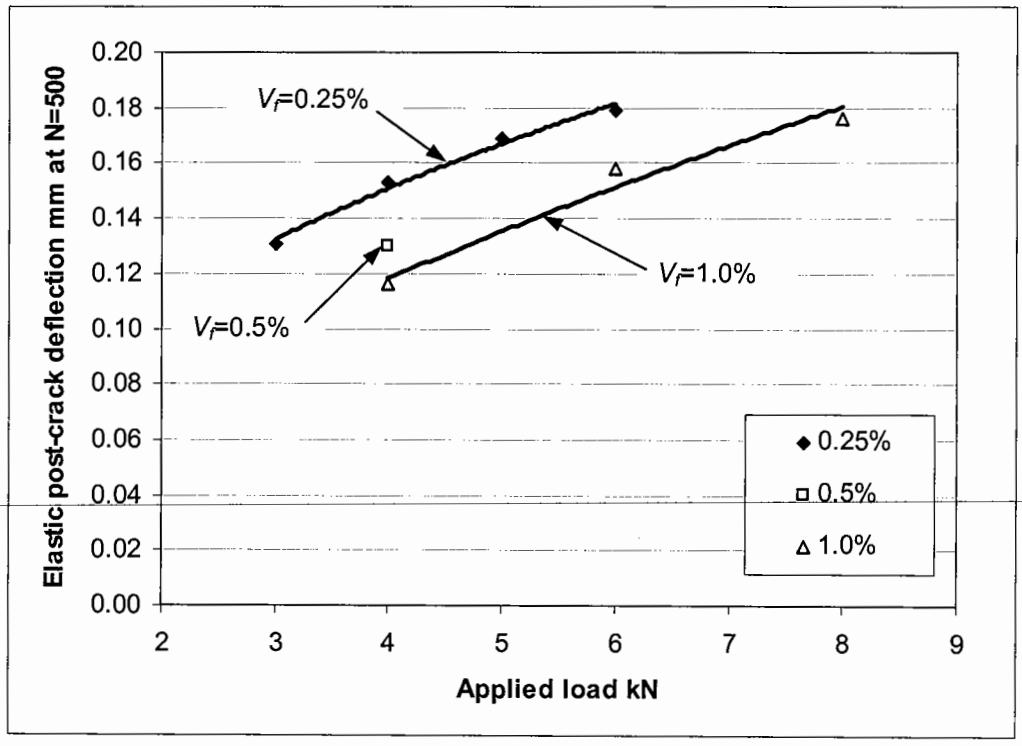

Figure 4-35 Relationship between applied load and elastic post-crack deflection for mix G3 at various fibre volume fractions

Generalised relationship for dynamic post-crack elastic deflection

The data in Figure 4-35 are represented in terms of a load ratio, the ratio of the applied load to the first crack load of the specimen in Figure 4-36. This is a first attempt at a generalised relationship that would allow the post-crack elastic deflection to be predicted for a range of strengths. Clearly, given the limited data this is based on, more data are required to support this.

The mix at a fibre volume fraction of 0.25% reached an upper limit at an approximate load ratio of 50%, shown by a rapid increase in elastic deflection per cycle and failure (shown in Figure 4-33). At a fibre volume fraction of 1.0%, this upper limit had not been reached by a load ratio of 64%. As tests had shown the material could carry load exceeding a cycle ratio of 100% (see Figure 4-31), it is assumed that the relationship is valid up to at least a load equal to the first crack load.

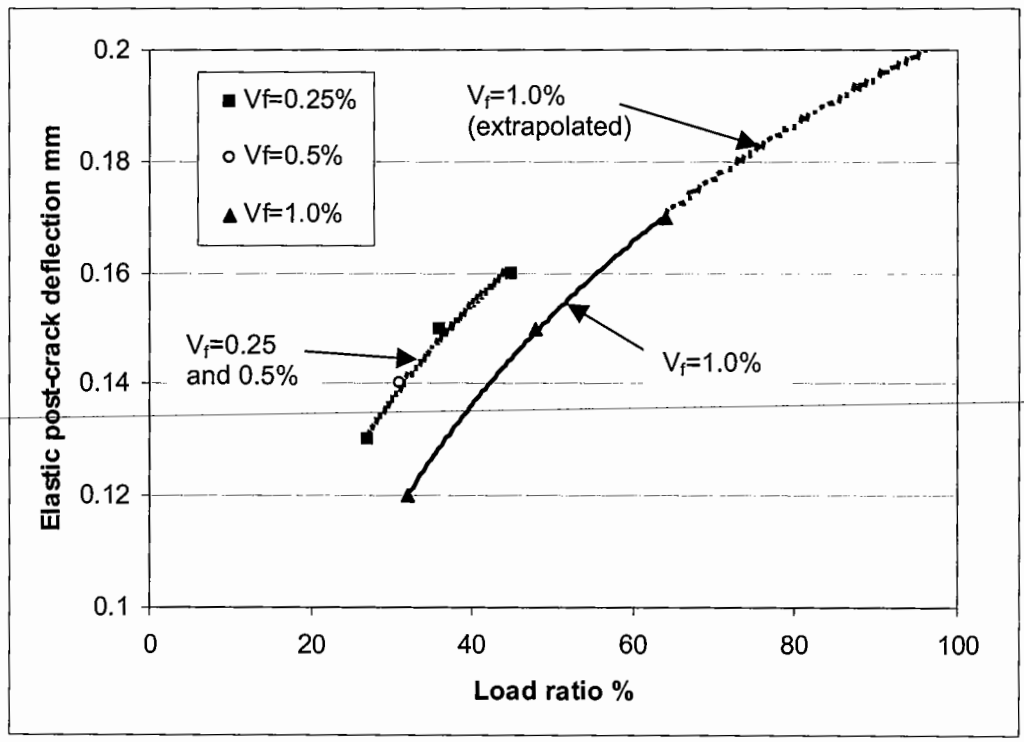

Figure 4-36 Relationship between load ratio and elastic deflection at various fibre volume fractions

Generalised relationship for dynamic post-crack permanent deflection

The number of load applications to reach a permanent deflection of 0.2mm is shown in Figure 4-37. At a given load ratio, fibre volume fraction has a significant influence on the post-crack life (or residual life) of the composite to a permanent deflection of 0.2mm. For a material that is loaded at a ratio of 50%, the material reinforced at 1.0% will potentially be able to carry approximately 45000 load applications compared to about 100 load applications at a fibre volume fraction of 0.25%.

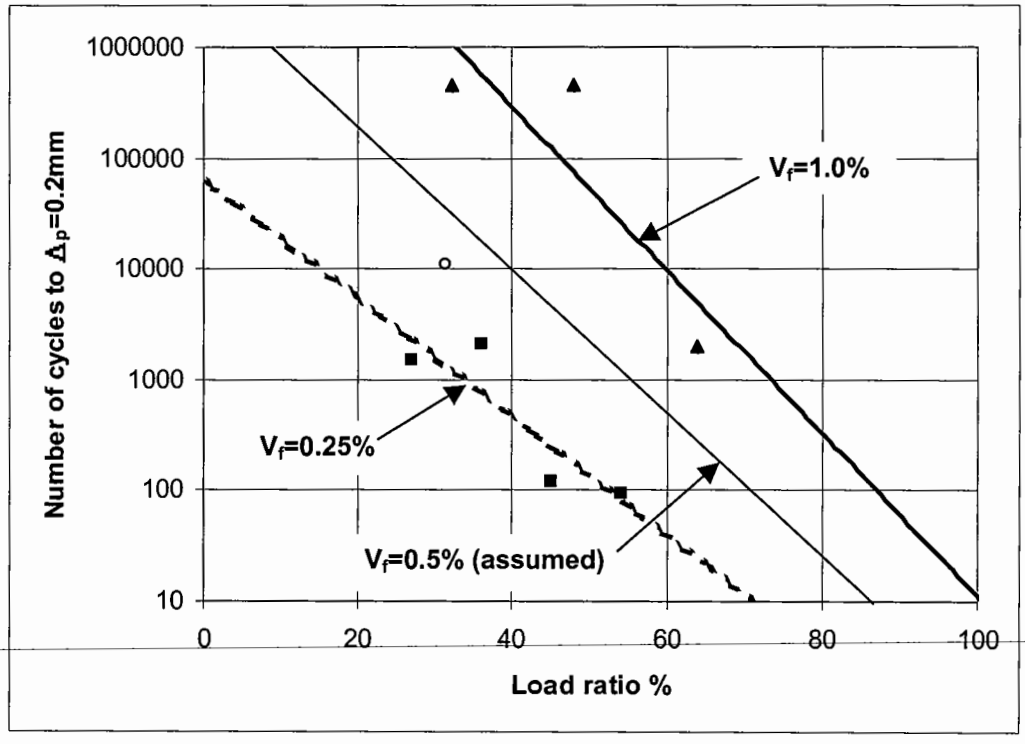

Figure 4-37 Relationship between load ratio and number of cycles to a permanent deflection of 0.2mm

Comments on dynamic post-crack test arrangement and applicability

The limited results from the post-crack dynamic tests outlined in this study have demonstrated that there are benefits in fibre reinforcement post-crack under dynamic load. The test arrangement is the same as the flexural endurance study, and can be used by researchers who carry out such investigations without modification of equipment. Further development of this type of test is required to confirm the findings shown here. There has been no attempt as part of this study to include these data into the design process. However, given the influence of the fibres on the composite post-crack, and the dynamic loading that occurs in the field, such data may be related more closely to the behaviour of a pavement than static tests. A challenge will be to find ways in which the benefits of fibre reinforcement on the dynamic post-crack data can be modelled in practice.

4.6.5 Conclusions and discussion based on dynamic test results

Fatigue endurance

1. Dynamic fatigue endurance tests suggested that there may be no significant benefit in fibre reinforcement prior to cracking occurring when expressed in terms of standard *S-N* curves. The fatigue lines for FRCBM and CBM measured in this study were similar to relationships reported for a wide range of concrete mix strengths. Many researchers had demonstrated an improvement in the fatigue properties of fibre reinforced concrete when compared to unreinforced concrete. The fact that no difference was observed in this study for FRCBM may be because there was no significant increase in first crack strength with fibre volume fraction, and therefore, perhaps there is no reason to expect an increase in fatigue endurance.

2. In order to use the fatigue behaviour of cementitious pavements in practice, engineers often apply safety factors. It should be borne in mind that the actual number of damaging loads applied may be lower than at first expected, based on data presented by Lister (1974). Lister showed that for a 40kN wheel load, the load spectrum for wagons in the UK was such that only 10% of these would result in measurable damage (see Section 2.3.1). It may therefore be assumed that 10 applied loads in the field is equal to 1 'damaging' cycle in the test, or 10

million standard axles equals 1 million laboratory cycles. The laboratory produced fatigue line may therefore be 'shifted' to take account of this.

3. Fatigue relationships should be considered in context with other material properties. This is particularly so in CBM, where the deterioration of the material may be influenced by factors other than traffic induced fatigue. In particular, a reduction in compaction has been shown to affect the material strength significantly (William 1986). Therefore, whilst fatigue must be assessed in the determination of any safety factors that are to be applied to the material, other factors might indeed be of relatively greater importance, and often these are not given equal merit.

Post-crack behaviour

4. A test arrangement has been presented to compare the post-crack performance of FRCBM at various fibre volume fractions under a dynamic load. The test equipment was the same as that used in the endurance tests. Measurements of permanent and elastic deflection showed that the test was able to distinguish between fibre volume fractions and load ratios.

5. Behaviour post-crack is potentially very significant in fibre reinforced composites, in particular as some cracking is expected (or even induced) in flexible composite roadbases. The fibres are not only able to carry a static load post-crack, but also exhibit some reduction in the rate of permanent strain accumulation under repeated loading. There has been no attempt to quantify this benefit as the use of the laboratory results for practical application is not straightforward.

6. Considering the potential of steel fibres to enhance the properties of this material post-crack, and based on the limited results reported here, further investigation of the post-crack dynamic properties in small scale laboratory tests, as described in this report, and larger scale studies on slabs, is recommended.

4.7 Cyclic shear tests

Cyclic shear tests were carried out on CBM and FRCBM specimens to investigate the crack interface properties at various fibre volume fractions and crack widths. Any improvement in the shear properties of a transverse crack would improve the load transfer characteristics in the FRCBM roadbase. This will benefit the structure in two ways:

i) By reducing the stresses imposed in bending on the roadbase; and
ii) By reducing the damaging strains that cause reflection cracking through the asphalt overlay.

The dynamic shear characteristics of CBM and FRCBM were investigated at crack widths between 0.2mm and 1.0mm using a test developed for this study. These widths were expected to cover the range of transverse crack widths that would occur naturally and by induced cracking. Tests were carried out on the high and low strength gravel aggregate CBM, referenced G1 and G3 respectively. Reinforcement was with fibre type 65/60 at volume fractions of 0.25%, 0.5% and 1.0% as shown in Table 4-15.

Mix ref.	Control	Fibre volume fraction (V_f) %		
		0.25	0.5	1.0
G1	x	x	x	x
G3	x	x	x	x

Note: Mix reference details shown in Table 4-1 and Figure 4-1.

Table 4-15 Details of tests carried out in cyclic shear

This section describes the cyclic shear test arrangement, the testing procedure and parameters used in the analysis of the results.

4.7.1 Cyclic shear testing arrangement

The testing arrangement comprised of a 100x100x500mm beam with two vertical cracks induced 100mm apart. The beams were prepared in steel moulds and cured in the same way as for the static flexure beams, described in Section 4.2.2. The cracks were induced in bending after firstly cutting notches around the perimeter of the beam to a depth of approximately 8mm, using a steel saw. Loading was applied in three point bending (Figure 4-39) at a stroke rate of 0.2mm/minute until a load reduction was detected by the software used to control the Zwick Universal Testing Machine (UTM), signifying the onset of cracking. The beam was then turned upside down and the process repeated so that a full depth crack was induced. The presence of a crack was confirmed by visual inspection of the beam and by measuring the crack width using DEMEC pips mounted on the face of the specimen, at the positions shown in Figure 4-38.

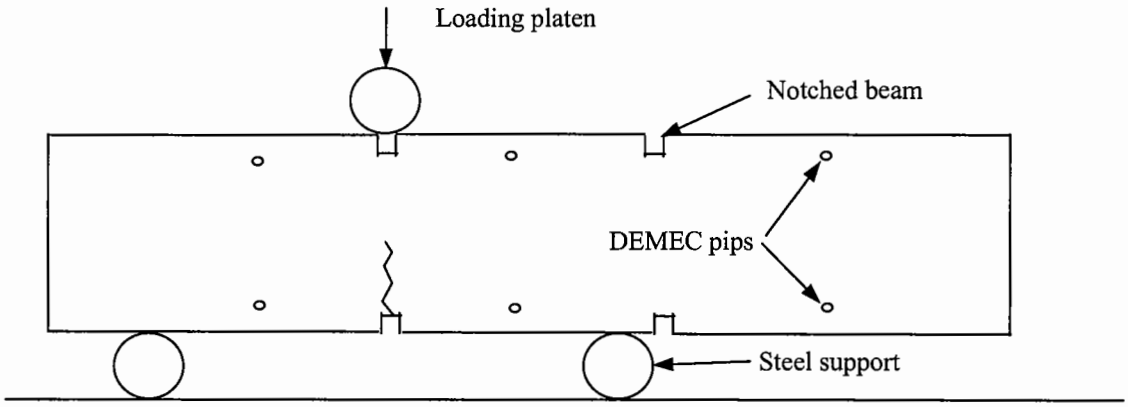

Figure 4-38 Method used to induce cracks in beam specimens

The technique of inducing cracks in bending had been criticised by Abdel-Maksoud (1997), who advocated inducing cracks in direct tension. A smoother interface had been shown to occur in hardened concrete fractured in flexure as failure often took place through the aggregate rather than around it. The shape of the crack was also shown to be influenced in direct tension by whether it was induced by pulling in one or both directions. Also, Abdel-Maksoud (1997) had observed that whilst some specimens had developed cracks as large as 2mm on the surface, subsequent observation showed that a large section of the block remained intact.

The cracking of the CBM specimens in flexure was seen as a practical method of inducing cracks. Without exception, the unreinforced specimens resulted in a vertical crack. The orientation of the crack in the reinforced specimens was more variable and often 'wandered', and this was assumed to have been due to the influence of the fibres. The shape of the formed crack would be expected to affect the behaviour in transferring load. The observation of a crack around the total perimeter of the specimen and its measurement at various points led to the assumption that the crack was continuous across the specimen. The test arrangement was therefore considered to be suitable to carry out comparative tests of CBM and FRCBM specimens. An aim of the study was to measure crack properties at very small crack widths. This presented special problems in producing small crack widths whilst ensuring a full crack had formed throughout the specimen.

The ends of the beam were clamped rigidly to the end supports, and the central block clamped to the loading platen (Figure 4-39). The central block could therefore be moved relative to the end sections.

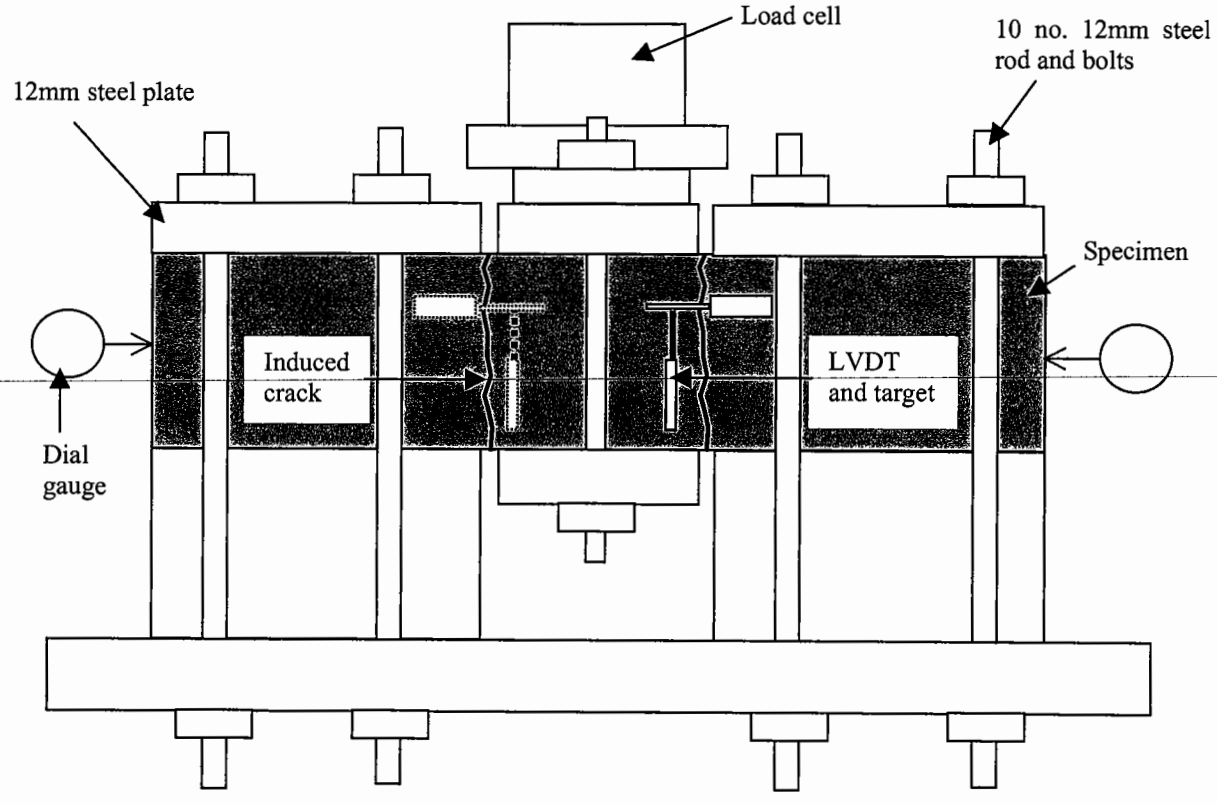

Figure 4-39 Cyclic shear testing arrangement

The movement of the central block was measured using two linear variable differential transformers (LVDT's), mounted on opposite faces of the beam. Targets were mounted on the end sections of the beam so that only relative movement of the central block was recorded, independent of small movements in the apparatus. Machine control and data acquisition were automated using Rubicon software, using a Mand hydraulically driven UTM. Dial gauges were used to ensure no horizontal movement took place due to slippage between the specimen and clamping points.

This testing arrangement had followed previous investigations into methods to measure shear. Initially a specimen with a single crack was used, with one end of the specimen clamped and the other loaded. Horizontal measurements during these tests showed that significant movement was taking place in this mode due to the normal stresses that were introduced under a vertical load. The two crack set-up developed for this study had the benefit of balancing out these horizontal forces, without causing movement of the end sections. This arrangement was considered a more realistic evaluation than the single crack test arrangement of what would occur in a confined pavement.

4.7.2 Testing procedure and definition of parameters

Prior to any test taking place, the saturated density of the beam was determined, and average cross sectional area at each notch calculated by measuring the breadth and depth of the beam with a vernier gauge. Crack widths were measured using a DEMEC gauge once the cracked beam had been mounted in the test rig and clamps fully tightened.

Tests were routinely carried out in load control at ±2kN, where a positive load was in the upward direction, and a negative load was in the downward direction. This resulted in shear stresses comparable to the shear stresses expected across transverse joints in rigid pavements (Buch 1994), though the actual magnitude of shear stress is dependent on the load transfer efficiency of the joint. The example in Section 3.4.3 showed this could vary between 20kPa and 220kPa at load transfer efficiencies of 5% and 95% respectively. A number of tests were carried out on gravel CBM mix G1 at fibre volume fractions of 0, 0.5 and 1.0% at three load levels; ±1kN, ±2kN and ±3kN. This was to determine the relationship between

load and shear slip, where shear slip was defined as the vertical distance moved under the applied load, measured as the average of two LVDT's.

Tests were carried out in series, each series comprising of a 'start' shear test, a deterioration test and an 'end' shear test. The start and end tests plotted the total load-shear slip response over five cycles and were used to monitor any difference in the behaviour across the cracks after the deterioration tests had been carried out. Example 'start' and 'end' load-shear slip plots from an unreinforced specimen with an average crack width of 0.49mm are shown in Figure 4-40.

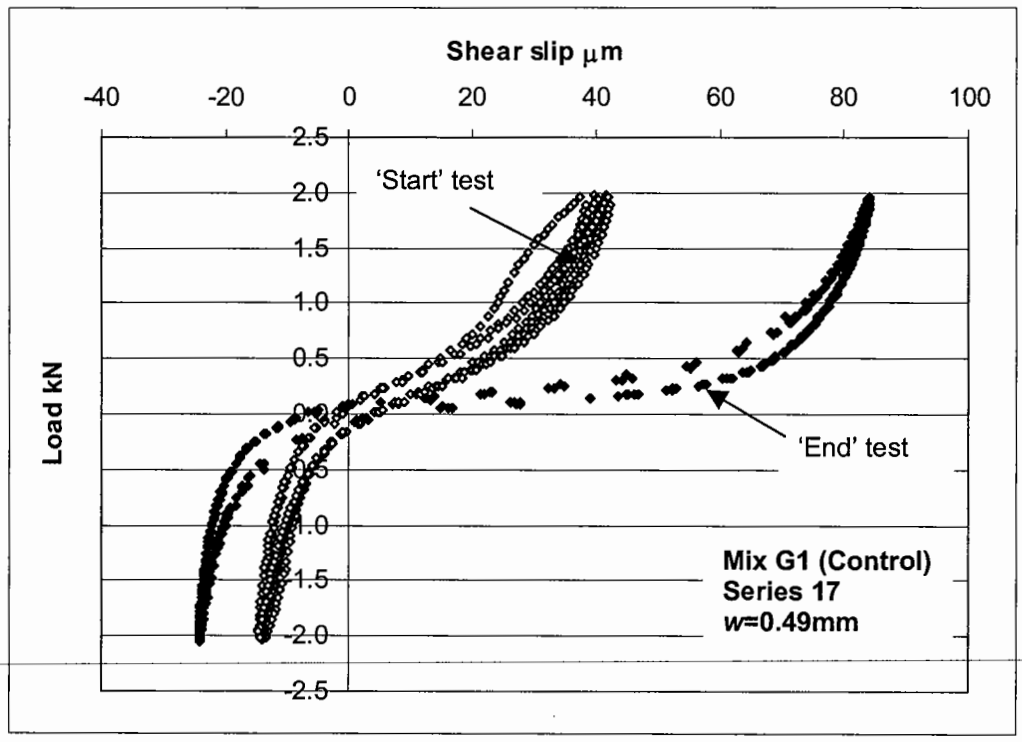

Figure 4-40 Load-shear slip output for 'start' and 'end' of deterioration test

Deterioration tests were performed over 10000 cycles. The change in load-shear slip response shown in Figure 4-41 demonstrated that some permanent damage had taken place to the specimen during the deterioration test. Deterioration tests recorded maximum and minimum shear slips that corresponded to the maximum and minimum load respectively. As the load-shear slip response was often not linear, the plotting of peak and trough points demonstrated the net shear slip only, under a given load, and not the actual crack response. A deterioration plot for the unreinforced specimen shown in Figure 4-40 is shown in Figure 4-41.

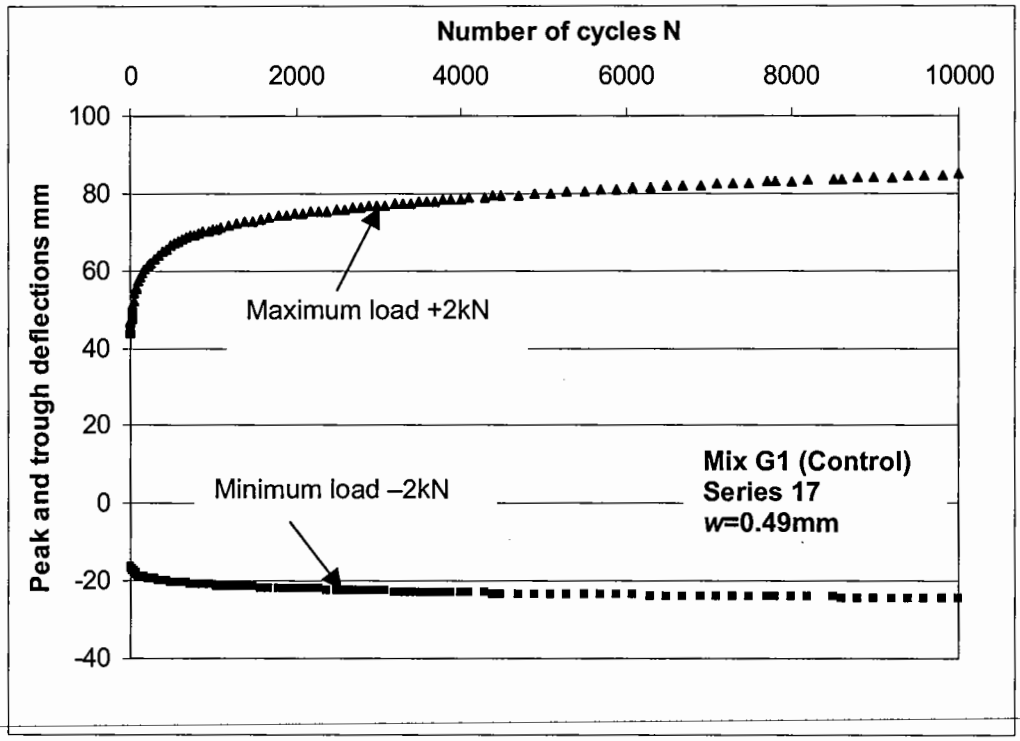

Figure 4-41 Typical peak and trough shear slip output from deterioration test

Following each test series, the crack width was increased and the test series repeated. Specimens were generally used in this way up to a maximum of three crack widths. Some specimens were also tested by re-closing the cracks, to investigate any permanent damage that may have taken place whilst cycling at a greater crack width.

The basic shape of the load-shear slip response was generally observed to be of the form of Figure 4-42. It was noted that the central region of the load-shear slip output tended to have a lower gradient in CBM when compared to FRCBM. The reduced gradient was considered to be an indication of the region not effectively contributing to the total shear slip of the specimen. A ratio was therefore defined to distinguish between specimens exhibiting this behaviour, which measured the proportion of the load (F_2/F_1) required to move the specimen through a proportion of the net shear slip (δ_2/δ_1). This ratio, expressed as a percentage, was defined as crack linearity. Crack linearity tended towards 100% when all the load contributed to the total shear slip. The linearity tended towards zero when a small proportion of the load contributed to most of the shear slip.

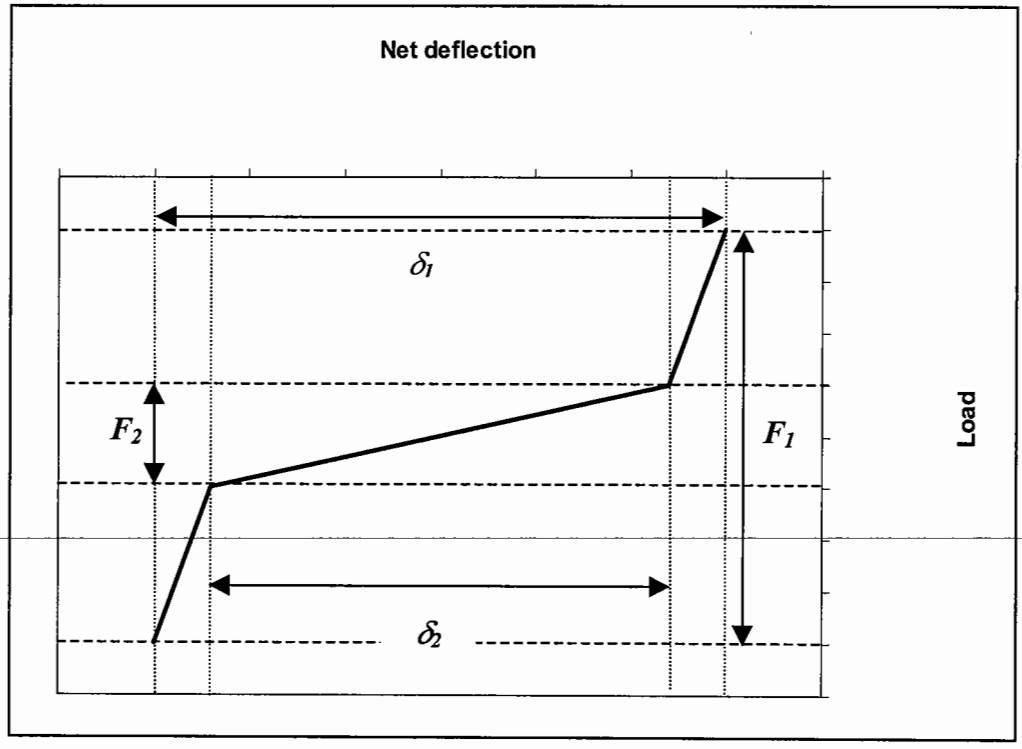

Figure 4-42 Load-shear slip model

The difference between the points in Figure 4-42 was the total distance moved by the central block (as an average of the two LVDT readings), resulting in a typical net shear slip-number of cycles plot as shown in Figure 4-43. Load was found to relate to the natural logarithm of the number of cycles. The relationship therefore took the form of:

$$y = a + m.Ln(x) \qquad \textbf{Eqn...4-6}$$

Constant 'a' corresponded to the total shear slip of the central block at the start of the test under the maximum and minimum load. Often, the behaviour up to approximately 10 cycles was not logarithmic, as illustrated by Figure 4-43. In such instances the constant 'a' will have been estimated to be less than what actually occurred.

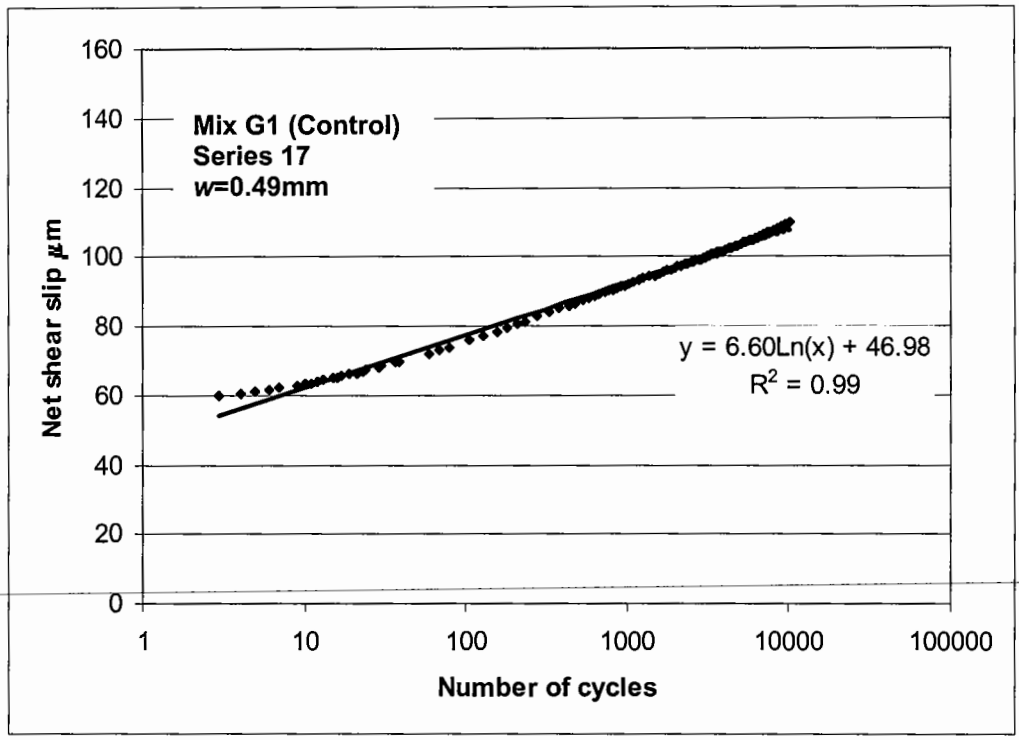

Figure 4-43 Net shear slip-cycle relationship at a load of ±2kN showing expression used to determine initial shear slip and deterioration

The constant 'm', given by the gradient of the graph, was a measure of the increase in net shear slip per cycle. This was assumed to be an indication of the deterioration that was taking place across the crack interface. On a small number of specimens, a constant gradient 'm' could not be determined as the shear slip-log cycles relationship was not linear, illustrated by Figure 4-44 at a load of ±3kN. Such specimens were considered to be subject to

'rapid deterioration'. These data are reported in the Tables below but not used in the analysis. Within the limits described, the constants a and m in Eqn...4-6 allowed a comparison of specimen behaviour at various crack widths and fibre volume fractions.

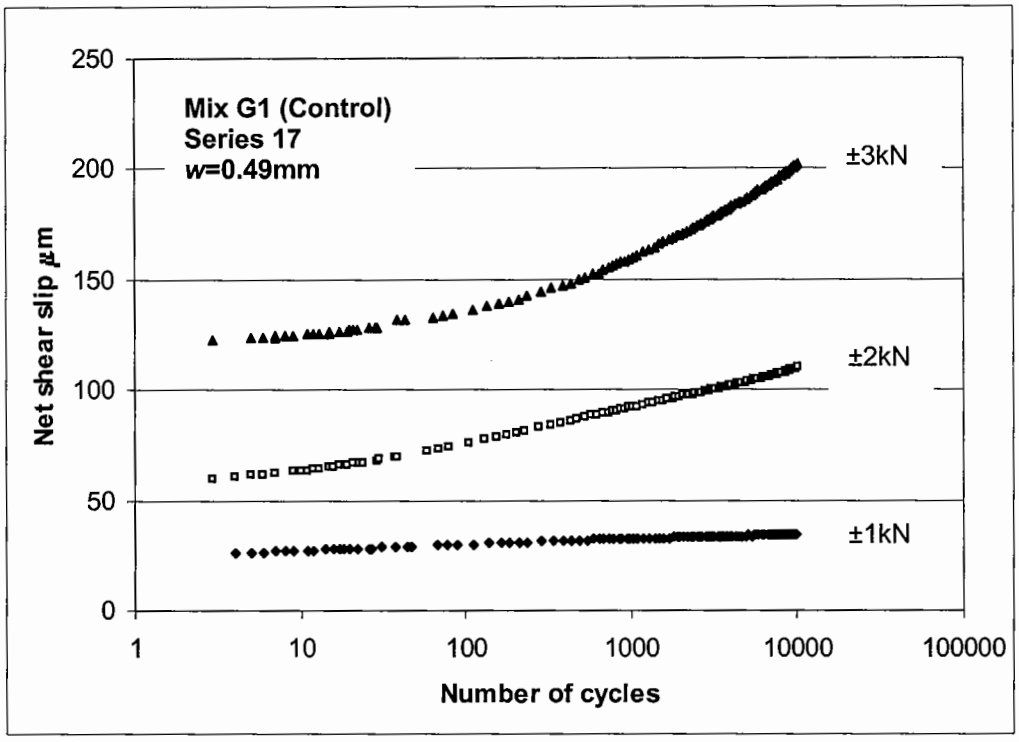

Figure 4-44 Shear slip-cycles plot at various load levels indicating rapid deterioration at ±3kN

From the shear slip data, load transfer stiffness (LTS) was defined as the applied shear stress (τ) per unit shear slip (y). For each test, the applied load (F) and the cross sectional area of both crack faces (A) remained constant. Therefore, any increase in the net shear slip (y) during the deterioration tests as determined using Eqn...4-7 resulted in a reduction in the load transfer stiffness. As the net shear slip was a measure of the total movement between the maximum and minimum loads, it was halved to calculate the load transfer stiffness in any given direction of movement.

$$LTS = \frac{\tau}{\left(y/2\right)} = \frac{F}{A.\left(y/2\right)} \qquad \textbf{Eqn...4-7}$$

4.8 Results from cyclic shear tests

Cyclic test results are presented in Table 4-16 in terms of initial shear slip (a) and deterioration gradient (m) at various crack widths (w) and fibre volume fractions (V_f).

Series	Beam no.	V_f %	Crack width mm	±1kN		±2kN		±3kN	
				a	m	a	m	a	m
16	1	0	0.09	2.6	0.02	7.2	0.43	15.0	2.0
17	1	0	0.49	25.0	1.06	60.0	6.6	120.0	10.7
18	2	0	0.43	5.9	0.13	16.6	1.4	44.0	9.1
19	2	0	0.80	113.6	4.18	190.0	21.1	300.0	20.0
22	3	0	0.55	4.7	0.04	13.5	0.28	25.0	2.0
23	3	0	1.00	42.6	9.74	200.0	44.0	300.0	20.0
12	1	0.5	0.14	3.1	0.01	8.8	0.08	14.1	0.37
13	1	0.5	0.19	4.6	0.01	11.4	0.12	21.0	0.57
14	1	0.5	0.36	5.6	0.00	14.2	0.21	25.2	0.89
15	1	0.5	0.83	25.4	0.61	74.5	4.7	128.4	9.4
25	2	0.5	0.39	1.3	0.00	2.8	0.03	4.8	0.10
26	2	0.5	0.68	4.6	0.00	10.8	0.10	19.0	0.28
27	2	0.5	0.95	6.2	0.04	15.4	0.39	30.6	0.79
20	1	1.0	0.52	4.0	0.07	10.6	0.62	25.0	2.0
21	1	1.0	0.81	17.2	0.53	64.5	5.1	140.0	9.2

Table 4-16 Summary of results for effect of cyclic shear stress on load transfer stiffness for mix G1

4.8.1 Load-shear slip response

The load-shear slip response from the 'start' and 'end' shear tests highlighted very different behaviour as the crack widths were increased, and with steel fibre reinforcement. At low crack widths (less than about 0.4mm), the load-shear slip response was often approximately linear (Figure 4-45). In such tests, invariably, the net shear slip was low, resulting in a high load transfer stiffness. This behaviour was similar for the control and fibre reinforced specimens. The deterioration gradient for these specimens was also low.

It appears that when the crack width is low, the whole crack face contributes to the shear resistance. This results in a linear load-shear slip relationship, and maintains small shear slips and deterioration rates. The contribution of fibres at such crack widths appears to be less significant than in wider cracks, as will be demonstrated.

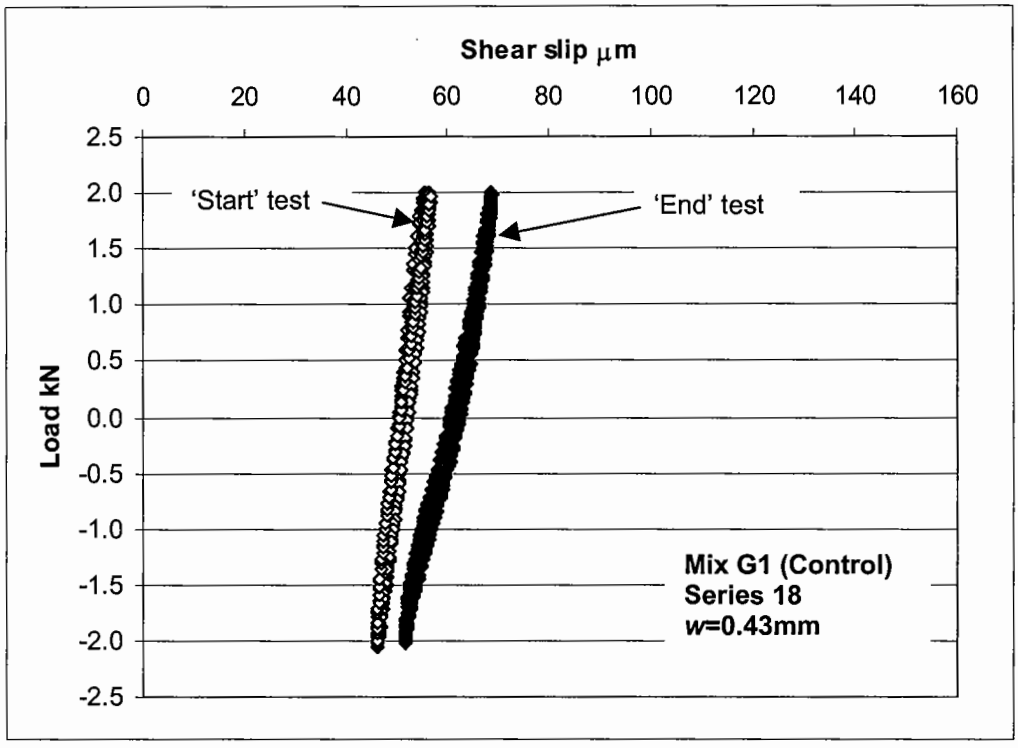

Figure 4-45 Load-shear slip plot demonstrating good interlock characteristics

At higher crack widths, the relationship between load and shear slip was non-linear (Figure 4-46). Similar behaviour was previously reported by Abdel-maksoud (1997). It appears that in these instances the total crack face is not contributing to the shear resistance. The explanation might be that the finer aggregate is no longer contributing to aggregate interlock, with the load being carried by the larger aggregate only. As these are spaced apart, the specimen must undergo some movement before the effects of the large aggregate can contribute significantly. Once the contribution of the larger aggregate is mobilised, the majority of the applied load is taken over a very small shear slip. The load transfer stiffness in unreinforced specimens at large crack widths might therefore be a function of the aggregate spacing and size.

The fact that this apparent lack of any load carrying exists between the large aggregate pieces means that the majority of the shear slip takes place at a very low load.

Figure 4-46 shows that approximately 270μm out of 340μm of movement took place under only 0.5kN of load. Put another way, 80% of the movement occurred at 12.5% of the total load. This means that in unreinforced specimens with wide cracks, very small loads cause large movements.

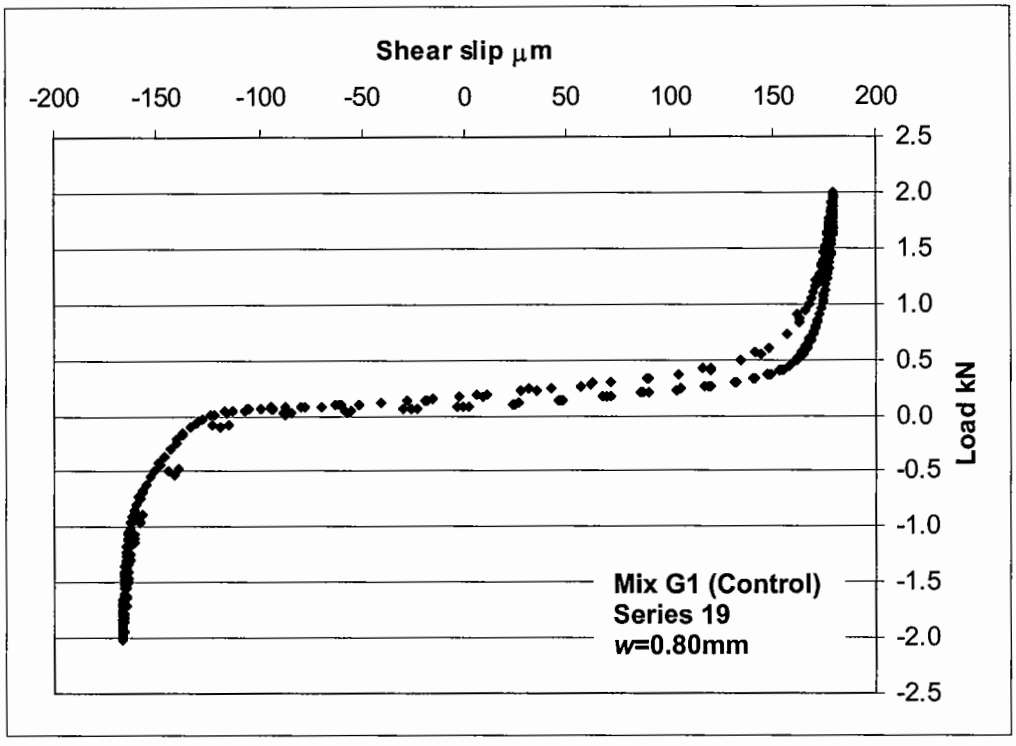

Figure 4-46 Load-shear slip relationship in an unreinforced specimen demonstrating poor aggregate interlock properties

This may have some practical significance if such behaviour also occurs in CBM pavements. Traditionally, only the heaviest traffic loads are considered to contribute to the damage of a pavement. If lower loads also cause significant deflection at the crack face, the implication is that more local distress could occur than is currently assumed. In a flexible composite pavement, this additional movement will not only add to spalling and deterioration of the CBM crack, but also contribute to the strains on the asphalt overlay.

The load-shear slip response was observed to be noticeably different at the larger crack widths in steel fibre reinforced specimens. The relatively flat load-shear slip portion observed in the unreinforced specimen appeared to be 'smoothed' out in the fibre reinforced specimens (Figure 4-47).

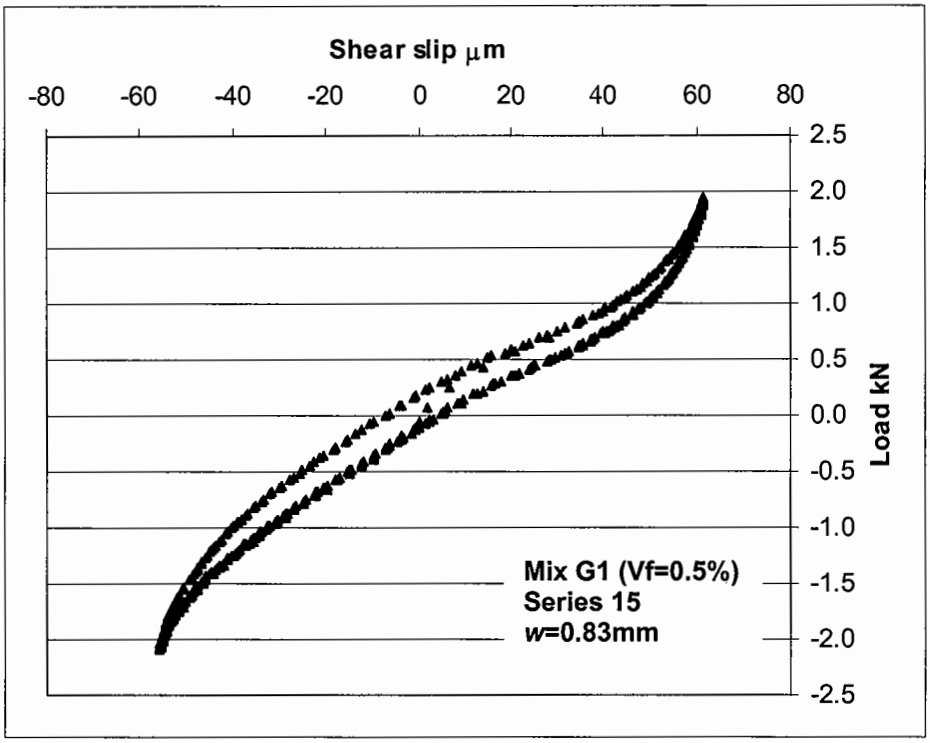

Figure 4-47 Load-shear slip relationship for a fibre reinforced specimen with a wide crack

It was observed during the tests that the fibres tended to bend around the aggregate as the central specimen block moved relative to the end sections. 'Snubbing' of the fibres had been recognised in static flexure tests as a possible cause of increased toughness (Paine 1998). The local frictional forces created by bending the fibres around aggregate may be an explanation of the mechanism for this smoothing action. Proportionally more load is required to move the specimen when compared to the unreinforced material. This smoothing behaviour creates a more efficient crack, as a greater load is required to cause movement than in the unreinforced material. The damage observed at lower load in the unreinforced material is less likely to occur when steel fibre reinforcement is used.

4.8.2 Crack linearity

The difference in 'crack efficiency' between CBM and FRCBM was modelled based on the crack linearity, a measure of the proportional load required to move the central block of the specimen through a proportion of its total movement.

At the end of the deterioration tests, the unreinforced specimens generally had low crack linearity (Figure 4-48). For mix G1, 8 out of 11 specimens had a crack linearity less than 25%. The fibre reinforced specimens tended to be more able to maintain high crack efficiencies; only specimens with a fibre volume fraction of 0.25% fell below 75%. It should be noted that the crack linearity was a measure of the free movement within each specimen; it did not describe the total movement, used to determine the load transfer stiffness. However, the crack linearity values show that there is a measurable difference in the load-shear slip behaviour of fibre reinforced specimens under cyclic shear. The 'smoothing' effect may help maintain a serviceable crack, reducing the risk of spalling and further damage across the cracked interface.

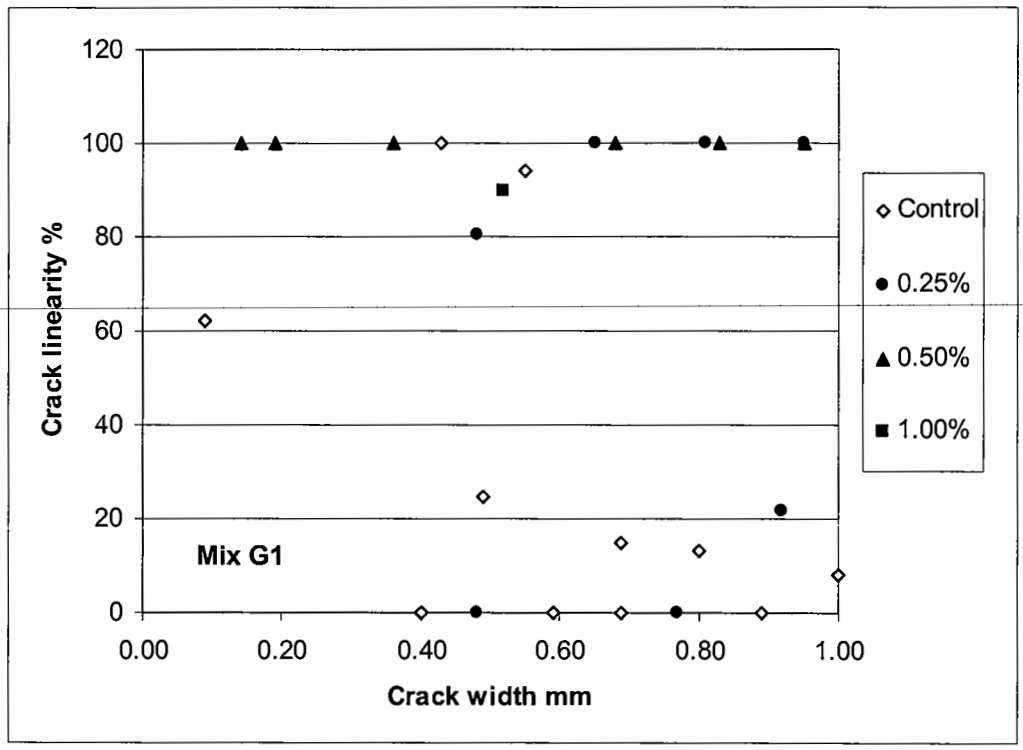

Figure 4-48 Increase in crack linearity due to fibre reinforcement

For practical purposes, shear slip was measured at maximum and minimum loads only during the deterioration tests. The load transfer stiffness calculated based on these values assumes a linear relationship between the shear slips measured, which simplifies greatly the actual behaviour at a crack interface. Any difference between CBM and FRCBM therefore relies on a measurable difference in the net shear slip. This may not take full account of the benefits of crack efficiency due to fibre reinforcement on account of the improved crack linearity when compared to CBM.

4.8.3 Effect of shear stress on load transfer stiffness

The relationship between load and shear slip is reasonably linear as shown by Figure 4-49.

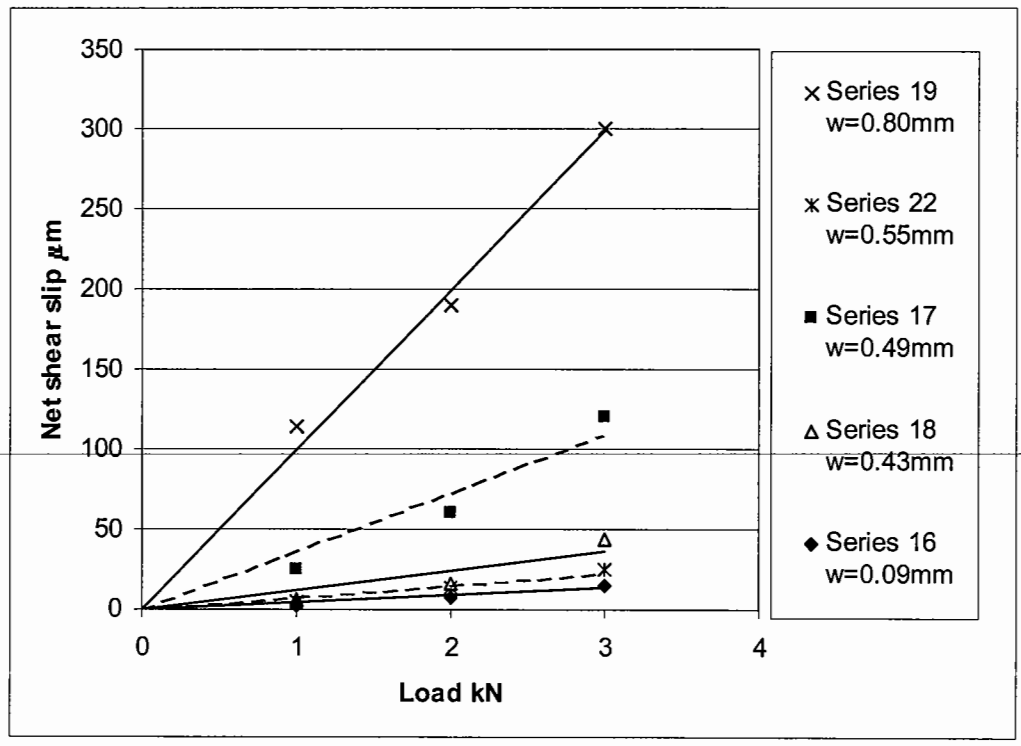

Figure 4-49 Relationship between load and net shear slip

The load transfer stiffness reduces approximately exponentially with increasing shear stress (Figure 4-50). Generally, as would be expected, greater crack widths resulted in lower load transfer stiffnesses. However, the pattern of reducing the crack width and increasing the load transfer stiffness does not always follow, as demonstrated at crack widths of 0.49mm and 0.55mm. The main variable was the coarse aggregate spacing within each specimen, which was not easily controllable but was considered likely to contribute to the load transfer stiffness. This may have accounted for a large proportion of the variability in load transfer stiffness. Despite this, the tests were able to distinguish between a range of load transfer stiffness values at differing crack widths in the control (unreinforced) specimens.

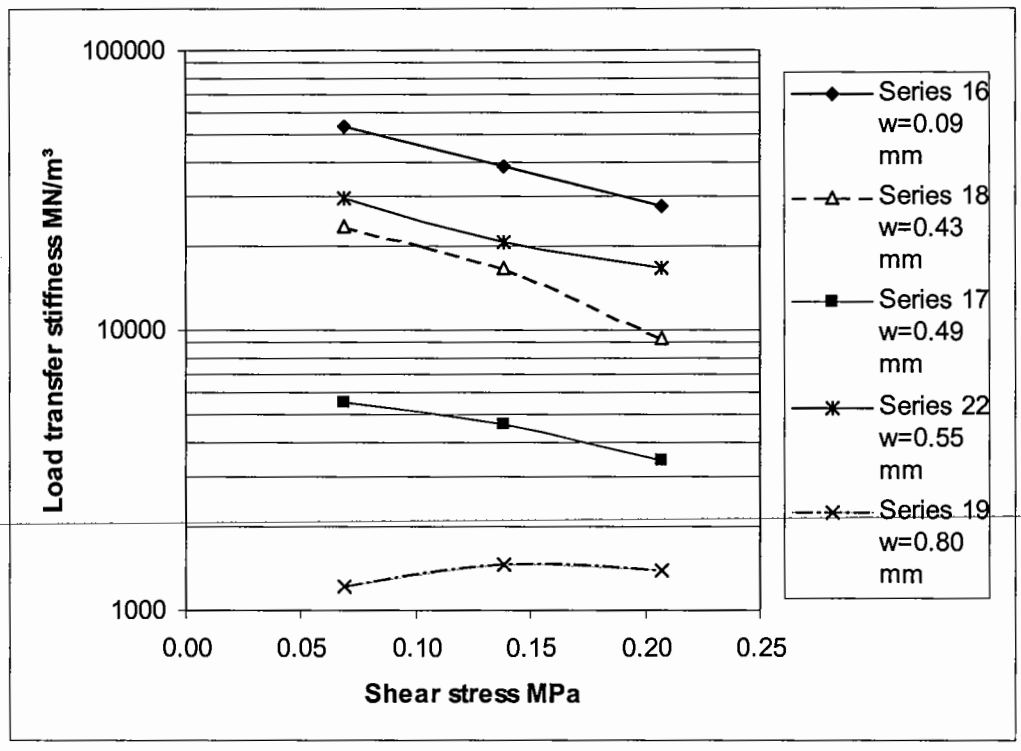

Figure 4-50 Relationship between shear stress and load transfer stiffness for control mix G1

Reinforced specimens, with the exception of series 15, were found to be more clustered around similar values of load transfer stiffness (Figure 4-51). The low values obtained for series 15 may only be explained by a reduced number of fibres bridging the cracks. The cluster of values at various crack widths demonstrates that fibre reinforcement has a significant influence on the load transfer stiffness, and that an increase in load transfer stiffness at high crack widths may occur when compared to the unreinforced material.

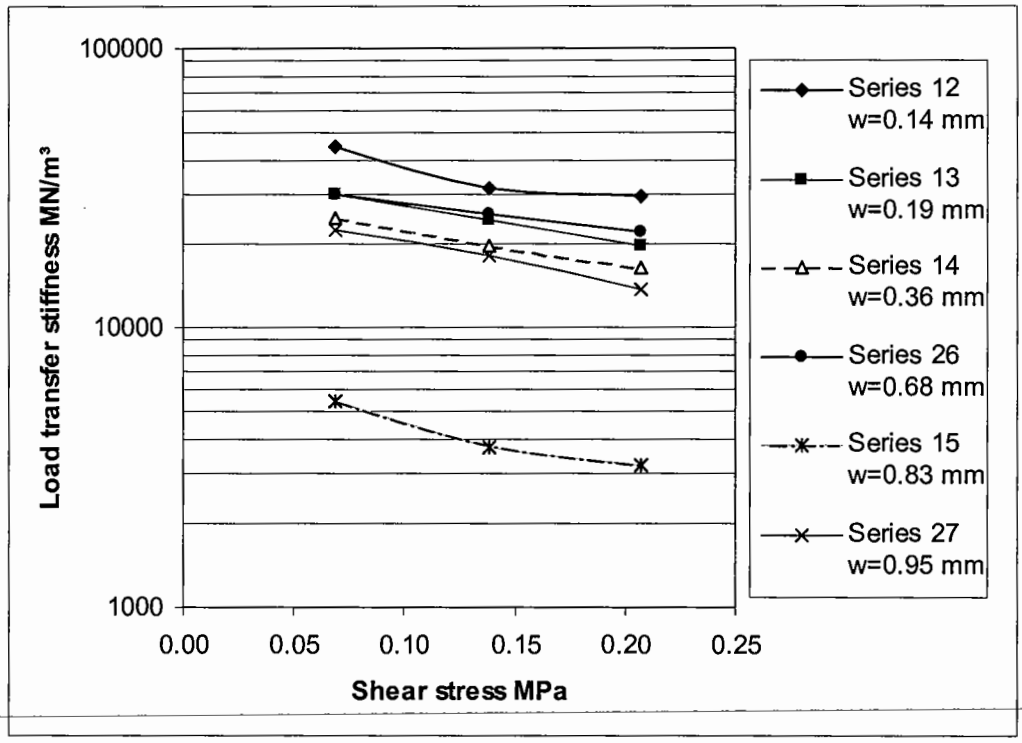

Figure 4-51 Relationship between shear stress and load transfer stiffness for mix G1 reinforced at a fibre volume fraction of 0.5%

4.8.4 Effect of fibre reinforcement on net shear slip and deterioration

The relationship between the net shear slip at the start of the test (a) and the crack width at various fibre volume fractions (V_f) is shown in Figure 4-52. This demonstrates that, as the crack width increased, the net shear slip tended to increase for all specimens. However, it was evident that the increase in shear slip was more marked for the unreinforced specimens. On the whole, the fibres were able to reduce significantly the net shear slip as the crack widths were increased, even at a volume fraction of 0.25%, when compared to the unreinforced specimens. However, no convincing pattern emerged whereby an increase in fibre volume fraction led to a proportional decrease in shear slip.

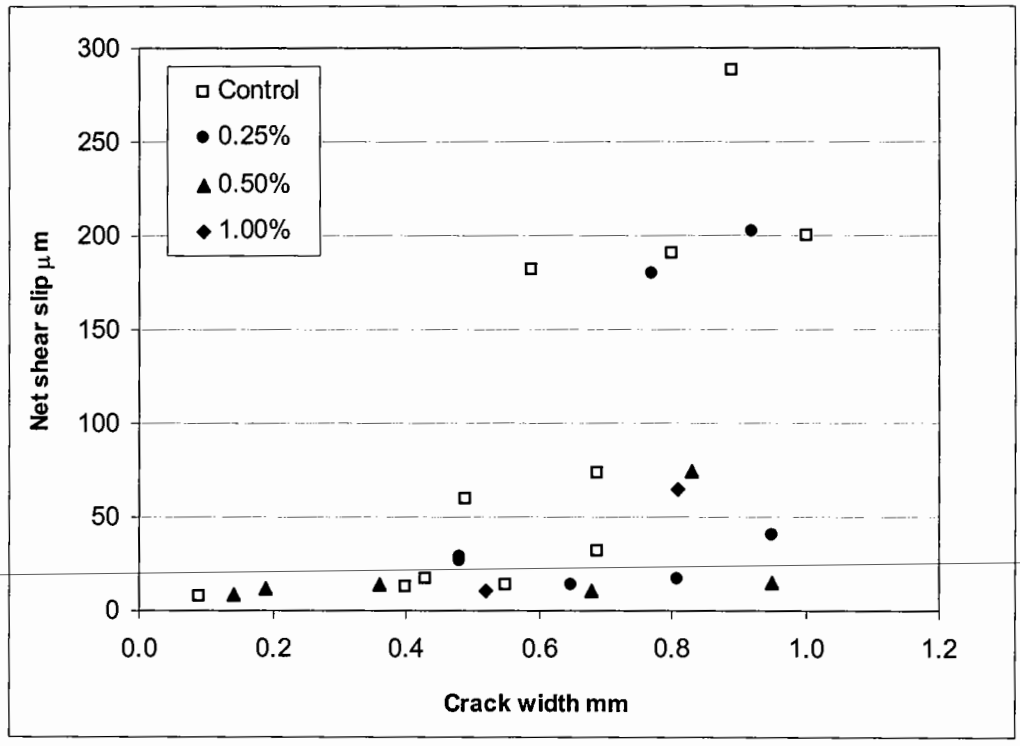

Figure 4-52 Relationship between net shear slip and crack width at various fibre volume fractions for mix G1 at ±2kN

The relationship between deterioration gradient and crack width was found to be similar to that of the net shear slip. Deterioration took place more rapidly in wider cracks than in narrower cracks. The fibres reduced the deterioration significantly (Figure 4-53). At fibre volume fractions of 0.5% and above, the deterioration was generally negligible.

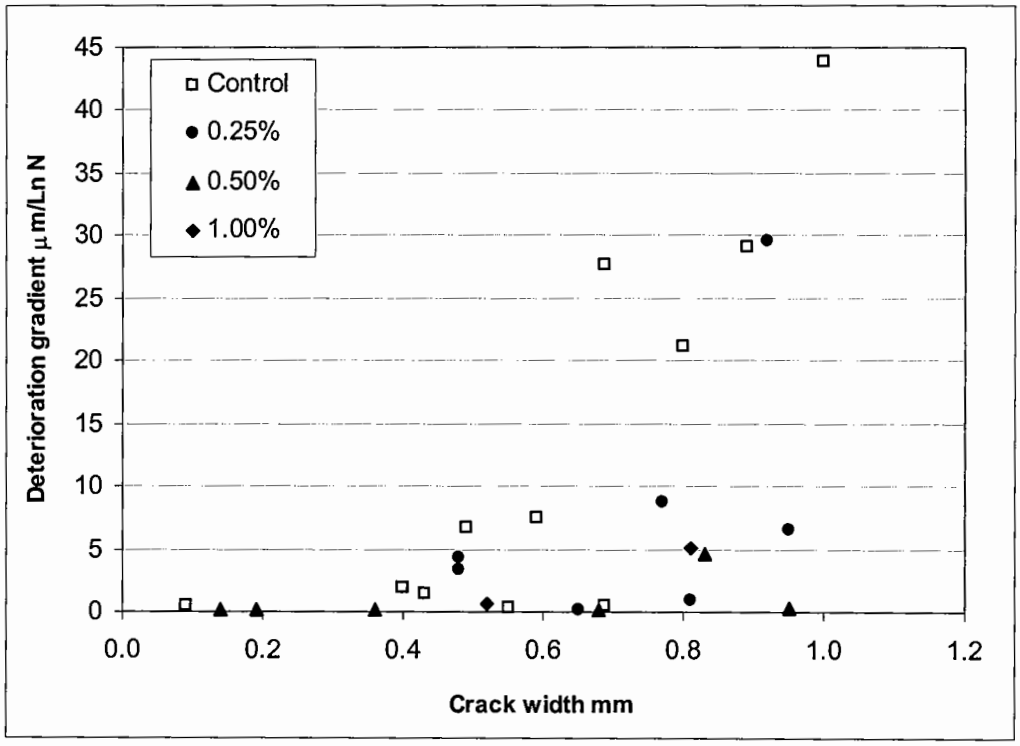

Figure 4-53 Relationship between deterioration gradient and crack width at various fibre volume fractions for mix G1 ±2kN

4.8.5 Effect of matrix strength

The data obtained from mix G3 at an applied load of ±2kN, which had a cement content of 8%, are shown in Table 4-17. These data are compared to the results for mix G1, previously presented in Table 4-16.

Series	Beam no.	V_f %	Crack width mm	±2kN	
				a	*m*
22	1	0	0.47	81.4	5.30
23	1	0	0.65	102.7	10.7
25	2	0	0.76	179.3	14.6
27	3	0	0.53	24.5	2.44
28	3	0	0.67	154.9	6.96
29	3	0	0.86	267.5	13.4
10	5	0.25	0.20	30.2	0.10
11	5	0.25	0.69	96.1	5.11
31	1	0.5	0.27	10.0	0.56
32	1	0.5	0.49	44.4	2.04
33	1	0.5	0.66	69.2	4.15
35	2	0.5	0.51	4.2	0.01
36	2	0.5	0.73	5.4	0.01
37	2	0.5	0.95	8.3	0.18
76	1	1.0	0.32	8.4	0.02
77	1	1.0	0.56	9.6	0.24
78	1	1.0	0.64	9.7	0.09
79	2	1.0	0.86 0.69	47.9	0.66

Table 4-17 Summary of cyclic shear results for mix G3

The expectation was for the higher strength mix (G3) to yield a lower net shear slip and deterioration gradient than the lower strength mix (G1) as the crack width increased. The unreinforced mixes showed that no significant difference at the start of tests between the two mix strengths could be determined (Figure 4-54). However, the deterioration gradients demonstrated that the higher strength G3 mix deteriorated at a lesser rate than the lower strength G1 mix (Figure 4-55).

Based on the data, it was concluded that the material strength has less of an influence on the load transfer stiffness and deterioration than fibre reinforcement and crack width, for the load and strength ranges tested. In subsequent analysis therefore, the two mix strengths were included together.

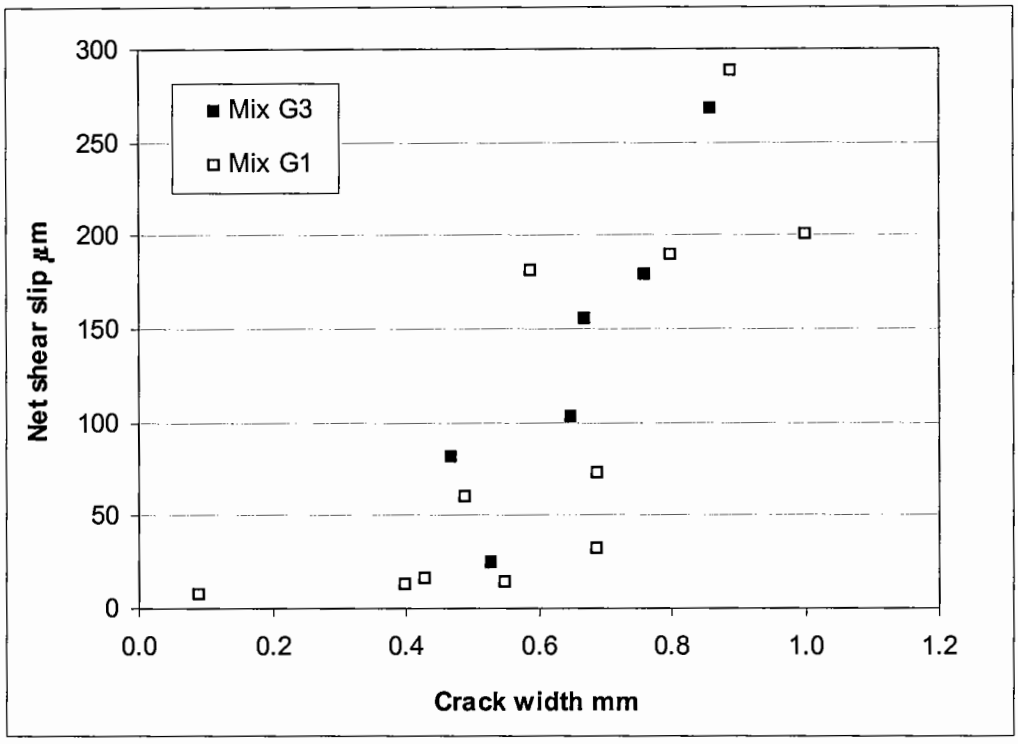

Figure 4-54 Effect of mix strength on net shear slip for unreinforced mixes G1 and G3

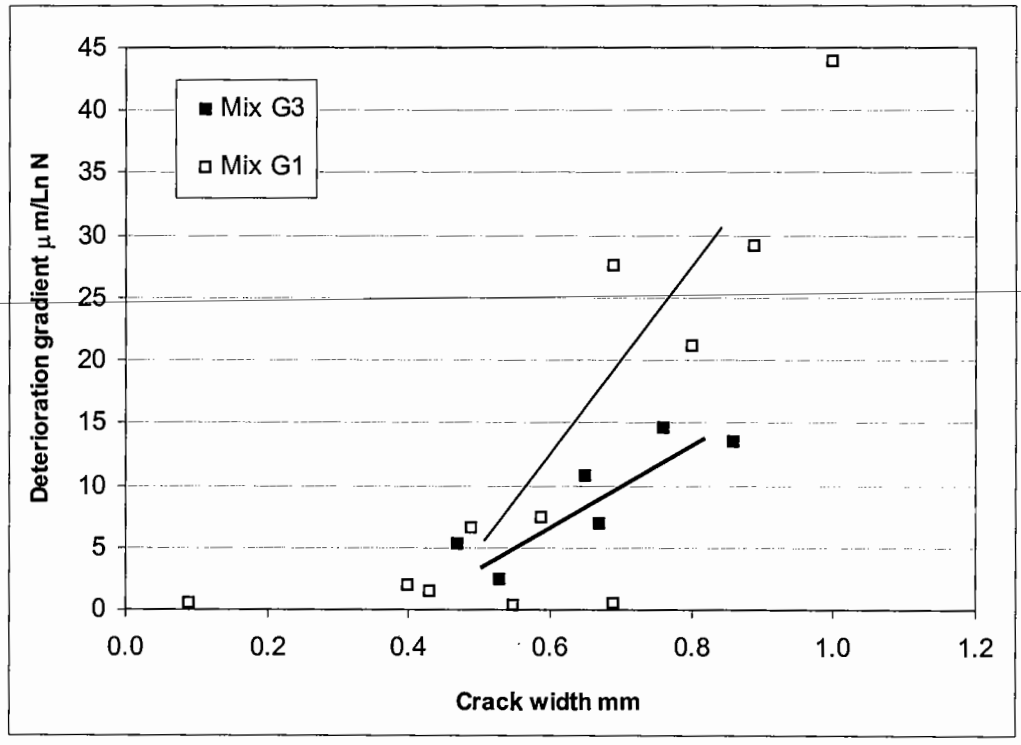

Figure 4-55 Effect of mix strength on deterioration gradient slip for unreinforced mixes G1 and G3

4.8.6 Effect of crack width and fibre reinforcement on load transfer stiffness

The load transfer stiffness was defined with a view to using the value as a design parameter. It was determined as a function of the net shear slip under a given load, using Eqn...4-7. As the net shear slip increased, the load transfer stiffness decreased. The relationship between load transfer stiffness and crack widths at various fibre volume fractions is shown in Figure 4-56. This includes data from mix G1 and mix G3. It is clear that at low crack widths, load transfer stiffnesses for unreinforced and reinforced mixes are similar. At high crack widths (greater than approximately 0.5mm), there is a greater difference between the load transfer stiffness values of CBM and FRCBM.

The data from the unreinforced specimens were reasonably predictable, as shown by the regression line in Figure 4-56. A regression line could not be fitted through the individual FRCBM specimens at various fibre volume fractions with any confidence, even though it was evident that the FRCBM performance was, on the whole, significantly better than CBM.

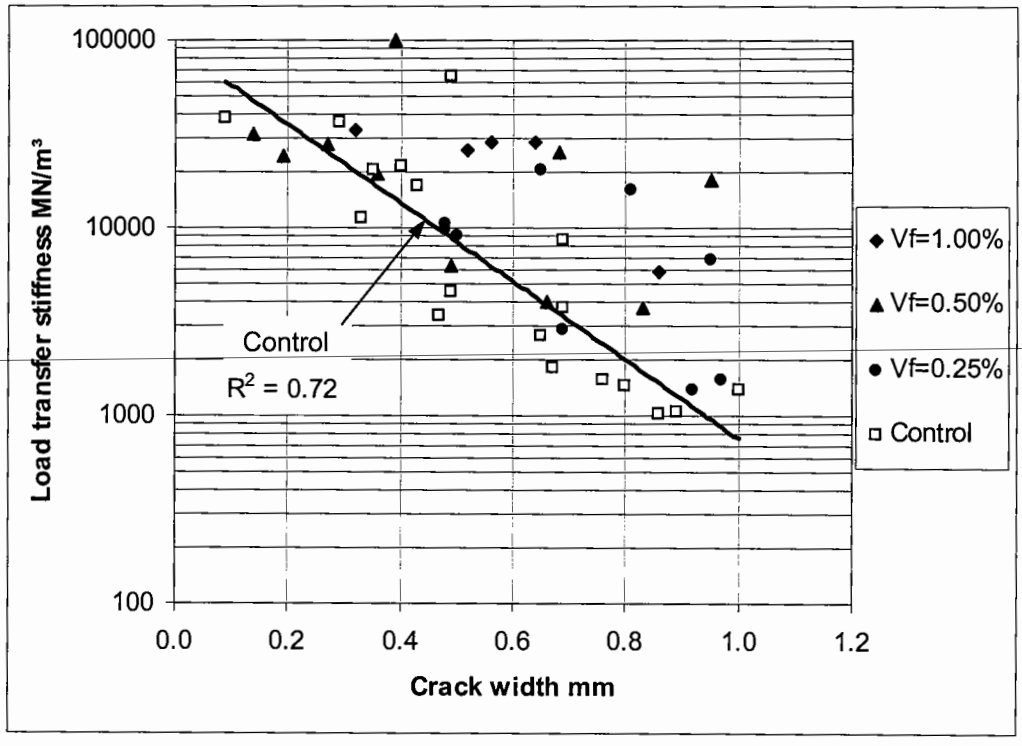

Figure 4-56 Relationship between load transfer stiffness and crack width at various fibre volume fractions for mix G1 and G3 at ±2kN

4.8.7 Effect of crack closure

A small number of tests were carried out at a load of ±2kN after crack widths had been decreased by pushing the specimen end sections together, thereby closing the crack. In almost every case, an irreversible reduction in load transfer stiffness had occurred (Figure 4-57).

This may be due to eroded fine material being captured within the crack face, facilitating slippage, or the inability to 'push' the crack faces back to their original positions. Such behaviour, if truly indicative of pavement behaviour in the field, will have significant consequences. Pavements with wide cracks, which will already have a significantly lower load transfer stiffness and increased deterioration rate than in narrower cracks, may be more prone to material collecting in the cracks. The permanent damage that appears to occur in wide cracks would be expected to result in a crack of poor load transfer efficiency, even throughout the warmer months when the cracks should be closed. By contrast, narrow cracks will maintain their load transfer efficiency, deteriorate at a relatively low rate and not be subjected to the permanent damage that occurs in wider cracks as material is not able to erode away to the same degree. It is therefore evident that inducing cracks to maintain narrow crack widths is of considerable benefit to flexible composite pavements.

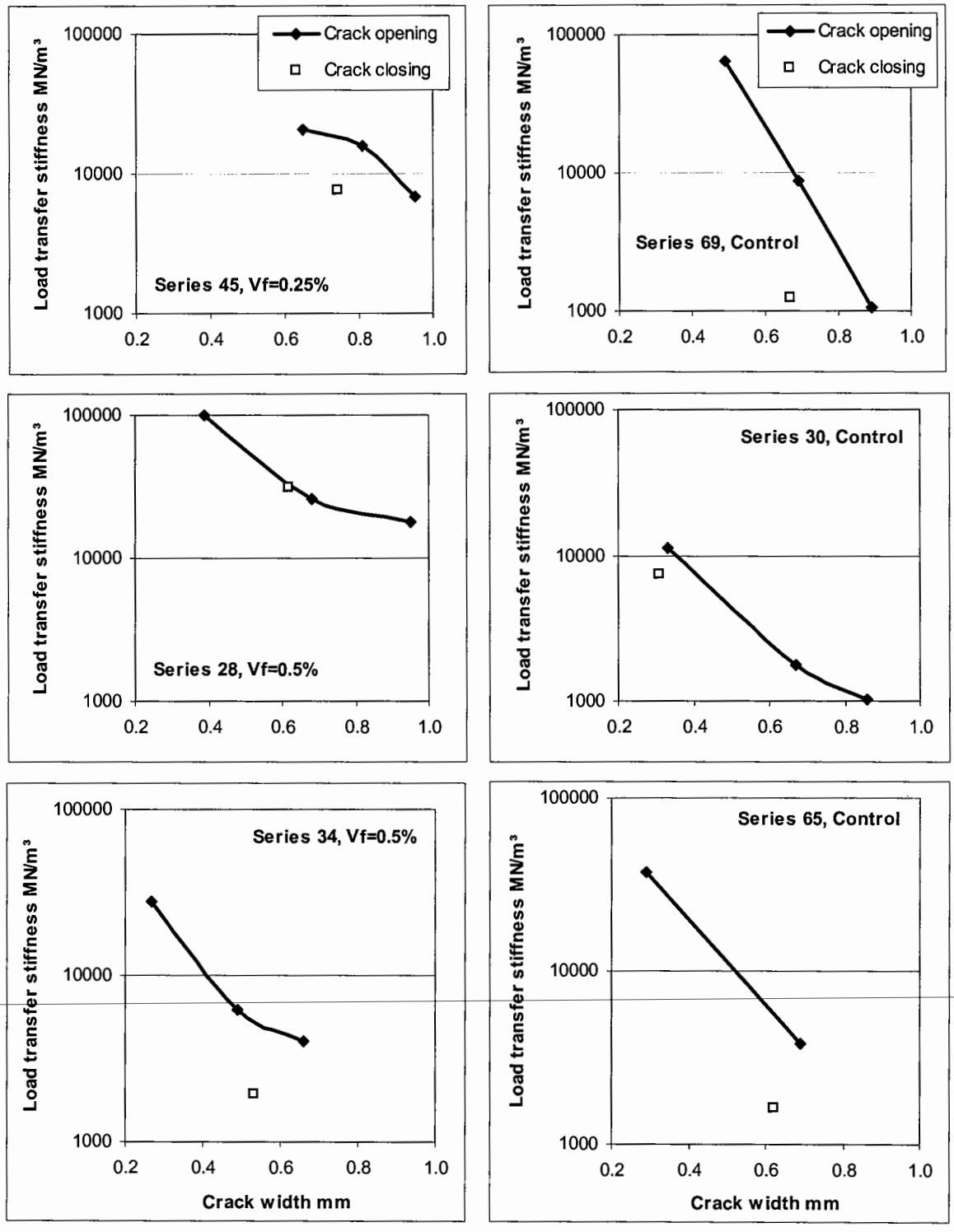

Figure 4-57 Effect of re-closing crack on load transfer stiffness

4.8.8 Conclusions and discussion based on cyclic shear tests

1. The cyclic shear test developed as part of this study was found to be a convenient tool to compare the shear characteristics of cracked CBM and FRCBM. The test allowed very small crack widths to be investigated. Crack widths in a CBM layer are predicted to be up to 1mm in naturally occurring transverse cracks, using a theoretical expression presented by Darter and Barenberg (1977). At closer crack spacings, the widths are reduced.

2. By examining the load-shear slip response from the cyclic shear tests, the unreinforced specimens almost universally showed signs of damage after a period of cycling. This resulted in relatively low loads contributing to most of the shear slip. The addition of fibres 'smoothed' out the load-shear slip response, improving its linearity. The mechanism for the smoothing behaviour was considered to have been derived from the fibres holding the sections of beam together under tension. It was concluded that the load transfer stiffness is most affected by the aggregate interlock, and that fibres help maintain this interlock rather than physically providing a means of load transfer themselves.

3. The cyclic shear tests showed that a reduction in the crack width is the most effective way to increase the load transfer stiffness. In practice, this may be realised by inducing cracks in the cementitious layer at closer spacings than would occur naturally. The benefits of induced cracking are significant and should be continued even where fibre reinforcement is used. Additionally, fibre reinforcement might indirectly contribute further by reducing transverse crack widths brought about by a resistance to the direct tensile stresses due to thermal effects.

4. Load transfer stiffness is increased and deterioration rate reduced significantly in fibre reinforced cracks, which if unreinforced, would be expected to exhibit poor crack interface characteristics. Fibres therefore provide a mechanism to enhance load transfer.

5. There was evidence to suggest that once some damage had occurred at the crack interface, re-closing of the crack would not return the load transfer stiffness to the original state. This may be due to aggregate breaking free and detritus falling into the crack opening, reducing the aggregate interlock effectiveness. Such behaviour in the field will result in a rapid deterioration at the crack face as the material contracts and expands during daily and seasonal temperature changes. Induced cracking will help maintain a crack of small width with a low amount of contraction and expansion, reducing the risk of damage and detritus falling into the crack.

6. Small scale tests such as these are an efficient way to investigate a relatively large sample. However, larger scale tests have the clear benefit of approximating in-service behaviour more closely. Large scale slab tests of the type carried out by Colley and Humphrey (1967) would enable a realistic validation of the results presented here, and allow the contribution of the sub-base properties to be included.

4.9 Closing remarks on laboratory testing

General

1. The laboratory tests demonstrated some particular traits of FRCBM. Primarily, it is evident that the major benefit of fibre reinforcement occurs post-crack; if the material does not crack, the fibre influence is negligible. A possible exception to this may be in fatigue, where tests demonstrated an enhanced ductility prior to cracking. As CBM often cracks for numerous reasons, fibre reinforcement potentially offers many advantages.

Static tests

2. Static flexure tests have demonstrated that the post-crack ductility observed in SFRC is also evident in FRCBM. This is in spite of the low matrix strength of FRCBM (to a minimum 7-day compressive cube strength of 10 MPa), low water content (and therefore paste content) and the method of surface compaction. Other than a study by Sobhan (1997), no other literature was found on a similar material at such a low strength.

3. There is no easy method for predicting the strength of a CBM without resorting to direct measurement, and the relationship between compressive cube strength and flexural strength is dependent on aggregate type, aggregate grading and water content. The first crack and ultimate flexural strength due to fibre reinforcement may be approximated based on semi-empirical expressions with a knowledge of the unreinforced strength. However, for all practical purposes the flexural strength of a CBM, and first crack and ultimate flexural strength of an FRCBM using fibre types and volume fractions considered in this study, may be considered equal.

4. There is no simple model available to predict the post-crack behaviour of a fibre reinforced composite, therefore direct measurement is required for each fibre type and volume fraction being considered. It should be noted that the apparatus and skills required for testing FRCBM are not widely available in the United Kingdom, with possibly half a dozen academic institutions currently able to perform instrumented flexure tests. However, as the ductility is

more sensitive to fibre type and fibre volume fraction than matrix strength, an approval process may allow a system whereby a manufacturer's fibres are tested in advance and certificated. In practice, fibre volume fraction for a given fibre type may than be selected from an approved list.

Dynamic flexure tests

5. Fatigue (endurance) tests did not demonstrate any difference between CBM and FRCBM. Current fatigue trends for CBM may therefore be used, and enhanced benefits reported for SFRC are not applicable. The failure mechanism is of interest, and the improved ductility pre-crack may increase the life in a composite structure. Such benefits require further investigation.

6. Post-crack dynamic behaviour demonstrates a reduction in the rate of permanent strain accumulation with increasing fibre volume fraction. The ability of the pavement to carry dynamic load post-crack offers the potential to produce a long-life, durable FRCBM pavement, though serviceability criteria would need to be investigated. This area also needs further investigation.

Cyclic shear tests

7. Cyclic shear tests demonstrated the increase in load transfer stiffness brought about by a reduced crack width, practically achieved using induced cracking techniques, though the actual measurement of crack width is by no means simple. Steel fibres were shown to further increase the load transfer stiffness and reduce deterioration rates, in particular at wider crack widths. It is likely that, without fibres, cracks will open up at different rates, with some cracks dominating. Theoretical expressions, whilst useful in assessing the effect of parameters on crack width, may underestimate the actual width in some locations. In addition to increases in load transfer stiffness, fibres may also reduce the temperature movement of slabs by providing some restraint across transverse cracks, also aiding aggregate interlock and reducing strains on the overlay. Fibre reinforcement therefore has a significant role to play in improving the load transfer characteristics of cracks.

Chapter 5. Field Investigations

5.1 Introduction

The mixing of steel fibre reinforced concrete (SFRC) is very different from that of FRCBM. SFRC is mixed by batch, and the amount of free water within the concrete makes for a workable material. The production of CBM differs significantly in that continuous batching is often employed in order to maintain production rates. Also, the material is much drier than conventional concrete to allow surface compaction by rolling, and this therefore results in a less workable mix. The production rate coupled with a dry mix required investigation to ensure the fibres were dispersed evenly throughout the mix and the soluble glue on collated fibres dissolved adequately.

This chapter reports two field investigations. The first investigated primarily the mixing process, and the problems encountered on this occasion are briefly outlined. Based in part on the outcome of this first study, a more extensive investigation considered the whole construction process. This included mixing the CBM and fibres, laying FRCBM through an asphalt paver, roller compaction and curing. Induced cracking was carried out using a guillotine type breaker. The performance of the pavement was monitored over a period of 18 months under high traffic load. Measurements were taken in the laboratory to investigate the effects of compaction on strength, and the effective stiffness of the pavement was measured using a Falling Weight Deflectometer (FWD) after considerable cracking had occurred. Toughness characteristics of laboratory and field prepared specimens using the trial mix were compared to results from the laboratory study reported in Chapter 4.

Recommendations are made based on the field trials regarding dispensing fibres into the mix. Ways are discussed by which laying CBM reinforced with steel fibres could be improved, through better construction techniques, with a view to optimising fibre distribution and material density.

5.2 Pode Hole Quarry trial

A mixing trial was carried out in Pode Hole Quarry near Peterborough in December 1997, shortly after the start of the project. Mixing was carried out using a pug-mill type continuous batcher, which was being used by Sitebatch (Contracting) Ltd at that time to produce a gravel aggregate CBM for the A1 widening at Alconbury. The objective was to investigate whether collated fibres could be mixed continuously at a high rate, achieving an acceptable distribution of fibres.

Reinforcement was at volume fractions of 0.5% and 1.0% using the Bekaert collated fibre type 65/60, as used in the laboratory investigation. Collated fibres rely on water to dissolve the glue that holds the fibres in bundles. Whilst this type of fibre had been used successfully for a number of years in structural grade concrete when mixed in batches, a concern was that the glue would not dissolve in such a dry mix, resulting in a poor fibre distribution.

A fibre dispenser was commissioned by Sitebatch for the trial. This distributed fibres onto the inlet belt along with the aggregate, whence they were introduced into the mixing drum where cement and water were added. The mixed material was collected via an outlet belt, from where material for beam and cylinder specimens was taken and visual inspection of the fibre distribution was made.

The results from this first trial demonstrated:

- The dispenser was unable to distribute the fibres evenly and at a rate compatible with the continuous batching process.

- Collated fibres on the whole remained collated.

The trial therefore showed the need for effective dispensing equipment to maintain production rates and even fibre distribution, and the possible preference for loose fibres over collated fibres.

5.3 Cloud Hill Quarry trial

The Cloud Hill trial was carried out in June 1999. It aimed in part to resolve mixing problems encountered in the previous field investigation. Additionally, this trial was more extensive in that the whole construction process was investigated by laying, compacting and curing the material and inducing transverse cracks. The trial area was not overlaid with asphalt so that the cracking that occurred under traffic loading could be visually inspected.

The experience gained was used to produce a Material Specification and Notes for Guidance (Appendix B) to be used as a basis for the specification of subsequent trials and contractual work.

5.3.1 Mix design and test specimens

Constituent materials

Single size 20 and 10mm carboniferous limestone was blended with a graded limestone of nominal maximum size 6mm in the ratio 1:1:3. The grading is shown in Figure 5-1. The aggregate was taken from stockpiles in the quarry and taken to the laboratory to obtain natural moisture contents and, after being oven dried, to be graded and subjected to laboratory tests. Two fibre types were used in the study: fibre type 45/50FL, which was a modification of the 45/50 fibre used in the earlier laboratory investigation in that it had a 'flanged leg'; and collated fibre type 65/60.

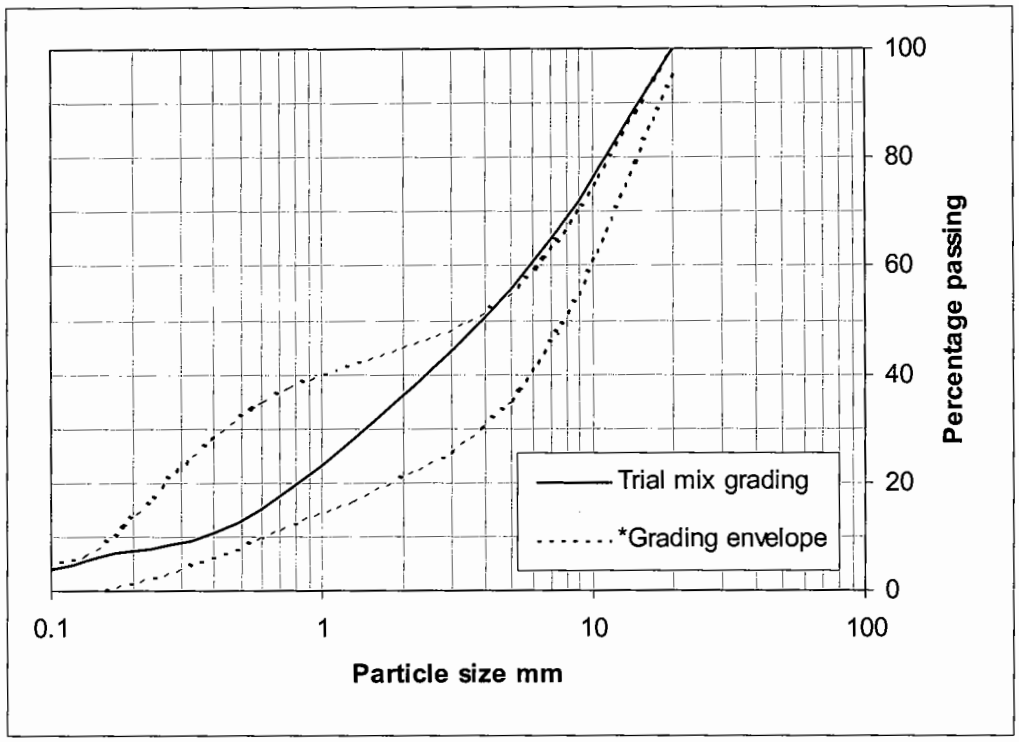

Note: *Grading envelope from Specification for Highway Works (Highways Agency 1998)

Figure 5-1 Particle size distribution for limestone aggregate used in Cloud Hill Quarry trial

The mix proportions adopted for the trial were based on experience gained in the laboratory study and from technical advice on site (Table 5-1). This was at a cement content of 7% by mass of dry aggregate to achieve the 'target' flexural strength of 4MPa. The structural design of the pavement was based on this value.

Laboratory prepared specimens

Following the trial, compressive cube and flexural strengths were obtained at 7-days from laboratory prepared specimens at cement contents of 6%, 7% and 8% by mass of dry aggregate. This allowed a retrospective study into the relationship between strength and

cement content for this material. These were compared to results obtained in the laboratory study.

Two additional beams and cubes were produced in the laboratory applying less compaction effort to investigate the effect of reduced density on material strength and toughness. All laboratory specimens were prepared using fibre type 45/50FL at a volume fraction of 0.4% because, as the analysis later will demonstrate, this represented the fibre content in the field.

Material	Mix proportions kg/m^3
Dry aggregate	2250.00
Cement	158.00
Natural moisture in aggregate	47.92
Added water	94.15
TOTAL MASS	*2550.07*

Cement content (by mass of dry aggregate)=7.0% and water content (by mass of aggregate and cement)=5.9%.

Table 5-1 Cloud Hill mix design

Site prepared specimens

During the trial, cube specimens of dimension 100mm and beams of dimension 100x100x500mm were produced in steel moulds and compacted using a vibrating hammer in the same way as described for the laboratory study (see Section 4-X). 3 no. beams and 3 no. cubes were prepared using the 45/50FL fibre at target volume fractions of 0.5% and 0.25% (referenced 4550-50 and 4550-25 respectively), 3 no. beams were produced for the type 65/60 fibre at a volume fraction of 0.5% (referenced 6560-50) and 3 no. cubes for the unreinforced material. These were tested at 6-days.

5.3.2 Mixing and laying

Mixing and laying was carried out using plant and techniques conventionally used in CBM paving work. Mixing was by means of a pug-mill type paddle mixer belonging to Sitebatch (Contracting) Ltd, which was sited in the quarry. The fibres were placed on the conveyor belt with the aggregate, using a commercially available fibre dispenser provided by Bekaert (Plate 5-1). This dispensed the fibres via a vibrating plate, which was factory calibrated for the collated 65/60 fibre. Site adjustments were necessary to dispense the loose 45/50FL fibres at the required rate and, in the event, this led to large variations in output, as will be discussed later. Batching was carried out in 20T loads at a production rate of 4T per minute. The batched material was transported to the trial area in wagons.

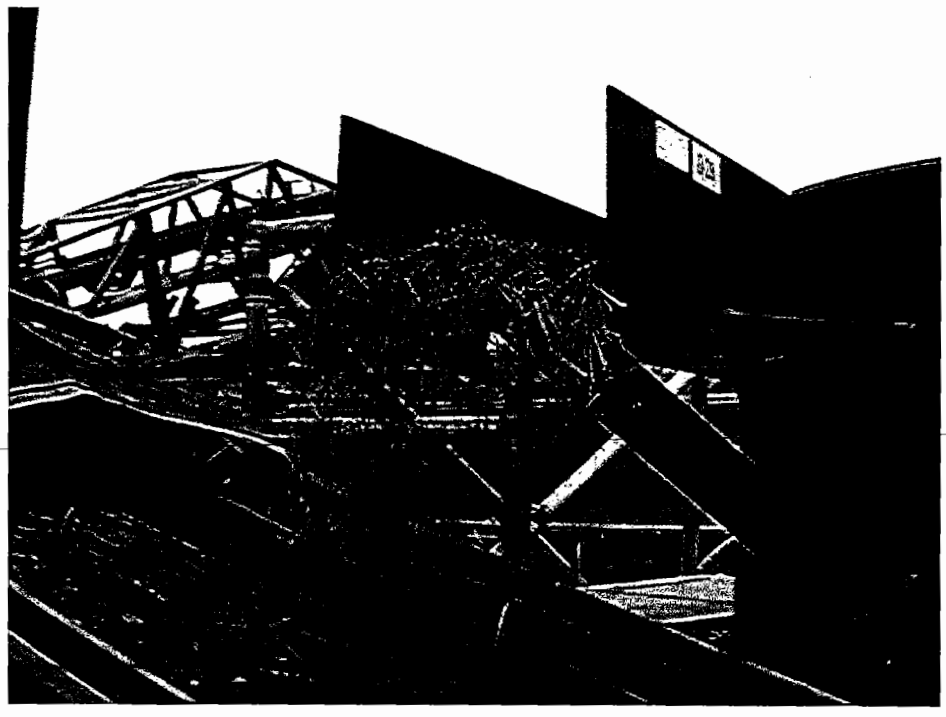

Plate 5-1 Fibre dispenser placing steel fibres onto aggregate belt during Cloud Hill Trial

The trial pavement was laid over a badly deteriorated section of concrete pavement that had collapsed along its centreline. A typical cross section is shown in Figure 5-2. The existing collapsed pavement was covered with unbound limestone aggregate to an approximate maximum depth of 300mm, to form a sub-base. Compaction was not controlled, although the sub-base was trafficked by site vehicles over a period of 24 hours. A 50mm deep regulating course using graded limestone of 6mm nominal maximum aggregate size was laid through the paver the evening before the trial to provide an even platform. Measurements were taken on the regulating course using the Dynamic Plate test (Highways Agency 1994) to assess the *in situ* stiffness.

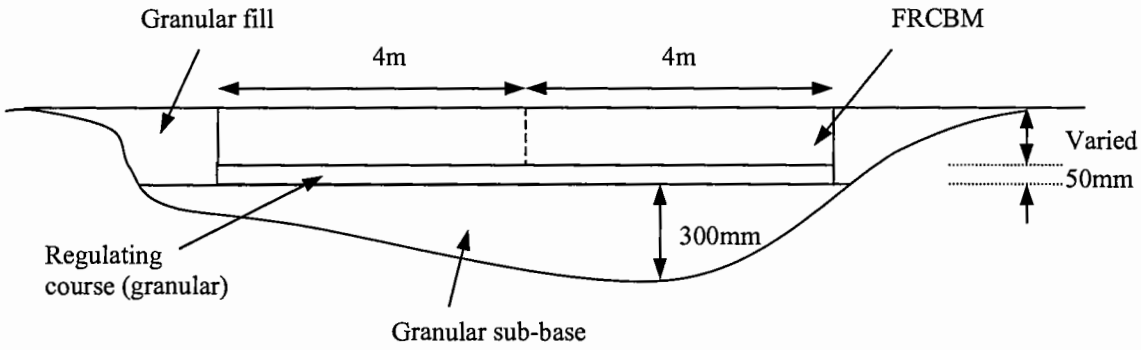

Figure 5-2 Typical cross section through trial area (exaggerated vertical scale)

A plan of the trial layout is shown in Figure 5-3. The material was laid through a paving machine in two lanes, each 4m wide. The central joint was formed by inducing a groove in the material using a vibrating plate with an attached fin (Plate 5-2), which was filled with bitumen before the layer was rolled. This technique of inducing longitudinal and transverse joints in CBM is proven to be effective (Ellis *et al.* 1997). The vibrating plate was also used to form transverse joints in the left lane at chainages 28, 31, 34 and 37. Induced cracking at 3 metre spacings was applied to the remainder of the pavement after 5 days using a guillotine type breaker (Plate 5-3). The guillotine was the preferred method of inducing

cracks as it ensured the fibres were not disturbed. It was felt that the fin on the vibrating plate would push fibres aside whilst inducing a discontinuity, therefore reducing the number of fibres bridging the crack. The material was compacted using a tandem vibratory roller (Bomag 160) and cured with a bituminous emulsion, and was opened to quarry vehicles after 7-days.

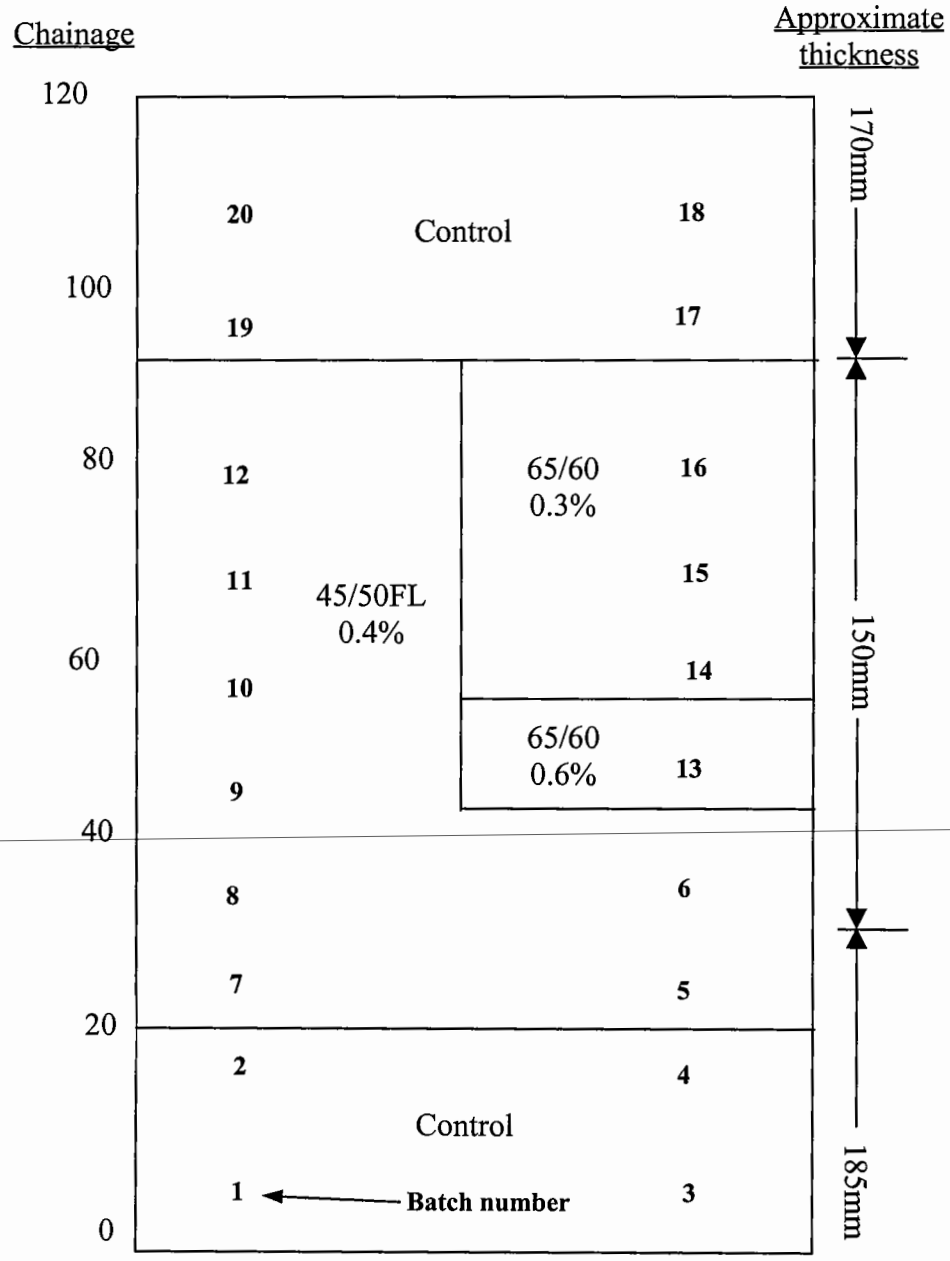

Figure 5-3 Plan of trial layout

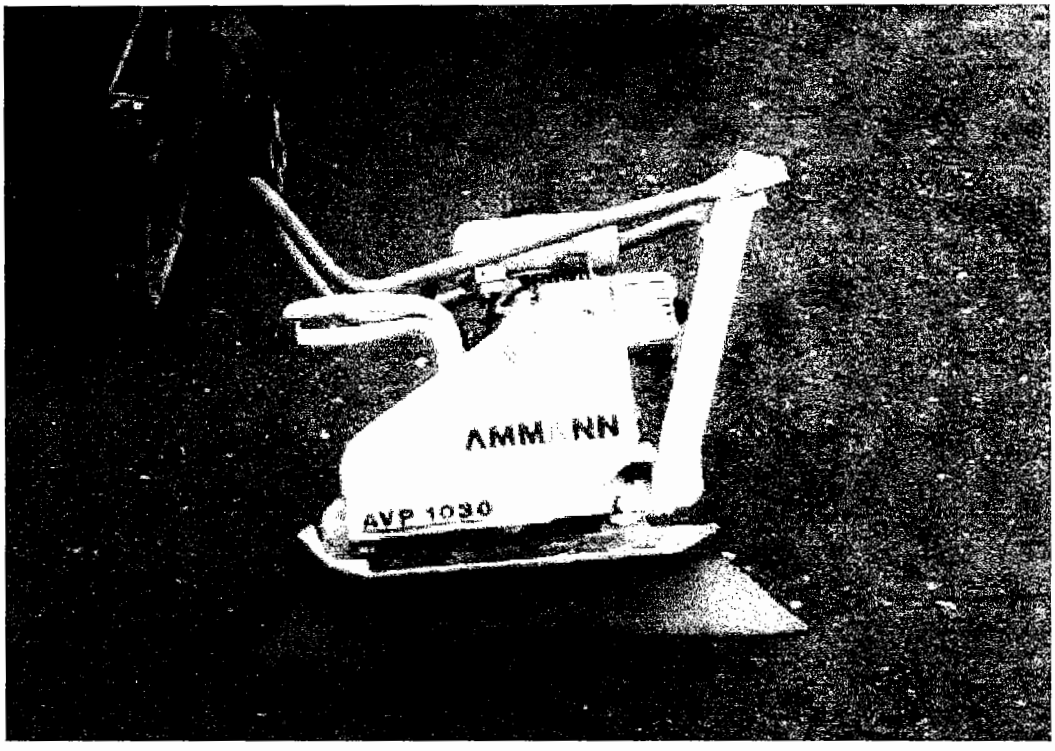

Plate 5-2 Vibrating plate with fin

Plate 5-3 Guillotine breaker used to induce cracks in FRCBM

5.3.3 Monitoring

The laid material and its subsequent deterioration was monitored by measurements from site cores, visual inspections and direct measurement using the Falling Weight Deflectometer (FWD) (Plate 5-4). A set of 35 no. cores was taken 5-days after laying the material. These cores were used to measure the pavement thickness, material density, indirect tensile (cylinder-splitting) strength and the indirect tensile stiffness. They were also used to assess the success of induced cracking. These were taken at the locations shown in Figure 5-4.

The FWD was used on three visits. It applied a load of 120kN using a 450mm diameter plate, resulting in an applied stress of approximately 750kPa. Geophones were positioned under the loading platen, and at distances of 0.3, 0.5, 0.6, 1.0, 1.5 and 2.1m. The FWD was used to measure the effective stiffness of the materials between transverse cracks after 5 days, 4 months and 13 months. Additionally, load transfer efficiencies were measured across induced transverse cracks. These were based on ratios of vertical deflections taken from the geophones at 0.5 and 0.6m from the load, either side of a crack.

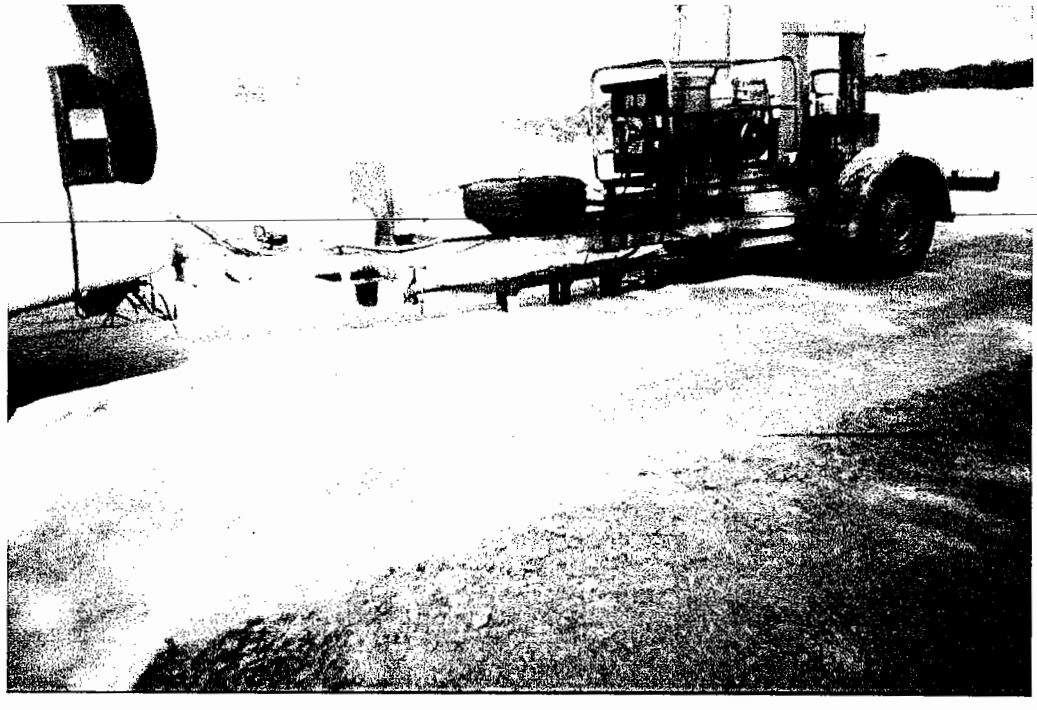

Plate 5-4 FWD used in site trial

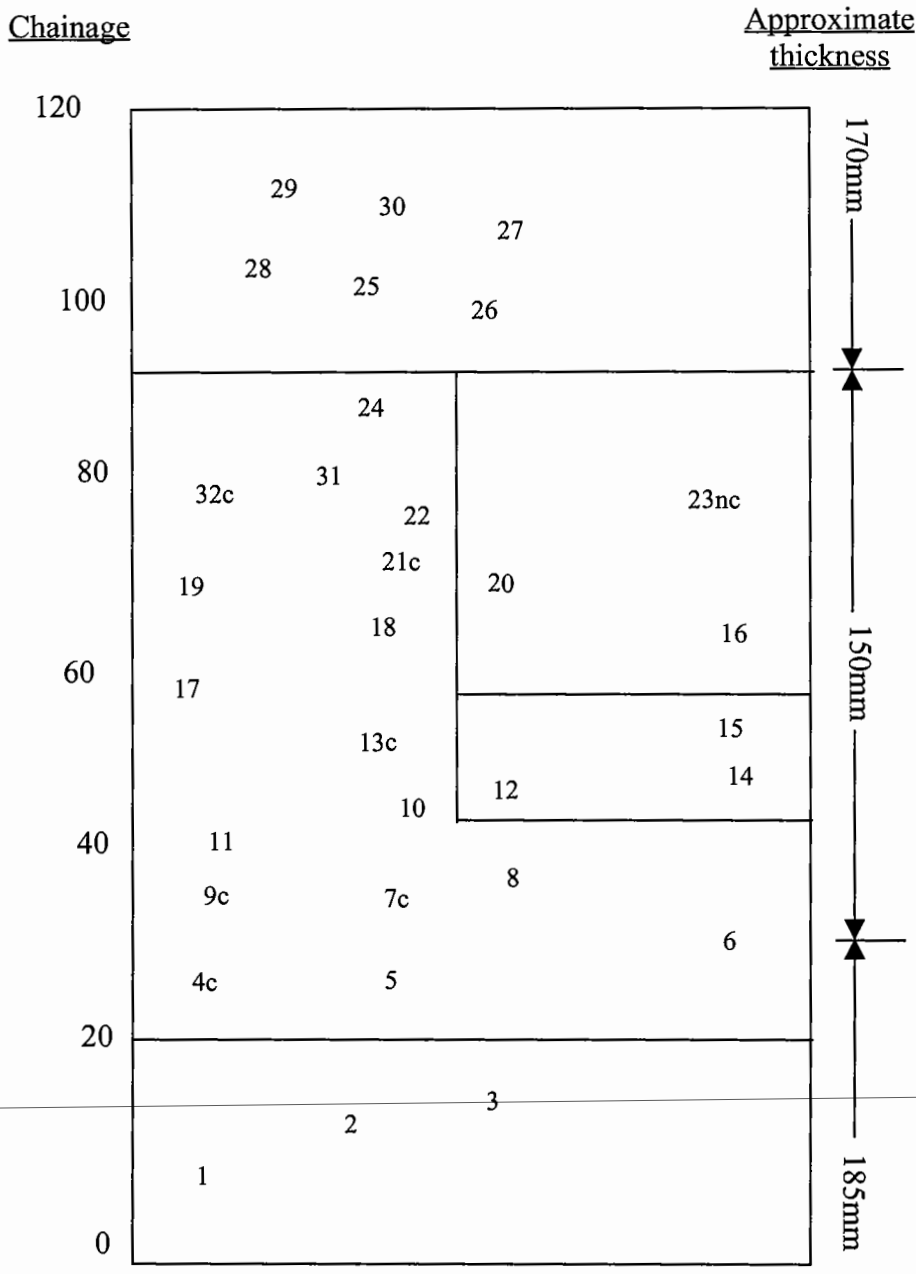

Figure 5-4 Location of cored specimens

5.3.4 Pavement design

The ultimate strength of the slab was calculated using plastic analysis (after Meyerhof 1962), and an allowable stress was determined using elastic analysis (after Westergaard 1926). Both methods are described in Technical Report 34 (Concrete Society 1994) for the design of ground bearing slabs. The modulus of subgrade reaction (k) was assumed to be 0.08N/mm³. The pavement was to withstand an assumed rear axle load of 650kN, based on a fully laden dumper load of 900kN and a known tyre pressure of 586kPa (85psi). A parameter to characterise the post-crack load carrying ability of the pavement ($R_{e,3}$) was estimated to be 50% based on design values provided in Bekaert product data sheets for SFRC.

Ultimate strengths based on plastic analysis and allowable stresses based on elastic analysis for pavement thicknesses of 150mm, 175mm, 200mm and 225mm are shown in Table 5-2. The 'target' flexural strength was 4MPa. Based on the analysis, it was anticipated that the unreinforced pavement with a thickness of 175mm would begin to crack over a short period as the critical stress is approximately equal to the flexural strength of the material, and the reinforced pavement would carry more load.

Slab thickness mm	Allowable stress (after *Westergaard 1926*) MPa	Ultimate (collapse) strength (after *Concrete Society 1994*) MPa	
		CBM ($R_{e,3}$=0%)	FRCBM ($R_{e,3}$=50%)
150	4.10	5.30	3.52
175	3.41	4.18	2.78
200	3.19	3.40	2.26
225	2.90	2.83	1.88

Table 5-2 Comparison of theoretical allowable stress/ultimate strength for purpose of thickness design

Analysis following the trial indicated that the pavement thicknesses, material strength and fibre volume fractions differed from the design. This resulted in a 'weaker' pavement than anticipated, although significant differences between the reinforced and unreinforced sections were observed, as described in the following sections.

5.4 Results from construction phase

5.4.1 Fibre dosage

The fibre dispenser used in the trial was designed for use with a batch mixer. The fibre dispenser operated on a frequency of vibration of the outlet, which was calibrated for use with type 65/60 collated fibres. To accommodate different fibre types and volume fractions, the machine required re-calibration. This was found to be impractical during the trial, so adjustments were made to the frequency of vibration on site by the operator. This did not allow the target fibre volume fractions of 0.25% and 0.5% to be achieved. Fibre volume (V_f) varied between 0.22% and 0.43% for the target fibre volume fraction of 0.25%, and between 0.37% and 0.52% for the target fibre volume fraction of 0.5% (Table 5-3 and Figure 5-5). Consequently, the 45/50FL fibres were dispensed at an average fibre volume fraction of approximately 0.4% (Batches 5 to 12). The 65/60 fibres were dispensed at an average of approximately 0.6% (Batch 13) and between 0.2-0.3% (Batches 14 to 16).

Fibre type	Batch no.	Target V_f		Actual V_f		Deviation %
		kg	%	kg	%	
45/50	5	320	0.5	330	0.52	+3
45/50	6	320	0.5	286	0.45	-11
45/50	7	320	0.5	268	0.42	-16
45/50	8	320	0.5	255	0.40	-20
45/50	9	320	0.5	238	0.37	-26
45/50	10	320	0.5	230	0.36	-28
45/50	11	160	0.25	272	0.43	+70
45/50	12	160	0.25	250	0.39	+56
65/60	13	320	0.5	380	0.59	+19
65/60	14	160	0.25	140	0.22	-13
65/60	15	160	0.25	187	0.29	+17
65/60	16	160	0.25	202	0.32	+26

Table 5-3 Fibre dispensing rates per batch

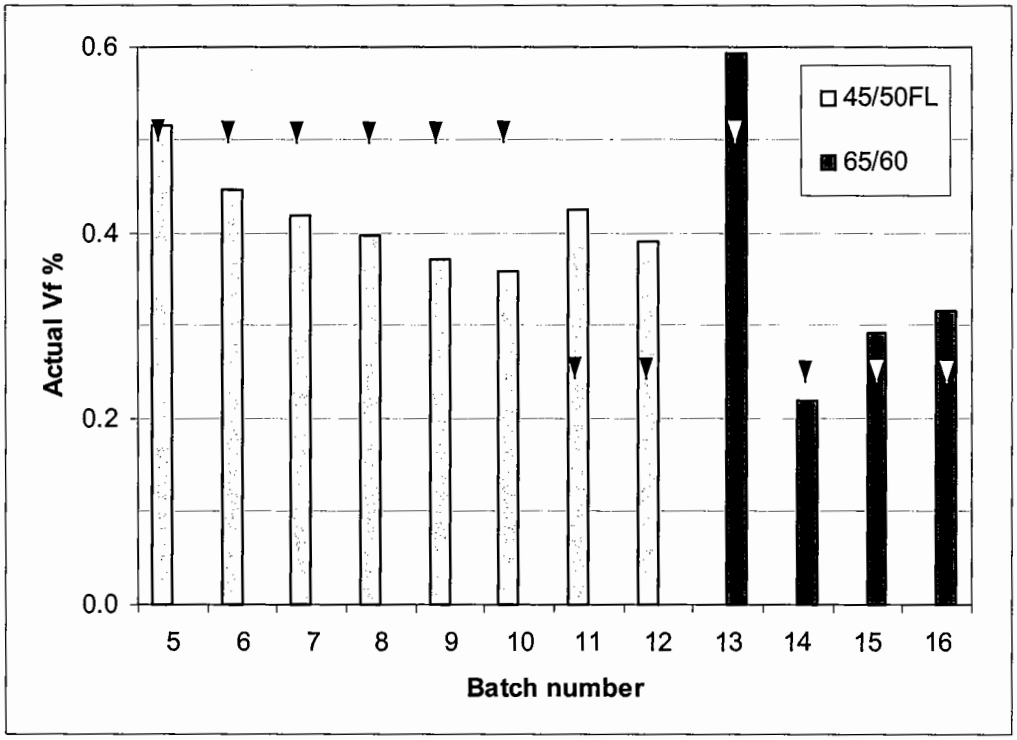

Note: ▼ denotes target fibre volume fraction

Figure 5-5 Fibre volume fraction in each batch

For Batches 14 to 16, the dispensing rate was recorded every 30 seconds (Figure 5-6). This showed that considerable variations occurred in dispensing rates during each batch. This was in spite of the fact that the dispenser had been calibrated for the fibre type 65/60 used in these batches.

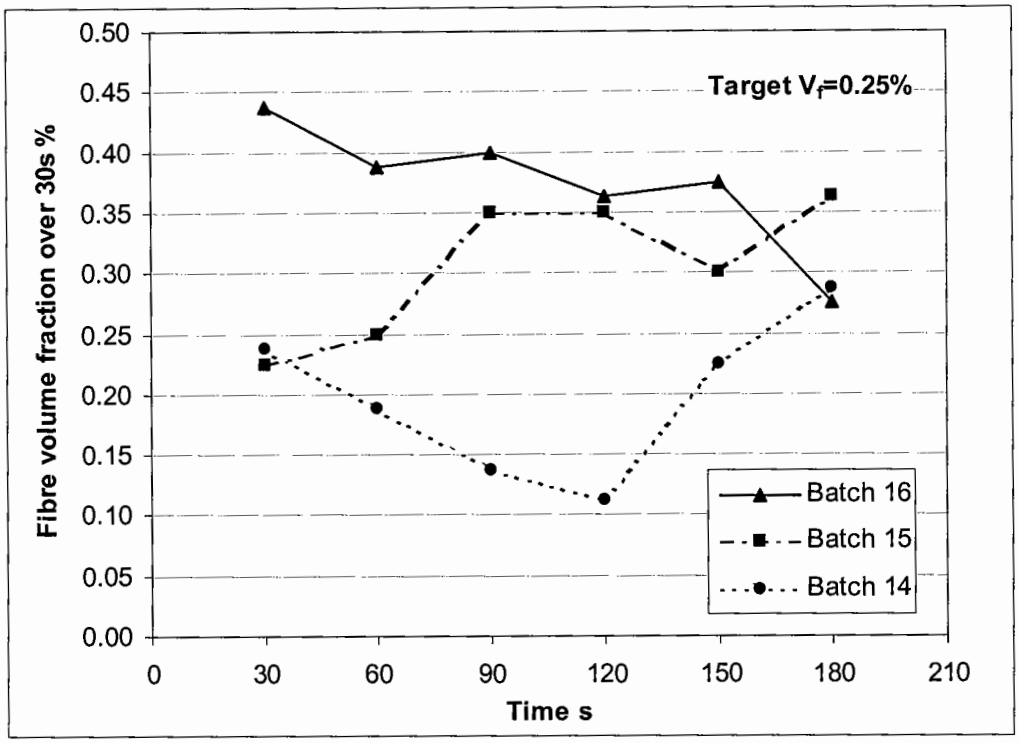

Figure 5-6 Variation in fibre volume fraction for Batches 14, 15 and 16

It was apparent, based on this study, that existing dispensing plant is not capable of distributing fibres evenly at the high production rates required of an FRCBM. Such problems could restrict the use of fibres with continuous mixers if the inadequacies of the current plant are not addressed. The variation in dispensing rates throughout batches would be expected to result in uneven fibre dispersion throughout the mix, leading to a loss in toughness where the quantity of fibres was less than expected. Since the trial, the fibre manufacturer Bekaert have taken steps to improve the dispensing plant based on lessons learnt from this study. This has since been tested, apparently successfully, on a scheme at Charles de Gaulle Airport in France, though to date the results of the study are not in the public domain (Nemegeer 2000). Should FRCBM gain acceptance within the United Kingdom and elsewhere, the impetus to find a solution to the dispensing problem, and the availability of suitable plant, will no doubt increase.

5.4.2 Pavement thickness

The control of level of the pavement is an important factor in ensuring the design thicknesses are achieved. A plot of the pavement thickness, obtained from the cored specimens, against chainage, shows that the depths achieved in the trial were lower than originally anticipated on account of inadequate level control during construction (Figure 5-7). Some were found to be as low as 130mm. As the critical stress is particularly sensitive to thickness, a large reduction in the load carrying capacity of the slab would be expected due to this thickness reduction. No specific difficulties with regard to laying the fibre reinforced sections were experienced by the paving contractor, and line and level of the reinforced sections were no worse than the control sections.

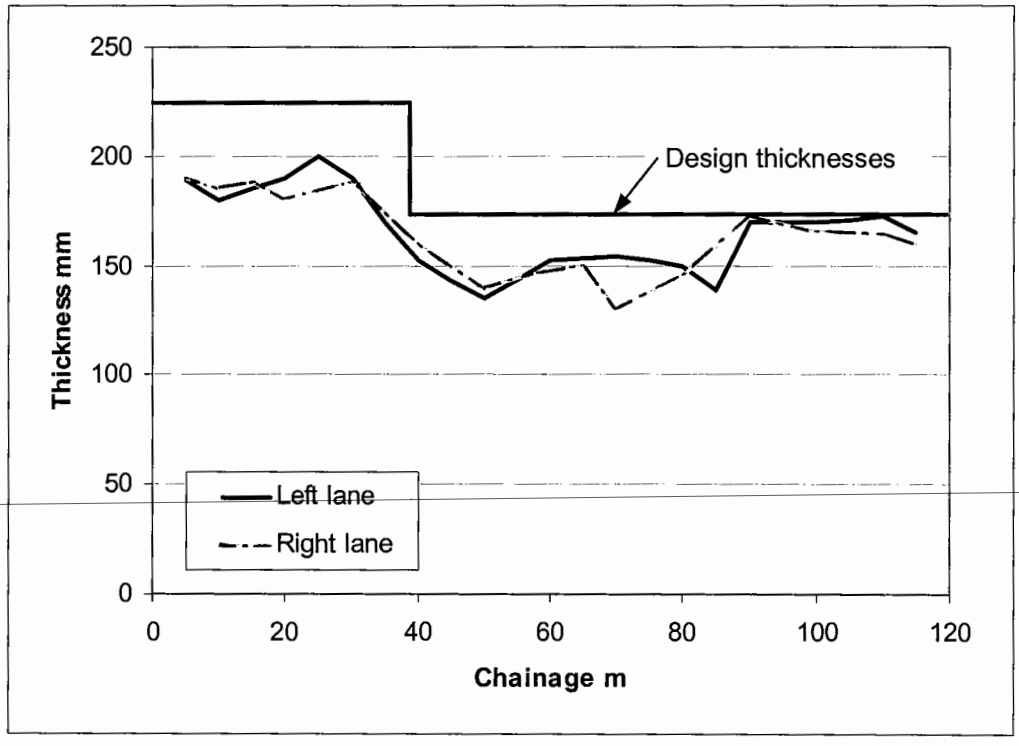

Figure 5-7 Material thicknesses from cored specimens

Such variability is in no way representative of CBM paving generally. As no guide wires were provided to control the paving depth, site operatives were reliant on measuring the depth of the material behind the paver and controlling the depth manually. The Specification

for Highway Works (Highways Agency 1998) requires depths to be within ±15mm, and through the use of guide wires or lasers, such tolerances are readily achievable. However, where no basecourse is used, which may be the case if a minimal asphalt overlay is deemed acceptable for an FRCBM pavement, the accepted tolerance is ±8mm.

5.4.3 Induced cracks

Induced cracking was carried out using a vibrating plate modified with a fin during construction, and using a guillotine type breaker five days after the pavement had been laid. Cores were taken at 5-days through a sample of both types of induced crack, immediately after the guillotine breaker had been used.

The cores demonstrated that full-depth vertical cracking was not visible in the cores using either the vibrating plate or the guillotine. However, after the area had been trafficked over a two week period, a visual inspection highlighted the occurrence of transverse cracks at the designated 3m spacings throughout the pavement. It is likely that these cracks occurred as a consequence of the high quarry traffic loading, rather than by temperature induced stress. This may have been due to an insufficient length of pavement (120m) to enable closely spaced cracks to develop. Even so, the fact that cracks appeared where the guillotine breaker had operated demonstrates that a plane of weakness was imposed on the CBM which, over time, would be expected to open up under ambient temperature changes when traffic loading was less severe.

The guillotine breaker is preferred over the vibrating plate for FRCBM as it does not disturb the fibres. As the vibrating plate induces a joint up to half the thickness of the layer, the fibres bridging this zone would be pushed aside. The guillotine breaker therefore offers the advantage that the full thickness of the layer is fibre reinforced. At the trial, an early age shrinkage crack appeared half way along the trial section. The optimum time for induced cracking may therefore be before 5-days, but clearly after the material has gained sufficient strength to carry the load of the plant. Perhaps the occurrence of some cracking should not be of concern, as once induced cracking has been completed, the opportunity for these naturally occurring cracks to open up significantly will be restricted.

It is worth noting that in practice, the material is likely to be overlaid with asphalt before induced transverse cracks open, therefore the verification of the success of induced cracking may present a challenge in terms of supervision.

5.4.4 Dynamic plate tests on sub-base

Immediately before laying the material, a series of dynamic plate tests was carried out on the sub-base using the Dynamic Plate (Highways Agency 1994). This is a hand held instrument currently being investigated by the Highways Agency in the United Kingdom to measure the *in situ* stiffness of capping and sub-base material (Plate 5-5). Trials in the United Kingdom have shown that the Dynamic Plate typically under-estimates *in situ* stiffness by varying factors, when compared to the FWD. At this stage, the data are presented here to help to assess the viability of this testing method for end product specifications.

Plate 5-5 Dynamic Plate testing of the surface modulus of the sub-base

The tests carried out on this site indicated an average surface stiffness of 107MPa (Table 5-4), which is considered reasonably high for a sub-base. However, the values were higher than expected considering the lack of controlled compaction applied to the sub-base. The concern with the Dynamic Plate was that it was measuring stiffness in close proximity to the surface, and lower stiffnesses within the pavement, which would influence the composite behaviour, might not be detected.

Chainage	Dynamic Plate Stiffness MPa	
	Left lane	Right lane
10		80
20		130
30	115	109
40	123	58
50	70	117
60	121	97
70	88	147
80	95	102
90	109	118
100	147	105
Average	*107MPa*	

Table 5-4 Sub-base stiffness values from the Dynamic Plate test

5.4.5 Collated fibres

It was observed in the FRCBM that many of the collated fibres (type 65/60) remained collated. This was consistent with observations from the first trial in Pode Hole Quarry. Samples of FRCBM from batches 13 and 14, weighing approximately 5kg, were taken from the trial area and fibres separated from the CBM. The fibres were then sorted according to the number still collated. The results showed that on average over half the fibres remained stuck to at least one other fibre (Figure 5-8). Over 10% were in bundles of 5 fibres or more. The reason the fibres remained collated was thought to be due to the low water content of the mix and the speed of the production process. The expectation must be for the toughness

characteristics of sections containing these fibres to be reduced. To some extent, this was demonstrated by the I_{50} indices for specimens referenced 6560-50, taken from batch 13. Although the fibre volume fraction was (on average) 0.6%, the toughness values were comparable to the loose fibres with average volume fractions of 0.4%.

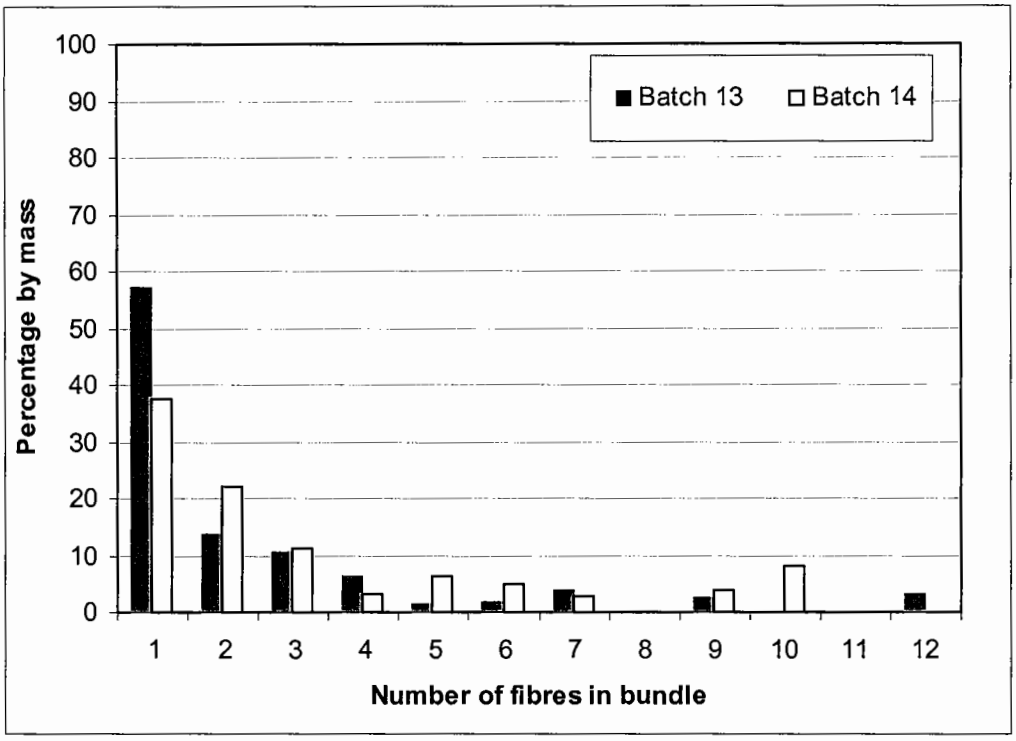

Figure 5-8 Percentage of 65/60 fibres remaining collated from 2 no. samples

In spite of the 65/60 fibres remaining collated, there remain advantages in using collated fibres - dispensing is better controlled and the aspect ratio may be increased without the risk of balling. The increase in aspect ratio was shown to increase the effectiveness of the fibres at a given fibre volume fraction, as demonstrated in the laboratory study. The most likely solution to the problem of collated fibres may be through weaker glue, which is able to break down during the mixing process.

5.5 Results from laboratory tests

5.5.1 Material properties of laboratory prepared specimens

Following the trial, 7-day flexural and compressive cube strengths were measured from individual laboratory prepared specimens at cement contents (CC) of 6, 7 and 8% by mass of dry aggregate (Table 5-5). The specimens were reinforced with the 45/50FL fibre at a volume fraction (V_f) of 0.4% as this was approximately the volume fraction obtained in the field (see Figure 5-5).

			Cube results		Beam results				
Ref.	[1]CC %	[2]WC %	Sat. density kg/m^3	7-day comp. strength MPa	Sat. density kg/m^3	7-day flexural strength MPa	ASTM toughness index I_{50}	Equiv. flexural strength MPa	Flexural strength ratio $R_{e,2}$
1	6.0	5.9	2585	21.4	2573	2.7	27.1	2.1	76
2	7.0	5.9	2585	25.8	2569	4.1	37.1	2.8	68
3	8.0	5.9	2588	28.6	2557	*3.3	30.9	1.9	59

Notes: [1]by mass of dry aggregate, [2]by mass of dry aggregate and cement, *failed outside central zone

Table 5-5 Laboratory mix results using fibre type 45/50FL at V_f=0.4%

The relationship between compressive cube strength and cement content is shown in Figure 5-9. Based on the scatter within the flexural test results, it was difficult to establish with any certainty the cement content at which the target 4MPa flexural strength would have been achieved. As it has been demonstrated that there is a linear relationship between compressive cube strength and flexural strength, the regression line for the cube strength suggests approximately 8% cement by mass of dry aggregate would be required to achieve the target flexural strength. At the cement content used in the trial (7%), it may be surmised that the flexural strength at the maximum density would be approximately 3.6MPa.

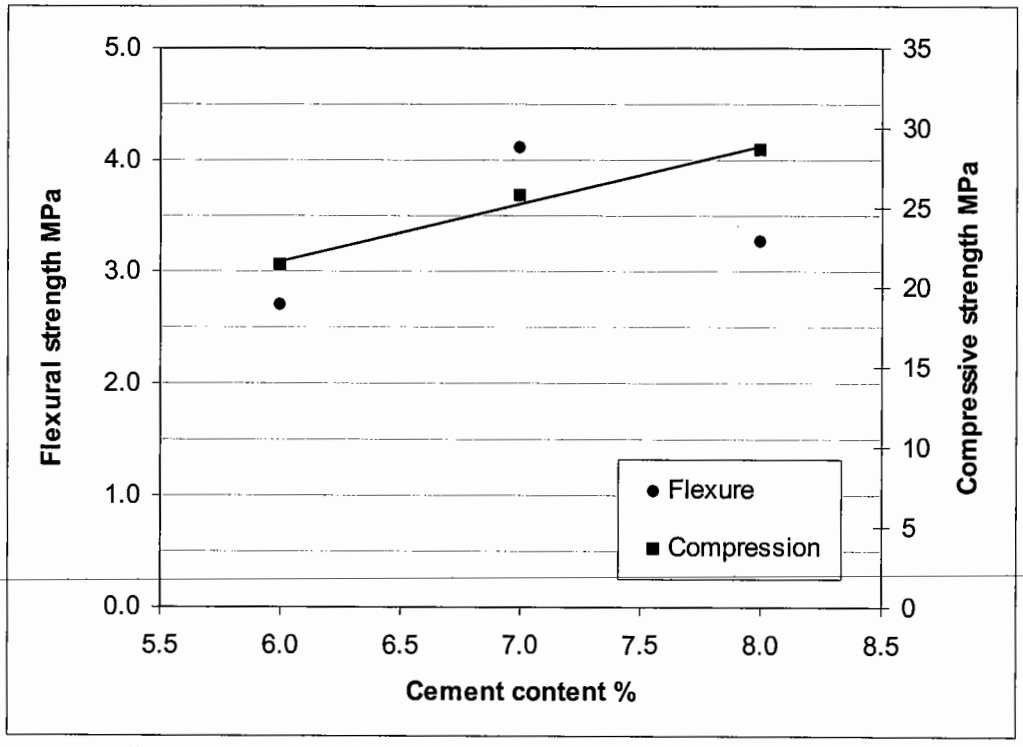

Regression line shown based on compressive strength

Figure 5-9 Laboratory mixes - relationship between strength and cement content

In the laboratory, the results from two additional beams produced by applying a reduced compaction effort are shown in Table 5-6. These demonstrated that at densities lower than the maximum, a significant reduction in both compressive cube and flexural strength occurred. A relationship between this reduction in density and the strength is described further in Section 5.5.2, and the effect of under-compaction on toughness in Section 5.5.4.

Ref.	Cube results			Beam results					
	Sat. density kg/m^3	[1]% of max. density	Compres. strength MPa	Sat. density kg/m^3	[1]% of max. density	Ultimate flexural strength MPa	ASTM tough. index I_{50}	Equivalent flexural strength MPa	Flexural strength ratio $R_{e,2}$ %
2	2585	100.0	25.8	2569	99.4	4.1	37.1	2.9	71
2b	2550	98.6	23.1	2543	98.4	3.1	21.7	1.3	42
2c	2509	97.1	15.8	2450	94.8	1.8	28.8	1.1	61

Notes: [1]based on 2585kg/m^3 obtained from Specimen 2.

Table 5-6 7-day laboratory results at reduced compaction at cement content 7% using fibre type 45/50FL at V_f=0.4%

5.5.2 Cored specimens

Saturated densities and layer thicknesses were measured from 35 cores taken at 5-days. The locations were shown in Figure 5-4. Eight cores were taken at induced or natural crack locations. Additionally, at 27-days, indirect tensile stiffnesses (from a repeated load test) and indirect tensile strengths were obtained from four of the cores and compressive strengths were obtained from three of the cores. The results are summarised in Table 5-7. The flexural strength was estimated from the indirect tensile strength using a relationship presented by Shahid (1997).

Core no.	Depth mm	Saturated density kg/m³	% max density	[1]Indirect tensile stiffness MPa	Indirect tensile strength (σ_{SP}) MPa	[2]Flexural strength (σ_u) MPa	Compressive strength MPa
		[3]2629	100				
1	188	2502	95.2				11.0
2	190	2478	94.3				
3	185	2458	93.5				
4	205	2466	93.8				
5	195	2507	95.3	29830	2.0	2.5	
6	200	2468	93.9				
7	190	2464	93.7				
8	182	2450	93.2				
9c	168	2499	95.1				
10c	152	2490	94.7				
11	130	2507	95.4				
12	135	2481	94.4				
13c	136	2495	94.9				
14	152	2436	92.7	24285	1.3	1.6	
15	142	2446	93.1				
16	140	2473	94.1	25975	2.0	2.5	
17	150	2469	93.9				
18	154	2489	94.7				
19	147	2484	94.5				
20	130	2488	94.6				
21c	158	2491	94.8				
22	*	2473	94.1				
23nc	165	2479	94.3				
24	138	2488	94.6	20997	1.4	1.8	
25	167	2470	93.9				16.4
26	155	2450	93.2				18.2
27	176	2412	91.8				
28	178	2469	93.9				
29	183	2438	92.7				
30	172	2418	92.0				
31	*	2472	94.0				
32c	140	2491	94.7				
33c	152	2492	94.8				
34	150	2454	93.4				
35	155	2462	93.6				
		Average (95% Confidence)	**94.0** (0.3)				

Notes: c=induced crack, nc=natural crack, *=damaged core, [1]taken from repeated load test, [2]assumed $\sigma_{flex}=1.25x\sigma_{sp}$, [3]maximum cube density shown in Table 5-2.

Table 5-7 Results from *in situ* cores at 27-days

The effect of layer thickness on density

The density of each core was calculated as a percentage of the maximum density obtained in the cube specimen, found to be 2629kg/m^3 (shown later in Table 5-8). The average density was 94.0% of the maximum. A plot of the FRCBM thickness against densities is shown in Figure 5-10. Densities appeared not to follow a specific pattern, and could not be correlated with thickness, as might have been expected. Although a reduction in density with thickness is not apparent from this study, such a reduction may occur at greater depths or with reduced compaction capability. Nanni and Johari (1989) showed from cored specimens that the lower half of the specimens were significantly less compacted than the upper half (see Figure 2-7 in Section 2.3.1). Such reductions in density result in lower strengths, as will be demonstrated, and the loss in strength in the lower portion of the layer is detrimental as it is here where the maximum tensile stress occurs.

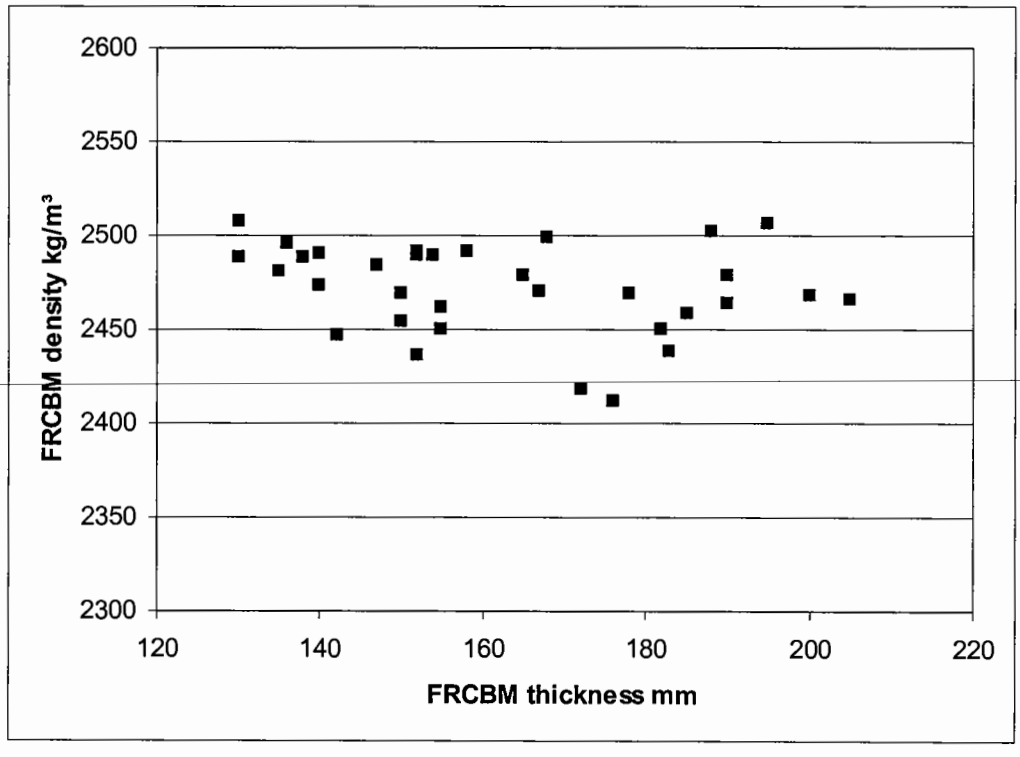

Figure 5-10 Plot showing there was no relationship between FRCBM thickness and density

The Specification for Highway Works requires a minimum density of 95%, obtained as the ratio of the maximum density from a cube and *in situ* nuclear density gauge measurements (Highways Agency 1998). Notwithstanding the different methods of determining the density ratio, the values obtained in the trial would appear to be on average below the limit of the specification requirements.

Despite indications in Nanni's study that the density in the top of the material approached the maximum density from tests, there were visual indications from this study that the top of the layer may not have been fully compacted. This manifested itself by 'plucking' out of larger aggregate from the matrix in the reinforced trial sections, under the wheel path. The reasons for this failure were not clear, though it appeared that in some way the fibres provided a mechanism that allowed this to occur as similar problems were not evident in the control sections. A solution may be to finish the layer by compacting it with a pneumatic tyre roller, as Nanni did, to ensure the material close to the surface is well compacted.

The effect of under-compaction on strength

The indirect tensile strengths ranged between 1.3MPa and 2.0MPa, from which flexural strengths of 1.6MPa and 2.5MPa were estimated (Table 5-7). The percentage densities of these cores were between 92.7% and 95.3%. Compressive strengths varied between 11.0MPa and 18.2MPa at a similar density range. The strength data were plotted against percentage density, and data from the laboratory flexure tests, used to assess under-compaction, were also included (Figure 5-11). There was a clear trend for the strength to decrease as the percentage density decreased, so that at a density of 94.0% of the maximum density, the strength was more than halved. Based on a density of 94%, the average *in situ* flexural strength was assumed to be approximately 2.2MPa.

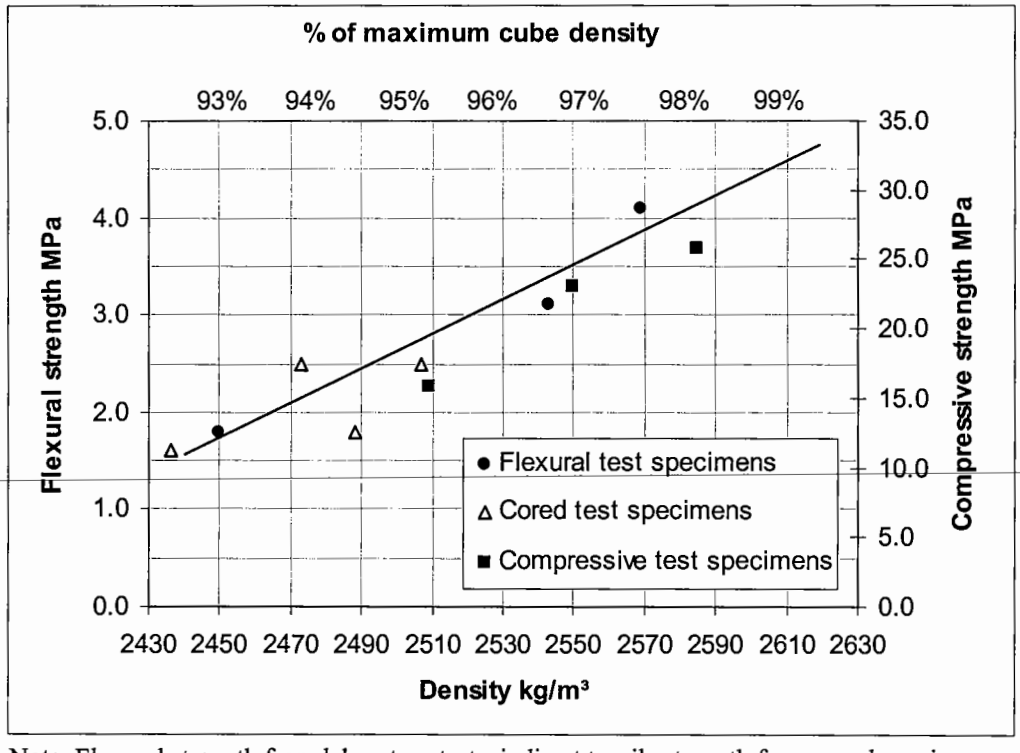

Note: Flexural strength from laboratory tests, indirect tensile strength from cored specimens (see Table 5-7), compressive strength based on laboratory tests.

Figure 5-11 Effect of under-compaction on strength.

Williams (1986) noted the difficulty in assessing the air void content, and observed that up to 3% air voids may be present in the mixture used to denote the 'maximum' density. The determination of *in situ* density to indirectly assess the strength of the material is convenient and immediate (using a nuclear density gauge). Due to the close relationship between density and strength, it would seem prudent to take special care at the design stage to ensure these characteristics can be optimised.

The effects of under-compaction are potentially more problematic than fatigue, yet this is often overlooked. The advantages of increased compaction are not explicitly accounted for in design charts for flexible composite pavements in the United Kingdom (Highways Agency 1994), though the practically achievable level of compaction of 95% is presumably included in the calculation of strength and therefore the base thickness. Nor is there an incentive for a contractor to significantly exceed the minimum density. An increase in the density should result in a more durable pavement of higher strength, which would result in less maintenance and a longer serviceable life. The obvious remedy might be to increase the minimum specified density, although critics will argue that the target density should be readily achievable, and stringent specifications will increase the cost. A case may be made for designers and contractors who take the care to achieve a high density to be rewarded for their efforts.

5.5.3 Material properties of site prepared specimens

A summary of results for the cube and beam specimens prepared on site is shown in Table 5-8. The densities were generally found to be higher than those of the laboratory prepared specimens. Compressive cube strengths were found to be almost 50% greater than those obtained in the laboratory (approximately 38MPa on site compared to 26MPa in the laboratory – comparing the results from Table 5-8 and Table 5-5), although ultimate flexural strengths were comparable (approximately 4MPa).

Ref.	Batch no.	Cube results		Beam results				
		Sat. density kg/m³	Comp. strength MPa	Sat. density kg/m³	Ultimate flexural strength MPa	ASTM toughness index I_{50}	Equivalent flexural strength MPa	Flexural strength ratio $R_{e,2}$ %
4550-50-1	5	2616	35.4	2590	5.2	24.8	2.8	53.5
4550-50-2	5	2636	41.7	2609	4.5	30.3	2.6	58.4
4550-50-3	5	2634	38.6	2574	1.9	29.0	1.4	72.6
Average		**2629**	**38.6**	**2591**	**3.9**	**28.0**	**2.3**	**61.5**
95% confidence		12	3.6	20	2.0	3.3	0.9	11.2
4550-25-1	11	2622	40.4	2595	3.7	20.4	1.4	37.7
4550-25-2	11	2613	37.3	2573	4.1	21.2	1.9	45.5
4550-25-3	11	2621	37.7	2594	4.5	15.9	1.2	27.4
Average		**2619**	**38.5**	**2587**	**4.1**	**19.2**	**1.5**	**36.9**
95% confidence		6	1.9	14	0.5	3.2	0.4	10.3
6560-50-1	13	-	-	2605	3.6	28.1	1.9	52.5
6560-50-2	13	-	-	2608	4.2	30.9	3.3	78.3
6560-50-3	13	-	-	2606	3.7	29.5	2.6	69.6
Average				**2606**	**3.8**	**29.5**	**2.6**	**66.8**
95% confidence				1	0.4	1.6	0.8	14.8
Control-1	17	2601	35.0	-	-	-	-	-
Control-2	17	2609	36.1	-	-	-	-	-
Control-3	17	2613	40.8	-	-	-	-	-
Average		**2608**	**37.3**					
95% confidence		7	3.5					

Table 5-8 Results from site prepared specimens at 6-days

The differences in strength may have been due to variations in grading, water content or compaction effort (due to different operators). On site these parameters would not be expected to be as well controlled as in the laboratory. The fact that the site prepared specimen properties were more favourable was probably fortuitous. It demonstrates again, as did the laboratory investigation, the difference that can occur in material properties with nominally the same constituent materials.

5.5.4 Toughness

For each beam specimen, the first crack and ultimate flexural strengths were found to be comparable, a characteristic expected at such a fibre volume fraction based on the laboratory study.

The ASTM toughness index I_{50} varied between a minimum of 15.9 (specimen 4550-25-3) and a maximum of 37.1 (specimen 2) as shown in Figure 5-12. As there appears to be no relationship between I_{50} and density or strength, it must be concluded that the differences are due to the variability in the distribution of fibres in the mix. Mix 4550-25 indicated significantly lower toughness than the other mixes, and this may have been due to the poor distribution of fibres. The expectation was for the 65/60 fibres at V_f=0.6% (6560-50, batch 13) to have a greater toughness than the 45/50 fibres at V_f=0.5% (4550-50, batch 5). This was not the case, possibly due to the poor distribution of collated fibres, as previously described.

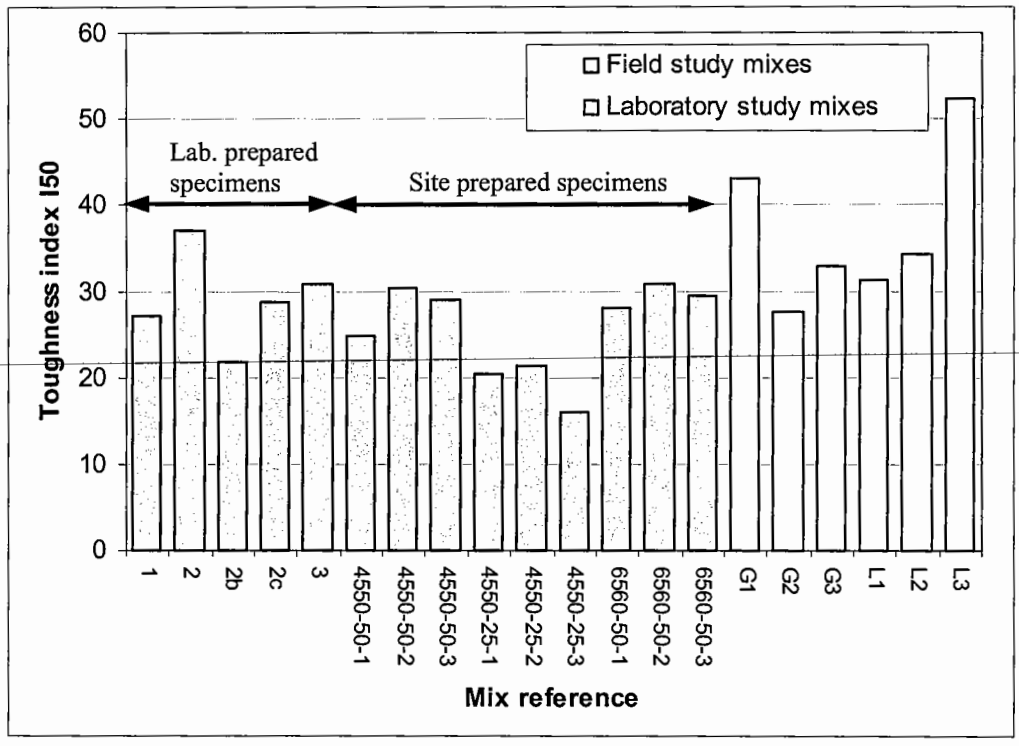

Figure 5-12 Toughness index I_{50} for laboratory and site prepared specimens compared to laboratory tests

The I_{50} indices obtained were compared to those reported in the laboratory investigation for a range of material strengths for the gravel (G1, G2 and G3) and limestone (L1, L2 and L3) CBM using the 65/60 fibre at V_f=0.5%. The higher toughness indices reported from the laboratory study are considered to be due to the higher fibre volume fraction (0.5% compared to the field study V_f of 0.4%) and the use of the higher aspect ratio fibre.

5.6 Falling weight deflectometer measurements

5.6.1 In situ stiffness

The falling weight deflectometer (FWD) was used to assess *in situ* effective stiffnesses after 5 days, 4 months and 13 months of quarry traffic. This stiffness measurement was based on the back-analysis of deflection readings to a radius of 2.1m. The values obtained during the three visits would therefore be an indication of the severity of cracking that had taken place in the test sections under traffic. The applied stress was 750kPa over a plate radius of 225mm.

The results indicated that the effective stiffness values of the reinforced sections were slightly higher than the unreinforced sections on Visit 1, after 5-days of traffic (Table 5-9, Figure 5-13). The values obtained were slightly lower, but comparable, to those obtained through the indirect tensile stiffness tests from cored specimens (see Table 5-7). Visit 2 indicated a significant reduction in effective stiffness in the control sections, a modest reduction in the section containing the 65/60 fibres and a smaller reduction in the sections reinforced with fibre type 45/50.

Trial section	Visit 1 (29 July 1999)		Visit 2 (30 November 1999)		Visit 3 (21 September 2000)	
	Average	95% Confidence	Average	95% Confidence	Average	95% Confidence
Control	17427	±5067	8071	±3224	7315	±2772
65/60	21261	±4771	14087	±7056	12029	±4091
45/50FL	23652	±4593	19339	±4574	18063	±3784

Table 5-9 Average effective stiffnesses back-analysed from FWD measurements and 95% confidence limits for trial sections on three visits

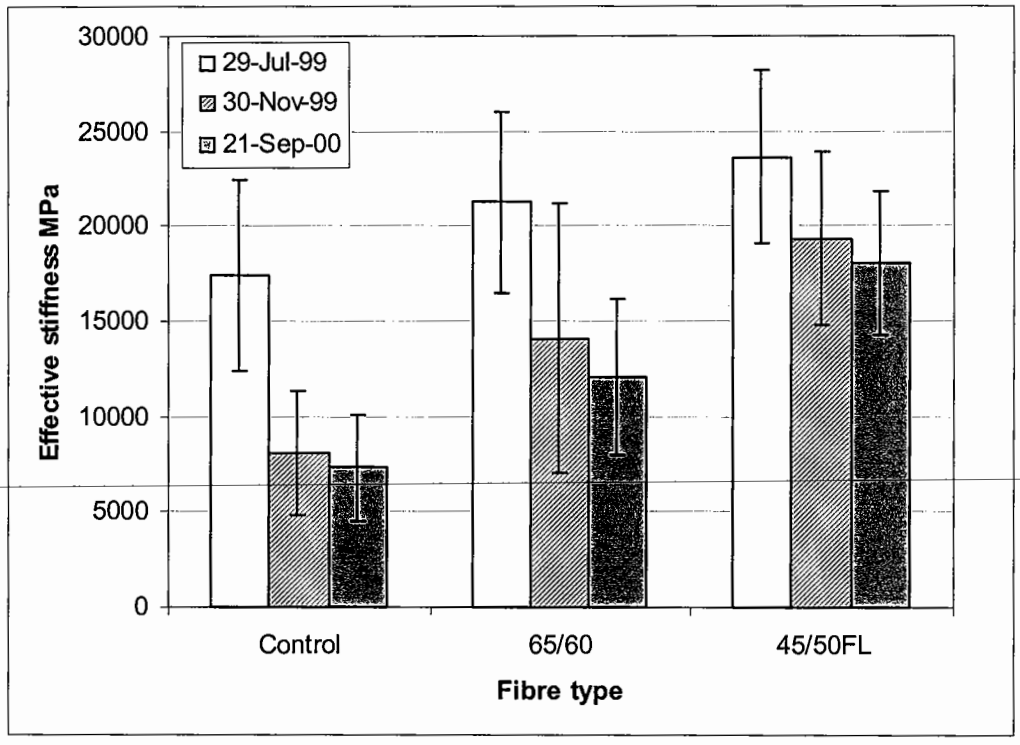

Figure 5-13 Effective stiffness reduction at three test sections (control, 65/60 and 45/50FL) over a 13 month period

The relative effective stiffness measurements on Visits 1 and 2 were consistent with the degree of cracking observed in the respective test areas (Figure 5-14). As was expected, most of the cracking occurred within the wheelpath of the vehicles, which tended to drive on the left side of the trial area fully laden. (Returning vehicles were unloaded, and would not be expected to contribute significantly to the damage). It was also evident that the magnitude of the cracks in the reinforced sections was less than in the unreinforced sections, showing the fibres were resisting crack widening.

Visit 3 demonstrated that the relative reduction in stiffness of all sections between visit 2 and visit 3 was significantly less than between visits 1 and 2. The implication was that the majority of the damage that occurred in the material did so over a short period of time, and thereafter deterioration took place at a reduced rate. The reason for this is thought to be the contribution of the foundation; once cracking has occurred the foundation must carry a higher proportion of the applied load. The base layer therefore deteriorates less rapidly, though the expectation would then be for damage to occur to the lower layers.

The fibre reinforced sections resulted in a higher effective stiffness than the control sections as, in this instance, the load was carried by the foundation and the steel fibres.

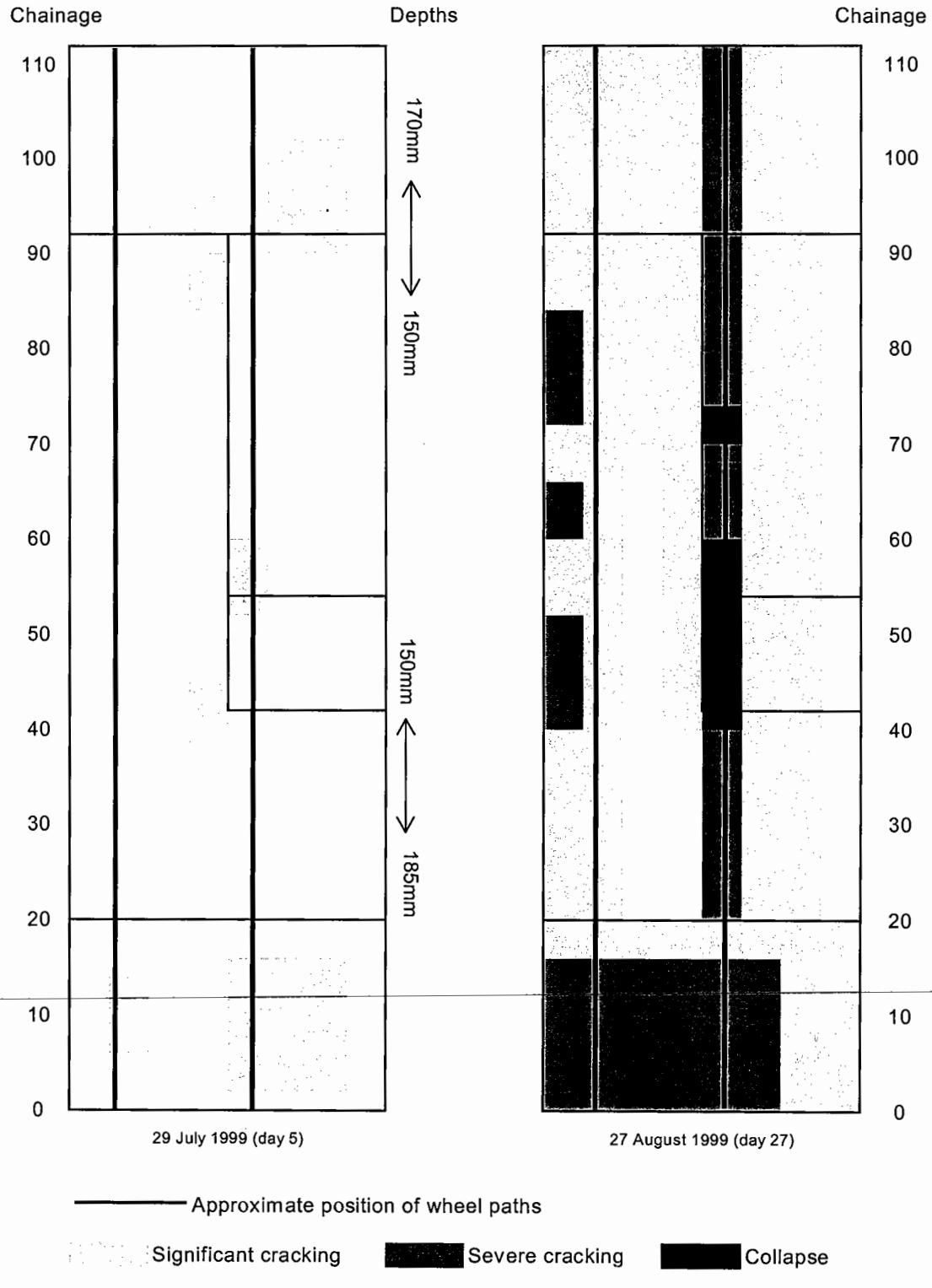

Figure 5-14 Observed severity of cracking in test sections after Visit 1 and Visit 2

5.7 Conclusions

1. Existing plant and methods currently used for CBM construction may also be used for FRCBM. The only additional equipment required is a fibre dispenser, although these have been developed for batch mixers rather than continuous mixers. This study showed that the dispenser used was unable to achieve a consistent distribution of fibres in a continuous mix. Modifications in the fibre dispensing plant are therefore required to improve this distribution.

2. The trials demonstrated that collated fibres may not currently be used in an FRCBM. Due to the continuous mixing and dry material, the soluble glue holding the fibres together did not dissolve. However, advantages of using collated fibres exist in terms of ease of mixing and superior potential performance and therefore a solution to the problems highlighted are worthy of investigation.

3. A significant amount of variability was found in the flexural strength of both the FRCBM and CBM specimens at full compaction. Furthermore, a reduction in density resulted in a significantly reduced strength, such that at 95% of the maximum density, the strength was reduced by 40%. The various stresses imposed on this material (temperature, shrinkage and traffic) and the large variability in strength increases the probability of cracks occurring.

4. Fibre reinforcement will not prevent cracks occurring in the material, but visual inspection and FWD measurements of the deteriorated pavement has shown that the severity of cracks in FRCBM is less than CBM. The fibres appear to bind cracks together, enabling the material to retain significant load carrying capacity even after severe cracking was visible within the material. It is expected these neatly bound cracks will reduce the propagation rate of a crack through the bituminous surface, enabling a significant reduction in the thickness of that layer.

5. Plastic and elastic analysis was used to determine the strength of the pavement. Based on the *in situ* pavement thickness and strength, the resulting rapid failure under the heavy quarry loads was to be expected. Plastic analysis was preferred over elastic analysis as it allowed some of the obvious benefits in the increase in load carrying capacity due to fibre reinforcement to be modelled.

6. Induced cracking using a guillotine breaker showed that cracks may not be expected to appear to the naked eye in the short term. However, it was evident that the breaker had induced a weakness in the pavement as cracks appeared over a two week period, although in this study it was thought such cracks appeared due to traffic rather than temperature variations. In practice, it is thought that the guillotine breaker will induce cracks in an FRCBM, although such cracks may not be visible before the material is overlaid.

7. The trial has allowed a draft Material Specification and Notes for Guidance (Appendix B) to be produced for use with FRCBM. These describe the performance criteria required to ensure acceptable fibre distribution, material strength and toughness.

Chapter 6. Development of a design method

6.1 Introduction

This chapter discusses the influence of various material parameters on the performance of a flexible composite structure using the finite-element computer program ILLISLAB95 and presents a design method for flexible composite pavements allowing for an FRCBM or CBM roadbase. It also allows the benefits of both induced and natural cracking on the structure to be quantified.

The objectives of the analytical study were to investigate the relative influence of the foundation and roadbase properties on the ability of the structure to carry load and to extract actual values, which are incorporated into the design method. In addition, the design method includes data obtained in the laboratory and field investigations.

Comparisons of various flexible composite pavement alternatives are shown, with costs, and recommendations are made as to how the program may be verified through field investigations.

6.2 Theoretical analysis of a cracked CBM

The finite-element computer program ILLISLAB95 was used to investigate the influence of a number of common variables in a concrete pavement. The program was developed at the University of Illinois in the United States to analyse concrete slabs on grade (Tabatabaie and Barenberg 1978). The inclusion of an overlay using this program is not possible. The effect of an asphalt overlay was modelled indirectly by assuming that the applied stress was reduced due to the load spreading characteristics (stiffness) of the layer. The magnitude of this reduction was therefore dependent on the thickness of the asphalt layer.

Since its initial development, the program has been improved and thoroughly checked for accuracy and reliability (Ioannides and Korovesis 1990). The perceived advantage of this particular finite element program over multi-layer linear elastic programs was that it allowed stresses and deflections to be computed based on the effectiveness of a transverse crack under a static load. Whilst deterioration at the crack interface is not predicted directly by the computational process, the effects of a dynamic load may be considered indirectly using laboratory data determined from the cyclic shear tests. The program therefore lent itself to the analysis of a cracked FRCBM roadbase.

The critical stress in the cementitious pavement base, under a standard 80kN axle, was investigated assuming various foundation support conditions and aggregate interlock factors. Longitudinal surface profiles were plotted so that the vertical deflections and slab rotations on either side of a loaded and unloaded crack could be compared, assuming various material parameters. From this, and based on laboratory and field data, a design method is presented and recommendations made as to how flexible composite pavement performance may be improved in practice.

6.2.1 Parameters and variables used in the ILLISLAB95 analysis

The two-dimensional mesh used in the finite element analysis is shown in plan in Figure 6-1. Dimensions of 3.6m x 3.0m were designed to replicate a typical CBM pavement with induced cracks at 3m spacings.

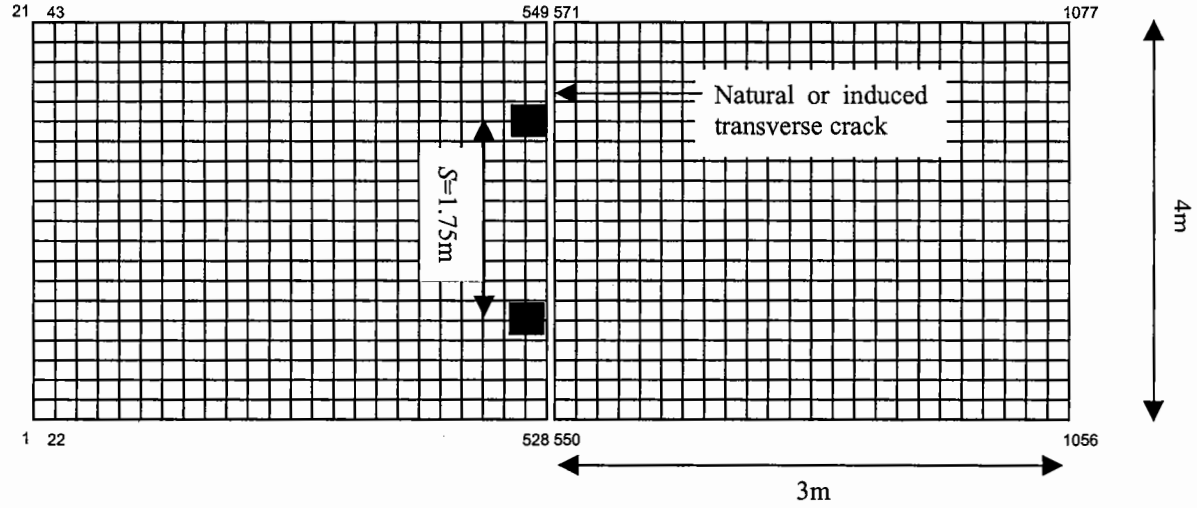

Figure 6-1 Standard mesh in plan used in ILLISLAB95 analysis

In the analysis, a standard axle load was placed directly on the cementitious slab near a transverse crack – the influence of the asphalt overlay was not considered at this stage. The constant parameters were; slab length (3.0m); slab width (3.6m); wheel load (F=40kN); tyre pressure (P=595kPa); wheel spacing (S=1.75m); and number and position of nodes. In order to achieve the required pressure, the load was made to act through a square plate of dimension 258mm. The input variables were; modulus of subgrade reaction (k); slab stiffness (E); slab depth (D); aggregate interlock factor (AIF); and asphalt overlay depth (D_a) – considered later. The range of values analysed for each parameter were k=0.04, **0.08**, 0.16, 0.25N/mm³; E=10000, **15000**, 20000, 25000MPa; D=150, **200**, 250mm; and AIF=7, **70**, 700, 3500, 7000MPa. The figures in bold were held constant in the investigation of other parameter sets.

The AIF was defined as the joint spring stiffness per unit length. This may therefore be compared to the load transfer stiffness (LTS) obtained in the cyclic shear tests, which was defined as the joint spring stiffness per unit area. Thus:

$$AIF = LTS \times D \qquad \textbf{Eqn...6-1}$$

The effects of a load offset from the crack (as shown in Figure 6-1) were found to be the most onerous scenario, creating the highest stress, vertical deflections and rotations at the crack interface. The output data were the maximum deflection of the loaded side of the crack (δ_L), the deflection of the unloaded side of the crack (δ_{UL}), the angle of the loaded side (θ_L) and the angle of the unloaded side (θ_{UL}). From these, the differential vertical movement ($\Delta\delta$), total rotation (θ_T) and load transfer efficiency as a percentage (LTE) were calculated as defined in Figure 6-2. A summary of the input, output and calculated parameters is shown in Table 6-1.

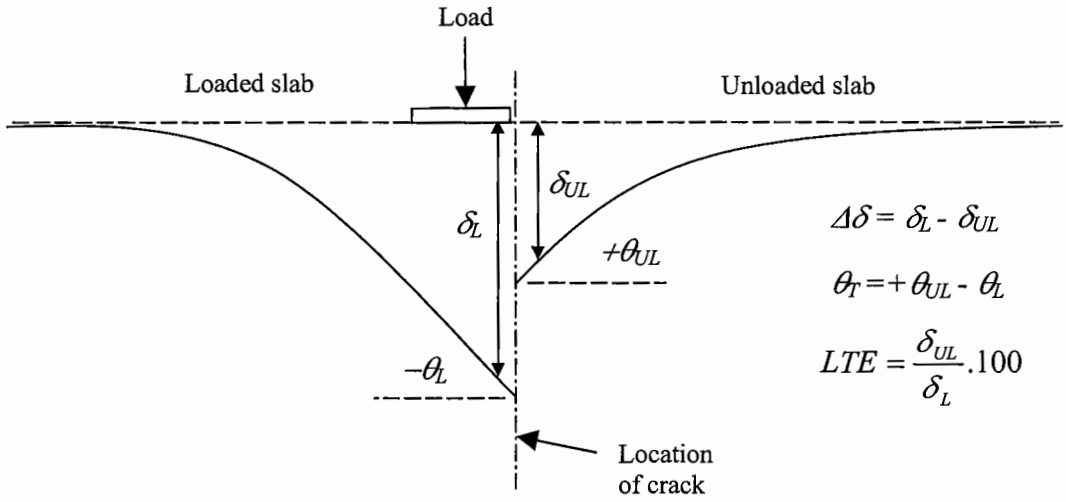

Figure 6-2 Definition of output and calculated values from ILLISLAB95 based on a plot of the longitudinal surface profile close to a transverse crack (exaggerated vertical scale)

Additionally, the critical stress (σ_t) was determined, found to be near the crack, at the underside of the slab and under the wheel load, as shown in Figure 6-3. It should be noted that at this stage no account of the overlay has been included. The contribution of the asphalt is considered later.

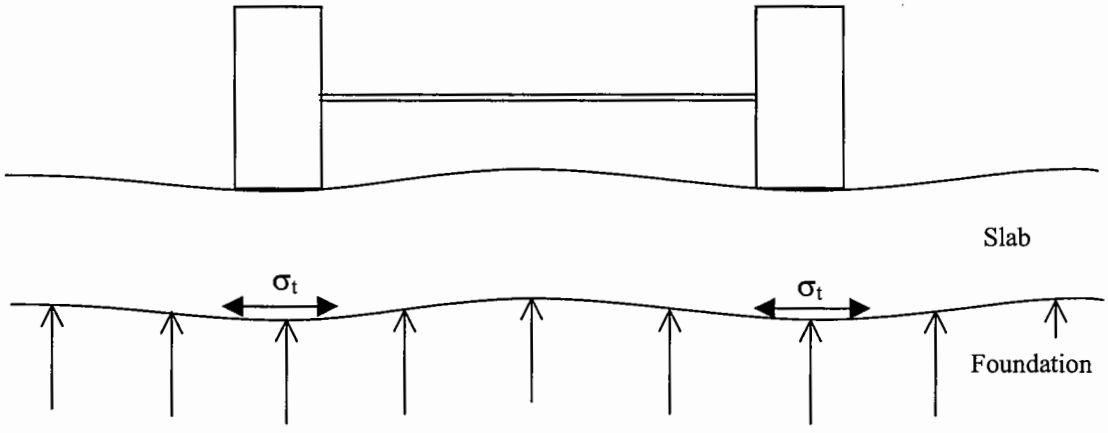

Figure 6-3 Cross section through flexible composite pavement showing critical stress

No.	Input variables				Output variables					Calculated values		
	E MPa	D mm	k N/mm³	AIF MPa	σ MPa	δ_L μm	δ_{UL} μm	θ_L x10^{-5} rad	θ_{UL} x10^{-5} rad	$\Delta\delta$ μm	θ_T x10^{-5} rad	LTE %
1	15000	200	0.08	70	1.64	384	221	-36	28	163	64	58
2	15000	150	0.08	70	2.60	496	292	-51	43	204	94	59
3	15000	250	0.08	70	1.12	322	183	-27	18	139	45	57
4	15000	200	0.08	7	1.77	528	77	-40	8	451	48	15
5	15000	200	0.08	700	1.32	320	286	-32	28	34	60	89
6	15000	200	0.08	3500	1.12	307	298	-25	57	9	82	97
7	15000	200	0.08	7000								
8	15000	200	0.04	70	1.69	589	413	-48	41	176	89	70
9	15000	200	0.16	70	1.58	259	109	-27	16	150	43	42
10	15000	200	0.25	70	1.53	208	76	-23	12	132	35	37
11	10000	200	0.08	70	1.56	-	-	-	-	-	-	-
12	20000	200	0.08	70	1.69	-	-	-	-	-	-	-
13	25000	200	0.08	70	1.73	-	-	-	-	-	-	-

Table 6-1 Results from analytical study using ILLISLAB95

The following presentation of the results from the analytical study and discussion outlines the relative influence of the input parameters on the deflections, rotations and critical stresses close to a transverse crack.

6.2.2 Stresses near a transverse crack

When the load is offset from the crack, the stress distribution across the loaded side of a transverse crack at various *AIF* is as shown in Figure 6-4. The distance between the two wheel loads (*S*) was such that the stresses on the slab were not superimposed. As the *AIF* increases, the critical stress in the slab decreases.

The *AIF* may be related to the load transfer efficiency (*LTE*) with knowledge of the modulus of subgrade reaction (*k*) and the radius of relative stiffness, as described in Section 2.4.5. The radius of relative stiffness is itself a function of k, and the depth (*D*), stiffness (*E*) and Poisson's ratio (ν) of the slab (see Eqn...2-1). For the slab used in this study, where k=0.08N/mm^3, D=200mm, E=15000Mpa and ν is assumed to be 0.2, the *LTE* at *AIF* of 7, 70, and 3500MPa are 15%, 58%, and 89% respectively.

Therefore, in Figure 6-4, an increase in *LTE* between 58% and 89% resulted in a critical stress reduction from 1.6MPa to 1.1MPa, or by 30%.

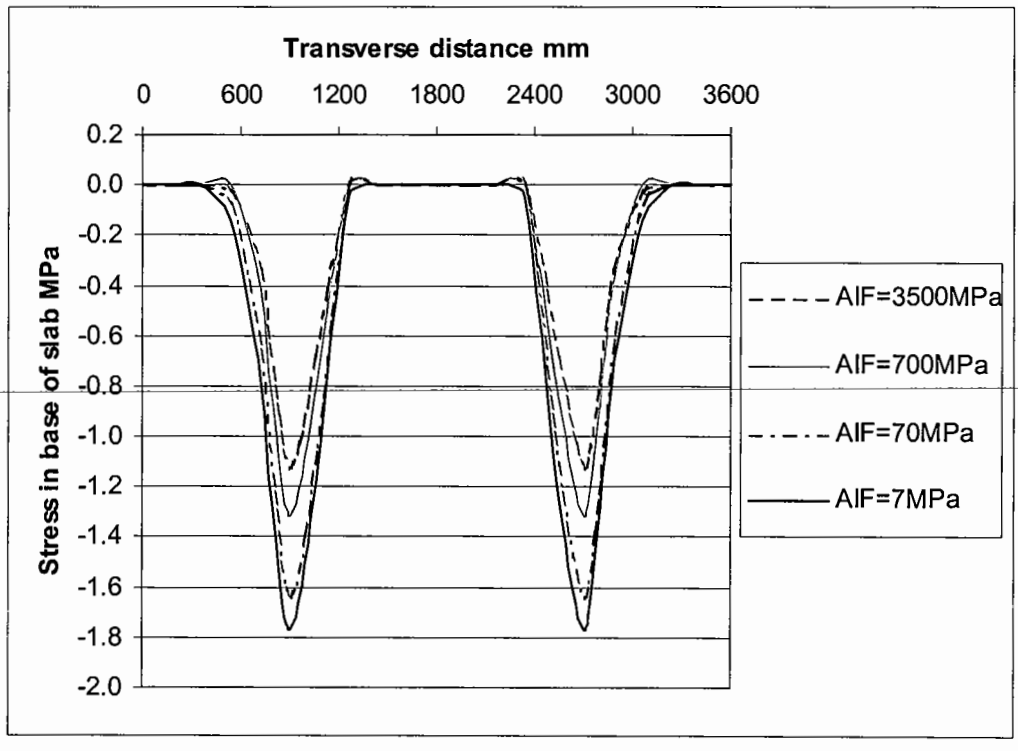

Figure 6-4 Typical stress distributions at underside of slab at various aggregate interlock factors as predicted by ILLISLAB95

An increase in the aggregate interlock factor reduces the critical stress significantly (Figure 6-5). The relationship is broadly logarithmic between *AIF* of 70MPa and 7000MPa, the reduction being of the order of 30% between these values. Cyclic shear tests on unreinforced specimens demonstrated that the load transfer stiffness (and hence the *AIF*) decreases dramatically when the crack width is increased (as shown by Figure 4-57 in Section 4.8.6). Steel fibre reinforcement was shown to result in significantly higher load transfer stiffness when compared to the unreinforced specimens, in particular at the greater crack widths. In practice a reduction in the average crack width may be engineered by inducing cracks at closer spacings than would occur naturally. This would reduce the critical stress in the slab, although any deterioration at the crack interface would result in a lower *AIF* over time, and in such instances the critical stress would increase. However, the cyclic shear laboratory results also demonstrated that at reduced crack widths deterioration also reduced.

It can therefore be seen that from the laboratory results, an *AIF* may be determined from the load transfer stiffness and slab depth (Eqn...6-1), and with a knowledge of the coefficient of subgrade modulus (k), the critical stress can be determined.

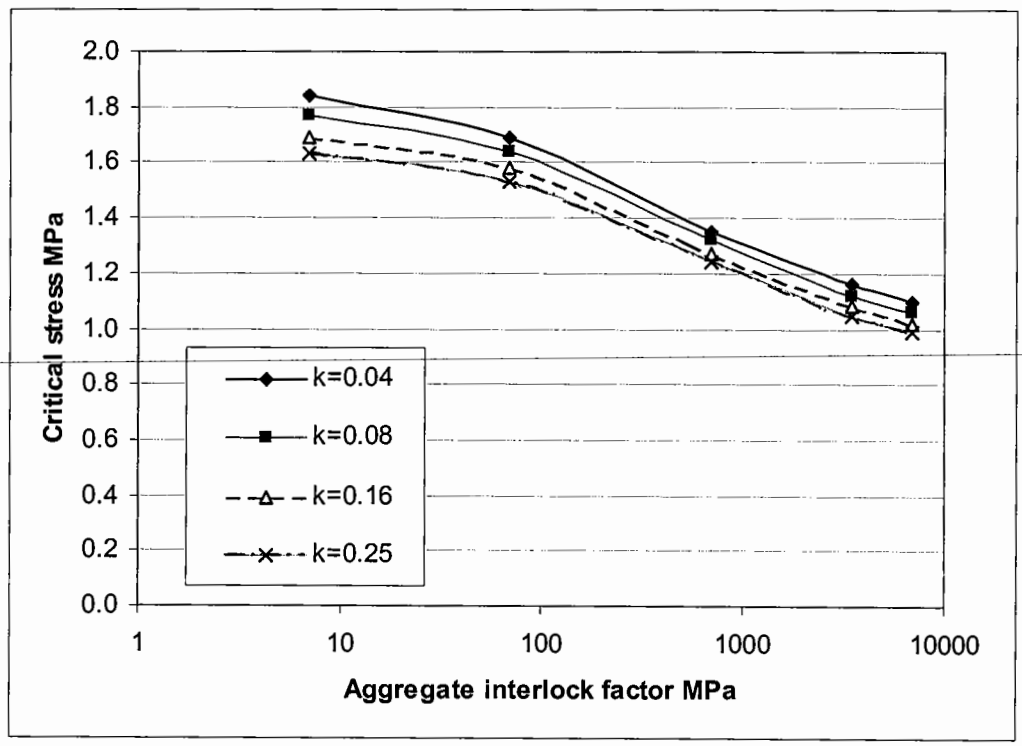

Figure 6-5 Relationship between aggregate interlock factor and critical stress at various moduli of subgrade reaction

The relative influence of the modulus of subgrade reaction (k) and elastic stiffness (E) of the material on the bending stress is significantly less than that of the *AIF*. For an *AIF* of 70MPa, over the range of subgrade moduli studied, the critical stress varied by less than 10%. An increase in E from 10000MPa to 25000MPa would increase the stress by approximately the same percentage (Figure 6-6).

In practice the effective elastic stiffness would reduce over time as the material deteriorates under traffic loads, resulting in some stress relaxation in the base, but requiring the lower layers to carry a higher proportion of the load. The loss of aggregate interlock would also result in an increase in vertical deflection at the crack, and again, require the underlying layer to carry more load. The magnitude of the deterioration is complex and is dependent on not only the mechanical properties of the FRCBM layer, but also on environmental factors. In particular, the ingress of water through surface (reflection) cracks and from the side of the pavement may wash out fine aggregate in a granular sub-base and soften subgrade clays. Damage may further be exacerbated through pumping and intermixing of the subgrade and sub-base under load, reducing significantly the load carrying capacity of the foundation. Whether or not there are effective water control measures, a cement treated sub-base will assist in maintaining the integrity of the foundation.

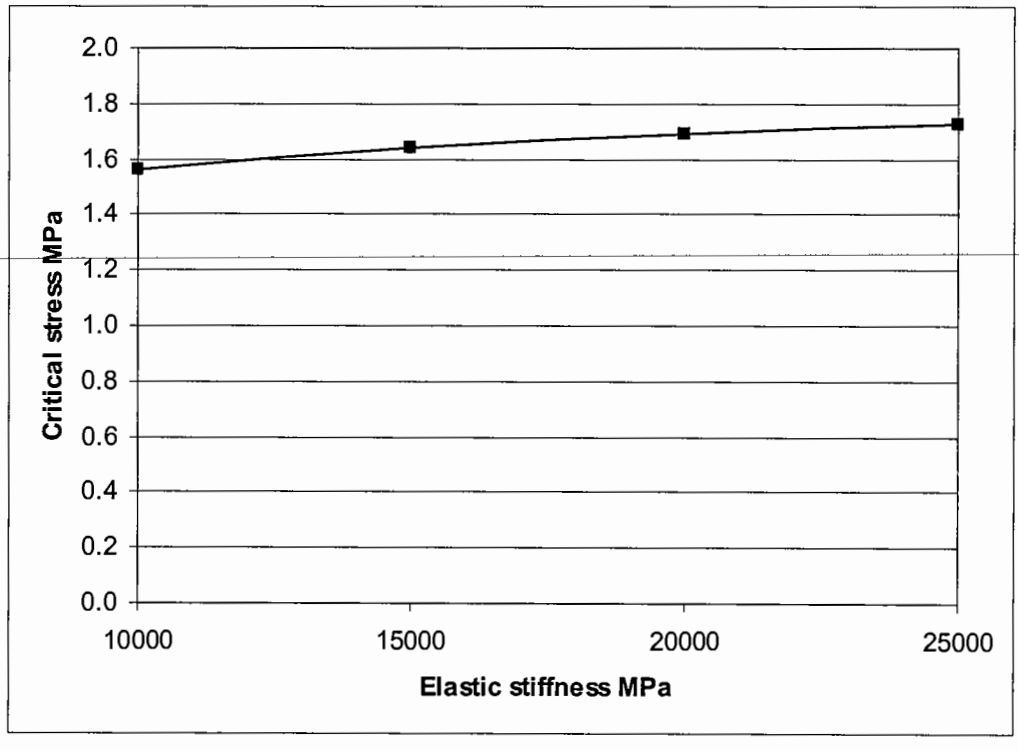

Figure 6-6 Effect of elastic stiffness (E) on the critical stress when k=0.08N/mm³, *AIF*=70MPa and D=200mm

Whilst the influence of k and E on the bending stress is not great, the effect on vertical deflections and rotation near a transverse crack is more significant; this will be addressed later.

The slab thickness affects the critical stress significantly; a small increase in the depth (D) will have a pronounced effect on the critical stress. The stress reduced by almost 60% between depths of 150mm and 250mm at an *AIF* of 70MPa (Figure 6-7). The reduction in stress was approximately 55% between *AIF* of 7 and 3500MPa at 150mm slab depth, and approximately 33% at a depth of 250mm over the same *AIF* range.

The temptation is often to reduce the layer thickness to reduce material costs. However, these costs may be small compared to the total cost that are incurred in pavement construction, and any additional thickness has significant mechanical advantages. It will be demonstrated in this thesis that thickness reductions are possible in FRCBM, although it is worth noting at this stage that a balance must be struck between the economic savings and loss in mechanical performance that occurs at reduced thicknesses.

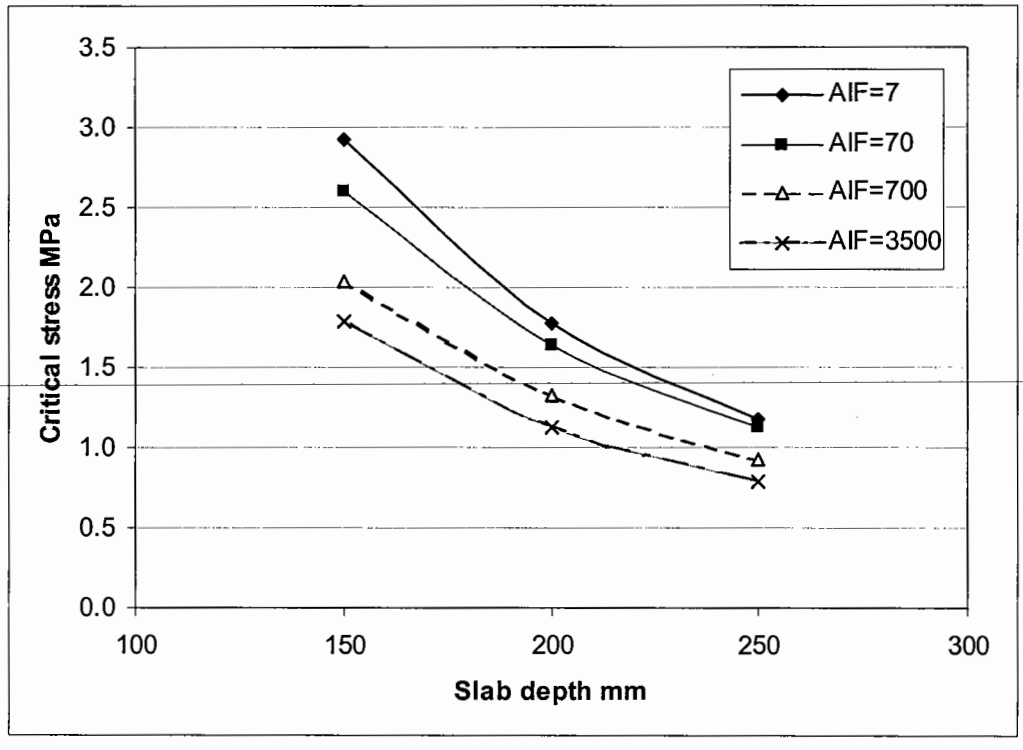

Figure 6-7 Effect of base depth on bending stress at various aggregate interlock factors for k=0.08N/mm³

6.2.3 Deflections and rotations near a transverse crack

Effect of aggregate interlock factor across width of slab

For an offset load, the deflection profile across the width of the loaded side of a transverse crack is dependent on the *AIF* (Figure 6-8). The longitudinal deflection profile and rotation at the crack will be affected by this, and material properties of the various layers in the structure, such as layer thickness, stiffness and foundation support. The deflection and rotation parameters being investigated were defined in Figure 6-2.

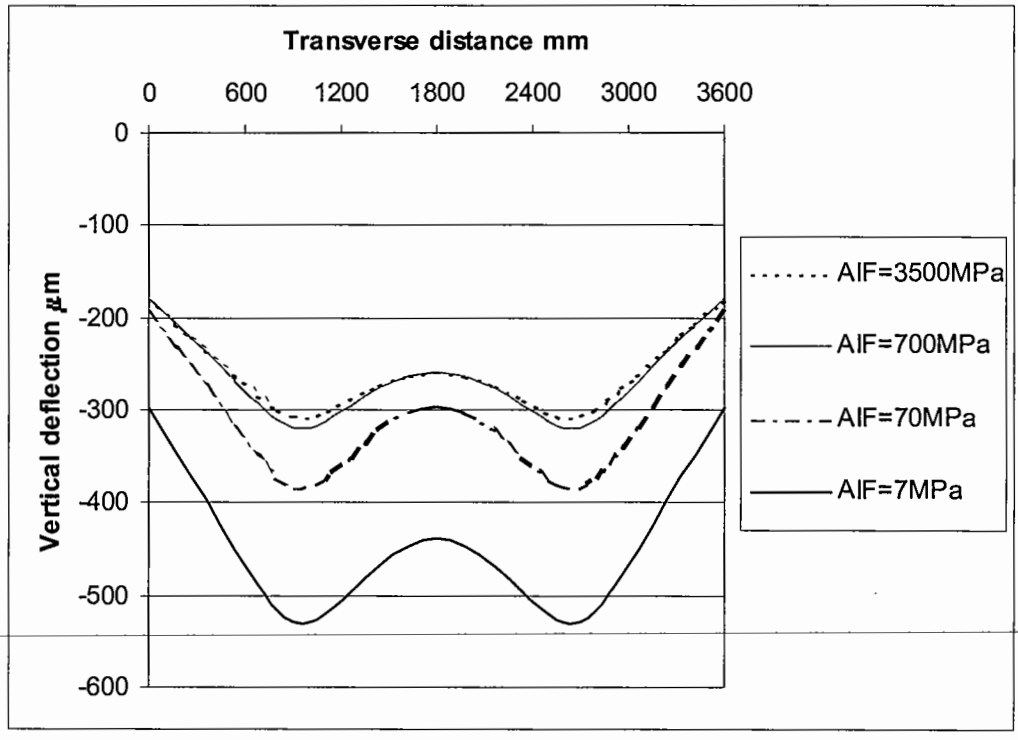

Figure 6-8 Typical vertical deflection profiles across slab section at various *AIF*

The influence of the *AIF*, modulus of subgrade reaction (k) and slab depth (D) on the rotation and vertical deflection on the loaded and unloaded sides of a crack are shown in Figures 6-9 to 6-14. The differential vertical movement ($\Delta\delta$) and total rotation (θ_T) are also shown.

Effect of aggregate interlock factor on longitudinal deflection profile

The *AIF* had little affect on the total rotation (Figure 6-9), which was found to be approximately $62x10^{-5}$ rad for the pavement properties investigated. A decrease in the rotation in the loaded side of the crack and an increase on the unloaded side of the crack occurred as the *AIF* increased. The increase in the *AIF* is indicative of the loaded and unloaded sides of the crack being 'tied together' more efficiently. This is further demonstrated by the reduction in the relative vertical deflection (Figure 6-10), which shows that an increase in the *AIF* decreases markedly the differential vertical movement at the crack interface ($\Delta\delta$). Between an *AIF* of 7MPa and 700MPa, the differential vertical movement was reduced by 95%.

Effect of modulus of subgrade reaction on longitudinal deflection profile

The modulus of subgrade reaction had a significant effect on the rotation, decreasing the loaded, unloaded and therefore net values (Figure 6-11). As the subgrade modulus increases from 0.08N/mm³ to 0.16N/mm³, the rotation decreases from 61 $x10^{-5}$ rad to $43x10^{-5}$ rad, or by 30%. The subgrade modulus had very little effect on the relative vertical deflection (Figure 6-12), though the deflections on the loaded side of the crack were reduced by approximately 30%, and the deflections on the unloaded sides of the crack were reduced by approximately 50% over the same modulus range.

Effect of slab thickness on longitudinal deflection profile

An increase in the slab thickness significantly decreased rotations, and to a lesser extent the deflections (Figures 6-14 and 6-15). As the depth increases from 150mm to 250mm, the rotation decreases by over 50%. Over the same range, the relative deflection decreases by 32%.

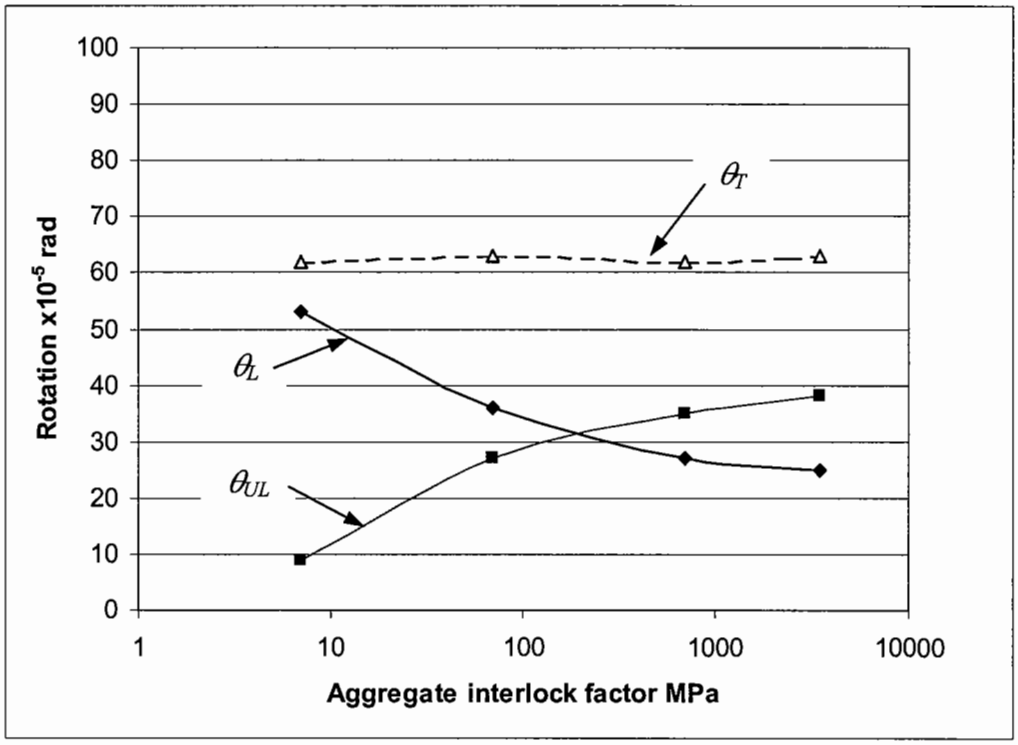

Figure 6-9 Relationship between rotation and AIF, when k=0.08N/mm³, E=15000MPa and D=200mm.

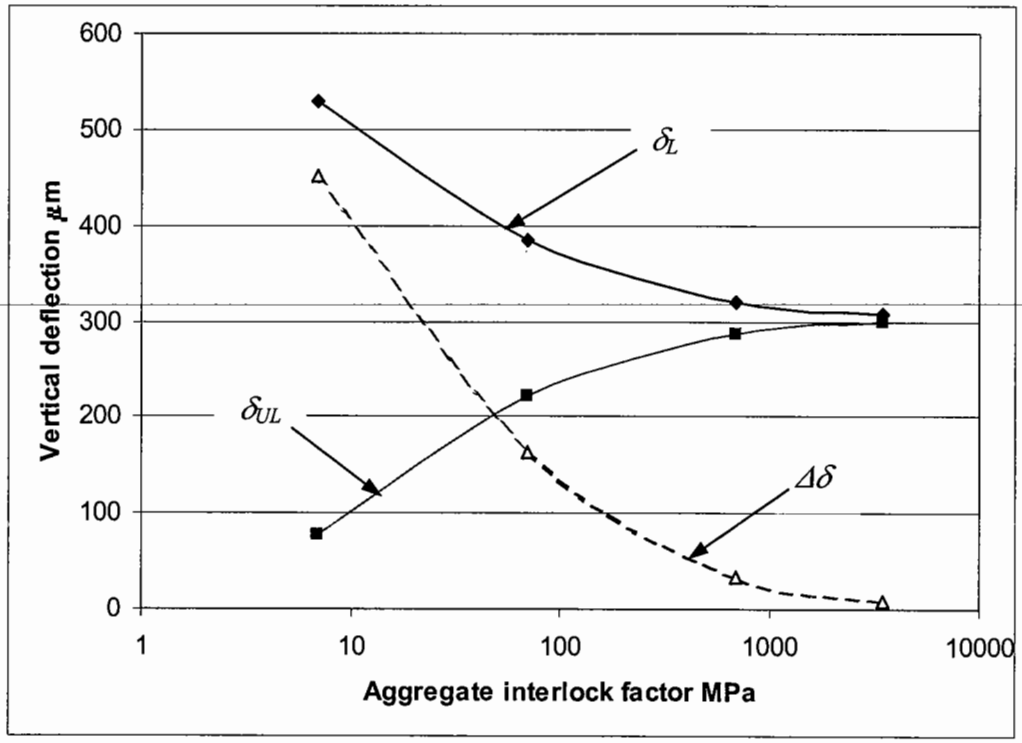

Figure 6-10 Relationship between vertical deflection and *AIF* when k=0.08N/mm³, E=15000MPa and D=200mm

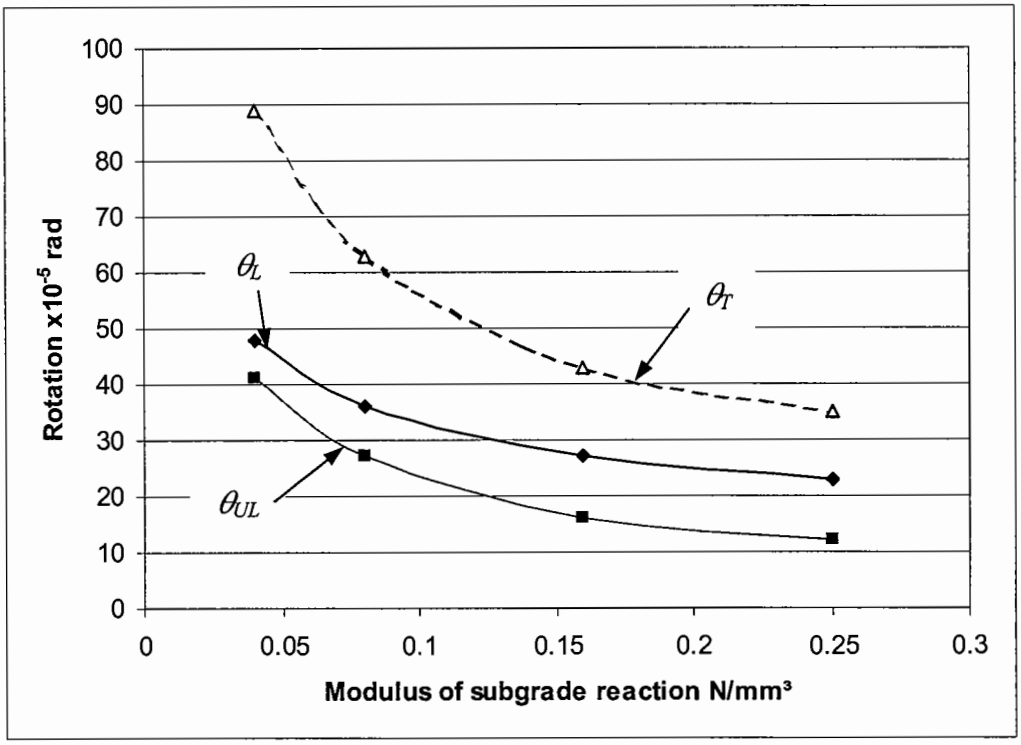

Figure 6-11 Relationship between rotation and modulus of subgrade reaction when *AIF*=70MPa, *E*=15000MPa and *D*=200mm

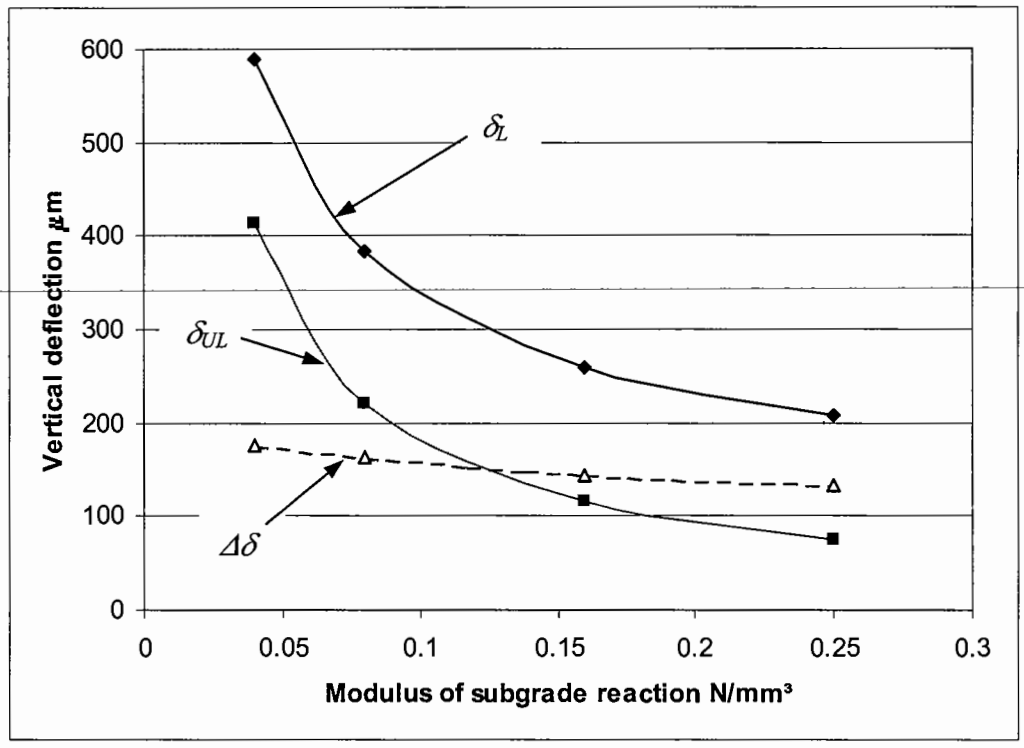

Figure 6-12 Relationship between vertical deflection and modulus of subgrade reaction when *AIF*=70MPa, *E*=15000MPa and *D*=200mm

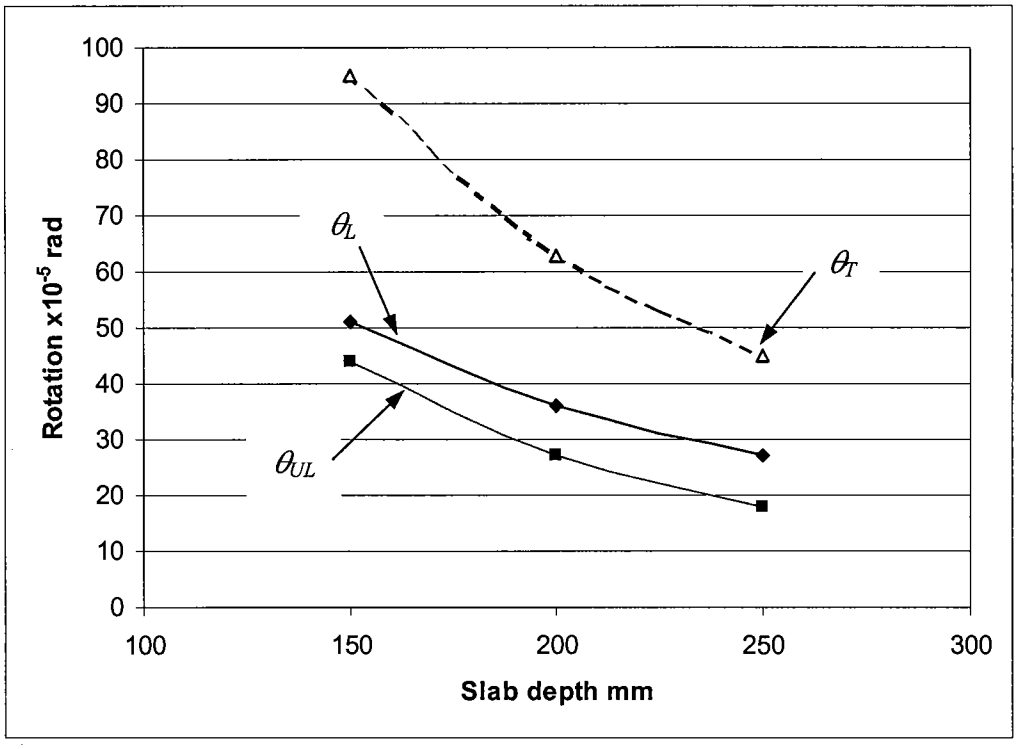

Figure 6-13 Relationship between rotation and slab depth when *AIF*=70MPa, *k*=0.08N/mm³ and *E*=15000MPa

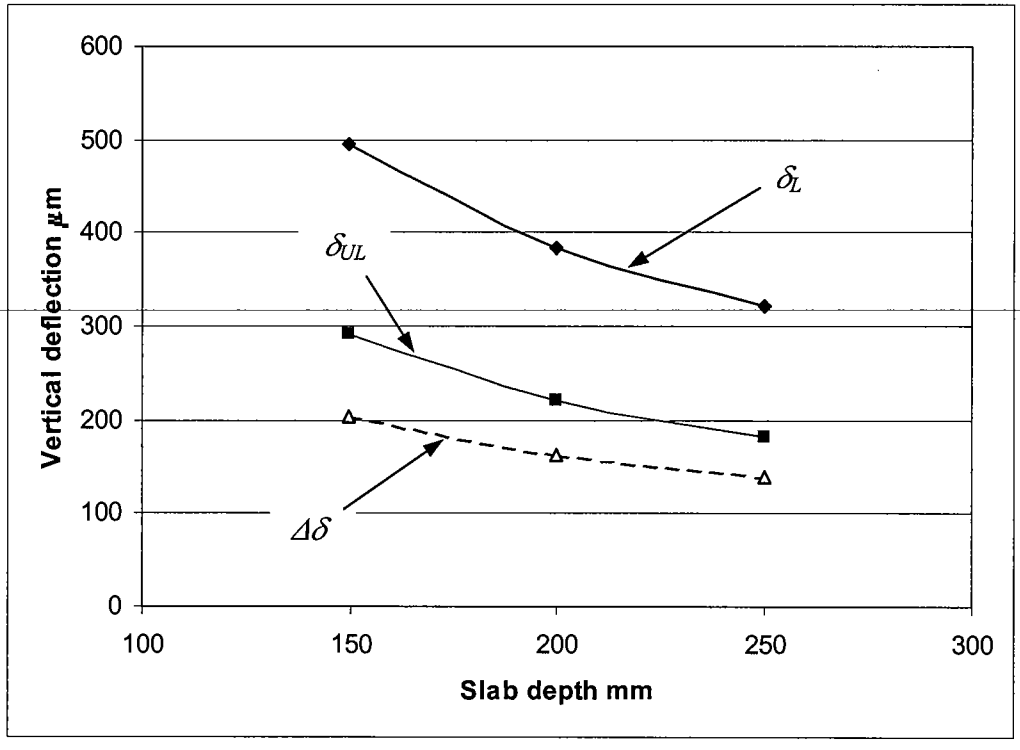

Figure 6-14 Relationship between vertical deflection and slab depth when *AIF*=70MPa, *k*=0.08N/mm³ and *E*=15000MPa

Summary of effects of material characteristics on stresses, deflections and rotations

The preceding brief analytical investigation serves to highlight the relative influence of the slab and foundation properties on the structure as a whole. In summary, the following is noted:

- Increases in **slab thickness** have universal benefits, decreasing the stresses, rotations and deflections significantly close to a transverse crack. However, a practical upper thickness limit exists for CBM based on compactability, as already discussed.

- Increases in the **aggregate interlock factor** decrease significantly the differential movement across a crack, and reduce the critical stress. The total rotation was found to be unaffected.

- The **modulus of subgrade reaction** was found not to have a significant affect on the critical stress or the differential movement across a crack. However, an increase in the modulus reduces the actual magnitude of the deflection on both the loaded and unloaded side of a crack and reduces the total rotation. This would be expected to reduce the distress at the crack face under dynamic load.

Relationship between aggregate interlock factor and load transfer efficiency

The influence of the subgrade modulus on the deflections is worthy of study. For a given *AIF*, the load transfer efficiency (*LTE*), calculated using Figure 2-18, reduces with increasing subgrade modulus (Figure 6-15). The magnitude of the reduction is a function of the *AIF*. This reduction in *LTE* is in spite of the vertical deflections and rotations on the loaded and unloaded sides of the crack being significantly reduced at a higher subgrade modulus, demonstrating improved behaviour. In large-scale load transfer tests, Colley and Humphrey (1967) demonstrated convincingly the reduction in deterioration at the crack interface due to reduced deflections brought about by a stiffer support.

It is reasonably common practice to record load transfer efficiencies (*LTE*) from Falling Weight Deflectometer (FWD) field measurements as an indicator of the performance of transverse cracks and joints. Unless the effect of the subgrade modulus on the *LTE* is

appreciated, the erroneous conclusion might be drawn that the aggregate interlock is poor, when in fact it is a function of the support properties that is being measured. A solution to this would be to back-calculate a value of *AIF* using the method described by Ioannides and Korovesis (1990). This takes account of the contribution of the support conditions (which may also be assessed from the FWD measurements) and does not give the misleading impression of crack performance that can occur with *LTE*.

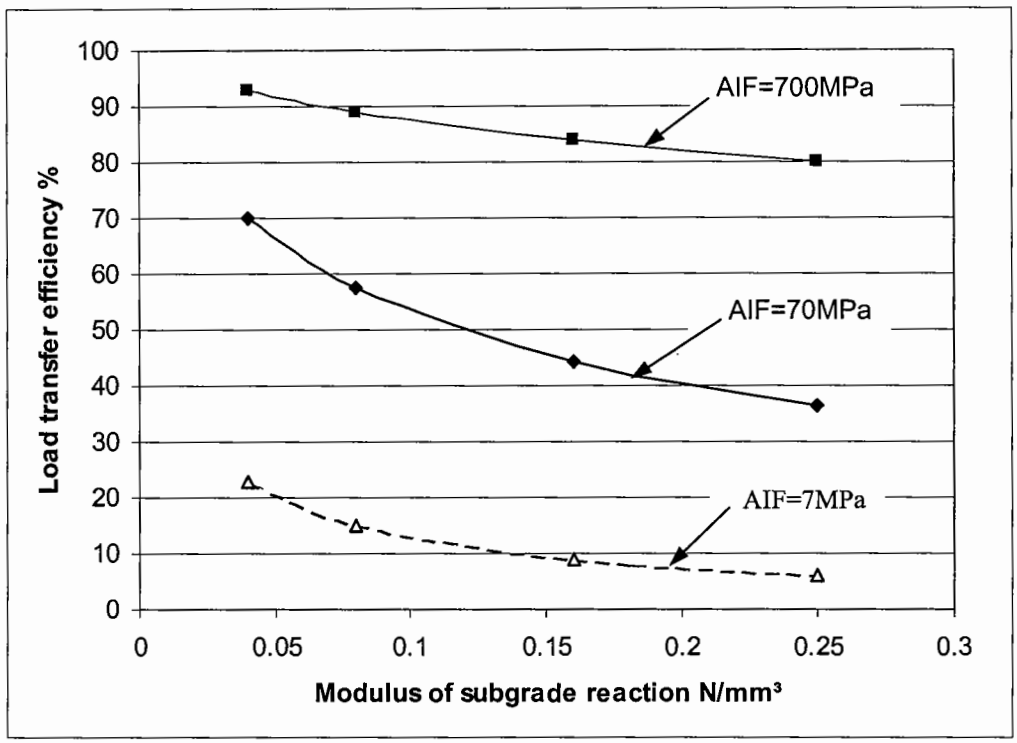

Figure 6-15 Effect of subgrade modulus on load transfer efficiency (*LTE*) at various *AIF*, *D*=200mm, *E*=15000MPa

6.2.4 Consideration of the asphalt overlay

The preceding discussion considered only the behaviour of a slab without an overlay. However, a number of benefits to the pavement result from using an asphalt overlay. These include a reduction in stress at the surface of the slab due to load spreading, and some transfer of load by the asphalt across the transverse cracks. Also, the insulation provided by the overlay reduces the horizontal movement across a crack by reducing the temperature variation in the slab, as reported by Lister (1972) and shown in Figure 2-8.

The effect of an overlay was investigated indirectly assuming asphalt depths (D_a) of 50, 100 and 150mm. The simple assumption was made that the asphalt spread the applied load over an angle of 45°, thereby reducing the imposed stress on the surface of the slab (Figure 6-16). However, this did not take account of the possible additional benefit of the transfer of load across a crack brought about by an overlay. This was not considered due to the complexity of the analysis, and since these benefits would be lost should reflective cracking occur. There is therefore a degree of conservatism within the analysis.

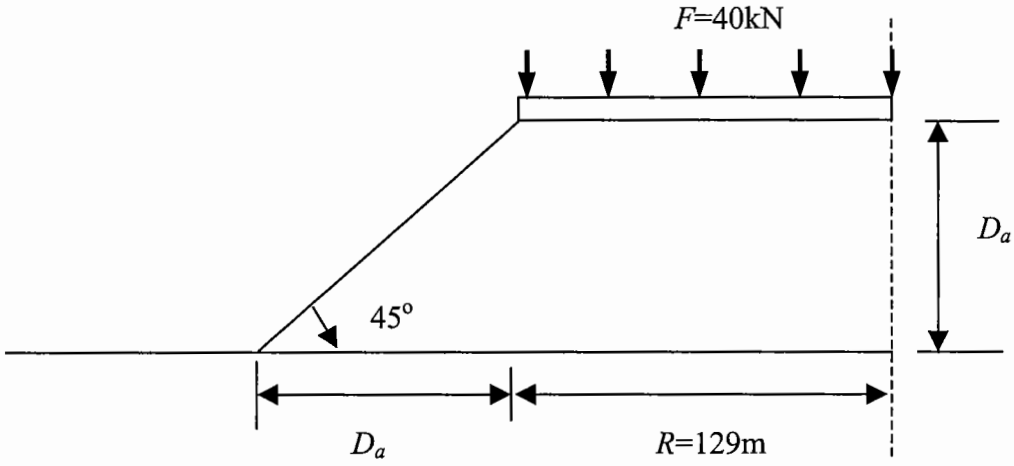

Figure 6-16 Assumed load spreading characteristics of asphalt overlay as used in FRCBM design method

In the analysis, half the tyre contact length (R) was assumed to be 129mm. Therefore, the contact area (A), for a given depth of asphalt in mm (D_a), was calculated as:

$$A=4(D_a+129)^2 \qquad \textbf{Eqn...6-2}$$

And the stress imposed on the top of the slab (P MPa) was:

$$P=\frac{10000}{(D_a+129)^2} \qquad \textbf{Eqn...6-3}$$

ILLISLAB95 was used to investigate the influence of a reduced imposed stress on the vertical deflections and rotation due to a load near a transverse crack. The results are shown in Table 6-2.

D_a mm	A mm²	P kPa	Deflection μm			Rotation x10^{-5} rad		
			δ_L	δ_{UL}	$\Delta\delta$	θ_L	θ_{UL}	θ_T
0	66564	595	490	220	170	37	26	61
50	128164	312	325	225	100	33	25	58
100	209764	191	275	220	55	24	24	48
150	311364	128	235	230	5	23	23	46

Table 6-2 Results of ILLISLAB95 runs using reduced imposed stresses with k=0.08N/mm³, E=15000MPa, D=200mm

The reduced stress due to a 150mm overlay reduces the total rotation by 25% when comparing it with a slab with no overlay (Figure 6-17). Only the loaded side of the crack is affected due to the assumption that no load is transferred by the asphalt. In fact, the asphalt contribution may be significant, and the considerable reduction in vertical deflection at increasing asphalt depths could only be improved as long as reflective cracking did not occur (Figure 6-18). The *AIF* used in the analysis for Figure 6-17 and Figure 6-18 is relatively low (70MPa), which might be indicative of a naturally cracked CBM. The preceding study has demonstrated that rotation and deflection may be improved by improving the support and crack properties, all achievable in practice. In theory, improvement of these properties should allow a reduction in the expensive asphalt overlay depth whilst maintaining the deflections and rotations currently experienced in 'untreated' slabs.

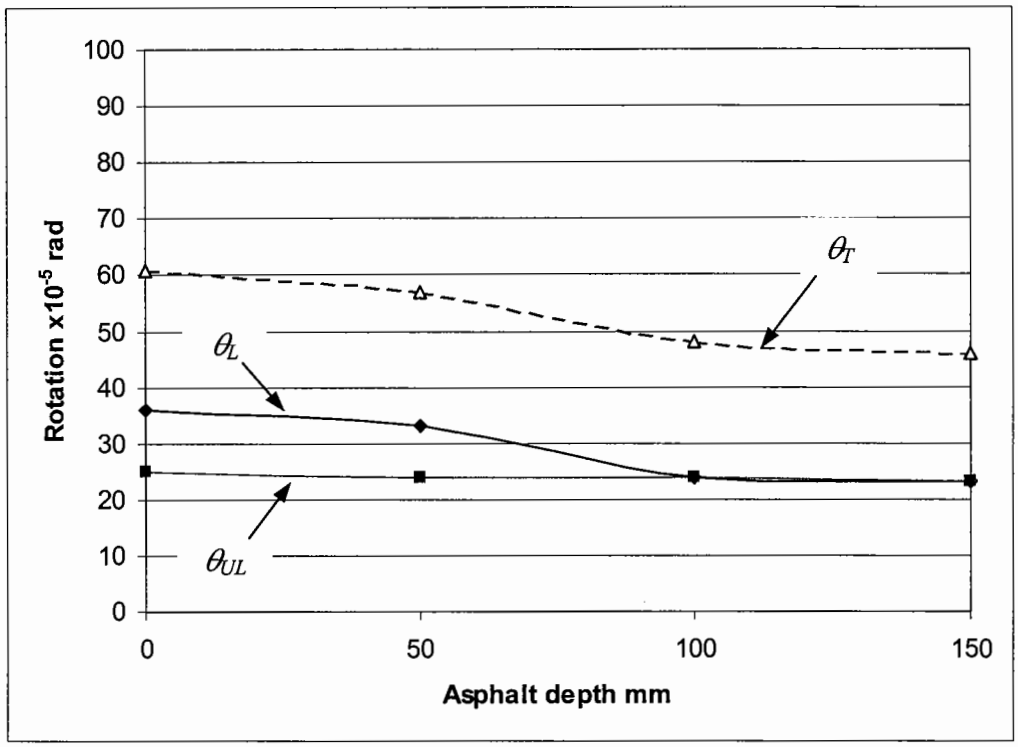

Figure 6-17 Relationship between rotation and asphalt depth when *AIF*=70MPa, *k*=0.08N/mm³, *E*=15000MPa and *D*=200mm

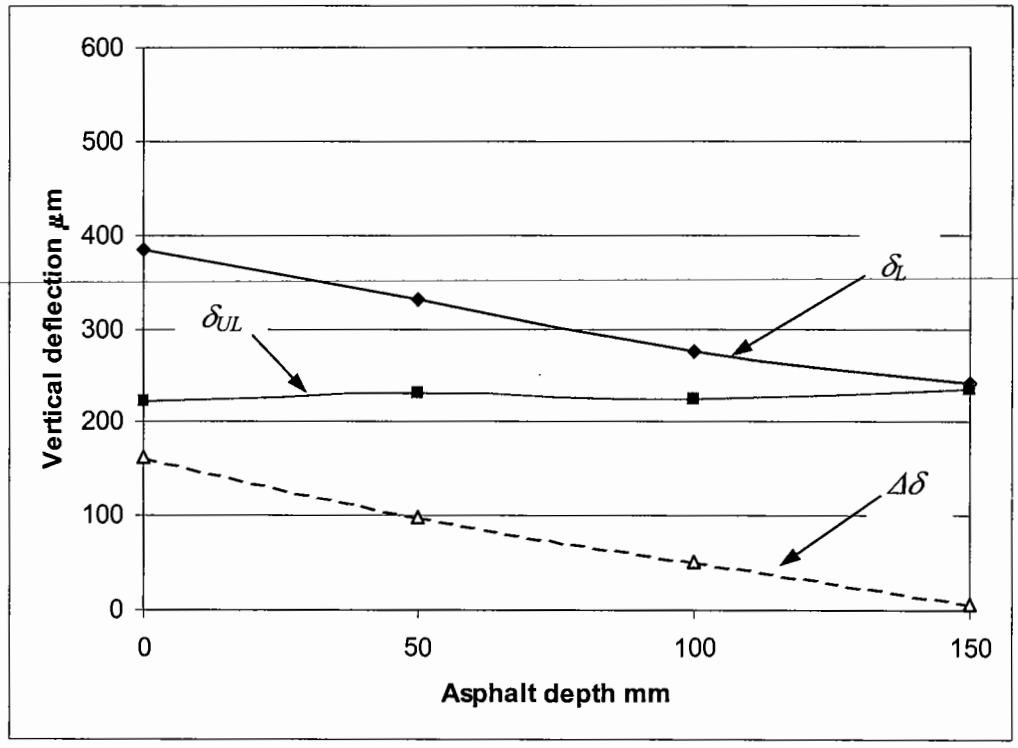

Figure 6-18 Relationship between vertical deflection and asphalt depth when *AIF*=70MPa, *k*=0.08N/mm³, *E*=15000MPa and *D*=200mm

In order to assess the relationship between the asphalt depth (D_a) and other parameters, the effect of the vertical deflection and rotation on the critical strain within the asphalt overlay was investigated for a wheel load offset from, and directly over, a transverse crack. The models were based on a two dimensional beam of asphalt in bending.

Strains imposed on asphalt due to a wheel offset from a transverse crack

For an offset load, the relationship between critical strain (ε_t), overlay depth (D_a), differential vertical deflection ($\Delta\delta$), rotation (θ) and de-bond length (L_{db}) is shown by Eqn...6-4 and defined in Figure 6-19. A full derivation of Eqn...6-4 is shown in Appendix C.

$$\varepsilon_t = \frac{D_a}{L_{db}}\left(\frac{3.\Delta\delta}{L_{db}} - 2\theta_T\right) \qquad \textbf{Eqn...6-4}$$

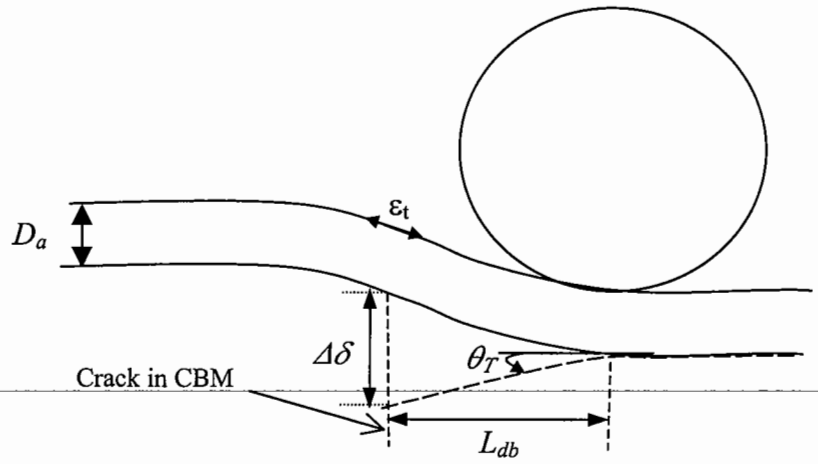

Figure 6-19 Schematic showing parameters used in derivation of cracking due to a load offset from the crack

Inspection of Eqn...6-4 shows that the strain is dependent on the de-bond length (L_{db}). As the de-bond length tends to zero, the strain tends to infinity. However, the actual value of L_{db} is not simple to determine and is rarely, if ever, known.

Despite this, it can be shown that de-bond length has a significant effect on the magnitude of the asphalt strain. For a slab with D_a=100mm, AIF=70MPa, D=200mm and

k=0.08N/mm^3, Figures 6-17 and 6-18 show that θ_T=48x10^{-5} rad and $\Delta\delta$=50μm. Based on assumed de-bond lengths of 50mm, 100mm and 150mm, the calculated strains are 4080με, 540με and 27με respectively (Figure 6-20). By using similar principles, Figures 6-10 and 6-18 was used to determine the effect of an *AIF* of 700MPa and of D_a on asphalt strain, assuming de-bond lengths indicated (Table 6-3).

AIF MPa	D_a mm	θ_T x10^{-5} rad	$\Delta\delta$ μm	Strain (με) at de-bond length (L_{db})		
				L_{db}=50mm	L_{db}=100mm	L_{db}=150mm
70	50	57	100	4840	920	280
	100	48	50	4080	540	27
	150	46	5	-1800	-1125	-800
700	50	60	21	76	-281	-258
	100	50	1	-709	-673	-520
	150	47	0.1	-2599	-1347	-909

Table 6-3 Asphalt strains at various *AIF*, asphalt depth and de-bond length

To put this into perspective, Powell *et al.* (1984) showed that Dense Bitumen Macadam under a strain of 200με would theoretically be able to carry traffic loads of 1 million standard axles (msa) before cracking occurred. At a strain of 50με it would be able to carry in excess of 300msa. For asphalt depths of 150mm, the strains were negative (which based on Figure 6-19 would result in a compressive, non-damaging strain). Figure 6-20 is based on an *AIF* of 70MPa, which may be expected in a CBM that has cracked naturally (see Section 2.4.5). In practice it has been found that 150mm of asphalt results in a long-life pavement, implying reflective cracking is not a significant problem at these overlay depths (Parry et al. 1999). The results presented here are not inconsistent with such a finding.

At an *AIF* of 700MPa, the strains are almost universally negative, and therefore non-damaging for the load scenario under consideration (Figure 6-21). The parameter that can be improved the most is $\Delta\delta$, either by increasing the *AIF* and/or increasing the overlay depth.

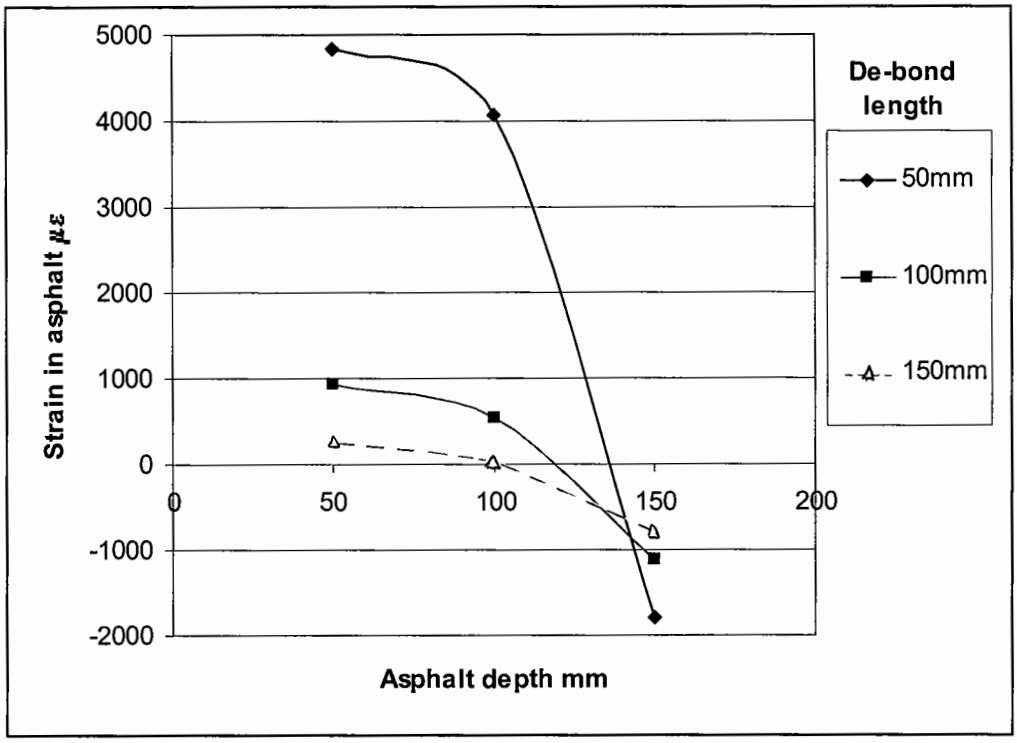

Figure 6-20 Strain in asphalt at various asphalt depths and de-bond lengths for an AIF of 70MPa

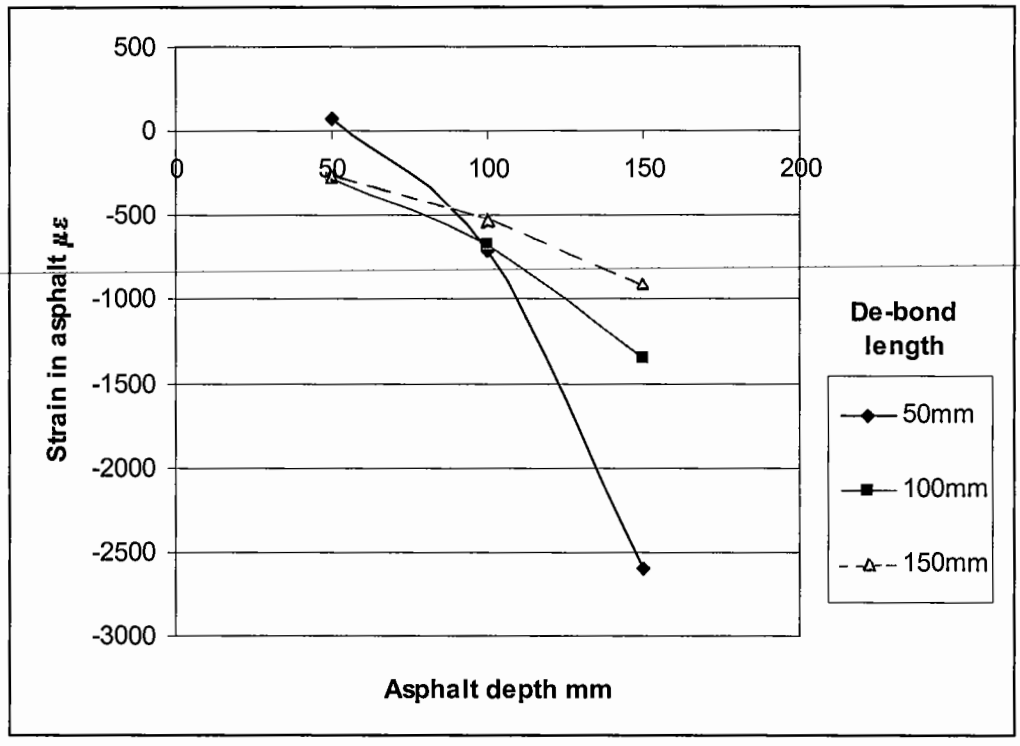

Figure 6-21 Strain in asphalt at various asphalt depths and de-bond lengths for an AIF of 700MPa

For a de-bond length of 100mm, the intersects of zero strain were plotted at *AIF* of 70MPa and 700MPa (from Figures 6-20 and 6-21), and following similar principles as described above, at an *AIF* of 350MPa. This shows a relationship between *AIF* and asphalt depth, which is referred to as the 'line of zero strain' (Figure 6-22). Below the line of zero strain, damaging strains will be imposed on the overlay. Above the line, the strains are negative and therefore considered non-damaging. As *AIF* and asphalt depth are determinable quantities within a pavement, the relationship between these values may be used in design to ensure damaging strains due to a traffic load offset from a crack will not occur.

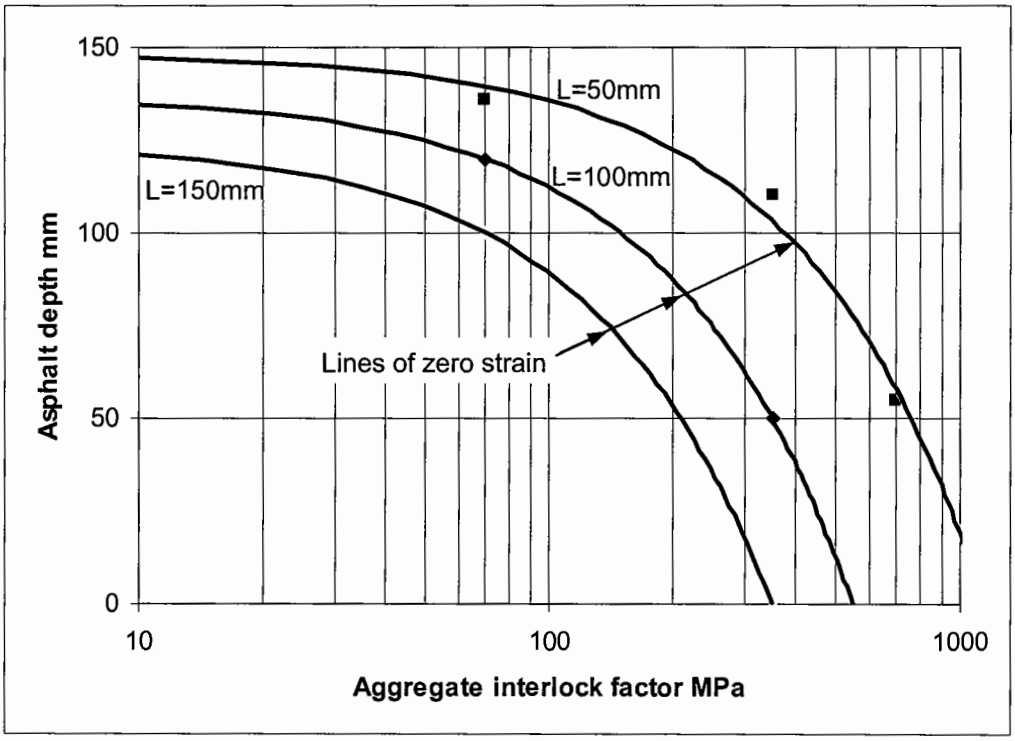

Figure 6-22 Relationship between *AIF* and overlay depth for asphalt de-bond lengths of 50mm, 100mm and 150mm

It was noted that in naturally cracked CBM, the average *AIF* prior to any traffic was 217MPa (Table 2-2, Section 2.4.5). As flexible composite pavements are expected to have an 'indeterminate' life with an overlay greater than 150mm (see Figure 2-2 in Section 2.2.1), it may be deduced from Figure 6-22 that a de-bond length less than 50mm is present. A de-bond length of 50mm has therefore been assumed in the design method presented below.

The preceding discussion illustrates the numerous variables to consider in assessing the conditions under which reflection cracking will occur. Cracks that occur based on a wheel load near a transverse crack, as presented, will result in a crack appearing first in the top of the asphalt (rather than the underside) as it is here where the strain is critical (refer to Figure 6-20). Nunn (1990) produced cores that showed evidence of so called 'top-down' cracking, but argued this was most likely a consequence of temperature effects. In flexible composite pavements with an overlay of over 150mm, it is likely based on the theoretical analysis presented that traffic induced strains are non-damaging. This agrees with Nunn's conclusions that such cracking is temperature induced. However, in pavements with overlays less than (say) 100mm, it seems probable that differential vertical deflections across cracks would be sufficient to result in reflective cracking due to traffic loading.

The implication of the above analysis is that a design will not result in a significant asphalt strain provided the combined influence of the *AIF* and asphalt depth ensure the differential deflection across a crack is below a certain value; this value is dependent on the de-bond length. Once the differential deflection has exceeded the limiting value, cracking would be expected to occur as the strains in the asphalt would then be damaging.

In addition to the load close to a transverse crack, a second situation must be considered, when the load is directly over the transverse crack. This too will impose bending strains in the asphalt, potentially resulting in reflective cracking.

Strains imposed on asphalt due to a wheel over a transverse crack

A wheel load directly over a crack results in the asphalt bending, with the critical strain in the base (Figure 6-23). Only a portion of the total tyre contact radius would contribute to the critical strain (ε_t), which would be dependent on the de-bond length (L_{db}).

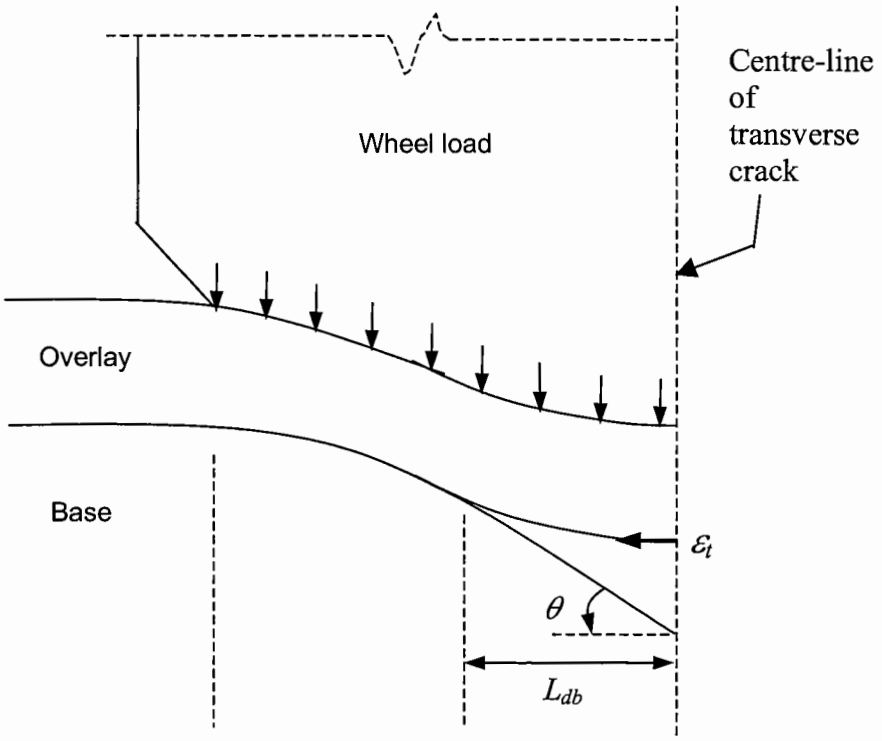

Figure 6-23 Schematic showing parameters used in the derivation of cracking for a load positioned over a crack

Relationships were derived to estimate the asphalt strain under an 'equivalent load' (P_{eq} - described below) and de-bond length, assuming a beam in bending; full derivations are shown in Appendix C. The de-bond length (L_{db}) was determined as a function of the asphalt depth (D_a) and rotation (θ), as shown in Eqn...6-5, so unlike the load offset from the crack, did not have to be assumed.

$$L_{db}=\left(\frac{ED_a^{\,3}\theta}{4P_{eq}}\right)^{\frac{1}{3}} \qquad \textbf{Eqn...6-5}$$

ILLISLAB95 computes deflections in three planes, yet Eqn...6-5 is based on two dimensions. To overcome the differences in applied stress that will occur in computing the rotation, an equivalent load (P_{eq}) was defined based on a strip load cross the width of the slab (Figure 6-24).

The vertical deflection based on the strip load (δ_w) was compared to a deflection obtained from a standard axle (δ), allowing the stress to be factored (Eqn...6-6).

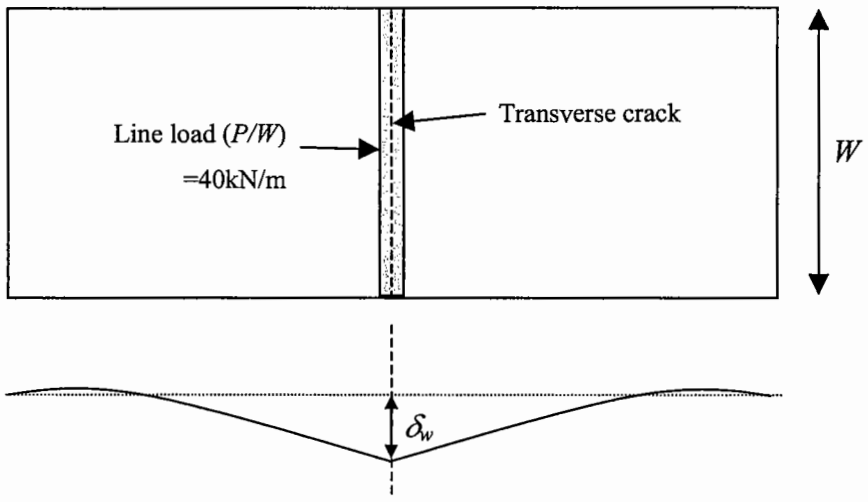

Figure 6-24 Definition of parameters in determination of equivalent load based on a strip load

$$P_{eq} = \left(\frac{\delta_w}{\delta}\right)\left(\frac{P}{W}\right) \qquad \textbf{Eqn...6-6}$$

For the computation, the following material parameters were used: modulus of subgrade reaction, k=0.08N/mm³; slab depth, D=200mm; and AIF=70MPa. It was found that δ_w=537μm and δ=331μm. Hence, for a standard 40kN wheel load P_{eq}=24.7kN, or 0.10kN/mm uniformly distributed load across a tyre of diameter 258mm. It was also found, for a subgrade modulus of 0.25N/mm³, δ_w=223μm and δ=159μm, that P_{eq}=28.5kN, or 0.11kN/mm. As the third root is taken in the determination of the de-bond length (Eqn...6-5), the difference in the calculated value of de-bond length between the two subgrade parameters was considered small.

The de-bond length determines the proportion of the equivalent load that contributes to the asphalt strain (as shown in Figure 6-23). For a given equivalent load per unit length of tyre (P_{eq}) and asphalt stiffness (E), the critical strain in the asphalt (ε_t) was found to be dependent on the de-bond length (L_{db}) and overlay depth (D_a), as shown in Eqn...6-7. The full derivation is shown in Appendix C.

$$\varepsilon = \frac{3P_{eq}L_{db}^2}{ED_a^2} \qquad \textbf{Eqn...6-7}$$

For a given overlay thickness (using the assumed load spreading angle of 45^0 outlined in Section 6.2.4), rotations were investigated under a standard 80kN axle load for various support conditions. As the aggregate interlock factor (*AIF*) in ILLISLAB95 transfers shear stress only, any benefits brought about by moment transfer cannot be modelled using this parameter. However, any increase in moment transfer, which may occur due to fibre reinforcement, will affect the rotations, and this aspect is worthy of further study.

Using a fatigue relationship for Dense Bitumen Macadam (DBM), the number of standard loading applications, for permissible strains within the asphalt, can be computed, as reported by Powell *et al.* (1984) and shown in Eqn...6-8. These data can then be used to determine a relationship between overlay depth and traffic loading, using Eqn...6-7.

$$Log\ N = -9.38 - 4.16\ log\ \varepsilon \qquad \textbf{Eqn...6-8}$$

The results of the ILLISLAB95 investigation and calculated values of L_{db}, ε_t and N are shown in Table 6-4. The relationship between asphalt depth and traffic based on this analysis is shown in Figure 6-25.

k N/mm^3	D_a mm	θrad x10^{-5}	L_{db} mm	ε_t (microstrain)	N msa
0.08	25	36	37	165	3.7
	50	35	73	158	4.3
	100	32	140	148	5.8
	150	29	204	138	7.8
0.16	25	26	33	133	9.3
	50	25	65	126	11.5
	100	22	124	115	17.0
	150	19	177	105	25.7

Table 6-4 Effect of rotation on de-bond length (L_{db}), asphalt strain (ε_t) and traffic (N) at various asphalt depths (D_a) and two subgrade moduli (k)

The life of DBM computed in this study is compared to that presented by Powell, which was derived from field studies. It can be seen that the effect of the overlay depth using the theoretical relationship determined in this study has a lesser affect on the life of the material than was observed by Powell *et al.* (1984). However, Powell's did not attempt to distinguish between thermal movement of the CBM, or 'top-down' or 'bottom-up' cracking brought about by traffic. Therefore, the failure curve presented by Powell may be expected to give a lower life, considering all the above effects are contributing to the asphalt strain.

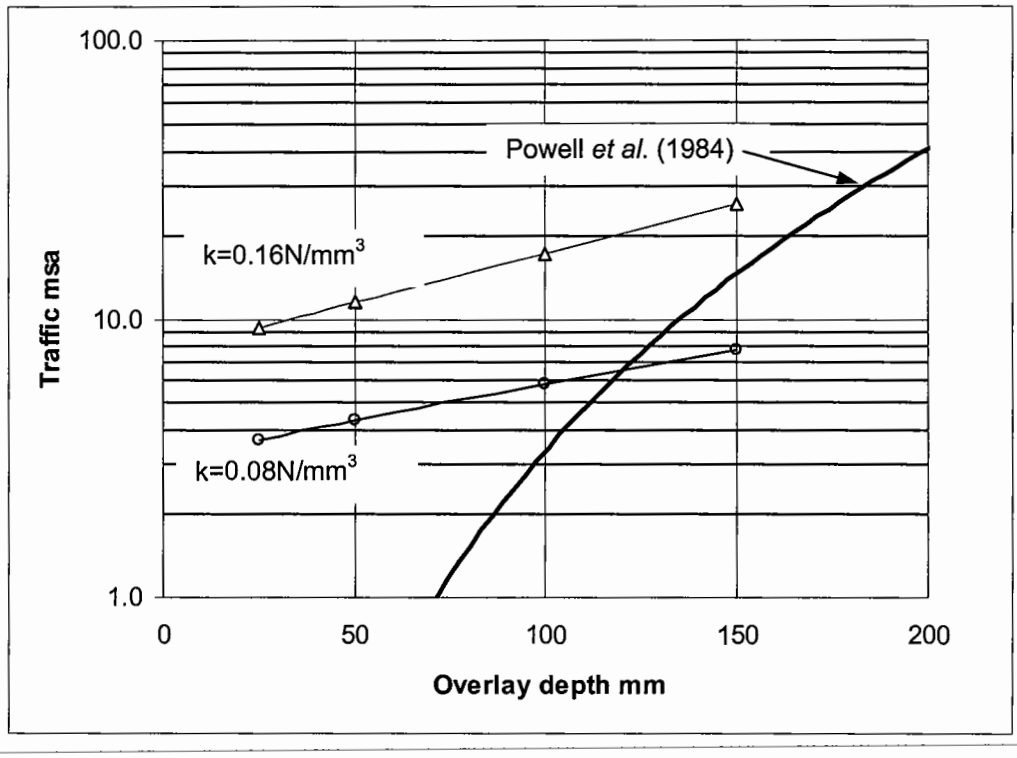

Figure 6-25 Predicted load applications to cause cracking in a DBM due to a load directly over a transverse crack at two subgrade moduli

An advantage of the theoretical relationship presented in this study is that it enables the relative influence of the modes of cracking caused by traffic to be compared. Additionally, the relationship shown in Figure 6-25 demonstrates the potential benefits of an improved subgrade modulus on decreasing the rate of reflective cracking. Between k=0.08 and 0.16N/mm^3, at an overlay depth of 100mm, the life is predicted to increase from 5.8msa to 17.0msa, the increase being due to a decrease in the rotation of the crack.

The opportunity exists for further improvements in the rotation due to steel fibre reinforcement to be investigated, either theoretically or in the field (using the FWD). Changes in rotation may be applied to Eqns...6-5 and 6-6, and the potential increase in asphalt life can be readily computed as demonstrated in the aforementioned discussion.

Field observations have demonstrated that top-down cracking is the primary cause of reflective cracking in flexible composite pavements (Nunn 1990), which is supported by the preceding discussion. Therefore, in the design method presented below, bottom-up cracking as a failure mechanism was not considered.

6.2.5 Discussion of material properties

The theoretical analysis using ILLISLAB95 has highlighted that the changes in the behaviour of a CBM with a transverse crack occur as a function of the aggregate interlock factor, modulus of subgrade reaction, base depth and overlay depth. The changes were assessed in terms of critical stress, vertical deflection and rotation at the loaded and unloaded sides of a transverse crack.

The results demonstrate that a reduction in the rotation is most readily achieved by increasing the modulus of subgrade reaction. This can be achieved by ensuring the foundation has a high stiffness. Cement bound sub-bases would seem to be appropriate, not only to reduce the rotation, but also to help with compaction of the overlying FRCBM layer. It should be noted that the use of a stiff sub-base will have little effect on the critical stresses in the slab; its main purpose in the completed works is to decrease the rate of deterioration of cracks and provide some additional load carrying capability once cracks have formed in the base.

An effective foundation will also reduce markedly the total deflection on the loaded and unloaded sides of the cracked CBM slab. Relative deflections can be further, and more significantly, improved by increasing the aggregate interlock factor. In practice, this can most effectively be achieved by reducing the crack spacing by inducing cracks at closer spacings than would occur naturally. Laboratory tests have demonstrated that smaller crack widths increase significantly the aggregate interlock factor (measured in terms of load transfer stiffness – refer to Section 4.8.6) and decrease the deterioration of the cracks. Steel fibres

further enhance this behaviour, particularly in wider cracks. An additional influence on the aggregate interlock factor is the aggregate type. The coefficient of thermal expansion, which governs the magnitude of the expansion that takes place under a temperature change, will affect the crack width, and aggregate strength and angularity will contribute to the overall load transfer mechanism. The mixture strength may also have a role to play. The expectation would be for a higher strength material to be more durable, yet if the fracture surface is through the aggregate, rather than around the aggregate, a crack interface with poor interlock characteristics may result.

An increase in the aggregate interlock factor also significantly reduces the critical stress. Based on the analytical study, it is proposed that the *AIF* is increased through induced cracking at 3m centres, steel fibre reinforcement and aggregate selection. Hard, angular aggregate with a low coefficient of thermal expansion is preferred. Further tests may be required to investigate the fracture surface of higher strength CBM using weaker aggregate than the gravel used in the cyclic shear tests.

Increases in slab depth appear to have universal benefits, though the maximum depth of a CBM is limited by the need for achievable compaction. Paradoxically, a more slender section might be stronger if compaction is facilitated due to the reduced depth. However, greater shear stress across transverse cracks would be expected in more slender sections.

The benefits of an asphalt overlay are to reduce the thermally induced movement of cracks, provide some transfer of load and reduce the imposed the stress on the FRCBM by 'spreading' the traffic load. The asphalt is by far the most costly single item within flexible composite construction, therefore a reduction in the overlay depth is economically attractive. Maintaining both the economics and performance of the pavement at a reduced overlay depth will be dependent on the relative influence and cost of improving these parameters.

6.3 Design method overview

The FRCBM design method is based on the relationships described above using theoretical analysis, and laboratory and field data. The design criteria were to avoid longitudinal cracking in the FRCBM layer, and to limit the reflective transverse cracking through the asphalt overlay by designing an overlay of minimum thickness. The analysis assumes a load offset from a crack; the load directly over the crack would result in a bottom-up crack, and as previously discussed, there is no evidence such cracks occur. Therefore, only top-down cracking is assumed in the design.

The design method uses plastic analysis to determine the magnitude of the critical stress in the FRCBM roadbase under a standard axle load. The load transfer stiffness across a transverse crack after a number of traffic loads is used to determine the critical stress in the base. The stress is factored to provide a design strength based on the level of compaction and fatigue characteristics of the material and the asphalt overlay depth.

In the analysis, a CBM sub-base is assumed. The reason for this is that there are many benefits, in particular by increasing the endurance of cracks, but also by providing a compliant platform to compact the FRCBM onto. Also, a CBM enables the use of marginal materials, and is less susceptible to softening should water enter the pavement.

The design methodology is shown by the flow chart in Figure 6-26. There follows a discussion of the various design elements, presentation of the design charts and some design examples. The method allows comparison of flexible composite constructions using FRCBM with induced cracks, CBM with induced cracks and naturally cracked CBM. Finally, approximate costs are used to illustrate the economics of the various options.

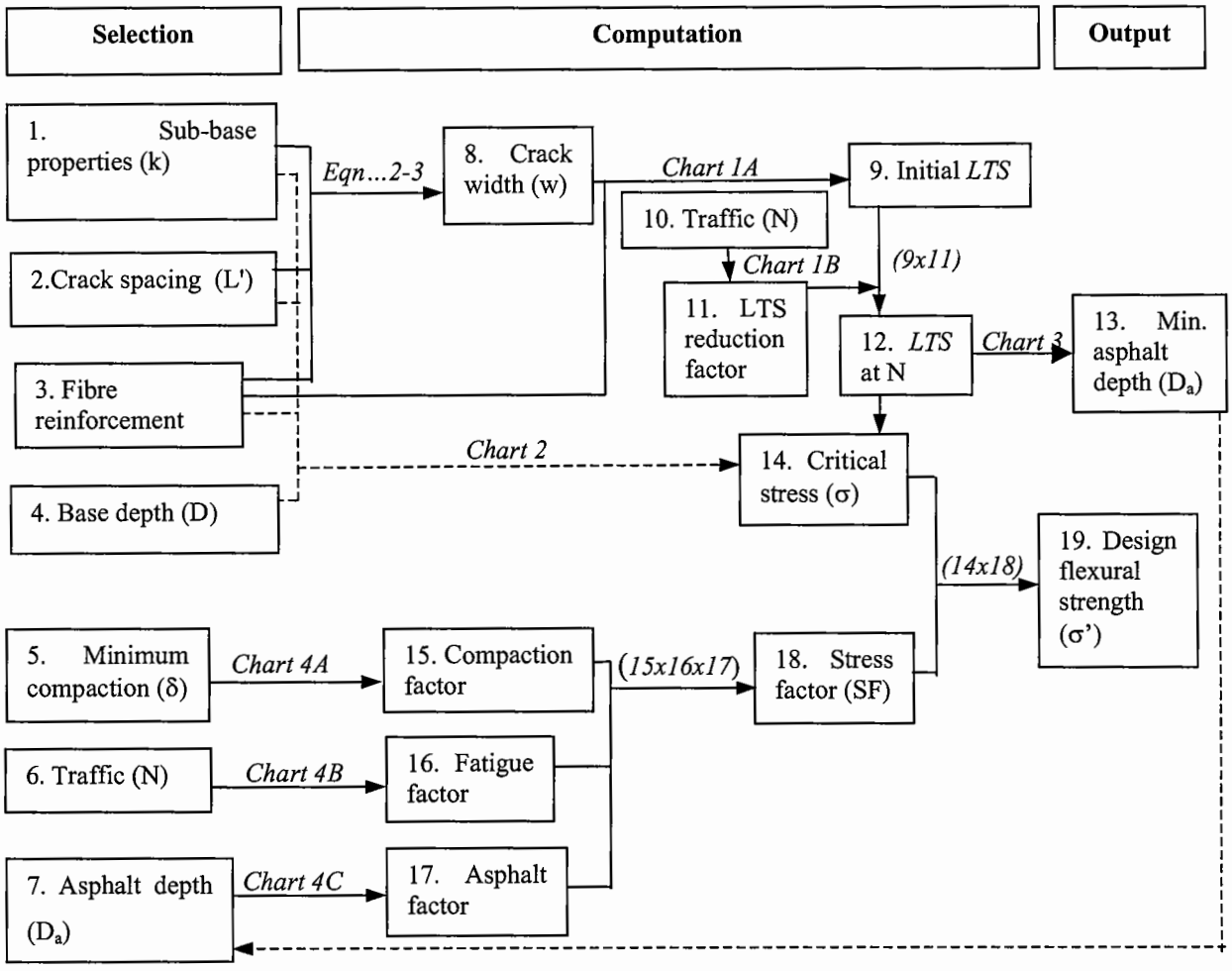

Figure 6-26 FRCBM design method flow chart for flexible composite pavements

6.3.1 Sub-base

The function of the sub-base is primarily to protect the subgrade from excessive strains and to provide a platform upon which the base may be constructed. It is assumed in the analysis that the sub-base layer will be cement bound. The finite element analysis demonstrated that the foundation properties do not affect the stress in the base significantly. However, the vertical deflections on the loaded and unloaded side of the slab are reduced significantly, increasing the overall durability of the crack. Additionally, once a crack has formed, its propagation will be dependent in part on the sub-base properties.

The modulus of subgrade reaction (k) was assumed to be 0.16N/mm^3, a value suitable for CBM sub-base according to (Tayabji and Halpenny 1998). It is derived in the field using the plate bearing test (BSI 1990) which is an accepted method for testing foundations in the United Kingdom (Highways Agency 1994). The modulus of subgrade reaction has found widespread use in the design of heavy duty roller compacted pavements in the United States (Tayabji and Halpenny 1988). A disadvantage of using this parameter is that it only measures the properties relatively close to the surface, and may not take full account of material properties at some depth, although relationships between sub-base values and subgrade values have been determined (Tayabji and Halpenny 1988). Care must therefore be taken not to overestimate this value, in particular on cement treated layers.

6.3.2 Load transfer stiffness

The load transfer stiffness (LTS), as defined in Section 4-7 from the cyclic shear tests, is a function of the crack width (w), fibre type and volume fraction (V_f) and effectiveness of the crack based on the fracture surface. The fracture surface is dependent on the aggregate strength and angularity, and material strength in that this will determine whether the material fractures through or around the aggregate. The design assumes a river gravel aggregate blended with sand as used in the laboratory tests. The expectation might be for a granite to perform better as it is more angular. It is not clear if a limestone aggregate would perform better or not. Whilst the angularity of a limestone should improve load transfer over gravel, the relatively low strength of limestone when compared to gravel may result in a less favourable fracture surface if fracture occurs through the aggregate. More tests are required to verify this.

The relationship between crack width and initial load transfer stiffness for the gravel aggregate CBM based on the laboratory study was shown in Figure 4-57. Deterioration was shown in Figure 4-54. The relationship between crack spacing and crack width was as shown by Eqn...2-3, assuming a mean annual temperature change of 15°C, a coefficient of thermal expansion of 10×10^{-6} per °C for a gravel aggregate and sub-base restraint values of 0.65 for CBM, as discussed in Section 2.3.2.

6.3.3 Critical stress (σ)

The finite element analysis showed that the critical stress was at the base of the cementitious layer directly beneath the wheel load. Analysis using ILLISLAB95 illustrated the relationship between the modulus of subgrade reaction, aggregate interlock factor (*AIF*), base depth and critical stress. Within the range of *AIF* values considered, the stress decreased linearly for a logarithmic increase in aggregate interlock factor (shown in Figure 6-5).

The laboratory study on beam specimens tested in flexure showed that the dynamic elastic stiffness and first crack strength of both CBM and FRCBM were comparable. Also, no tangible improvement in fatigue properties of FRCBM over CBM was observed. However, the laboratory and field investigations have demonstrated conclusively the improvement in FRCBM toughness and effective stiffness post-crack. As elastic analysis was unable to take account of the post-crack ductility of the composite and hence the benefits brought about by fibre reinforcement, plastic analysis was used in the determination of the critical stress.

The analysis considered the ultimate (critical) stress at the centre and edge of the slab. Neither centre nor corner loads were considered appropriate to the analysis, as the critical stress was known to occur near to a transverse crack, and corner loads are uncommon.

It was also assumed that an edge load (i.e. when no load transfer occurred) equated to a load transfer stiffness of 1000MN/m³. Such values were found to occur in unreinforced specimens at a crack width of approximately 0.9mm, as shown in Figure 4-57, and found to be realistic field values based on *in situ* measurements of naturally cracked CBM by Ellis *et al.* (1997), as shown in Table 2-2. The critical stress assuming no load transfer (σ_0) was calculated at the edge of the CBM from Eqn...6-8. The radius of relative stiffness (l), which was previously defined in Eqn...2-1 and R denotes the tyre contact radius. The contribution of the fibres was included following a similar approach to that used in the Design of Ground Bearing Floor Slabs (Concrete Society 1994). The flexural strength ratio ($R_{e,3}$) was discussed in Section 3.5.5.

$$\sigma_0 = \left(\frac{1.7F}{D^2}\right)\left(\frac{l}{l+3R}\right)\left(\frac{100}{100+R_{e,3}}\right) \qquad \textbf{Eqn...6-8}$$

An upper limit of load transfer stiffness was assumed to occur at 30000MN/m³, based on results from the laboratory study, shown in Figure 4-57. This was assumed to occur at a load transfer efficiency of 100%. The critical stress (σ_{100}) was determined in this instance by applying half the stress imposed by the wheel at the edge of the slab:

$$\sigma_{100} = \left(\frac{1.0F}{D^2}\right)\cdot\left(\frac{l}{l+3R}\right)\cdot\left(\frac{100}{100+R_{e,3}}\right) \qquad \textbf{Eqn...6-9}$$

Relationships between load transfer stiffness and critical stress for the unreinforced material (i.e. when $R_{e,3}$=0%) and for a fibre reinforced material with an assumed $R_{e,3}$=50% are shown in Chart 2 for various CBM or FRCBM thicknesses.

6.3.4 Stress Factor (*SF*)

The critical stress is multiplied by the stress factor to determine the design strength of the base. The stress factor is based on three components: percentage density (degree of compaction), traffic (fatigue of the base) and asphalt depth. Increasing the relative density (i.e. compaction factor) and traffic increases the stress factor, whereas increasing the asphalt depth reduces the stress factor. It should be noted that the stress factor is not a safety factor. It merely modifies the critical stress to take account of the three components. If a safety factor is deemed necessary (and for thin asphalt overlays it would), this is to be applied in addition to the stress factor and has the effect of increasing the flexural strength of the material further.

The effect of density was determined from site trials, and fatigue from laboratory tests. Under-compaction was found to reduce the density of the material. At 95% of the maximum density, the material strength was shown to be halved, shown in Figure 5-11, which is consistent with observations by Williams (1986). The relationship used in the design method is shown by Chart 4A.

Fatigue tests on CBM and FRCBM specimens in flexure did not convincingly distinguish between them. Therefore a single design line was used for both materials (Chart 4B). However, laboratory investigations showed that the failure mechanism of the fibre

reinforced material was different to that of the unreinforced material, which might be expected to result in a greater life, as described in Section 4.6.2. This potential improvement warrants further study, but no attempt has been made to include it here.

The influence of the asphalt depth (D_a) on the critical stress was determined using multi-layer linear elastic analysis by computing stresses in the underside of the base layer at various asphalt depths, as shown in Table 6-5, and converted to factors for design (Chart 4C). In the analysis, the asphalt stiffness and Poisson's ratio were assumed to be 4000MPa and 0.35 respectively.

Overlay thickness mm	Stress at overlay depth MPa	Stress factor
0	0.81	1.00
50	0.67	0.83
100	0.57	0.70
150	0.48	0.59

Table 6-5 Determination of stress factor

6.3.5 Design of asphalt thickness

The asphalt thickness was designed assuming a load offset from a transverse crack with a de-bond length of 50mm, as shown in Figure 6-22. The *AIF* was converted to a LTS for this purpose, and shown in Chart 3. The relationship between *LTS* and asphalt depth in Chart 3 indicated the minimum overlay thickness required for the design to be 'safe'. For a design thickness of asphalt that was below the line, transverse base cracks were shown in the theoretical analysis to result in a very high strain.

The asphalt thickness determined from Chart 3 is used to determine the stress factor. It should be noted that an under-estimation of the stress factor (by over-estimating the asphalt thickness) would result in the FRCBM base being under-designed, as the imposed stresses will in fact be greater than those assumed. If a thin asphalt overlay is proposed, it may be wise to assume a thickness of zero to provide a margin of safety.

6.4 Design charts

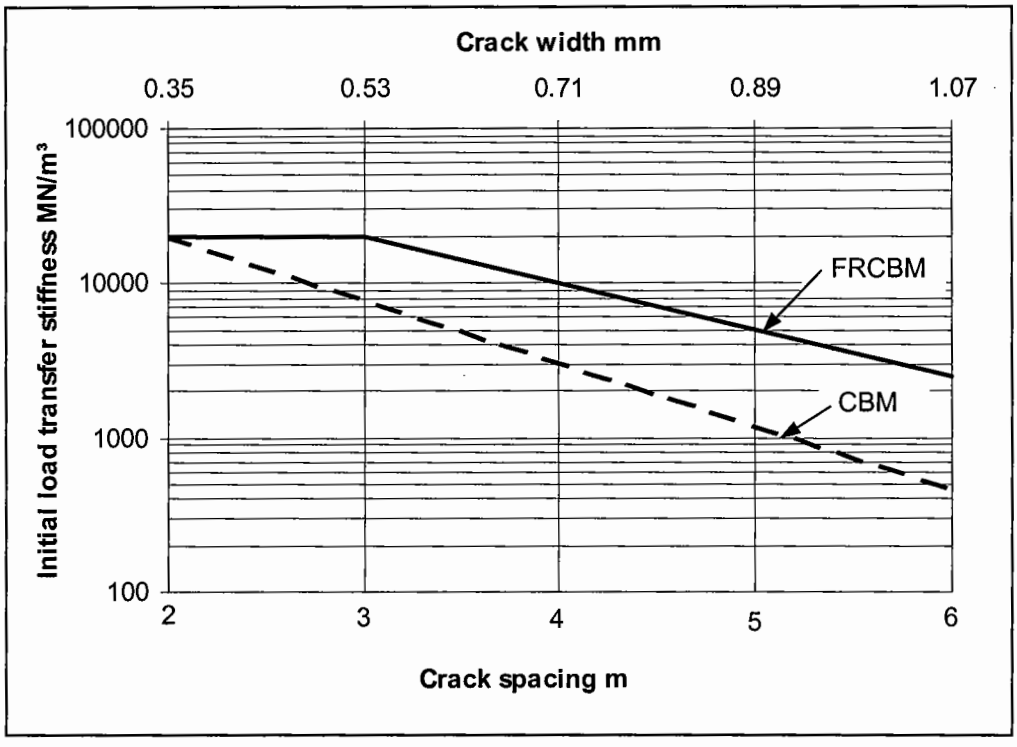

Chart 1A Determination of initial load transfer stiffness based on induced or natural crack spacing

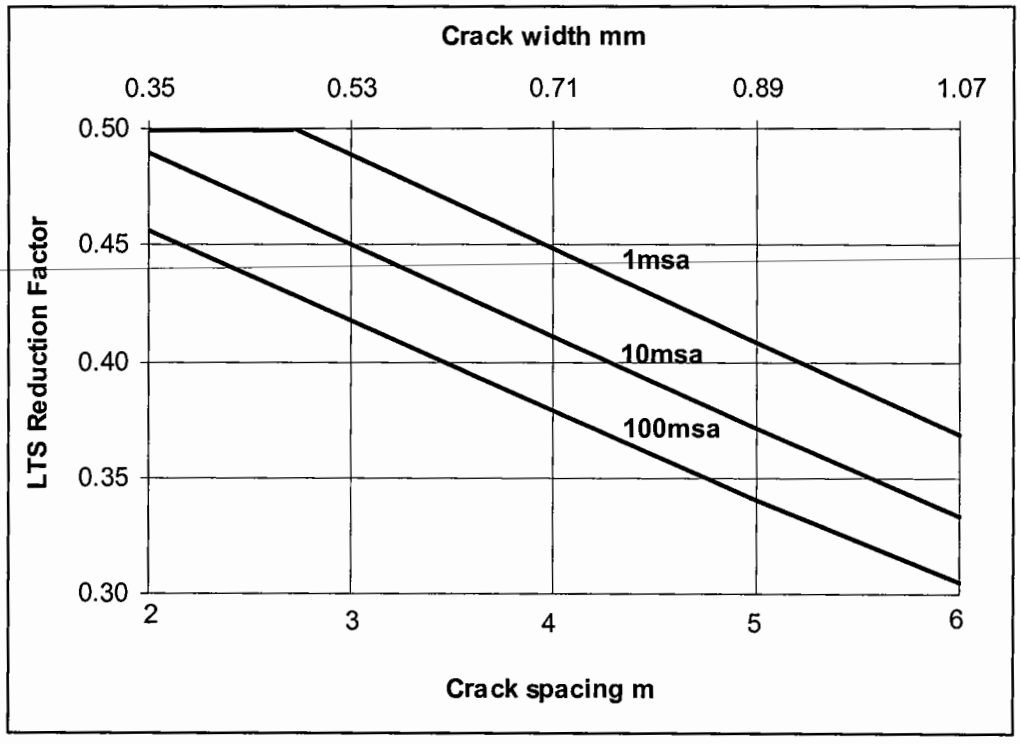

Chart 1B Load transfer stiffness (*LTS*) reduction factor based on induced or natural crack spacing at traffic of 1, 10 and 100msa

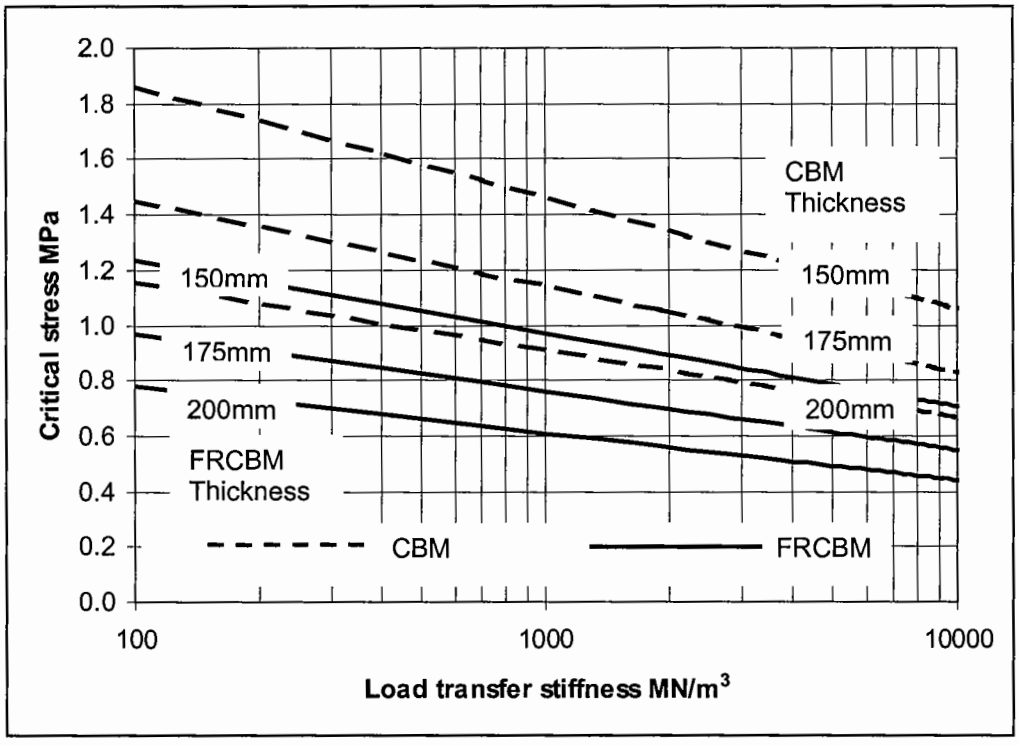

Chart 2 Determination of critical stress based on load transfer stiffness

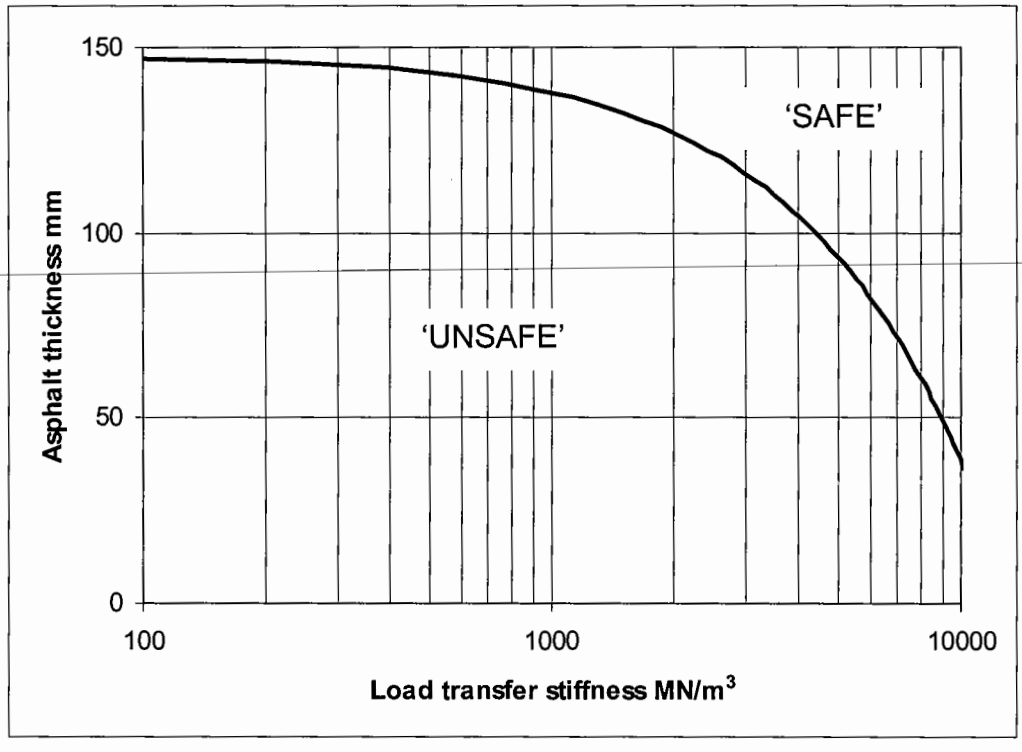

Chart 3 Determination of asphalt depth based on load transfer stiffness to limit 'top-down' cracking

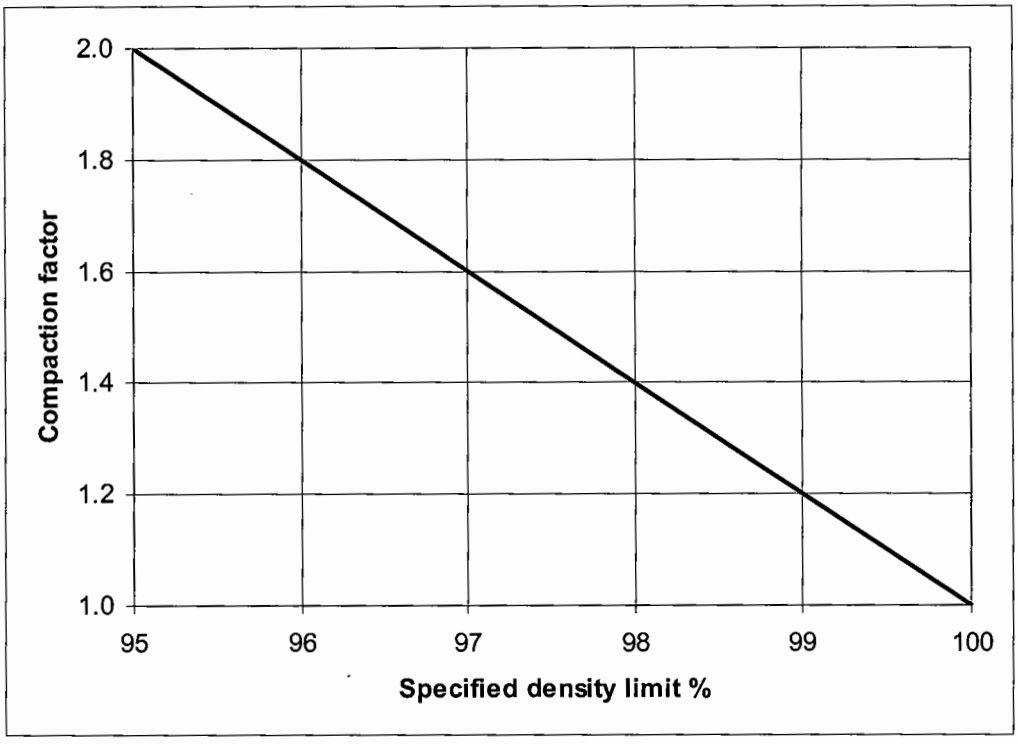

Chart 4A Determination of compaction factor based on density limit

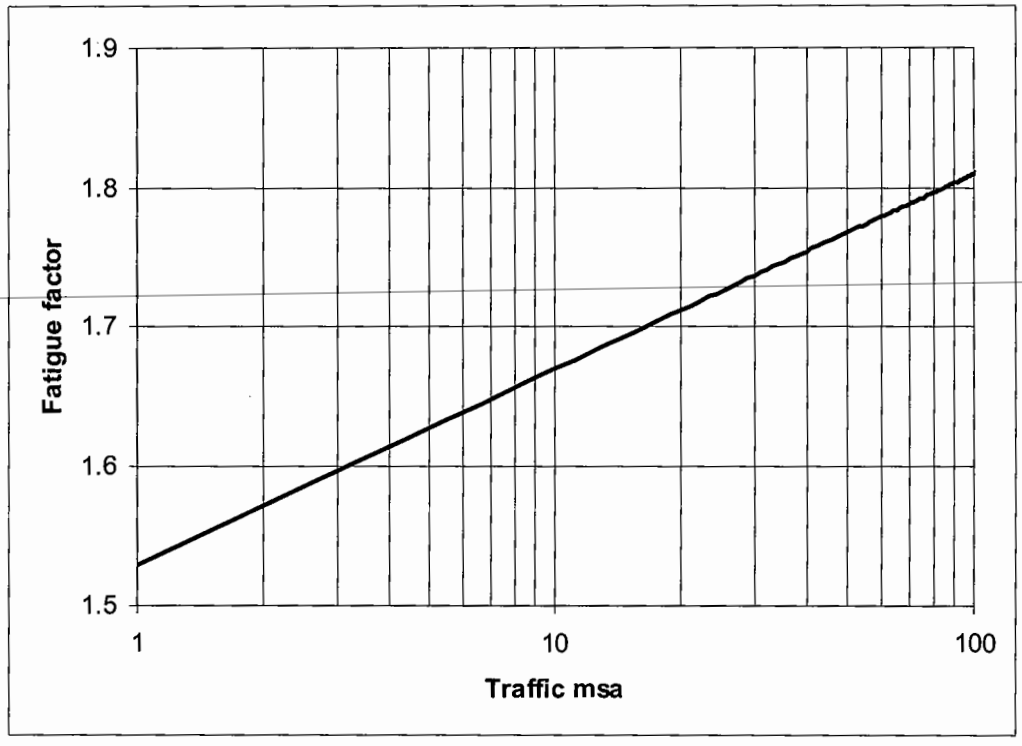

Chart 4B Determination of fatigue factor based on traffic

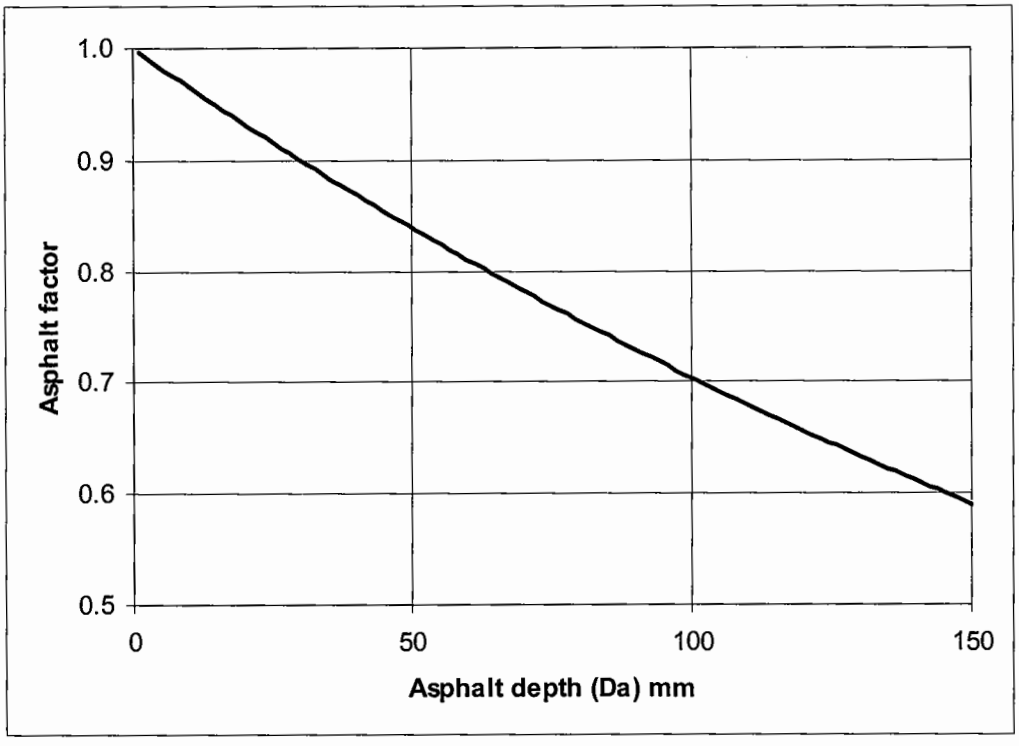

Chart 4C Determination of asphalt factor based on asphalt depth

6.5 Design examples

Using the design charts, comparisons are made between flexible composite pavements using a CBM base with natural and induced cracks, and an FRCBM base with induced cracks, at traffic loads of 1, 10 and 100msa.

A worked example is shown below for a CBM with cracks at 5m spacings, for traffic up to 100msa (Figure 6-27). The assumed natural crack spacing was to ensure an initial load transfer stiffness of 1200MN/m³ (from Chart 1A), on the basis that this was the average load transfer stiffness determined from FWD measurements on naturally cracked CBM in the field, shown in Section 2.4.5. (Note that Section 2.4.5 refers to the aggregate interlock factor, from which the load transfer stiffness may be calculated by dividing this parameter with the layer thickness, as shown in Eqn…6-1).

Design Reference: Worked Example

A	Crack spacing m	5				
B	Fibre reinforced? (Y/N)	N	Chart 1A	C	Initial LTS MN/m^3	1200
D	Traffic msa	100	Chart 1B	E	LTS reduction factor	0.34
			(CxE)	F	LTS at traffic in D MN/m^3	408
G	**Base depth mm**	**200**	Chart 2	H	Critical stress MPa	1.00
			Chart 3	I	**Asphalt depth D_a mm**	**150**
J	Specified density %	95	Chart 4A	M	Compaction factor	2.00
K	Traffic msa	100	Chart 4B	N	Fatigue factor	1.81
L	Asphalt depth D_a mm	150	Chart 4C	O	Asphalt factor	0.59
			(MxNxO)	P	Stress factor	2.14
			(HxP)	Q	**Flexural strength MPa**	**2.14**

Figure 6-27 Worked design example for a naturally cracked CBM base

In the design example, the CBM base thickness is 200mm with a flexural strength of 2.1MPa and an asphalt overlay thickness of 150mm. The calculated strength is designed to limit cracking in the CBM base for the stated traffic. The design CBM strength and thickness is comparable to a high strength CBM used in the United Kingdom for high volume traffic. The asphalt thickness is less than the 200mm currently specified.

There is currently no guide, either in the United Kingdom or overseas, as to the asphalt thicknesses required when induced cracking of the CBM takes place. Recommendations as to design thicknesses and strengths are therefore presented here based on the design charts. Example pavements are shown in Table 6-6 using a CBM base with natural cracks (assumed to be at 5m) and induced crack spacings of 3m, and FRCBM with induced cracks at 3m spacings. The load transfer stiffness of the CBM with induced cracks was assumed to be 5300MN/m^3, which was based on reported data from FWD field measurements, shown in Table 2-2. Traffic loads of 1,10 and 100msa are also compared. The

design criteria in the examples are to limit cracking in the base and 'top-down' reflection cracks through the overlay (through the use of Chart 4A).

Traffic msa	Calculated parameters	[1]CBM (cracked naturally)	[1]CBM + induced cracks at 3m	FRCBM + induced cracks at 3m
1	D mm σ MPa D_a mm	200 1.8 145	180 2.0 125	160 1.7 50
10	D mm σ MPa D_a mm	200 2.0 150	180 2.2 125	160 1.9 50
100	D mm σ MPa D_a mm	200 2.4 150	180 2.3 130	160 2.0 60

[1]Initial *LTS* determined from data based on aggregate interlock factor shown in Table 2-2

Table 6-6 Design parameters of various CBM and FRCBM options

Table 6-6 demonstrates that the increase in traffic between 1msa and 100msa does not significantly effect the flexural strength requirement of the base or the asphalt depth. The accumulation of traffic reduces the load transfer stiffness and increases the fatigue factor, although overall these factors do not greatly influence the design. Induced cracking significantly reduces the overlay depth, demonstrated by the CBM and induced cracking design. The expectation would be for a reduction in the flexural strength due to the increased load transfer stiffness that occurs at closer crack spacings. However, the flexural strength was similar to the naturally cracked CBM as a consequence of the reduced asphalt depth reducing the asphalt factor when compared with higher asphalt depths.

The FRCBM with induced cracks allowed a significant reduction in the asphalt depth and flexural strength. The asphalt depth was reduced due to the increase in load transfer stiffness. The flexural strength was decreased due to the increase in post-crack ductility of the composite allowing an increase in the ultimate bearing capacity of the FRCBM base.

It should be noted that the flexural strength calculated does not include a factor of safety. In flexible composite pavements with deep asphalt overlays a factor of safety may not be required, as the gradual deterioration of the base may not have a significant effect on the

structure. However, for pavements with a thin overlay, a factor of safety may be prudent as the effects of cracking in the base are more likely to be reflected through the surface. On a general note, the design of flexible composite pavements with deep overlays should be driven by the ability of the asphalt to carry load; the design of the CBM, whilst required to carry load, is not required to be of high strength. In designs with a thin asphalt overlay, the CBM and FRCBM govern the design, and must be of sufficient strength to carry the design traffic without cracking under this load. In designing such pavements, more attention must be paid to the design of transverse cracks than on pavements with deep overlays. Additionally, more care is required in the construction of the CBM and FRCBM to achieve finished surface tolerances so that the design thicknesses are achieved, particularly at the pavement edges.

To compare the total cost of the pavement options, the CBM and FRCBM pavements presented in Table 6-5 are estimated based on the unit cost of the materials shown in Table 6-7 (Table 6-8).

Material	Estimated unit cost
CBM	£35/m³
Fibres	£24/m³
Asphalt	£75/m³

Note: £1/m² added for induced cracking. Fibres based on content of 32kg/m³ at a unit cost of 75p/kg.

Table 6-7 Estimated material costs

The costs show that, considering the 100msa design, the naturally cracked CBM costs £18.25/m², the CBM with induced cracks costs £17.05/m² and the FRCBM with induced cracks costs £14.94/m². Therefore, on the basis of the design above, the cost saving using FRCBM over the current flexible composite pavements (naturally cracked) is over 20%. In fact, the current Highways Agency design considers such a pavement to have a CBM 150mm thick with 200mm of asphalt overlay, at a cost of £20.25/m²; the saving over this option would be 30%.

Traffic msa	Cost estimate £/m²		
	CBM (cracked naturally)	CBM + induced cracks at 3m	FRCBM + induced cracks at 3m
1	17.88	16.68	14.19
10	18.25	16.68	14.19
100	18.25	17.05	14.94

Table 6-8 Cost comparison of CBM and FRCBM options

6.6 Discussion and recommendations from design method

1. The HA asphalt design depth is based on field observations of reflective cracking reported in LR1132 (Powell *et al.* 1984). Theoretical expressions developed in this section approximate to these observations. Additional curves demonstrate the theoretical improvement brought about by induced cracking and fibre reinforcement, determined using an FE program to investigate variations in step and rotation at a crack under various load transfer and sub-base properties. Lower values (100mm) and upper values (200mm) were imposed by the HA for practical reasons. The minimum asphalt depth is proposed to be 50mm for FRCBM. A practical consideration in achieving this may be based on surface tolerances. The Specification for Highway Works (Department of Transport 1998) currently demands a roadbase surface tolerance of ±15mm. The current tolerance for an upper roadbase without base-course is ±8mm.

2. Both the current HA method and the FRCBM method accept that some reflective cracking through the overlay at transverse crack locations in the base will occur. The severity of this will be dependent on numerous factors relating to temperature variations and traffic loading. These include; sub-base restraint, CBM aggregate type, crack spacing (natural or induced), CBM strength and asphalt overlay depth. A reduction in the asphalt overlay depth will adversely affect the CBM by increasing the temperature variation, increasing the imposed stress and reducing the load transfer created by the asphalt. The effect will be an increase in asphalt strain. However, induced cracking and fibre reinforcement will reduce significantly the crack movement under any temperature change and increase the load transfer, reducing

the asphalt strains. The relationship between asphalt depth, crack spacing, load transfer and asphalt strain is complex. The FRCBM design method makes some effort to quantify the relationship based on traffic load and thermal movement. Provided the base is designed to withstand the required traffic load, assuming a minimal overlay depth, some reflective cracking may be considered a risk worth taking if the lowest cost design is to be determined in the field.

3. Following the current Highways Agency design, there would be good reason to try to limit the maximum CBM strength (although this is not a specification requirement). Deep asphalt overlays reduce considerably the stress in the CBM. Furthermore, the temperature movement in weakly bound materials is significantly less than higher strength CBM when cracks occur naturally. Induced cracking reduces considerably the movement due to temperature variations. An upper strength limit on this basis is therefore no longer a requirement, which would allow higher base strengths, more able to carry greater loads without requiring the protection offered by the asphalt overlay. The emphasis of flexible composite design may therefore change from a low strength CBM with deep overlay to a high strength CBM with a reduced overlay. Economically, the relative costs of asphalt and bitumen would make this a very attractive alternative. A thinner overlay may provide opportunities to investigate alternative asphalt mixes. Thinner asphalt depths may allow a less stiff asphalt mixture than is currently specified for deeper overlays, and these would be less susceptible to cracking.

4. The recommended pavement would be one with a cement bound sub-base. The depth of this layer may be investigated based on current criteria to protect the subgrade, though it is likely to be in the range of 150mm to 200mm. An FRCBM base of between 150 and 175mm is proposed of flexural strength 3MPa, with induced cracks at 3m spacings. This approximates to 7-day cube strengths of 40MPa for a gravel aggregate and 35MPa for a limestone aggregate based on the results reported in this study. A thin bituminous overlay is proposed, though it should be noted that some hairline reflective cracking should be expected. However, the overlay is a wearing surface, and will be replaced periodically.

6. The initial cost of this type of construction is significantly less than current flexible composite alternatives and it offers the additional benefit of having high residual strength characteristics.

Chapter 7. Conclusions and further work

7.1 Conclusions

Literature review

1. CBM is a graded aggregate or crushed rock, mixed with cement and water, and compacted from the surface using a vibrating roller. As part of a flexible composite pavement, the set material offers good protection to the lower layers, provides a firm platform on which the higher layers may be laid, and is able to carry many traffic loads. It is therefore very suitable as a roadbase. CBM costs significantly less than asphalt and is able to be used with a wide range of aggregate types. Flexible composite pavements can therefore offer environmental, financial and mechanical benefits over alternative types of construction.

2. Despite the benefits of flexible composite construction, reflective cracking continues to be a problem. The current solution for this is to increase the thickness of the asphalt overlay. The asphalt reduces the stress on the CBM and provides insulation from temperature changes. Whilst increasing the asphalt depth is an acceptable solution to limit the occurrences of reflective cracking, the asphalt does not allow the properties of CBM to be used to their full potential and adds to the cost of the pavement. If reflective cracking can be controlled, the potential exists to utilise the CBM as the roadbase with a reduced overlay thickness.

3. Flexible composite designs in the United Kingdom and France aim to limit reflective cracking by specifying an asphalt overlay up to 200mm thick. In such designs, the CBM is relatively weak (when compared to some roller compacted concrete used outside the United Kingdom) and inherent cracking in the CBM is generally not problematic, as any inadequacies of the material are 'masked' by the asphalt overlay. A variation on the composite design in France allows the use of a thinner overlay with the acceptance that reflection cracking will occur. In such designs the cementitious base material is designed not to crack under the action of traffic, and the determination of the critical stresses within this material is more critical than when the thicker overlay is an option.

4. There is currently no method that allows flexible composite pavement thicknesses and strengths to be designed based on the load transfer characteristics of transverse cracks. Potential benefits from recent developments into induced cracking may not therefore be included in designs. This has meant that the cost savings envisaged from induced cracking cannot yet be determined. However, it is expected that the Highways Agency will soon require induced cracking as part of flexible composite construction, although indications are that only a 10mm reduction in asphalt thickness, from the current thickness of 200mm for high volume roads, will be permitted.

5. Fibre reinforcement in concrete has been shown not to significantly increase the ultimate flexural strength compared to unreinforced concrete at low fibre volume fractions. The main benefit is to increase the post-crack ductility. Steel fibres ensure any cracks that develop remain narrow, in effect allowing an increase in the ultimate bearing capacity of the pavement.

Laboratory investigations – strength

6. The compressive cube strength of fibre reinforced specimens was found to be the same as, or less than, that of unreinforced specimens. The lower strengths were attributed to the direction of the fibres with respect to the applied load. Compressive cube strength is therefore not recommended as a performance indicator. It is proposed that the flexural test is more widely adopted for the design of FRCBM pavements, as such a test will not only measure the flexural strength of the material, but will also allow the post-crack ductility (toughness) to be quantified.

7. The flexural strength of CBM was found not to increase using steel fibre reinforcement at fibre volume fractions less than approximately 0.5%. At a fibre volume fraction of 1%, an increase in the ultimate over the first crack flexural strength of up to 30% occurred. In practice, at the fibre volume fractions considered economic, the flexural strength of CBM, and the first crack and ultimate flexural strength of FRCBM, may be considered equal.

8. Considering the relative cost of fibres and cement, increases in flexural strength are more economically achieved by adding cement. Steel fibres are not therefore added to increase the strength of the material.

9. Increases in indirect tensile strength occurred at fibre volume fractions as low as 0.2%. However, specimens exhibited wedging, and the effect of this on the strength is not known. This test is therefore not currently recommended to be used to measure the strength of FRCBM.

Laboratory investigations - toughness

10. The main benefit of fibre reinforcement is to provide a mechanism whereby load can be carried post-crack. The post-crack ductility of the composite is readily demonstrated in instrumented flexure tests, and is measured in terms of toughness. It is the toughness of the composite more than any other parameter that is improved by steel fibre reinforcement.

11. Toughness was measured in this study using the ASTM index I_{50}, the equivalent flexural strength (σ_{eq}) following JSCE-SF4 and the flexural strength ratio ($R_{e,2}$). Toughness parameters are necessary as the performance of the fibres in the composite material is dependent on the relationship between fibre type and volume fraction. Direct measurement is currently the only reliable option for comparing the toughness properties based on fibre type and volume fraction.

12. The applicability of the toughness parameters is summarised:

- The ASTM index was shown to be a measure of toughness independent of material strength and could readily distinguish between fibre type and volume fraction based on this study. However, the determination of the index was not straightforward, and it requires the interpretation of first crack strength and deflection. It also does not obviously lend itself to design.

- The equivalent flexural strength is dependent on material strength, and may therefore only be used to compare fibre types and volume fractions in materials of the same strength. The advantages of this parameter over the ASTM index were that interpretation of first crack was not required and that that the value would be widely understood by engineers.

- The flexural strength ratio was shown not to distinguish between fibre volume fractions where the ultimate strength exceeded the first crack strength. At fibre volume fractions where the first crack and ultimate strength are equal, however, this parameter is a measure of fibre performance independent of material strength, and was shown to provide consistent results with the ASTM index.

13. Tests carried out at 7-day flexural strengths between 1MPa and 4MPa indicated that at the lowest fibre volume fractions tested (0.25%), significant toughness was achieved. The increase in toughness between fibre volume fractions of 0.5% and 1% was less marked.

14. Tests also showed that significant toughness was achieved in the lowest strength mix (7-day compressive cube strength of 10MPa). Steel fibres may therefore be used to reinforce CBM, and the philosophy of utilising the post-crack properties, as is current practice for concrete floor slabs in the United Kingdom, is considered equally valid for FRCBM pavements.

15. Significant toughness occurred in indirect (cylinder-splitting) tensile tests at fibre volume fractions as low as 0.1%. Wedges already noted in regard to the determination of indirect tensile strength meant that the validity of the results was not known. However, it was shown that indirect tensile toughness related well to flexural toughness, and therefore there is merit in pursuing the test. Until the effects of wedging are understood however, it is recommended that flexural testing is used in practice.

Laboratory investigations – dynamic flexure

16. The fatigue endurance of FRCBM appears to be no different from that of CBM, where failure is defined as the first observed crack. For practical purposes therefore, current fatigue relationships may be used for the design of FRCBM pavements.

17. Measurement of the mid-span deflection during the dynamic flexure tests showed that the accumulation of elastic and permanent deflection was found to be dependent on fibre volume fraction. In the fibre reinforced mixes, the elastic and permanent deflection increased progressively throughout the tests. Little increase in deflection occurred in the unreinforced specimens, and failure was sudden. The progressive increase in elastic deflection of the fibre reinforced specimens resulted in a progressive decrease in elastic stiffness. This would result in a progressive reduction in the tensile stress at the underside of a pavement layer. In a pavement, which has a continuous support, this should result in an increase in the life of the material. The increase in deflection will result in the lower layers carrying additional load, and these should be designed taking account of this.

18. A post-crack dynamic flexure test was developed as part of this study. The limited results showed that FRCBM was able to carry dynamic load following cracking of the matrix. The number of cycles the specimens were able to carry post-crack was dependent on the load magnitude and fibre volume fraction. Considering the post-crack improvements already demonstrated from the static tests, and the importance of post-crack dynamic behaviour in any cementitious pavement material, the dynamic behaviour is worthy of further study.

Laboratory investigations – cyclic shear

19. The load transfer stiffness, a measure of the dynamic shear effectiveness of a cracked CBM, was shown to increase significantly when the crack width decreased. Fibre reinforcement increased the load transfer stiffness further, in particular at high crack widths. The deterioration of the specimens was significantly lower in CBM with low crack widths and, for higher crack widths, with fibre reinforcement.

20. Relationships between load transfer stiffness, crack width, fibre reinforcement and crack deterioration were used in the development of a design method.

Field investigations

21. FRCBM may be mixed and laid using equipment and techniques that are currently employed on CBM. So that the fibres are distributed evenly within the mix, fibre dispensing must be controlled. Fibre dispensers are available, which were designed to dispense fibres into a batch. CBM is often mixed continuously, and at a high rate, and modifications may be required to existing dispensers to ensure an even rate of distribution is achieved.

22. The glue used to adhere collated fibres was found not to be able to dissolve in the CBM, possibly due to the low water content of the mixture coupled with the high dispensing rate. Collated fibres allow an increase in the aspect ratio with reduced risk of balling; as the post-crack ductility and toughness has been shown also to improve with increasing aspect ratio, the impetus to find a solution to this problem is likely to be pursued by fibre manufacturers.

23. Effective stiffness measurements using the FWD demonstrated that the fibre reinforced sections had a significantly higher effective stiffness than the unreinforced sections. At the end of the design period it is therefore expected that FRCBM will offer greater protection to the lower layers and continue to be able to carry traffic load. Whilst for the unreinforced material, the expectation might be to replace the CBM roadbase, FRCBM is expected to remain serviceable, requiring only replacement of the asphalt overlay. The whole life cost of a structure using FRCBM will therefore be less than with an unreinforced CBM.

Design method

24. The relative influence of the numerous parameters in a concrete slab with no overlay, in particular the effect of the load transfer characteristics of a transverse crack, were investigated using the finite element programme ILLISLAB95. This allowed values of

critical stress in the FRCBM, and relative deflection and rotation across a transverse crack at various aggregate interlock factors to be made.

25. ILLISLAB95 demonstrated that the critical stress in the FRCBM is significantly reduced by increasing the layer thickness and by increasing the aggregate interlock factor (or the load transfer stiffness). The modulus of subgrade reaction has little influence on the critical stress. However, it does decrease the vertical deflection across a transverse crack, decreasing the rate of deterioration of a transverse crack.

26. An asphalt overlay was included in the design method by using theoretical expressions derived assuming a beam in bending. These allowed relationships between asphalt life, de-bond length and crack characteristics to be determined.

27. The design criteria for the FRCBM method is to avoid traffic induced cracking in the FRCBM roadbase and limit reflective cracking in the asphalt overlay. The design is based on the determination of a critical stress close to a transverse crack. The stress is modified to give a design strength based on crack characteristics, FRCBM thickness, traffic, degree of under-compaction and asphalt overlay thickness. The asphalt thickness is based on a load offset from a crack, and is designed to avoid 'top-down' cracking.

28. Pavement thicknesses determined using the FRCBM design method were compared assuming a naturally cracked CBM, a CBM with induced cracks at 3m spacing and an FRCBM with induced cracks at 3m spacing. The results show that induced cracks in CBM allow an asphalt reduction of 30mm compared to naturally cracked CBM, and the FRCBM allows a further asphalt thickness reduction of 70mm and roadbase thickness reduction of 25mm. Comparative costs show that FRCBM is approximately 20% less expensive than the current flexible composite design.

7.2 Further work

Laboratory investigation

1. The formation of 'wedges' in the indirect tensile (cylinder-splitting) tests was highlighted in this study. The effects of these wedges on the ultimate strength and toughness in indirect tension is unknown. Given the practicality of taking *in situ* cores to assess field performance, the further study of the effects of wedging may provide some confidence in the use of this test. Data from this study showed consistent comparative performance between the indirect tensile and flexural test, therefore there is some hope that the problems outlined may be resolved or explained.

2. The dynamic flexure tests carried out as part of this study suggested that there was no increase in life of FRCBM over CBM from a simply supported test. However, other work on fibre reinforced cementitious materials cited in the text did show a significant difference between the life of such specimens and the unreinforced material. This aspect therefore requires further investigation. As part of this, a common test standard in fatigue would allow researchers to more easily compare the results obtained.

3. A dynamic flexure test to measure post-crack characteristics was developed as part of this study. The results showed that the test is able to relate load level, fibre volume fraction and number of load applications. Given the improvements already demonstrated post-crack from static tests, and considering the in-service dynamic loading imposed on a pavement, this type of test is proposed to be more widely adopted. Data collected may be used to further demonstrate the increased post-crack ductility, and methods should be investigated to enable any benefits to be used in design.

4. Cyclic shear tests carried out as part of this study demonstrated that fibre reinforcement improved the load transfer stiffness across a crack, and therefore the load transfer capability of the material. However, these data were at odds with those reported by Abdel-Maksoud (2000), who found that the fibres in fact resulted in less favourable load transfer. This aspect has significant consequences on the behaviour close to a transverse crack, for both the flexural stress in the material and damaging strain in the asphalt. More extensive research is required in this area, and should be extended to slab size specimens, of the kind used by Colley and Humphrey (1967).

5. The cyclic shear tests in this study were carried out using a gravel aggregate. Given the influence of aggregate type on load transfer (and aggregate size as demonstrated by Abdel-Maksoud 2000), the study of other aggregates is worthwhile. In particular the use of weaker aggregate, which may result in a less favourable fracture surface, should be investigated.

Field investigation

6. There was some indication from the literature review that early age cracking would result in more frequent transverse cracking than in unreinforced concrete. Given benefits of induced cracking (narrower cracks, increased load transfer, less thermal movement), the natural formation of more frequent cracking during hydration may be of interest.

7. The *in situ* measurement of load transfer, using for example an FWD, would allow validation of the design method presented in this study. An extensive study over a period of time would also allow the effects of thermal movement and deterioration on the load transfer to be measured. Data relating to thermal movement are particularly important as it is thought that expansion and contraction of the material contributes to reflective cracking, and fibres theoretically provide a mechanism to resist the tensile stresses generated, thereby maintaining aggregate interlock.

8. This report has presented a design method, including theoretical models to predict the traffic required to cause reflective cracking at various crack load transfer stiffnesses. On-site monitoring and testing of a full scale trial is required to validate the relationship between crack width, load transfer stiffness, asphalt thickness and traffic, to determine if the design method presented is realistic. In particular, this should be carried out at reduced crack widths and thin asphalt overlays, as it is here that there is little site data.

Design

9. A number of points were already raised regarding the design process, and these and others are listed below as areas that could be explored to improve the design of FRCBM pavements.

- Further investigation into the effects of wedging on the indirect tensile strength and toughness is required, to enable in situ verification (i.e. from cores) of the FRCBM properties measured in the laboratory.

- Verification of initial load transfer stiffness, deterioration and thermal effects are required from field measurements.

- The verification of the reflection cracking model is required by some accelerated testing device, such as the pavement test facility or heavy vehicle simulator.

- The relationship between flexural toughness and load transfer stiffness should be investigated further.

References

Abdel-maksoud M.G, Hawkins N and Barenberg E, 1997. *Behaviour of concrete joints under cyclic shear.* ASCE. Frank and Herman, August. pp. 190-204.

Abdel-maksoud M.G, 2000. *Behaviour of concrete joints under cyclic shear.* PhD thesis, The University of Illinois, USA.

ACI Committee 544, 1998. *State-of-the-art report on fiber reinforced concrete, ACI 544.1R-96.* ACI Manual of Concrete Practice part 5, ACI, Detroit, Michigan, pp 544.1R –1 to –66.

ACI Committee 544, 1998. *Guide for specifying, proportioning, mixing, placing and finishing steel fiber reinforced concrete, ACI 544.3R-93.* ACI Manual of Concrete Practice part 5, ACI, Detroit, Michigan, pp 544.3R –1 to –10.

ACI Committee 544, 1998. *Design considerations for steel fiber reinforced concrete, ACI 544.4R-88 (reapproved 1994).* ACI Manual of Concrete Practice part 5, ACI, Detroit, Michigan, pp 544.4R –1 to –18.

American Society for Testing and Methods, 1995. Standard specification for steel fibers for fiber reinforced concrete. ASTM *Annual Book of Standards*, ASTM, Philadelphia, **04.02**. ASTM A 820-85.

American Society for Testing and Methods, 1994. Standard test method for flexural toughness and first-crack strength of fiber-reinforced concrete (using beam with third-point loading). *ASTM Annual Book of Standards*, ASTM, Philadelphia, **04.02**, pp. 509-516. ASTM C 1018-94b.

Balaguru and Shah, 1992. *Fiber reinforced cement composites.* McGraw-Hill, London.

Barnes G.E, 1995. *Soil mechanics principles and practice.* MacMillan Press Ltd, Basingstoke, UK.

Batson G, Ball C, Bailey L, Landers E and Hooks J, 1972. *Flexural fatigue strength of steel fiber reinforced concrete beams*. ACI Journal, Title no.69-64, pp. 673-677.

Beckett D and Humphreys, 1989. *Comparative tests on plain, fabric reinforced and steel fibre reinforced concrete ground slabs*. Report **TP/B/1**, Thames Polytechnic, London.

Bentur A and Mindess S, 1990. *Fiber reinforced cementitious composites*. Elsevier Applied Science.

Bischoff P.H and Valsangkar A.J, 1999. *Assessment of slab-on-grade design and comparison with model slab behaviour*. Source Unknown. pp. 153-158.

Bischoff P.H. Valsangkar A.J. and Irving J., 1997. *A performance evaluation of steel fibre reinforced concrete slabs on grade*. Asia-Pacific Specialty Conference on Fibre Reinforced Concrete, Singapore, August 28-29, pp. 25-32.

Bischoff P.H. Valsangkar A.J. and Irving J., 1998. *Concrete slab-on-grade construction: to reinforce or not*. Annual Conference of the Canadian Society for Civil Engineering, Halifax, Nova Scotia, June 10-13, pp. 309-318.

British Standards Institution, 1983. *Aggregates from natural sources for concrete*. BSI, London. BS 882.

British Standards Institution, 1983. *Determination of compressive cube strength*. BSI, London. BS 1881.

British Standards Institution, 1990. *Determination of particle size distribution*. BSI, Section 9, London. BS 1377: Part 2.

British Standards Institution, 1983. *Method for determination of flexural strength*. BSI, London. BS 1881: Part 118.

British Standards Institution, 1990. *Methods of test for cement-stabilised and lime-stabilised materials*. Stabilised materials for civil engineering purposes, Section 2, London. BS 1924: Part 2.

British Standards Institution, 1990. *Plate bearing test*. BSI, London. BS 1377.

Brown S.F, 1979. *The design of pavements with lean concrete bases*. TRR 725, Transport Research Board, pp51-57.

Buch N, 1994. *Factors affecting load transfer across transverse joints in jointed concrete pavements*. Recent Developments in Concrete Pavement Systems. SP 181-3. pp. 43-64.

Colley B.E and Humphrey H.A, 1967. *Aggregate interlock at joints in concrete pavements*. In *Highway Research Record 189,* HRB, National Research Council, Washington, D.C., pp. 1-18.

Colombier G, 1997. *Cracking in pavements: nature and origin of cracks*. Prevention of reflective cracking in pavements, RILEM Report **18**.

Concrete Society, 1994. *Concrete industrial ground floors – a guide to their design and construction*. Technical Report 34, Slough, UK.

Cornelissen H.A.W and Reinhardt H.W, 1984. *Uniaxial tensile fatigue of concrete under constant amplitude and programme loading*. Magazine of Concrete Research, V.**36**, No.129, pp. 216-227.

Croney D and Croney P, 1991. *The design and performance of road pavements*. McGraw-Hill, Berkshire.

Ellis S.J, Megan M.A and Wilde L.A, 1997. *Construction of full-scale trials to evaluate the performance of induced cracked CBM roadbases*. Transport Research Laboratory, Crowthorne. LR 289.

Ficheroulle B, 1998. Fiber-reinforced roller-compacted concrete (rollfiber) for continuous concrete pavements. *Proc. 8th International Conference on Concrete Pavements*, Lisbon, Theme 3, pp 319-323.

Foulkes M.D, 1988. *Assessment of asphalt materials to relieve reflection cracking of highway surfacings.* PhD Thesis. Plymouth Polytechnic.

Foulkes M.D, and Kennedy C.K, 1986. *The limitations of reflection cracking in flexible pavements containing cement bound layers. Proc. Int. Conf. On Bearing Capacity of Roads and Airfields.* Plymouth, UK.

Galloway J.W, Harding H.M and Raithby K.D, 1979a. *Effects of age on flexural, fatigue and compressive strength of concrete.* Transport and Road Research Laboratory, Crowthorne. LR 865.

Galloway J.W, Harding H.M and Raithby K.D, 1979b. *Effects of moisture changes on flexural and fatigue strength of concrete.* Transport and Road Research Laboratory, Crowthorne. LR 864.

Galloway J.W and Raithby K.D, 1973. *Effects of rate of loading on flexural strength and fatigue performance of concrete.* Transport and Road Research Laboratory, Crowthorne. LR 547.

Grzybowski M and Meyer C, 1993. *Damage accumulation in concrete with and without fiber reinforcement.* ACI Materials Journal. Title no. 90-M60.

Grzybowski M and Shah S.P, 1989. *Model to predict cracking in fibre reinforced concrete due to restrained shrinkage.* Magazine of Concrete Research, V.**41**, No.148, pp. 125-135.

Grzybowski M and Shah S.P, 1990. *Shrinkage cracking of fibre reinforced concrete.* ACI Materials Journal, Title no.87-M16, pp. 138-148.

Hannant D.J, "Fibre cements and fibre concretes," John Wiley and Sons, 1978.

Highways Agency, 1998. *Manual of contract documents for highway works, Specification for Highway Works, Series 1000, volume 1.* TSO, London.

Highways Agency, 1994. *Design Manual for Roads and Bridges, Pavement Design and Maintenance, Structural assessment methods.* Vol. **7**. TSO, London. HD 29/94.

Huang Y.H, 1993. *Pavement analysis and design.* Prentice-Hall, Inc., Englewood Cliffs, New Jersey, USA.

Ioannides A.M and Korovesis G.T, 1990. *Aggregate interlock: pure-shear load transfer mechanism.* Transportation Research Record 1286, TRB, National Research Council, Washington D.C. pp. 14-24.

Japan Concrete Institute, 1983. Method of test for flexural strength and flexural toughness of fiber reinforced concrete. *JCI Standards for Fiber Reinforced Concrete*, pp. 35-36. JCI Standard SF4.

Johnston, C.D., 1982. *Steel fibre reinforced and plain concrete: Factors influencing flexural strength measurement.* ACI Journal, Title no.79-14, pp. 131-138.

Johnston, C.D., 1998. *Toughness of steel fibre reinforced concrete.* Steel fibre concrete US-Sweden joint seminar, Stockholm, pp. 333-359.

Jenq Y.S and Shah S.P, 1986. *Crack propagation in fiber reinforced concrete. Journal of Structural Engineering,* ASCE, **112** (1), January, pp. 19-34.

Jun Z. and Stang H., 1998. *Fatigue performance in flexure of fiber reinforced concrete.* ACI Materials Journal, Title no.95-M7, pp. 58-67.

Kennedy J., 1983. *Cement-bound materials for sub-bases and roadbases.* Cement and Concrete Association, Slough.

Knapton J., 1998. *The structural design of heavy duty pavements*. The Structural Engineer, Vol. **76**, No 8.

Kolias S. and Williams R.I.T., 1978 *Cement bound road materials: strength and elastic properties measured in the laboratory*. Transport and Road Research Laboratory, Crowthorne. SR 344.

Lanu M., 1995. Testing fibre reinforced concrete in some structural applications. Technical Research Centre of Finland, Espoo, Finland. Report no. 237.

Laws V, 1983. *On the mixture rule for strength of fibre reinforced cements*. Journal of Materials Science Letters, Vol. **2**, Buildings Research Establishment, Watford, UK, pp. 527-531.

Lemaitre J, 1996. *A course on damage mechanics.* Second edition, Springer, Berlin.

Li V.C. and Liang E., 1986. *Fracture processes in concrete and fibre-reinforced cementitious composites*. ASCE Journal of Engineering Mechanics, Vol. **12**(6), pp 566-586.

Lim T.Y, Paramasivam P and Lee S.L., 1987. *Analytical model for tensile behaviour of steel-fiber concrete*. ACI Materials Journal, 84-M30, pp 286-298.

Lister N.W, 1972. *Design and performance of cement-bound bases. Journal of the Inst. of Highways Engineers*. February.

Maidl B.R., 1995. *Steel fibre reinforced concrete*. Ernst and Sohn, Berlin.

Mallet G., 1991. *Fatigue of reinforced concrete.* TRRL State of the Art Review, HMSO, London.

Mangat P.S and Gurusamy K, 1987. *Flexural strength of steel fibre-reinforced cement composites*. Journal of Materials Science, **22**(9), pp. 3103-3110.

McCall J.T., 1958. *Probability of fatigue failure of reinforced concrete.* ACI Journal, **55**, pp 233-444.

Megson T.H.G, 1987. *Strength of materials for civil engineers - 2nd Edition.* ISBN 0-7131-3612-X. Hodder and Stoughton Ltd., United Kingdom.

Meyerhof G.G., 1962. *Load carrying capacity of concrete pavements*. Journal of the Soil Mechanics and Foundation Division, *Proc. ASCE.*

Millard S.G and Johnson R.P, 1984. *Shear transfer across cracks in reinforced concrete due to aggregate interlock and to dowel action. Magazine of Concrete Research,* **36** (126), March. pp. 9-21.

Munt K, 1999. *Steel fibre reinforcement in cement bound material.* MEng thesis, School of Civil Engineering, The University of Nottingham (unpublished).

Neville A.M., 1995. *Properties of concrete.* 4th edition, Longman Group Ltd, Essex.

Nanni A., 1988. *Splitting-tension test for steel fibre reinforced concrete.* ACI Materials Journal, Title no.85-M27, July/August. pp229-233.

Nanni A. and Johari A., 1989. *RCC pavement reinforced with steel fibres.* Concrete International, March, pp. 64-69.

Nemegeer D. and Tatnall P.C, 1995. *Measuring toughness characteristics of SFRC – A critical view of ASTM C 1018.* ACI SP-155 Testing of Fibre Reinforced Concrete.

Nunes M.C.M., 1997. *Enabling the use of alternative materials in road construction.* The University of Nottingham, Department of Civil Engineering.

Nunn M.E., 1990. Reflection cracking in composite pavements. *Highways Asphalt 90 Supplement*, **58** (1957), January. pp. 7-11.

Paine K., 1998. *Pre-stressed fibre reinforced concrete.* PhD thesis, The University of Nottingham, School of Civil Engineering.

Parry A.R, Phillips S.J, Potter J.F and Nunn M.E, 1999. *Design and performance of flexible composite road pavements. Proc. Inst. Civ. Engrs. Transp., February.* **135**, pp. 9-16.

Pittman D.W, 1993. *Development of a design procedure for roller-compacted concrete (RCC) pavements.* PhD Dissertation, The University of Texas at Austin.

Powell W.D. Potter J.F. Mayhew H.C. and Nunn M.E., 1984. *The structural design of bituminous roads*. Transport and Road Research Laboratory, Crowthorne. LR 1132.

Raja Z.I and Snyder M.B, 1991. *Factors affecting deterioration of transverse cracks in jointed reinforced concrete pavements.* Transportation Research Record 1307, TRB, National Research Council, Washington. D.C. pp 162-168.

Ramakrishnan V, and Josifek C, 1987. Performance characteristics and flexural fatigue strength of concrete steel fibre composites. *Proc. of the International Symposium on Fibre Reinforced Concrete*, Madras, India, December 1987, pp. 2.73-2.84.

Ramakrishnan V, Oberling G and Tatnall P, 1987. *Flexural fatigue strength of steel fiber reinforced concrete.* ACI Journal, pp. 225-245. SP 105-13.

Romualdi J.P and Batson G.B, 1963. *Behaviour of reinforced concrete beams with closely spaced reinforcement.* ACI Materials Journal, Title no.60-40, **60**(6), pp775-789.

Shahid M.A., 1997. *Improved cement bound base design for flexible composite pavements.* PhD thesis, University of Nottingham.

Shahid M.A., 1996. *Investigation of site trials with controlled cracking of cement bound bases.* University of Nottingham. PGR 96 021.

Shahid M.A and Thom N.H., 1999. Steel fibre reinforcement in cement bound bases. *Proc. Instn Civ. Engrs Transp.,* 129, pp. 34-43.

Sherwood, P. 1993. *Soil-stabilisation with cement and lime*. TRL State-of-the-Art Review HMSO, London.

Silfwerbrand J, 1998. *Ultimate load-carrying capacity of steel fibre reinforced concrete pavements*. Royal Institute of Technology, Department of Structural Engineering, Sweden.

Smith M.R and Collis L., 1993. *Aggregates. Sand, gravel and crushed rock aggregates for construction purposes*. Second edition, The Geological Society, Special Publication No.9, Bath.

Sobhan K, 1997. *Stabilized fiber-reinforced pavement base course with recycled aggregate.* PhD Thesis, Northwest University, Evanston, Illinois.

Swamy R.N, Mangat P.S and Rao C.V.S.K., 1974. *The mechanics of fiber reinforcement of cement matrices*. ACI Publication SP-44, Fiber Reinforced Concrete International Symposium, Ottawa.

Tabatabaie A.M and Barenberg E.J, 1978. *Finite-element analysis of jointed or cracked concrete pavements.* Transportation Research Record 671, TRB, National Research Council, Washington. D.C. pp 11-19.

Tayabji S.D and Halpenny D.J, 1988. *Thickness design of roller-compacted pavements.* Transportation Research Record 1136, TRB, National Research Council, Washington. D.C. pp 23-32.

The University of Nottingham, 1998. *Bituminous pavements: Materials, design and evaluation*. Department of Civil Engineering, Residential course lecture notes, March.

Thomlinson J, 1940. *Temperature variations and consequent stresses produced by daily and seasonal temperature cycles in concrete slabs.* Concrete and Constructional Engineering. **XXXV**. pp. 298-360.

Thompson I, 2000. *Dynamic testing and fatigue properties of fibre reinforced cement bound material.* MSc thesis, Construction Engineering, Design and Management, Department of Civil and Structural Engineering, The Nottingham Trent University.

Vermeeren J, 1999. *Site trial – UK.* Faxed communication, 13 September 1999.

Weiler B and Grosse C, 1996. *Pullout behaviour of fibers in steel fiber reinforced concrete.* (unknown source), pp. 116-127.

Williams R.I.T, 1986. *Cement treated pavements: Materials, design and construction.* Elsevier Applied Science, UK.

Westergaard H.M, 1926. *Stresses in concrete pavements computed by theoretical analysis.* Public Roads, **7**, p.25.

Westergaard H.M, 1927. *Analysis of the stresses in concrete roads caused by variations in temperature.* Public Roads, **8** (3), May, pp. 54-60.

Appendix A

Mix ref.	[1]Cement content (Water content) %	Fibre type	Fibre volume fraction %	[2]Test date	7-day static flexure tests										7-day compressive cube tests	
					Density kg/m^3	σ_{cr} MPa	σ_u MPa	ASTM toughness indices				T_{JSCE} kNmm	σ_{eq} MPa	$R_{e,2}$ %	Density kg/m^3	Cube strength MPa
								I_5	I_{10}	I_{20}	I_{50}					
G1	4.5 (5.0)	-	-	25.3.99	2344	1.2	1.2	-	-	9.4	13.2	0.6	0.09	8	2380	9.4
					2347	1.3	1.4	-	-	10.6	16.7	0.8	0.12	9	2371	9.6
					2338	1.5	1.5	-	-	9.9	13.8	0.6	0.09	6	2359	8.6
				Average	*2343*	*1.3*	*1.4*	-	-	*10.0*	*14.6*	*0.7*	*0.10*	*7*	*2370*	*9.2*
				St. Dev.	5	0.2	0.2	-	-	0.6	1.9	0.1	0	1.3	11	0.5
				CoV	0.2	11.5	11.2	-	-	6.0	12.8	17.3	17.3	17.7	0.4	5.8
				95% Con	5	0.2	0.2	-	-	0.7	2.1	0.1	0	1.5	12	0.6
G2	6.0 (5.2)	-	-	19.2.98	2338	2.2	2.2	2.6	4.0	6.3	9.2	1.4	0.21	10	2389	18.2
					2338	2.1	2.1	3.9	5.7	7.8	9.8	1.0	0.15	7	2366	15.8
					2336	2.3	2.3	3.4	-	-	-	-	-	-	2390	16.6
				Average	*2337*	*2.2*	*2.2*	*3.3*	*4.9*	*7.1*	*9.5*	*1.2*	*0.18*	*8*	*2382*	*16.9*
				St. Dev.	1	0.1	0.1	0.7	1.2	1.1	0.4	0.3	0.1	5.0	14	1.2
				CoV	0	4.5	4.5	19.9	24.8	15.0	4.5	23.6	60.1	60.7	0.6	7.2
				95% Con	1	0.1	0.1	0.7	1.7	1.5	0.6	0.4	0.1	6.9	15	1.4
G3	8.5 (5.2)	-	-	27.5.98	2402	2.9	2.9	3.4	5.3	7.3	9.0	1.2	0.18	6	2422	31.8
					2400	3.0	3.0	3.5	4.9	6.5	8.1	1.5	0.23	8	2415	34.6
					2391	2.5	2.5	3.2	4.7	6.5	7.9	1.2	0.18	7	2413	32.2
				Average	*2398*	*2.8*	*2.8*	*3.4*	*5.0*	*6.8*	*8.3*	*1.3*	*0.20*	*7*	*2417*	*32.9*
				St. Dev.	6	0.3	0.3	0.2	0.3	0.5	0.6	0.2	0	0.7	5	1.5
				CoV	0.2	9.4	9.4	4.5	6.2	6.8	7.0	13.3	13.3	9.7	0.2	4.6
				95% Con	7	0.3	0.3	0.2	0.3	0.5	0.7	0.2	0	0.8	5	1.7

Notes: [1]Cement content by mass of dry aggregate; water content by mass of dry aggregate, cement and fibres. [2]St.dev. = Standard deviation, CoV = Coefficient of variability, 95% Con = ±95% confidence limit.

A1 Table of 7-day flexural and compressive cube test results – Gravel aggregate - Control specimens

Mix ref.	[1]Cement content (Water content) %	Fibre type	Fibre volume fraction %	[2]Test date	7-day static flexure tests										7-day compressive cube tests	
					Density kg/m^3	σ_{cr} MPa	σ_u MPa	ASTM toughness indices				T_{JSCE} kNmm	σ_{eq} MPa	$R_{e,2}$ %	Density kg/m^3	Cube strength MPa
								I_5	I_{10}	I_{20}	I_{50}					
G1	4.5 (5.0)	65/60	0.5	29.6.99	2373	1.3	1.4	2.5	5.0	11.3	33.6	7.4	1.1	79	2405	12.0
					2371	1.4	1.5	4.8	9.4	18.7	46.6	8.4	1.3	84	2408	12.9
					2380	1.4	1.5	5.0	10.0	19.7	49.0	8.2	1.2	82	2410	13.7
				Average	*2375*	*1.4*	*1.5*	*4.1*	*8.1*	*16.6*	*43.1*	*8.0*	*1.2*	*82*	*2408*	*12.9*
				St. Dev.	5	0.1	0.1	1.4	2.7	4.6	8.3	0.5	0.1	2.4	3	0.9
				CoV	0.2	4.2	3.9	33.9	33.6	27.7	19.2	6.6	6.6	2.9	0.1	6.6
				95% Con	5	0.1	0.1	1.6	3.8	5.2	9.4	0.6	0.1	2.7	3	1.0
G2	6.0 (5.2)	65/60	0.5	27.3.98	2384	1.8	1.9	3.7	6.5	12.2	28.3	11.2	1.7	88	2397	18.6
					2404	2.0	2.1	3.9	6.6	11.7	28.5	12.9	1.9	92	2397	17.6
					2378	1.9	1.9	3.6	6.5	11.8	25.7	8.2	1.2	65	2386	17.0
				Average	*2389*	*1.9*	*2.0*	*3.7*	*6.5*	*11.9*	*27.5*	*10.8*	*1.6*	*82*	*2393*	*17.7*
				St. Dev.	14	0.1	0.1	0.2	0.1	0.3	1.6	2.4	0.4	14.9	6	0.8
				CoV	0.6	5.3	5.9	4.1	0.9	2.2	5.7	22.1	22.1	18.1	0.3	4.6
				95% Con	15	0.1	0.1	0.2	0.1	0.3	1.8	2.7	0.4	16.8	7	0.9
G3	8.5 (5.2)	65/60	0.5	17.9.98	2424	3.3	4.3	4.4	9.3	19.9	41.6	16.6	2.5	58	2422	27.4
					2428	3.2	3.2	3.7	6.7	12.3	27.2	11.8	1.8	55	2417	25.3
					2433	3.5	3.5	3.8	7.2	13.3	30.3	15.4	2.3	66	2419	24.9
				Average	*2428*	*3.3*	*3.7*	*4.0*	*7.7*	*15.2*	*33.0*	*14.6*	*2.2*	*60*	*2419*	*25.9*
				St. Dev.	5	0.2	0.6	0.4	1.4	4.1	7.6	2.5	0.4	5.6	3	1.3
				CoV	0.2	4.6	15.5	9.5	17.8	27.2	22.9	17.1	17.1	9.3	0.1	5.2
				95% Con	5	0.2	0.6	0.4	1.6	4.7	8.6	2.8	0.4	6.3	3	1.5

Notes: [1]Cement content by mass of dry aggregate; water content by mass of dry aggregate, cement and fibres. [2]St.dev. = Standard deviation, CoV = Coefficient of variability, 95% Con = ±95% confidence limit.

A2 Table of 7-day flexural and compressive cube test results – Gravel aggregate - Fibre 65/60 at a volume fraction of 0.5%

Mix ref.	[1]Cement content (Water content) %	Fibre type	Fibre volume fraction %	[2]Test date	7-day static flexure tests										7-day compressive cube tests	
					Density kg/m^3	σ_{cr} MPa	σ_u MPa	ASTM toughness indices				T_{JSCE} kNmm	σ_{eq} MPa	$R_{e,2}$ %	Density kg/m^3	Cube strength MPa
								I_5	I_{10}	I_{20}	I_{50}					
G2	6.0 (5.2)	65/35	0.5	27.2.98	2355	2.2	2.2	4.9	9.4	17.8	44.2	13.7	2.1	93	2402	17.2
					2360	2.0	2.0	5.1	9.2	17.8	43.9	11.1	1.7	83	2388	15.7
					2343	2.1	2.1	3.9	6.7	11.9	27.4	9.2	1.4	66	2400	17.9
				Average	*2353*	*2.1*	*2.1*	*4.6*	*8.4*	*15.8*	*38.5*	*11.3*	*1.7*	*81*	*2397*	*16.9*
				St. Dev.	9	0.1	0.1	0.6	1.5	3.4	9.6	2.3	0.3	14.0	8	1.1
				CoV	0.4	4.8	4.8	13.9	17.8	21.5	25.0	19.9	19.9	17.3	0.3	6.6
				95% Con	10	0.1	0.1	0.7	1.7	3.9	10.9	2.6	0.4	15.9	9	1.3
G2	6.0 (5.2)	45/50	0.5	13.3.98	2329	2.1	2.1	3.4	5.9	9.8	22.8	7.2	1.1	51	2405	16.5
					2341	2.2	2.2	3.5	6.2	11.2	23.5	7.5	1.1	51	2391	15.4
					2344	2.3	2.3	4.7	8.5	15.7	35.1	8.5	1.3	55	2389	15.0
				Average	*2338*	*2.2*	*2.1*	*3.9*	*6.9*	*12.2*	*27.1*	*7.7*	*1.2*	*53*	*2395*	*15.6*
				St. Dev.	8	0.1	0.1	0.7	1.4	3.1	6.9	0.7	0.1	2.4	9	0.8
				CoV	0.3	4.5	4.5	18.7	20.7	25.2	25.5	8.8	8.8	4.6	0.4	5.0
				95% Con	9	0.1	0.1	0.8	1.6	3.5	7.8	0.8	0.1	2.7	10	0.9

Notes: [1]Cement content by mass of dry aggregate; water content by mass of dry aggregate, cement and fibres. [2]St.dev. = Standard deviation, CoV = Coefficient of variability, 95% Con = ±95% confidence limit.

A3 Table of 7-day flexural and compressive cube test results – Gravel aggregate - Fibres 65/35 and 45/50 at a volume fraction of 0.5%

Mix ref.	[1]Cement content (Water content) %	Fibre type	Fibre volume fraction %	[2]Test date	7-day static flexure tests										7-day compressive cube tests	
					Density kg/m^3	σ_{cr} MPa	σ_u MPa	ASTM toughness indices				T_{JSCE} kNmm	σ_{eq} MPa	$R_{e,2}$ %	Density kg/m^3	Cube strength MPa
								I_5	I_{10}	I_{20}	I_{50}					
G1	4.5 (5.0)	65/60	1.0	8.6.99	2372	1.3	1.5	-	-	19.1	43.5	7.4	1.1	74	2407	8.6
					2376	1.5	1.9	-	-	21.2	55.1	10.9	1.6	86	2416	9.0
					2420	1.5	1.9	-	-	19.8	51.5	10.2	1.5	81	2390	10.0
				Average	*2389*	*1.4*	*1.8*	-	-	*20.0*	*50.0*	*9.5*	*1.4*	*81*	*2404*	*9.2*
				St. Dev.	27	0.1	0.2	-	-	1.1	5.9	1.9	0.3	6.0	13	0.7
				CoV	1.1	8.1	13.1	-	-	5.3	11.9	19.5	19.5	7.5	0.5	7.8
				95% Con	30	0.1	0.3	-	-	1.2	6.7	2.1	0.3	6.8	15	0.8
G2	6.0 (5.2)	65/60	1.0	2.4.98	2390	2.3	2.9	4.4	8.1	16.7	42.6	18.5	2.8	96	2414	17.4
					2389	3.0	3.0	3.5	7.3	13.9	33.1	17.2	2.6	86	2405	18.2
					2379	2.9	2.9	4.8	9.6	20.0	46.1	17.3	2.6	89	2413	18.2
				Average	*2386*	*2.7*	*2.9*	*4.2*	*8.3*	*16.9*	*40.6*	*17.7*	*2.7*	*90*	*2411*	*17.9*
				St. Dev.	6	0.4	0.1	0.7	1.2	3.1	6.7	0.7	0.1	4.9	5	0.5
				CoV	0.3	13.9	2.0	15.7	14.0	18.1	16.6	4.1	4.1	5.4	0.2	2.6
				95% Con	7	0.4	0.1	0.8	1.3	3.5	7.6	0.8	0.1	5.6	6	0.5

Notes: [1]Cement content by mass of dry aggregate; water content by mass of dry aggregate, cement and fibres. [2]St.dev. = Standard deviation, CoV = Coefficient of variability, 95% Con = ±95% confidence limit.

A4 Table of 7-day flexural and compressive cube test results – Gravel aggregate - Fibre 65/60 at a volume fraction of 1.0%

Mix ref.	[1]Cement content (Water content) %	Fibre type	Fibre volume fraction %	[2]Test date	7-day static flexure tests										7-day compressive cube tests	
					Density kg/m^3	σ_{cr} MPa	σ_u MPa	ASTM toughness indices				T_{JSCE} kNmm	σ_{eq} MPa	$R_{e,2}$ %	Density kg/m^3	Cube strength MPa
								I_5	I_{10}	I_{20}	I_{50}					
G2	6.0 (5.2)	65/35	1.0	5.3.98	2381	2.3	2.8	5.4	11.4	23.5	57.0	14.9	2.2	80	2398	17.0
					2386	2.4	2.9	4.3	8.9	18.4	48.5	16.8	2.5	87	2412	16.0
					2379	2.1	2.1	3.8	6.5	11.1	25.6	7.2	1.1	51	2417	15.8
				Average	*2382*	*2.3*	*2.6*	*4.5*	*8.9*	*17.7*	*43.7*	*13.0*	*1.9*	*75*	*2409*	*16.3*
				St. Dev.	4	0.2	0.4	0.8	2.5	6.2	16.2	5.1	0.8	18.8	10	0.6
				CoV	0.2	6.7	16.8	18.2	27.4	35.3	37.2	39.2	39.2	25.1	0.4	4.0
				95% Con	4	0.2	0.5	0.9	2.8	7.1	18.4	5.8	0.9	21.2	11	0.7
G2	6.0 (5.2)	45/50	1.0	19.3.98	2356	2.3	2.7	4.1	8.2	17.0	42.3	11.6	1.7	64	2411	17.9
					2366	2.3	2.3	3.2	6.0	11.3	26.2	10.6	1.6	69	2396	17.8
					2366	2.3	2.3	3.2	6.0	10.9	24.2	10.8	1.6	70	2401	17.9
				Average	*2363*	*2.3*	*2.4*	*3.5*	*6.7*	*13.1*	*30.9*	*11.0*	*1.7*	*68*	*2403*	*17.9*
				St. Dev.	6	0	0.2	0.5	1.3	3.4	9.9	0.5	0.1	3.2	8	0.1
				CoV	0.2	0.3	9.5	14.8	18.9	26.1	32.1	4.8	4.8	4.6	0.3	0.3
				95% Con	7	0	0.3	0.6	1.4	3.9	11.2	0.6	0.1	3.6	9	0.1

Notes: [1]Cement content by mass of dry aggregate; water content by mass of dry aggregate, cement and fibres. [2]St.dev. = Standard deviation, CoV = Coefficient of variability, 95% Con = ±95% confidence limit.

A5 Table of 7-day flexural and compressive cube test results – Gravel aggregate - Fibres 65/35 and 45/50 at a volume fraction of 1.0%

Mix ref.	[1]Cement content (Water content) %	Fibre type	Fibre volume fraction %	[2]Test date	7-day static flexure tests										7-day compressive cube tests	
					Density kg/m^3	σ_{cr} MPa	σ_u MPa	ASTM toughness indices				T_{JSCE} kNmm	σ_{eq} MPa	$R_{e,2}$ %	Density kg/m^3	Cube strength MPa
								I_5	I_{10}	I_{20}	I_{50}					
L1	3.5 (4.5)	65/60	0.5	5.3.98	2487	2.1	2.4	4.5	9.0	18.0	42.5	13.4	2.0	83	2489	17.7
					2489	2.3	2.4	3.7	6.2	11.0	23.0	8.8	1.3	54	2479	17.6
					2466	2.3	2.3	4.3	7.4	13.1	28.4	9.9	1.5	66	2477	18.6
				Average	*2481*	*2.2*	*2.4*	*4.2*	*7.5*	*14.0*	*31.3*	*10.7*	*1.6*	*68*	*2482*	*18.0*
				St. Dev.	13	0.1	0.1	0.4	1.4	3.6	10.1	2.4	0.4	14	5.2	0.4
				CoV	0.5	3.6	4.4	10.0	18.6	25.6	32.2	22.4	22.4	21.1	0.3	3.0
				95% Con	14	0.1	0.1	0.5	1.6	4.1	11.4	2.7	0.4	16	5.9	0.5
L2	4.5 (4.5)	65/60	0.5	19.3.98	2497	3.6	3.6	4.8	7.9	13.4	32.9	18.2	2.7	75	2480	23.7
					2485	3.5	3.5	3.8	6.3	11.1	24.8	13.0	2.0	57	2484	23.4
					2491	3.6	3.9	4.8	9.4	18.4	45.5	21.2	3.2	82	2484	29.4
				Average	2491	*3.6*	*3.7*	*4.5*	*7.9*	*14.3*	*34.4*	*17.5*	*2.6*	*71*	*2483*	*25.5*
				St. Dev.	6	0.1	0.2	0.6	1.6	3.7	10.4	4.1	0.6	13	1.9	2.8
				CoV	0.2	2.8	5.8	12.9	19.7	26.1	30.3	23.8	23.8	18.6	0.1	13.0
				95% Con	7	0.1	0.2	0.7	1.8	4.2	11.8	4.7	0.7	15	2.1	3.1

Notes: [1]Cement content by mass of dry aggregate; water content by mass of dry aggregate, cement and fibres. [2]St.dev. = Standard deviation, CoV = Coefficient of variability, 95% Con = ±95% confidence limit.

A6 Table of 7-day flexural and compressive cube test results – Limestone aggregate - Fibre 65/60 at a volume fraction of 0.5%

Mix ref.	[1]Cement content (Water content) %	Fibre type	Fibre volume fraction %	[2]Test date	7-day static flexure tests										7-day compressive cube tests	
					Density kg/m^3	σ_{cr} MPa	σ_u MPa	ASTM toughness indices				T_{JSCE} kNmm	σ_{eq} MPa	$R_{e,2}$ %	Density kg/m^3	Cube strength MPa
								I_5	I_{10}	I_{20}	I_{50}					
L3	5.5 (4.5)	65/60	Control	5.3.98	2470	4.4	4.4	2.8	3.6	4.3	4.9	1.4	0.2	5	2504	38.4
					2457	4.5	4.5	2.8	3.6	4.3	4.9	1.4	0.2	5	2509	39.2
					2470	4.2	4.2	2.8	3.7	4.7	5.3	1.5	0.2	5	2513	39.1
				Average	2466	4.4	4.4	2.8	3.6	4.4	5.0	1.4	0.2	5	2509	38.9
				St. Dev.	8	0.1	0.1	0	0.1	0.2	0.2	0	0	0.2	3.7	0.4
				CoV	0.3	3.0	3.0	0	1.6	5.2	4.6	1.6	1.6	4.7	0.2	1.0
				95% Con	8	0.1	0.1	0	0.1	0.3	0.3	0	0	0.3	4.2	0.4
L3	5.5 (4.5)	65/60	0.25	5.3.98	2487	4.4	4.4	3.6	5.3	8.3	15.8	9.7	1.5	33	2483	29.5
					2485	4.5	4.5	3.5	5.4	9.6	24.0	16.5	2.5	55	2495	29.9
					2492	4.7	4.7	3.3	5.1	7.7	14.2	8.7	1.3	28	2496	29.1
				Average	2488	4.5	4.5	3.5	5.3	8.5	18.0	11.6	1.7	39	2491	29.5
				St. Dev.	4	0.1	0.1	0.2	0.2	1.0	5.3	4.2	0.6	14	5.9	0.3
				CoV	0.1	2.3	2.3	4.4	2.9	11.4	29.2	36.5	36.5	36.8	0.3	1.0
				95% Con	4	0.1	0.1	0.2	0.2	1.1	5.9	4.8	0.7	16	6.7	0.4
L3	5.5 (4.5)	65/60	0.5	19.3.98	2500	4.9	4.9	5.4	10.6	21.2	49.6	27.1	4.1	83	2513	34.8
					2496	4.5	4.7	5.0	10.5	20.5	53.0	30.0	4.5	95	2497	32.8
					2499	4.8	5.2	6.0	11.5	24.0	54.5	30.5	4.6	88	2502	34.9
				Average	2498	4.7	5.0	5.5	10.9	21.9	52.4	29.2	4.4	89	2504	34.2
				St. Dev.	2	0.2	0.2	0.5	0.6	1.9	2.5	1.8	0.3	6	6.7	1.0
				CoV	0.1	4.6	5.0	9.2	5.1	8.5	4.8	6.3	6.3	6.7	3.0	4.0
				95% Con	2	0.2	0.2	0.6	0.6	2.1	2.8	2.1	0.3	7	7.6	1.1
L3	5.5 (4.5)	65/60	1.0	19.3.98	2521	5.4	5.9	5.0	8.3	18.0	41.0	31.0	4.7	79	2517	32.8
					2524	4.9	6.8	6.3	13.7	25.7	65.7	39.4	5.9	86	2522	32.4
					2517	3.9	4.9	5.2	10.6	22.0	59.0	30.2	4.5	92	2504	27.4
				Average	2521	4.7	5.9	5.5	10.9	21.9	55.2	33.5	5.0	86	2514	30.9
				St. Dev.	4	0.8	1.0	0.7	2.7	3.9	12.8	5.1	0.8	7	7.6	2.5
				CoV	0.1	16.2	16.3	12.7	24.9	17.6	23.1	15.2	15.2	7.8	0.4	10.0
				95% Con	4	0.9	1.1	0.8	3.1	4.4	14.5	5.8	0.9	8	8.6	2.8

Notes: [1]Cement content by mass of dry aggregate; water content by mass of dry aggregate, cement and fibres. [2]St.dev. = Standard deviation, CoV = Coefficient of variability, 95% Con = ±95% confidence limit.

A7 Table of 7-day flexural and compressive cube test results – Limestone aggregate - Fibre 65/60 at various volume fractions

Appendix B

XX01 General

1 FRCBM shall comply with Series 700 and 1000 of the Specification for Highway Works together with the Clauses listed below.

XX02 Excavation, trimming and reinstatement of existing surfaces

1 The Contractor shall only excavate pits, trenches or other openings through the FRCBM with the prior approval of the Engineer. The reinstatement of such areas shall be as specified under sub-Clause 1035.

XX03 Grades of concrete and constituent materials for FRCBM

1 The target water content shall be the minimum water content required to provide the workability for compaction of the fibre reinforced material to the required minimum density, as determined by trial mixes.

2 The nominal size of coarse aggregate shall not exceed 20mm. The aggregate grading shall comply with Table 10/11.

3 The compressive cube strength and compaction requirements shall meet the requirements of Appendix 7/1 and comply with Table 10/8, and be carried out on specimens containing fibres at the specified volume fraction.

4 The flexural strength and equivalent flexural strength, measured as the mean less one standard deviation from five tests, shall exceed the value stated in Appendix 7/1. The flexural strength parameters shall be measured in accordance with JSCE SF-4 (Japan Society of Civil Engineers, Concrete Library International Number 3, JSCE, June 1984).

5 Fibres shall be cold drawn wire with a minimum mean tensile strength of 1000MPa complying with Table X/X below, as detailed in Table 1 of the Dutch National Assessment Guideline 5061 Steel Fibres for Application in Concrete and Mortars.

Property	Deviation of the individual value relative to the supplied value	Deviation of the average value relative to the supplied value
Length l_f	± 10%	± 1.5%
(Equivalent) diameter d_f	± 10%	± 0.015mm
Tensile strength f_t N/mm^2	± 15%	± 7.5%
Length/diameter ratio	± 15%	± 7.5%

Table X/X Requirements with regard to the characterisation of steel fibres

6 The aspect ratio (length/diameter ratio) shall not exceed 50 for fibres that are supplied loose, or 80 for fibres that are supplied collated.

XX04 Construction joints

1 Longitudinal and transverse construction joints shall be cut back to form a vertical face. The position of transverse construction joints shall be at least 0.5m from any transverse crack in a CBM sub-base layer. Cracks shall be induced 0.5m either side of a transverse construction joint.

XX05 Induced cracks

1 Induced cracks shall comply with Clause 1070AR.

XX06 Dispensing equipment

1 Fibres shall be dispensed to uniformily provide fibres in the completed CBM at a rate stated in Appendix 7/1. The total mass of fibres dispensed per m^3 shall be measured at the intervals stated in Appendix 7/1 and no mean or individual value shall deviate from the design value by more than that stated in Appendix 7/1.

2 A preliminary trial shall be carried out to demonstrate that the dispensing equipment proposed for introducing the fibres into the mix can perform uniformily at the required rate for the proposed fibres. Where collated fibres are to be used, the trial shall demonstrate that the fibres in the batched material are well dispersed and evenly distributed throughout the mix.

XX01 General

1 FRCBM is a CBM containing steel fibres to be used as the roadbase in flexible composite pavement. As the bond between the fibres and CBM increase with strength, the higher category CBM4, CBM5 and CBM6 would normally be used.

XX02 Excavation, trimming and reinstatement of existing surfaces

1 The edges of pits, trenches or other openings through the FRCBM would create a joint without continuity of fibres and eliminate load transfer provided by the aggregate and fibres. This will increase the tendency for reflective cracking in the asphalt overlay.

XX03 Grades of concrete and constituent materials for FRCBM

1 Steel fibre reinforcement will affect the workability and achievable density of the mix, therefore the target water content should be determined following trials over a range of water contents using the reinforced material. Some plucking out of gravel aggregate at the surface was observed in trial sections of FRCBM. Surface rolling using PTR plant should be considered to increase the density at the surface.

2 The fibre length should not normally be less than three times the maximum nominal aggregate size.

3 Using the value of target water content, the cement content needed to achieve the required strength may be determined by establishing the compressive strength of the FRCBM over a range of cement contents.

4 The flexural strength and equivalent flexural strength is determined in four point bending using beams with a 100mm cross section over a span of 300mm, instrumented to control the rate of mid-span deflection. The sensitivity of the testing machine must be such as to obtain the post-crack peak. JSCE SF-4 (Japan Society of Civil Engineers, Concrete Library International Number 3, JSCE, June 1984) describes the test and determination of the ultimate and equivalent flexural strengths. Due to the variability in post-crack ductility, a minimum of five tests must be carried out, from which the average ultimate and equivalent flexural strengths and respective standard deviations are determined.

5 Dutch National Assessment Guideline 5061 Steel Fibres for Application in Concrete and Mortars is published by Certification Institute BMC, PO Box 150, 2800 Gouda. Table 1 of the Guideline describes acceptable steel fibre length, diameter, tensile strength and length/diameter ratio.

6 Trials and laboratory studies have shown where the specified aspect ratios are exceeded, balling of the fibres can occur.

XX04 Construction joints

1 Longitudinal and transverse construction joints may be considered a weak point in that no fibres cross these joints. The effectiveness of the joint may be improved by ensuring the vertical face is rough to obtain the maximum aggregate interlock. Cracks induced 0.5m either side of transverse construction joints are required to locally limit expansion/contraction of the slab.

XX05 Induced cracks

1 Induced cracks within the FRCBM at specified centres result in a greater number of cracks than would occur naturally. This is beneficial in that the degree of expansion/contraction between cracks is reduced and load transfer increased. This reduces the stresses in the FRCBM and the strains in the asphalt overlay. Induced cracking using a guillotine type breaker has been shown in trials to be an effective method of inducing cracks. Experience has shown that often these cracks will visible to the naked eye.

XX06 Dispensing equipment

1 FRCBM must be plant mixed to ensure an even distribution of fibres. When using a continuous force action mixer, the fibres must be dispensed evenly and at a rate compatible with the output of the mixer.

2 Trials have demonstrated that loose fibres can be dispensed at a rate compatible with a forced action continuous mixer, although the existing dispensing equipment must be calibrated for each fibre type and fibre volume fraction. If the fibres are introduced into the mix evenly, the distribution of the fibres in the CBM can be satisfactory. Normally, no additional testing other than at the plant would be required. Collated fibres were shown in trials in the UK to remain glued together after the mixing process. New glue or dispensing techniques may overcome this difficulty, and trials in France have suggested that collated fibres might be mixed successfully. If collated fibres are proposed, more extensive testing would be required in the completed Works to ensure the fibres are no longer collated and are evenly distributed.

Appendix C

Derivation of asphalt strain for 'top-down' cracking

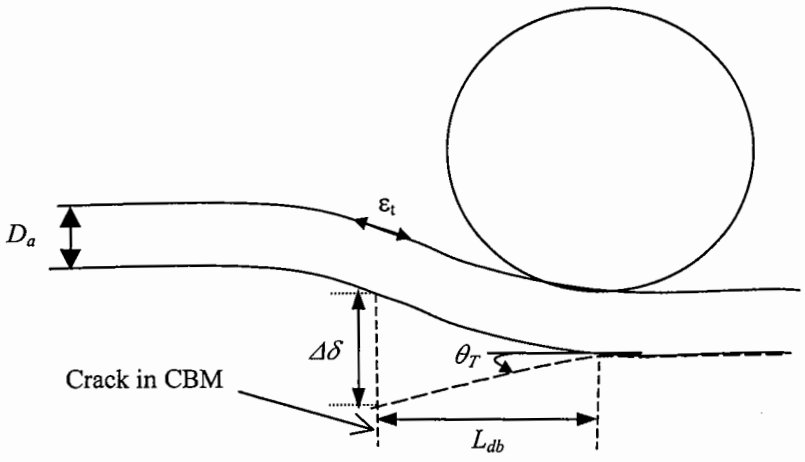

Considering moments on the asphalt (and neglecting the effects of shear), by superposition:

	M_{FA}	M_{FB}	End slope θ
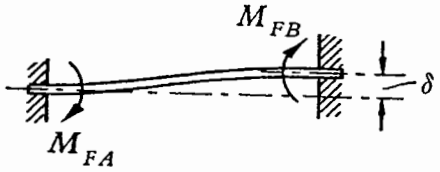	$+\frac{6EI\delta}{l^2}$	$+\frac{6EI\delta}{l^2}$	
+			
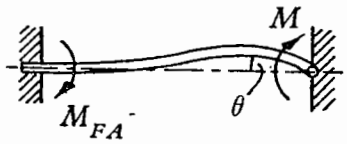	$+\frac{M}{2}$		$\frac{Ml}{4EI}$

Positive and negative moments (M_a and M_b) are given by:

$$M_a = \frac{6EI\delta}{L_{db}^2} \qquad \text{and} \qquad M_b = -\frac{4EI\theta}{L_{db}}$$

And therefore, the total moment M is given by:

$$M = \frac{2EI}{L_{db}}\left(\frac{3\delta}{L_{db}} - 2\theta\right)$$

Also, based on bending theory:

$$M = \frac{1}{6}\sigma D_a^2$$

Therefore:

And as:
$$\sigma = \frac{12EI}{L_{db}D_a^2}\left(\frac{3\delta}{L_{db}} - 2\theta\right)$$

$$I = \frac{D_a^3}{12} \quad \text{per unit width, and} \qquad \varepsilon = \frac{\sigma}{E}$$

It can be shown that:

$$\varepsilon = \frac{D_a}{L_{db}}\left(\frac{3\delta}{L_{db}} - 2\theta\right)$$

Derivation of asphalt strain for 'bottom-up' cracking

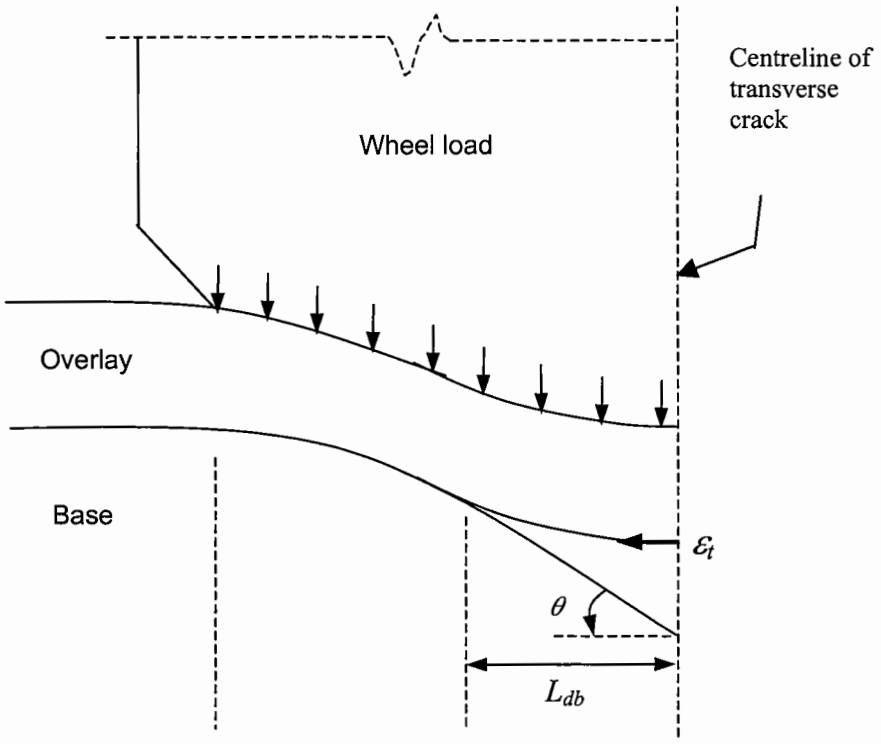

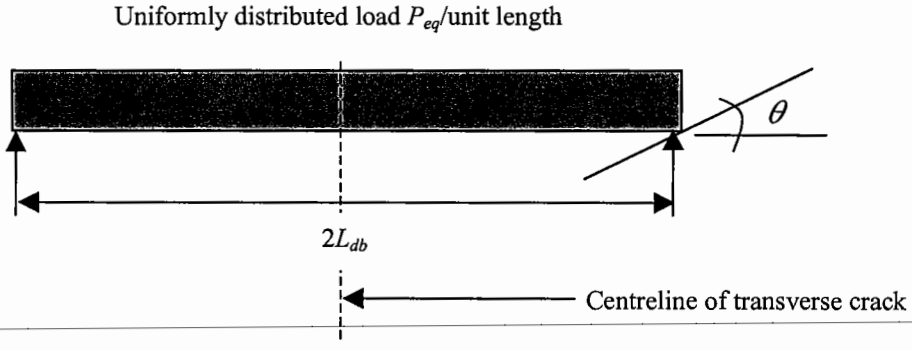

Rotation at the supports is given by:

$$\theta = \frac{wL_{db}^2}{24EI}$$

Therefore, assuming a uniformly distributed load of P_{eq} per unit length:

$$\theta = \frac{P_{eq} 2L_{db}(2L_{db})}{24EI} = \frac{P_{eq} L_{db}^3}{3EI}$$

Or

$$L_{db} = \left(\frac{3EI\theta}{P_{eq}} \right)^{\frac{1}{3}}$$

As:

$$I = \frac{D_a^3}{12} \quad \text{per unit width, then} \quad L_{db} = \left(\frac{ED_a^3\theta}{4P_{eq}} \right)^{\frac{1}{3}}$$

Based on bending theory:

$$M = \frac{wL_{db}^2}{8} = \frac{P_{eq}(2L_{db})^2}{8} = \frac{P_{eq} L_{db}^2}{2}$$

And:

$$M = \frac{1}{6}\sigma D_a^2$$

Therefore:

$$\sigma = \frac{3P_{eq} L_{db}^2}{D_a^2}$$

And as:

$$\varepsilon = \frac{\sigma}{E}$$

Then:

$$\varepsilon = \frac{3P_{eq} L_{db}^2}{ED_a^2}$$